



MINISTÉRIO DA
CIÊNCIA, TECNOLOGIA
E INOVAÇÕES



sid.inpe.br/mtc-m21d/2021/07.19.17.39-TDI

**HYBRID HYDRO-SOLAR POWER GENERATION FOR
INCREASING WATER AND ENERGY SECURITIES IN
THE SÃO FRANCISCO RIVER: EXPLORING LOCAL
AND REGIONAL EFFECTS DURING A SEVERE
DROUGHT**

Érica Ferraz de Campos

Doctorate Thesis of the Graduate
Course in Earth System Science,
guided by Drs. Enio Bueno Pereira,
and Pieter Richard Van Oel,
approved in July 23, 2021.

URL of the original document:

<<http://urlib.net/8JMKD3MGP3W34T/454UTPB>>

INPE
São José dos Campos
2021

PUBLISHED BY:

Instituto Nacional de Pesquisas Espaciais - INPE
Coordenação de Ensino, Pesquisa e Extensão (COEPE)
Divisão de Biblioteca (DIBIB)
CEP 12.227-010
São José dos Campos - SP - Brasil
Tel.:(012) 3208-6923/7348
E-mail: pubtc@inpe.br

**BOARD OF PUBLISHING AND PRESERVATION OF INPE
INTELLECTUAL PRODUCTION - CEPPII (PORTARIA Nº
176/2018/SEI-INPE):****Chairperson:**

Dra. Marley Cavalcante de Lima Moscati - Coordenação-Geral de Ciências da Terra
(CGCT)

Members:

Dra. Ieda Del Arco Sanches - Conselho de Pós-Graduação (CPG)
Dr. Evandro Marconi Rocco - Coordenação-Geral de Engenharia, Tecnologia e
Ciência Espaciais (CGCE)
Dr. Rafael Duarte Coelho dos Santos - Coordenação-Geral de Infraestrutura e
Pesquisas Aplicadas (CGIP)
Simone Angélica Del Ducca Barbedo - Divisão de Biblioteca (DIBIB)

DIGITAL LIBRARY:

Dr. Gerald Jean Francis Banon
Clayton Martins Pereira - Divisão de Biblioteca (DIBIB)

DOCUMENT REVIEW:

Simone Angélica Del Ducca Barbedo - Divisão de Biblioteca (DIBIB)
André Luis Dias Fernandes - Divisão de Biblioteca (DIBIB)

ELECTRONIC EDITING:

Ivone Martins - Divisão de Biblioteca (DIBIB)
André Luis Dias Fernandes - Divisão de Biblioteca (DIBIB)



MINISTÉRIO DA
CIÊNCIA, TECNOLOGIA
E INOVAÇÕES



sid.inpe.br/mtc-m21d/2021/07.19.17.39-TDI

**HYBRID HYDRO-SOLAR POWER GENERATION FOR
INCREASING WATER AND ENERGY SECURITIES IN
THE SÃO FRANCISCO RIVER: EXPLORING LOCAL
AND REGIONAL EFFECTS DURING A SEVERE
DROUGHT**

Érica Ferraz de Campos

Doctorate Thesis of the Graduate
Course in Earth System Science,
guided by Drs. Enio Bueno Pereira,
and Pieter Richard Van Oel,
approved in July 23, 2021.

URL of the original document:

<<http://urlib.net/8JMKD3MGP3W34T/454UTPB>>

INPE
São José dos Campos
2021

Cataloging in Publication Data

Campos, Érica Ferraz de.

C157h Hybrid hydro-solar power generation for increasing water and energy securities in the São Francisco River: exploring local and regional effects during a severe drought / Érica Ferraz de Campos. – São José dos Campos : INPE, 2021.
xxvi + 155 p. ; (sid.inpe.br/mtc-m21d/2021/07.19.17.39-TDI)

Thesis (Doctorate in Earth System Science) – Instituto Nacional de Pesquisas Espaciais, São José dos Campos, 2021.

Guiding : Drs. Enio Bueno Pereira, and Pieter Richard Van Oel.

1. Water-energy nexus. 2. Solar power. 3. Hybrid power plant.
4. Water security. 5. Integrated resources management. I.Title.

CDU 502.21:551.521.37



Esta obra foi licenciada sob uma Licença [Creative Commons Atribuição-NãoComercial 3.0 Não Adaptada](https://creativecommons.org/licenses/by-nc/3.0/).

This work is licensed under a [Creative Commons Attribution-NonCommercial 3.0 Unported License](https://creativecommons.org/licenses/by-nc/3.0/).



INSTITUTO NACIONAL DE PESQUISAS ESPACIAIS

DEFESA FINAL DE TESE DE ÉRICA FERRAZ DE CAMPOS BANCA Nº 191/2021 REG 142441/2017

No dia 23 de julho de 2021, às 09h, por teleconferência, o(a) aluno(a) mencionado(a) acima defendeu seu trabalho final (apresentação oral seguida de arguição) perante uma Banca Examinadora, cujos membros estão listados abaixo. O(A) aluno(a) foi APROVADO(A) pela Banca Examinadora, por unanimidade, em cumprimento ao requisito exigido para obtenção do Título de Doutor em Ciência do Sistema Terrestre. O trabalho precisa da incorporação das correções sugeridas pela Banca Examinadora e revisão final pelo(s) orientador(es).

Título: "Hybrid hydro-solar power generation for increasing water and energy securities in the São Francisco river: exploring local and regional effects during a severe drought."

Dr. Jean Pierre Henry Balbaud Ometto - Presidente - INPE
Dr. Enio Bueno Pereira - Orientador - INPE
Dr. Pieter Richard Van Oel - Orientador - Wageningen University
Dr. Francisco de Assis de Souza Filho - Membro Externo - UFC
Dr. Fernando Ramos Martins - Membro Externo - Unifesp



Documento assinado eletronicamente por **Jean Pierre Henry Balbaud Ometto, Pesquisador Titular**, em 26/07/2021, às 10:38 (horário oficial de Brasília), com fundamento no § 3º do art. 4º do [Decreto nº 10.543, de 13 de novembro de 2020](#).



Documento assinado eletronicamente por **Enio Bueno Pereira, Pesquisador Titular**, em 26/07/2021, às 11:32 (horário oficial de Brasília), com fundamento no § 3º do art. 4º do [Decreto nº 10.543, de 13 de novembro de 2020](#).



Documento assinado eletronicamente por **Fernando Ramos Martins (E), Usuário Externo**, em 26/07/2021, às 16:47 (horário oficial de Brasília), com fundamento no § 3º do art. 4º do [Decreto nº 10.543, de 13 de novembro de 2020](#).



Documento assinado eletronicamente por **FRANCISCO DE ASSIS DE SOUZA FILHO (E), Usuário Externo**, em 08/10/2021, às 15:13 (horário oficial de Brasília), com fundamento no § 3º do art. 4º do [Decreto nº 10.543, de 13 de novembro de 2020](#).



A autenticidade deste documento pode ser conferida no site



<http://sei.mctic.gov.br/verifica.html>, informando o código verificador **7912186** e o código CRC **E9F47D14**.

Referência: Processo nº 01340.004778/2021-32

SEI nº 7912186

*“The mind that opens up to a new idea
never returns to its original size.”*

Albert Einstein

*“A mente que se abre a uma nova ideia
jamais voltará ao seu tamanho original.”*

(In Portuguese)

To the people who did not have the chance of having their lives thoroughly transformed by human knowledge and innovation.

A todas as pessoas que não tiveram a chance de ter a vida plenamente transformada pelo conhecimento e inovação humanos.

(In Portuguese)

ACKNOWLEDGEMENTS

(In Portuguese)

Meus agradecimentos aos familiares, amigos, colegas e profissionais que fizeram parte dessa importante fase de minha história profissional.

Ao Fábio, meu companheiro de vida e incentivador na área acadêmica. Aos que cuidaram de mim em todas as fases da vida e foram modelos de dedicação, Antonio Carlos e Julieta. À Valéria pelo carinho e sábios aprendizados.

Aos queridos orientadores Prof. Dr. Enio Bueno Pereira e Prof. Dr. Pieter van Oel pela oportunidade de integrar os núcleos de pesquisa que lideram. O constante apoio e direção nos passos do doutorado, bem como a confiança depositada, foram fundamentais no desenvolver dessa pesquisa. Ao Prof. Dr. Vanderley M. John, uma fonte de inspiração que me abriu as portas e moldou como pesquisadora.

Aos colegas do grupo de pesquisa Labren (Laboratório de Modelagem e Estudos de Recursos Renováveis de Energia) pelo interesse em colaborar com informações, contatos, sugestões e trocas de ideias. Especialmente ao André Rodrigues Gonçalves e Rodrigo Santos Costa, que dedicaram tempo e energia nessa pesquisa; à Silvia Vitorino Pereira, sempre disponível para transmitir seu conhecimento e aprimorar nossa comunicação dos resultados científicos, e à Madeleine Sánchez Gácita Casagrande pelas valiosas orientações.

Aos colegas e docentes da Pós-graduação em Ciência do Sistema Terrestre (PGCST) pelos ensinamentos compartilhados. Aos pesquisadores da Divisão de Impactos, Adaptação e Vulnerabilidades (DIIAV) por constituir um centro de pesquisa de excelência, que tanto nos orgulha como brasileiros e que tenho muita honra em fazer parte. Especialmente ao Dr. Kleber Naccaratto, que nos conduziu com tanta sabedoria e dedicação durante sua gestão como coordenador da pós-graduação. Igualmente à Angelica Giarolla pelo fundamental apoio como coordenadora no PrInt Capes. Imprescindivelmente, ao Prof. Dr. Antônio Donato Nobre por renovar minha visão na ciência, nos sistemas, no planeta Terra, e no contraditório.

Aos meus colegas de “turma”, os Gaianos autores do Gaia em Jogo, amigos de muitas reflexões e conquistas. Juntos, nos oferecemos a oportunidade de criar esse produto de difusão do conhecimento, do qual tanto me orgulho em fazer parte.

Às amigas de longa data Bruna Fontes - pelas animadas conversas e deliciosas risadas nessas décadas de amizade, Vanessa Rosa e Camila Casas – que me impulsionaram para a busca de conhecimento em sustentabilidade. Às amigas que o doutorado trouxe e levo para a vida: Cristiane Pereira, Rafaela Bulgarelli, Anna Flávia Silva, Mariana Cicarelli e Maria Paula Yoshii pelo carinho brasileiro em terras estrangeiras. À Sarra Kchouk pelas doses diárias de entusiasmo e sabedoria durante nosso convívio.

Aos membros da banca examinadora, que ofereceram valiosas contribuições para o término da tese.

À Coordenação de Aperfeiçoamento de Pessoal de Nível Superior (CAPES) – Código 001 e CAPES PRINT - pelo financiamento integral da pesquisa na forma de bolsa de estudos no Brasil e no exterior, viabilização de visita técnica e aprimoramento de produto científico.

(In English)

I wish to express my gratitude to the professors, colleagues, and friends from the Wageningen University and Research for their support and warm welcoming. My special regards to Prof. Petra Hellegers, Hassnain Shah, George Kimbowa, Lena Hommes, Matthijs Wessels, Zerihun Gurmu, Wahib Al-Qubatee, Melle Nikkels, Timon Weitkamp, Maartje Sijtsema, and the 3DDD Louise Cavalcante de Souza Cabral and Germano Gondim Ribeiro Neto. To the dear friends Ara Cho, Wurska Hren, and Frances Widjaja for the shared culture and great moments.

ABSTRACT

Reservoirs of hydropower plants can amend water, energy, and food securities in semi-arid regions. However, during severe droughts, the priority of energy demand leads to critical conditions on the water storage and risk of availability for multiple uses. To reduce water use for energy, one possible measure is the adoption of solar power, an abundant energy source in semi-arid regions. This study assessed the influence of adding a floating photovoltaic powerplant in the large-scale reservoir of the Sobradinho hydropower plant, located in the São Francisco River, in the semi-arid region of Brazil, from 2009-2018. The simulated scenarios varied the installed solar power capacity from 50 to 1000 MW. For each scenario, water allocation was modified based on the solar-hydro equivalence that restrained the historical outflow of Sobradinho to maintain water in the reservoir. Additionally, a diverse set of rules for the operation of the reservoirs in cascade installed at the São Francisco River was adopted to avoid ecological impacts of low streamflow. The scenarios were assessed in water security, solar-hydro electricity output, capacity factor of the powerplant, and water and energy losses by evaporation and spilled water. Results show that a photovoltaic system starting from 250 MW was necessary to improve water security during the severe drought, reserving 0.7-2.3 years of water demand. Due to the water scarcity, the scenarios PV-750 and PV-1000 presented the same water storage level in the reservoirs after 2014, which restricted the influence of adding solar power. On the energy side, the capacity factor of the Sobradinho hybrid power plant was optimized from 29% to 34-47%. However, the water allocation of the simulated scenarios maintained the total electricity generation from the system in cascade for the solar power plant of 250 MW but reduced by 4.4% for the 750 MW. Although the reduction in total generation, all scenarios achieved an increment of the electricity output in the most critical years of the severe drought. We concluded that the solar source implied improvements for water and energy securities in the range of 250-750 MW. Additionally, we discussed opportunities and limitations in social, environmental, and economical aspects. This information can support decisions on the operation of water and energy supply

systems and subsidize the proposal of public policies and guidelines for governance focused on integrated resources management in semi-arid regions.

Keywords: Water-Energy Nexus. Solar power. Hybrid power plant. Water security. Integrated resources management. São Francisco river. Semi-arid.

GERAÇÃO DE ELETRICIDADE POR USINA HÍBRIDA SOLAR-HÍDRICA PARA APRIMORAMENTO DAS SEGURANÇAS HÍDRICA E ENERGÉTICA NO RIO SÃO FRANCISCO: EFEITOS LOCAIS E REGIONAIS DURANTE SECA SEVERA

RESUMO

Reservatórios de usinas hidrelétricas podem alterar a segurança hídrica, energética e alimentar em regiões semiáridas. No entanto, durante secas severas, a prioridade na gestão de água para produzir energia conduz a condições críticas no estoque de água e risco na disponibilidade para os diversos usos. Para reduzir o uso de água para fins energéticos, uma possível medida reside em adotar a fonte solar, abundante recurso em regiões semiáridas. Este estudo avaliou a influência da adição de usina fotovoltaica flutuante no reservatório da usina hidrelétrica de Sobradinho, localizada no rio São Francisco, na região semiárida do Brasil, no período 2009-2018. Os cenários simulados variaram a capacidade instalada de geração fotovoltaica entre 50 e 1000 MW. Para cada cenário, a alocação de água foi modificada com base na equivalência hídrica-solar para restringir a vazão histórica de Sobradinho e manter água no reservatório. Além disso, foram adotadas regras de operação dos reservatórios em cascata instalados no rio São Francisco para evitar impactos ecológicos advindos da baixa vazão praticada no período. Os cenários foram avaliados por indicadores de segurança hídrica, produção combinada de eletricidade pelas fontes solar e hidrelétrica, fator de capacidade da usina híbrida, e perdas de água e energia potencial por evaporação e defluência de água sem turbinamento. Os resultados mostram que uma planta fotovoltaica com porte superior a 250 MW seria necessária para melhorar a segurança hídrica durante a seca severa, reservando o equivalente a 0,7-2,3 anos da demanda de água. Devido à escassez hídrica, nos cenários PV-750 and PV-1000 os reservatórios apresentaram níveis similares de estoque de água após 2014, o que limitou a

influência da planta solar. No quesito energia, o fator de capacidade da usina híbrida de Sobradinho foi otimizado de 29% para 34-47%. Entretanto, a alocação de água nos cenários simulados manteve a geração total de eletricidade do sistema em cascata com a planta solar de 250 MW, porém houve redução de 4,4% com a planta solar de 750 MW. Apesar da diminuição total, todos os cenários obtiveram incremento da geração hidrelétrica nos anos mais críticos da seca. Concluímos que a adoção da fonte solar influenciou a condição hídrica do rio São Francisco, com melhorias da segurança hídrica e energética na faixa de plantas solares de 250 a 750 MW. Adicionalmente, foram discutidas oportunidades e limitações em aspectos sociais, ambientais e econômicos. Essas informações podem subsidiar decisões da operação de sistemas de abastecimento de água e energia, bem como subsidiar a proposição de políticas públicas e orientar medidas de governança voltadas à gestão integrada de recursos em regiões semiáridas.

Palavras-chave: Nexo água-energia. Energia solar. Usina híbrida. Segurança hídrica. Gestão integrada de recursos. Rio São Francisco. Semiárido.

LIST OF FIGURES

Figure 2.1 - Location of São Francisco Basin and the four sub-basins.	9
Figure 2.2 - Climate normals for 1981-2010 in Brazil: (A) annual precipitation (mm) and (B) annual evapotranspiration (mm).....	9
Figure 2.3 - Potential for photovoltaic production in (A) Brazil and (B) São Francisco Basin in kWh/kWp.year.....	10
Figure 2.4 - Population living in poverty (%) versus water access in 1,136 municipalities in the semi-arid region of the Brazilian Northeast (red dots), compared to 4,430 other municipalities in the rest of Brazil for 2010 (green dots).	10
Figure 2.5 – Location of the hydropower plants installed at the São Francisco River and the ratio of water demand and water availability in the São Francisco Basin.	12
Figure 2.6 - Annual volume of precipitation at São Francisco Basin from 1961 to 2018.	13
Figure 2.7 - Precipitation at São Francisco Basin: column bars express the seasonal volume of rainfall from 1961 to 2018; horizontal lines express the average values for wet (blue) and dry (orange) season in different periods: 1961-2008 (light color), 2009-2018 (medium-dark color), and 2012-2018 (dark color); the lines with variation express the annual precipitation rate of the four sub-basins (gray colors).	14
Figure 2.8 - Number of days in water deficit in the Brazilian Northeast from 2011-2016.	15
Figure 2.9 – (A) Inflow and (B) outflow of the Sobradinho reservoir (m ³ /s).....	17
Figure 2.10 – Effective water storage in reservoirs of hydropower plants installed in the São Francisco River from 1999 to 2018: (A) Três Marias, (B) Sobradinho, and (C) Itaparica.....	18
Figure 2.11 - Hydroelectricity generation (primary axis; orange bars) and average outflow (secondary axis; blue line) at Sobradinho from 1999 to 2018.	19
Figure 2.12 - Fruit production type of culture at IBGE microregions Petrolina and Juazeiro from 1990 to 2018.....	20

Figure 2.13 - Fruit production of the microregions Petrolina and Juazeiro from 1990 to 2018, in million tons.....	21
Figure 2.14 – Projections in the variation of precipitation minus potential evapotranspiration (mm/day) at Brazilian Northeast from 1970-2100.	22
Figure 3.1 – Classical schematization of the water-energy-food Nexus.	24
Figure 3.2 - Conceptual diagrams of different fields of knowledge.	25
Figure 3.3 - Monthly average irradiation at Petrolina meteorological station (kWh/m ²).....	27
Figure 3.4 – Solar irradiation at Petrolina meteorological station and precipitation rate at Middle sub-basin, on monthly average values.	28
Figure 3.5 - Potential power generation at Petrolina per installed capacity in monthly timestep.	29
Figure 3.6 - Productivity related to the level of water storage in the Sobradinho reservoir from 1999-2018.	30
Figure 3.7 – Productivity of Sobradinho HPP from 1999-2018.....	30
Figure 3.8 – Rules for outflow at Sobradinho at attention stage: quantified for solar scenarios based on saved flow (dashed lines) and adjusted by the minimum outflow of 800 m ³ /s (solid line).....	34
Figure 3.9 – (A) Schematic interface of WEAP and the elements of modeling São Francisco River at (B) Três Marias region (Upper sub-basin) and (C) Sobradinho and Itaparica region (Lower-Middle and Lower sub-basins).....	37
Figure 3.10 – Water flow (Sankey diagram) in the components of the San Francisco River model; values in Gm ³ for the average 2009-2018 refer to the y-axis.....	38
Figure 3.11 – Volume-elevation curve of the reservoir (A) Sobradinho, (B) Três Marias and (C) Itaparica (ANA, 2019a).	40
Figure 3.12 – Monthly precipitation rate at the São Francisco sub-basins Upper, Middle, Lower-middle, and Lower.....	42
Figure 3.13 – Correlation of the volume of water at the Sobradinho reservoir and the area of the lake.....	43
Figure 3.14 – Sub-catchment in the São Francisco reservoir with the contributing area of local runoff to the Sobradinho reservoir (in yellow).	44

Figure 3.15 – Water input (m ³ /s) in reaches: R1, R2, R3, and R4, local runoff at Sobradinho, precipitation (P) on the three reservoirs, and the linear trend of total input from 1999 to 2018.	45
Figure 3.16 – Volume of water of authorized withdrawal from Sobradinho Reservoir for 2001-2018. Primary data by (ANA, 2020c) in solid line; adjusted data incorporated to the model, per user, in dashed line.....	47
Figure 3.17 – Water demand from the reservoirs Três Marias (A) and Itaparica (B); and from the São Francisco River section downstream Três Marias (C), downstream Sobradinho (D), and downstream Itaparica (E).....	48
Figure 3.18 – Monthly variation of the water consumption from reservoirs and SFR sections.....	49
Figure 3.19 – Monthly evaporation rates on Três Marias, Sobradinho, and Itaparica reservoirs from 1999 to 2018, based on the evaporation rate dataset of Funceme (2020).	50
Figure 3.20 - Water output in the model distributed into demand, evaporation from the reservoirs, and outflow to the ocean from 1999 to 2018.....	51
Figure 3.21 – Annual flow of SFR: volume of input, output, variation of water storage in the reservoirs, and variance in data.....	52
Figure 3.22 – Volume of water in the modeled reservoirs (A) Três Marias, (B) Sobradinho, and (C) Itaparica (blue line) comparing to the ONS dataset (red line) at left; Nash-Sutcliffe efficiency (NSE) graph for the reservoir at right; and (D) NSE for the total storage in SFR reservoirs.....	54
Figure 3.23 – Outflow from the modeled reservoirs and at the wedge streamflow (blue line) comparing with the National Water Agency dataset (red line) at the gauges downstream.	56
Figure 3.24 – Hydroelectricity output in simulation (blue line) and ONS dataset (red line) for (A) Três Marias, (B) Sobradinho, (C) Itaparica, (D) Paulo Afonso, (E) Xingó, and (F) SFR HPPs, from 1999 to 2018.	57
Figure 3.25 - Nash-Sutcliffe efficiency (NSE) of hydroelectricity output comparing ONS dataset and the modeling of (A) Sobradinho and (B) the five hydropower plants installed at São Francisco River.	58

Figure 3.26 – Comparison of the water input in the model and the estimated runoff at São Francisco basin: (A) monthly volume and (B) correlation of the data.	59
Figure 4.1 – Water storage at Sobradinho reservoir using minimum streamflow from 550 to 1,100 m ³ /s in the period 2009-2018.....	64
Figure 4.2 - Water storage at Sobradinho for PV scenarios ranging from 50-1,000 MW: valid scenarios (blue line), invalid scenarios (orange line), and observed scenario (red line).....	65
Figure 4.3 – Outflow from Sobradinho reservoir in valid and observed scenarios.....	65
Figure 4.4 – Water flow in the components of the San Francisco River model: (A) Observed scenario for average 2009-2018, (B) Observed scenario in 2017, (C) Scenario PV-250, and (D) Scenario PV-1000. Values in billion cubic meters in the y-axis.....	67
Figure 4.5 – Frequency of months with water storage in the three operation stages defined by the National Water Agency (ANA).	71
Figure 4.6 - Frequency of the operating rule in prevalence in the simulated scenarios for the period 2009-2013 and 2014-2018.....	72
Figure 4.7 – (A) Ratio of the lowest level of water storage in Sobradinho and the yearly water withdrawal from the reservoir (D3) and between Sobradinho and Itaparica (D4); (B) result for 2017.	73
Figure 4.8 - Range of (A) monthly and (B) annual electricity generation of a PV installed power of 250MW located at the Sobradinho reservoir.....	73
Figure 4.9 – Scenarios of monthly electricity output from Sobradinho hybrid power plant per energy source: (A) PV-250, (B) PV-500, (C) PV-750, and (D) PV-1000, compared to the historical time-series 2009-2018 (red bold line).....	75
Figure 4.10 – Annual electricity generation for PV scenarios in Sobradinho: PV-250 (yellow), PV-1000 (orange), hydroelectricity outputs of the simulated scenarios (blue), the observed dataset from ONS (red), and the equivalent generation for HPP outflow of 800 m ³ /s.....	76
Figure 4.11 – Average electricity output in historical dataset 2009-2018 and simulated PV scenarios at (A) Sobradinho and (B) five HPPs at SFR.	77

Figure 4.12 - Loss of potential energy by spilled water at the hydropower plants Sobradinho, Itaparica, PAC, and Xingó for observed scenario, PV-250, PV-500, PV-750, and PV-1000.	79
Figure 4.13 – Range of evaporation from Sobradinho reservoir related to the water storage.....	80
Figure 4.14 – Loss of potential energy by evaporation from Sobradinho reservoir for the simulated scenarios compared to the observed scenario, excepting the evaporation of dead volume condition.....	81
Figure 4.15 - Monthly electricity output of Sobradinho hybrid power plant per energy source in scenario (A) PV-250 and (B) PV-1000 from 1999 to 2018 compared to the historical time-series (red bold line).	82
Figure 5.1 – Net balance of solar electricity output considering the loss of potential energy for evaporation.	87
Figure 5.2 – Commercial value of the electricity of the Northeastern sub-system.....	93
Figure 5.3 – Estimates of average cloud cover index (CEF) over the Sobradinho reservoir region for the two periods of the day (early and late afternoon) and season of the year [December, January, February (DJF); March, April, May (MAM); June, July, August (JJA); and September, October, November (SON)].	98
Figure 5.4 - Size of the floating PV power plants with an installed capacity of 250 and 1,000 MW in simulated insertion at the Sobradinho lake for the relative area in October 2011, 2015, and 2016.	100
Figure 5.5 - Monthly electricity output of Sobradinho hybrid power plant per energy source in scenario (A) PV-50 and (B) PV-100 from 1999 to 2008 compared to the historical time-series (red bold line).	101

LIST OF TABLES

Table 3.1 - Six scenarios with varying levels of installed power of photovoltaic panels, estimates of annual electricity from the solar source, and the equivalent volume and outflow of water.....	31
Table 3.2 - Water Agency Resolution 2081/2017 for the outflow of the reservoirs at São Francisco River related to the effective water storage volume in the reservoir (EV).	32
Table 3.3 - Operation rules of water allocation adopted in the simulations.	33
Table 3.4 – Indicators of assessment of the scenarios.....	35
Table 3.5 – Primary information on the hydropower plants and their reservoirs.....	39
Table 3.6 – Calculation of the runoff coefficient.....	59
Table 5.1 – Qualitative summary of indicators for the simulated PV scenarios. The colors express improvement (blue) or loss (red) compared to the observed scenario. The gradient expresses the intensity of the change.....	84
Table 5.2 - Installation and electricity production cost of the PV system in the simulated scenarios PV-250 and PV-1000.....	93
Table 5.3 – Potential advantages and disadvantages of the floating photovoltaic technology (FPV).....	95
Table 5.4 – Size of the PV system for the simulated scenarios and the covering area of Sobradinho lake.	99

LIST OF ABBREVIATIONS AND ACRONYMS

ANA	National Water Agency
CF	Capacity Factor
CBHSF	São Francisco River Basin Committee
EV	Effective water storage volume in the reservoir
FPV	Floating photovoltaic power plant
HPP	Hydropower Plant
IBGE	Brazilian Institute of Geography and Statistics
INMET	National Institute of Meteorology
MFR	Minimum Flow Requirement
ONS	National Electric System Operator
OS	Observed scenario (modeling of the historical dataset)
PAC	Paulo Afonso Complex hydropower plants
PV	Photovoltaic power plant
SFB	São Francisco Basin
SFR	São Francisco River
SIN	National Interconnected Power System

CONTENTS

1	INTRODUCTION	1
1.1	Hypothesis and goals.....	5
2	CONTEXTUALIZATION	8
2.1	Study area.....	8
2.2	Influence of severe drought.....	13
3	MATERIALS AND METHODS	23
3.1	Water-Energy Nexus.....	23
3.2	Selected scenarios.....	26
3.2.1	Solar power and solar-water equivalence	26
3.2.2	Operation rules for the reservoirs.....	31
3.3	Assessment of the scenarios	34
3.4	Water and energy system modeling.....	36
3.4.1	Hydropower plants and reservoirs	38
3.4.2	Water input.....	41
3.4.2.1	Incremental streamflow	41
3.4.2.2	Precipitation in the reservoirs	42
3.4.2.3	Runoff at the Sobradinho reservoir	43
3.4.2.4	Total water input	44
3.4.3	Water output	45
3.4.3.1	Demand	45
3.4.3.2	Evaporation.....	49
3.4.3.3	Total water output	50
3.4.4	Water balance.....	51
3.5	Validation	52
3.5.1	Model validation 1: reservoirs storage and streamflow	53
3.5.2	Model validation 2: hydroelectricity output	56
3.5.3	Model validation 3: Water input.....	58
3.5.4	Variables and uncertainties regarding solar generation	60
3.5.4.1	Performance ratio of the PV system	60
3.5.4.2	Measures of solar irradiance.....	61
3.5.4.3	Solar panel efficiency	61
3.5.4.4	Technical uncertainties	61
4	RESULTS	63

4.1	Limits for water allocation.....	63
4.2	Effect of solar power generation on water conditions.....	64
4.3	Water security	72
4.4	Solar electricity.....	73
4.5	Hydroelectricity	74
4.6	Capacity factor of Sobradinho	76
4.7	Electricity output from Sobradinho and SFR system	77
4.8	Loss of water and potential energy	78
4.8.1	Spilled water	78
4.8.2	Evaporation from the reservoirs	79
4.9	Effects of solar PV in typical and wet periods	81
5	DISCUSSION.....	83
5.1	Opportunities and limitations for hybrid solar-hydro powerplants.....	88
5.2	Opportunities and limitations for large-scale PV power plant.....	91
5.3	Opportunities and limitations for floating PV systems	94
5.4	Opportunities and limitations for small-scale PV power plant.....	100
5.5	Final remarks	101
5.6	Recommendations for future researches	102
6	CONCLUSIONS	103
	REFERENCES.....	106
	APPENDIX A - WATER EVALUATION AND PLANNING (WEAP) MODELING	130

1 INTRODUCTION

Reservoirs can provide water security to water-stressed regions (PEREIRA et al., 2019; SCOTT et al., 2020). However, for multi-purpose reservoirs, the prioritization for other functions such as hydropower generation may jeopardize water security (BAHRI, 2020). In this context, the inclusion of a second power source to the existing HPP, turning it into a hybrid powerplant, can help to save water in the reservoir and make it available for other purposes, providing a solution for developing integrated resources management and rising governance (HUNT et al., 2018; MAUÉS, 2019).

Resource availability is driven by environmental characteristics of the site (LINK; SCHEFFRAN; IDE, 2016) and the dynamic process of positive and negative feedbacks involving anthropogenic interventions (VAN OEL et al., 2014; VAN LOON et al., 2016; GARCIA; RIDOLFI; DI BALDASSARRE, 2020) and ecosystem regeneration (SRINIVASAN et al., 2013). In contemporary society, demographic growth, urbanization process, land-use change, shifts in the pattern of production, and increase in consumption are trends that intensify the demand for natural resources and, consequently, the pressure on ecosystems (Hoff, 2011; Howells et al., 2013; IRENA, 2015; NCR / FAO, 2014; Rodriguez et al., 2013; World Economic Forum Initiative, 2011). Water crises, food crises, and energy price shock are frequently listed by the World Economic Forum among the significant global risks related to resources security, human health, social cohesion, political and economic stability (WEF, 2020).

For the definition of resource security, United Nations declares water security as:

“The capacity of a population to safeguard sustainable access to adequate quantities of acceptable quality water for sustaining livelihoods, human well-being, and socio-economic development, for ensuring protection against water-borne pollution and water-related disasters, and for preserving ecosystems in a climate of peace and political stability.” (UN, 2013).

For energy security, there are several definitions. The International Energy Agency defines it as the broad availability of energy at affordable prices (IEA, 2016). The International Renewable Energy Agency states that energy security would be achieved by stabilizing the prices of petroleum products, combining different energy sources, and including the dimension of sustainability (IRENA, 2015). For the European Commission, energy security implies political-economic bias and means the transition to a competitive low-carbon economy, less dependent on imported fossil fuels. The United States of America has a broader definition: to develop flexible, transparent, and competitive markets; diversify energy sources and routes; reduce greenhouse gas emissions; improve energy efficiency and manage the demand; adopt clean and sustainable technologies; invest in research and innovation; improve systems resilience; and minimize imported fuels (USDE, 2017).

Natural and anthropogenic factors define the security in the use of resources by a population regarding availability, infrastructure, economic dependence, and governance. BIGGS et al. (2015) defend security as complementarily driven by: availability in nature, capability to access, dynamics of social power, strength of institutions, and operating governance. For KURIAN and ARDAKANIAN (2013), the security in the long-term is only met in balanced ecosystems, managed under sustainability principles, adopting technologies, and appropriate adaptations favorable to the quality of life. Recently, global environmental changes jeopardize security as it represents a direct driver of interference on water cycles, food production, and energy generation (IPCC, 2014). In this context, the management capacity plays an important role to concomitantly protect ecosystems, distribute the resources equitably, and apply them efficiently by the appropriate advances in research and new technologies. To create a globally-oriented effort, the United Nations (UN) organized the Sustainable Development Goals (SDGs), a set of guidelines for multi-scales public policies to promote the strategic management of resources with governance and social equity for quality of life, human well-being, and conservation of ecosystems (UN, 2015). Food (SDG 2), water (SDG 6), and energy (SDG 7) securities stand among the seventeen objectives that make up the 2030 Agenda. The SDGs denote the

importance of global and coordinated actions that are constantly monitored and periodically reviewed.

In semi-arid regions, environmental and anthropogenic factors jointly impose low availability of water resources, absence of access, and conflicts in the use. In these water-stressed regions, the population is constantly exposed to vulnerability in human health, economic development, social interactions, and cultural activities. Beyond the inherently compromised access to water, the low precipitation and high evaporation rates in periods of severe drought aggravate the scarcity and intensify the competition by its multiple uses (HUANG et al., 2019). For the Intergovernmental Panel on Climate Change, drought relates to a certain climatic pattern, meaning “*A period of abnormally dry weather long enough to cause a serious hydrological imbalance.*” (IPCC, 2018). Scenarios of global changes predict an increase in frequency and severity of drought events that will probably intensify the drivers of pressure (IPCC, 2018). Thus, in semi-arid regions, the appropriate management capacity and governance of the available resources are necessary for dealing with the drought and the most critical events towards security in their use.

In order to address contexts of jeopardized security, vulnerability, and conflicts, Nexus stands as an approach to assess resources availability and their interactions. The concept recognizes water, energy, and food securities as intrinsically connected (HOFF, 2011; FAO, 2014a) in different spatial and temporal scales (KURIAN; ARDAKANIAN, 2013). The studies on Nexus are supposed to capture the interrelations, synergies, and trade-offs associated with the resources use and their mutual influence (SCOTT; KURIAN; WESCOAT, 2015). The analysis of multiple scenarios – for instance, in the adoption of practices, technologies, infrastructures, or public policies – enables to estimate the outcomes and qualify the solutions to improve security in different scales. Beyond the diagnosis of the context and the assessment of a range of possibilities, to reach the objectives, the Nexus framework enhances the use of transdisciplinarity and governance: scientific knowledge and participatory decision-making applied to the proposal and implementation of strategic solutions to society and economic sectors (AL-SAIDI; RIBBE, 2017; MANNAN et al., 2018).

MARENGO et al. (2017) affirm that “*There is a need for actions in which the scientific and the decision-makers communities can work together on drought issues, focusing on reducing vulnerability, and building resilience.*”. Accordingly, in contexts of scarcity - such as water resources in semi-arid regions, Nexus can work as an adequate approach to identify feasible solutions based on synergies and resilience.

Semi-arid areas are abundant in solar energy (SOLARGIS, 2020). Solar PV panels are progressively being adopted to feed equipment that withdraws, pump or treat water or, alternatively, to substitute water to generate electricity. Semi-arid regions are target sites to install large-scale PV power plants (CROOK et al., 2011), which has the potential to improve the infrastructure and prioritize water for other purposes when associated with existing HPPs (BELUCO; KROEFF DE SOUZA; KRENZINGER, 2012; KOUGIAS et al., 2015, 2016; STIUBIENER et al., 2020). As a substitute for hydropower, the use of solar allows to change the water management, making it available to being conserved in the reservoir saving potential energy, or increasing its destination for other purposes, such as ecological aspects and crop irrigation. Accordingly, a hybrid solar-hydro powerplant may change the pattern of resource use by reversing the policy of *water for energy* into *energy for water*. This strategy has the potential to increase water and energy security by attaining the water demand and providing renewable electricity.

Hybrid power plants combining solar and wind sources with hydro present high potential in the Brazilian semi-arid region (VIVIESCAS et al., 2019; SANTOS et al., 2020). In this study, we analyzed the result of adding a floating photovoltaic solar powerplant into the Sobradinho hydropower plant, located in the semi-arid region of Brazil. The historical climate conditions of this basin show that the typical operation needs to be addressed with additional measures of integrated water and energy management. Scenarios in a range of PV power capacity were simulated to evaluate the influence of this strategy on water and energy securities regarding the water availability and conservancy on local and regional scales and the electricity dispatches to the national electric grid.

Previous studies have separately discussed water allocation strategies at the São Francisco River (LIMA; ABREU, 2016; BRAMBILLA; FONTES; MEDEIROS, 2017; BASTO; FONTES; MEDEIROS, 2020), the local effects of converting hydro into hybrid power plants (MAUÉS, 2019; VELLOSO; MARTINS; PEREIRA, 2019), the water-energy Nexus for increasing the performance of the Sobradinho HPP (HUNT et al., 2018), or investigated the gains for the energy sector from the optimized design of floating PV systems added to the HPPs of SFR (SILVÉRIO et al., 2018). The novelty of this study stands in providing sensitivity analysis for a range of PV plants to improve both water and energy securities and discuss the trade-offs on local and regional scales.

1.1 Hypothesis and goals

The hypothesis of this study was to partially replace hydro power with solar power to maintain the volume of water stored in the reservoir, equivalent to the quantity necessary to produce the electricity generated by the PV panels. We assumed that Nexus Water-Energy stands as an appropriate concept to manage resources under conditions of water scarcity. The São Francisco River was adopted as the study case due to the presence of hydropower plants with large-scale reservoirs operating in cascade in a semi-arid region. A floating PV system installed at the reservoir of the Sobradinho hydropower plant was the technology selected to convert it into a hybrid system. The solar PV scenarios were proposed in the wide range of 50 to 1000 MW of installed power to carry out a sensitivity analysis of the proposed solution. We defined the years 2009 to 2018 to evaluate the potential benefits in a period of severe drought and critical water shortage in the river and reservoirs.

Hence, this study investigated the *influence of adding solar PV into the Sobradinho HPP on the water management of the São Francisco River over a severe drought*. Besides this primary scientific question, we assessed the following specific objectives:

- Identify the maximum outflow value from the Sobradinho reservoir that was sufficient to sustain a higher river flow compared to the observed values adopted over the severe drought of 2009-2018;

- Define operative rules to allocate water among the three reservoirs installed at the São Francisco river to increase water security in dry climatic conditions;
- Quantify the solar-water equivalence to generate electricity based on the solar irradiation and the productivity of the Sobradinho hydropower plant;
- Identify the viable range of scenarios varying the solar PV installed power into Sobradinho hydropower plant and quantify the associated electricity output;
- Quantify indicators of water and energy security to assess the synergies and trade-offs of the simulated scenarios compared to the observed scenario;
- Analyze associated impacts in social, environmental, and economic aspect that the PV adding into Sobradinho HPP would have avoided;
- Analyze the adherence of the proposed scenarios of solar PV power plants to the national plans for the Brazilian electric sector regarding costs and installed power.

The investigation involved the following steps: 1) to model the study area to reproduce water allocation and power generation of São Francisco River from 1999 to 2018, designed based on governmental dataset (observed scenario); 2) to quantify the solar-hydro equivalence in power generation for each scenario of installed PV system; 3) to set operative rules for water storage and outflow among the reservoirs; 4) to model the simulated scenarios (based on step 1), modified by the hydro-solar energy equivalence (step 2) and the operative rules (step 3); 5) to quantify the water and energy indicators.

The model was designed in computer simulation using WEAP software, chosen due to its capacity to quantify the interactions on water allocation and energy generation, allowing to compare the results of multiple alternatives derived from the observed scenario. We validated the model using water and energy outputs of the hydropower plants installed at SFR and classified the simulated scenarios using the results at local and regional scales for water security, solar-hydro

electricity generation, capacity factor, water and energy losses by spilled water, and evaporation.

The thesis is organized as follows: Chapter 2 describes the conditions of the São Francisco River in terms of water availability and energy production during the severe drought that occurred during the study period. Chapter 3 defines the methodology and dataset used in the modeling of the observed and PV scenarios and the indicators of water and energy outputs used in the assessment. Section 4 provides the results of the proposed indicators. In Section 5, we discussed the results and presented additional analysis regarding the technical solution and the implications in social, environmental, and economic aspects. Section 6 summarizes the main conclusions and recommendations for future research.

Some of the results presented in this document are part of the paper *“Hybrid hydro-solar power generation for increasing water and energy securities during drought: exploring local and regional effects in a semi-arid basin”*, Journal of Environmental Management, September 2021, Volume 294, p. 112989, available at: www.sciencedirect.com/science/article/pii/S0301479721010513.

2 CONTEXTUALIZATION

2.1 Study area

The São Francisco River is inserted in a critical region of Brazil regarding climate, social and environmental aspects. The river basin extends for 638,576 km² in the Brazilian Northeast (geographical coordinates 7.3°S-20.9°S; 36.3°W-47.6°W) and is partially located inside the semi-arid boundary (Figure 2.1). The hydrological deficit comprehends annual precipitation lower than 1,500 mm and annual evapotranspiration higher than 1,750 mm (Figure 2.2) for the period 1981-2010 (INMET, 2020). As illustrated in Figure 2.1, the basin is administratively organized in four sub-basins: Upper (16% of the total area), Middle (63%), Lower-Middle (17%), and Lower (4%). In 2010, the SFB population was quantified as 14.3 million, living in 505 municipalities (CBHSF, 2016).

The wet season is reported from December to April, when the precipitation at Upper and Middle sub-basins charges the surface water of the São Francisco riverbed and the existing reservoirs. FUNCEME (2020) quantified the monthly average precipitation for the SF sub-basins based on the INMET (National Institute of Meteorology) stations using the Thiessen method for the period 1961-2018. The estimative of annual precipitation varied by 543–2,134 mm at Upper, 603–1,393 mm at Middle, 587–1,306 mm at Lower-Middle, and 221–1,068 mm at Lower sub-basins (FUNCEME, 2020).

Since more than half of the basin is inserted in the semi-arid¹ climate (SUDENE, 2017), the sub-basins are social and economically characterized by differences derived from the availability of water. The river is the main source of water for the semi-arid portion of the basin (EMBRAPA, 2020) and the multiple uses essentially depend on the river and existing reservoirs (MANETA et al., 2009; CBHSF, 2016; ALVALÁ et al., 2017). On the other side, as a consequence of the low cloudiness and the geographic position of the Brazilian semi-arid, solar irradiation is an abundant resource over the year. Standing as one of the most productive areas

¹ Defined by average annual rainfall inferior to 800 mm, aridity index inferior to 0.50 (Thorntwaite method), and daily water deficit in more than 60% of the days over a year.

in Brazil, the potential for photovoltaic production reaches 1,750 kWh/kWp.year (PEREIRA et al., 2017), consisting of an appropriate site for the installation of solar powerplants to generate electricity to the national grid (Figure 2.3).

Figure 2.1 - Location of São Francisco Basin and the four sub-basins.

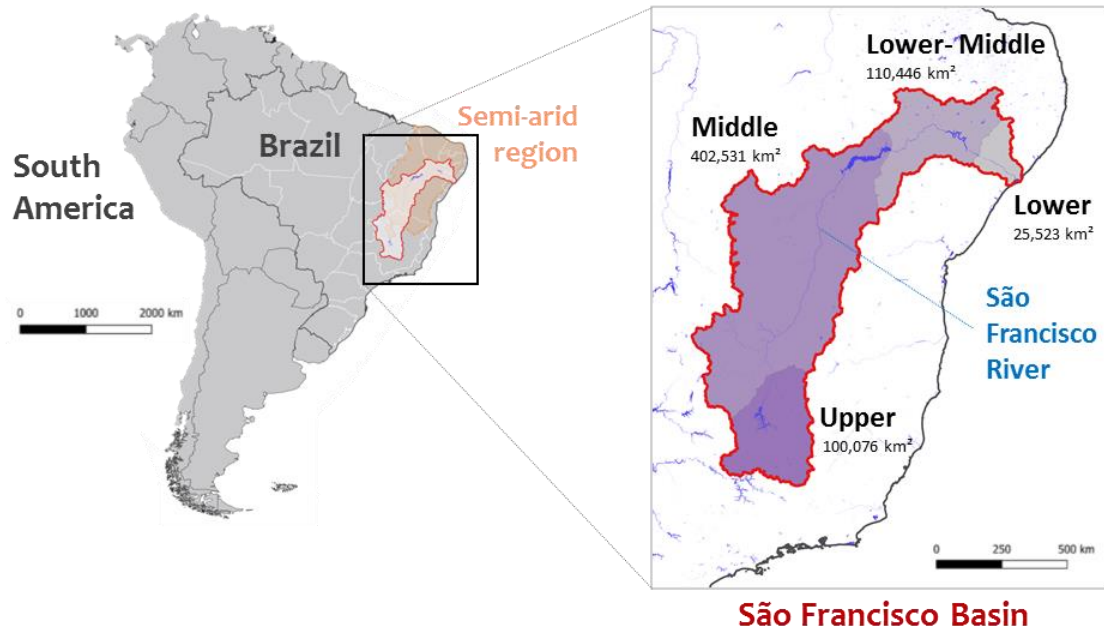
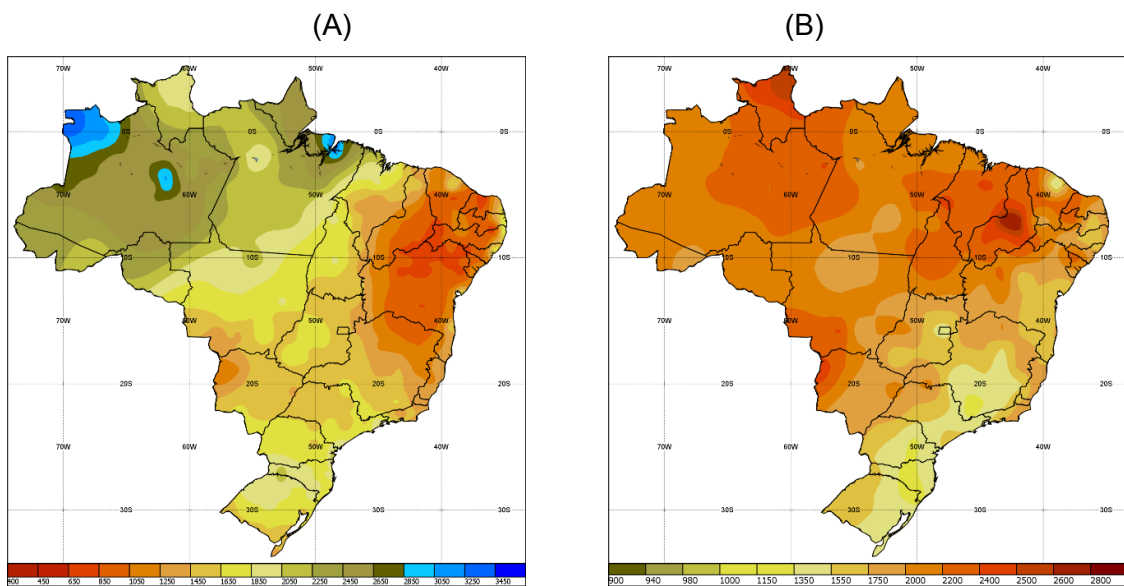
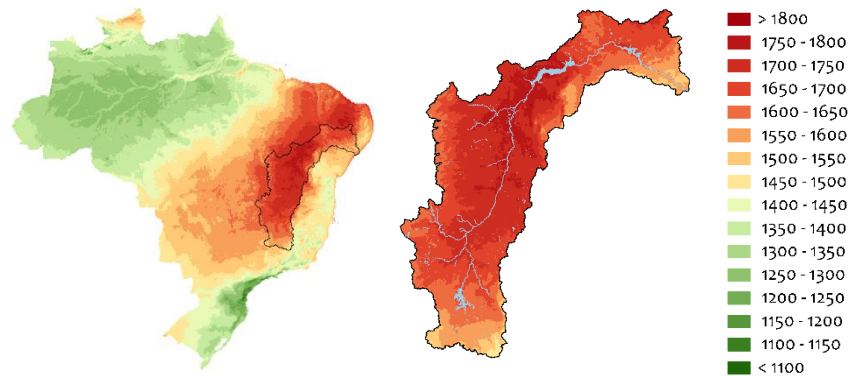


Figure 2.2 - Climate normals for 1981-2010 in Brazil: (A) annual precipitation (mm) and (B) annual evapotranspiration (mm).



Source: INMET (2020).

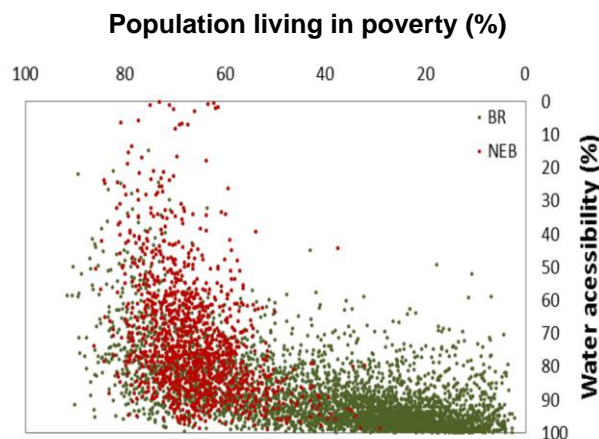
Figure 2.3 - Potential for photovoltaic production in (A) Brazil and (B) São Francisco Basin in kWh/kWp.year.



Source: Pereira et al. (2017).

The vulnerability in the access to water causes conflicts that have been gradually intensified by the control of the river flow imposed by the operators of the hydropower plants (MANETA et al., 2009; ANA, 2018a), the growth of water consumption (ANA, 2016a), and the events of severe drought (ALVALÁ et al., 2017; MARENCO et al., 2017). To represent the role of water to this population, Figure 2.4 associates the population with access to water and the level of poverty in municipalities located in the semi-arid region of the Brazilian Northeast in comparison to other parts of Brazil. These data express both the vulnerability triggered by the lack of access and the potential growth of the demand when reaching an equitable condition.

Figure 2.4 - Population living in poverty (%) versus water access in 1,136 municipalities in the semi-arid region of the Brazilian Northeast (red dots), compared to 4,430 other municipalities in the rest of Brazil for 2010 (green dots).



Source: Marengo et al. (2020).

Along the SF river, five HPP connected to the national electric grid take advantage of its streamflow. Three HPP contain large reservoirs (Figure 2.5): Três Marias (storage capacity: 19.5 Gm³; lake area: 1,040 km²), Sobradinho (34 Gm³; 4,214 km²), and Itaparica (10.7 Gm³; 60 km²), which jointly represented 15.8% of the water storage capacity of the national electric grid in 2017 (ANA, 2017a). The other two HPP – PAC and Xingó – work as run-of-river (ANA, 2020a), being influenced by the operating rules of the reservoir's system. The reservoirs were installed to provide two types of benefits: access to water during dry seasons at local and regional scales and control of electricity production at national scale.

After the installation of the HPP, the streamflow started to be intensively controlled by the SIN operators, leading to negative impacts on the natural environment (CORREIA; DA SILVA DIAS; DA SILVA ARAGÃO, 2006; BEZERRA et al., 2019; CAVALCANTE et al., 2020). Sobradinho started operating in 1979 and Xingó in 1994. As a consequence of the water allocation among the reservoirs, the river flow at the mouth was estimated in 1979-1994 in the range of 1,619-6,767 m³/s (average: 3,650 m³/s), being reduced in 1995-2012 to 1,326-2,549 m³/s (average: 1,805 m³/s) (VASCO; AGUIAR NETTO; SILVA, 2019). The Basin Decadal Plan 2016-2025, registered the streamflow in 1931-2013 by 2,790 m³/s, on average, with 811 m³/s of permanence flow Q95² (CBHSF, 2016).

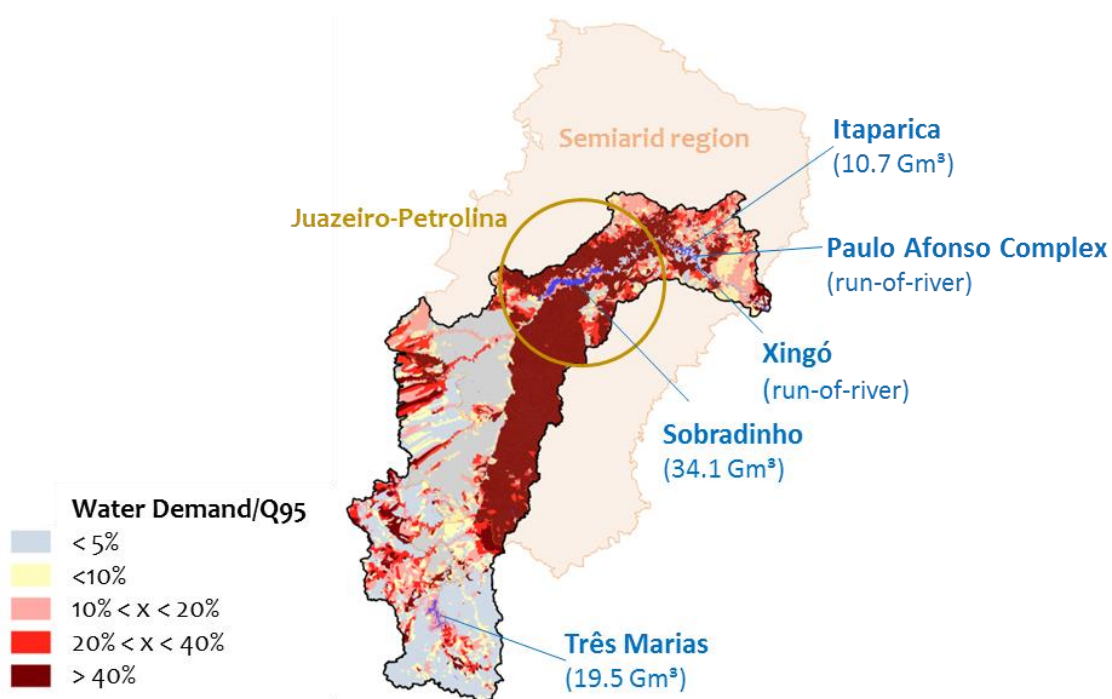
After the installation of the HPP, several public irrigation districts were installed nearby and downstream Sobradinho induced by the water provided by this reservoir (CODEVASF, 2017). Nowadays, Sobradinho supports an important regional economy, including a large-scale fruit culture (CARVALHO; KIST; BELING, 2020; CEPEA/ESALQ, 2020) that traded US\$ 480 million³ in 2018 (IBGE, 2019) with national and international markets (MAPA, 2018). The region is classified by the National Water Agency (ANA) as a special area for water resource management due to the intense demand and economic relevance (ANA, 2017b).

² Q95: streamflow value exceeded during 95% of the time.

³ 1 US\$ = R\$ 5.35 (02/02/2021)

In 2010, the water demand in SFB accounted for 279 m³/s, including irrigation (77%), human consumption (12%), industry (7%), and animal consumption (4%). The irrigation share is higher under semi-arid conditions: 87% at Middle (90m³/s) and 93% at Lower-Middle sub-basins (96m³/s) (CBHSF, 2016). Compared to the previous decade, the demand increased by 68% (166 m³/s in 2000), primarily driven by irrigation use, which increased 88%, from 114 m³/s in 2000 to 214 m³/s in 2010 (CBHSF, 2016). The relation between availability and demand is very critical in most of the semi-arid portion of the basin as expressed in Figure 2.5. To limit water use, in 2004, the basin committee set 360 m³/s as the limit for total withdrawal (CBHSF, 2004). However, the projections for the demand in 2025 are estimated in the range of 246-424 m³/s at Middle and 100-225m³/s at Lower-Middle sub-basins. Thus, the availability of water in the basin compared to the demand and its trend denote the urgency in managing the water resource.

Figure 2.5 – Location of the hydropower plants installed at the São Francisco River and the ratio of water demand and water availability in the São Francisco Basin.



Source: ANA (2017).

2.2 Influence of severe drought

In the 2010s, a prolonged and severe drought affected the Brazilian Northeast (ALVALÁ et al., 2017; MARENGO et al., 2017; MARENGO; TORRES; ALVES, 2017) with intense harm for water availability, energy generation, and agriculture at the SFB. Attributed to the effects of El Niño and a warm tropical North Atlantic Ocean influencing the Inter-Tropical Convergence Zone (MARENGO et al., 2017), the annual volume of precipitation was reduced from 646 Gm³ for the average 1981-2010 to 581 Gm³ for the average 2009-2018 (FUNCEME, 2020), the worst drought in 50 years (Figure 2.6 and Figure 2.7). For four years, the volume was registered below 480 Gm³ and classified as very dry in 2012, 2014, 2015, and 2017. The highest volume of precipitation occurred in 2011 at 709 Gm³, 10% higher than the average 1981-2010. For comparison, the years classified as wet exceed the average by 9-20% and very wet by 29-40%. Besides, the precipitation pattern in the two previous decades was already inferior and a very wet volume was only registered in 1992. The sequence of very dry years harmed the ecosystems and water-dependent activities (BRITO et al., 2018). For instance, 1,270 municipalities were listed in an emergency condition in 2016 (ALVALÁ et al., 2017).

Figure 2.6 - Annual volume of precipitation at São Francisco Basin from 1961 to 2018.

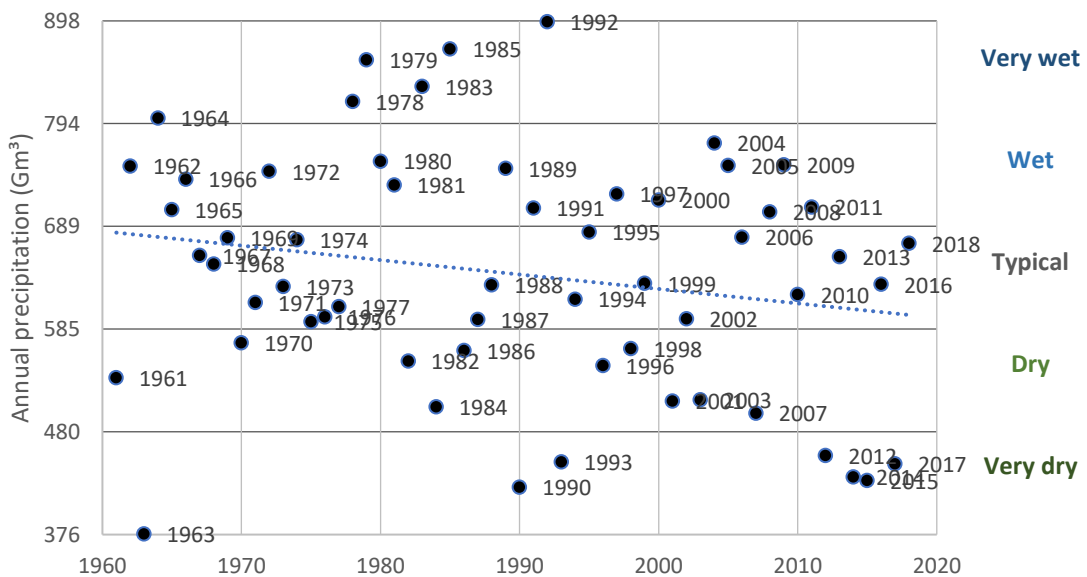
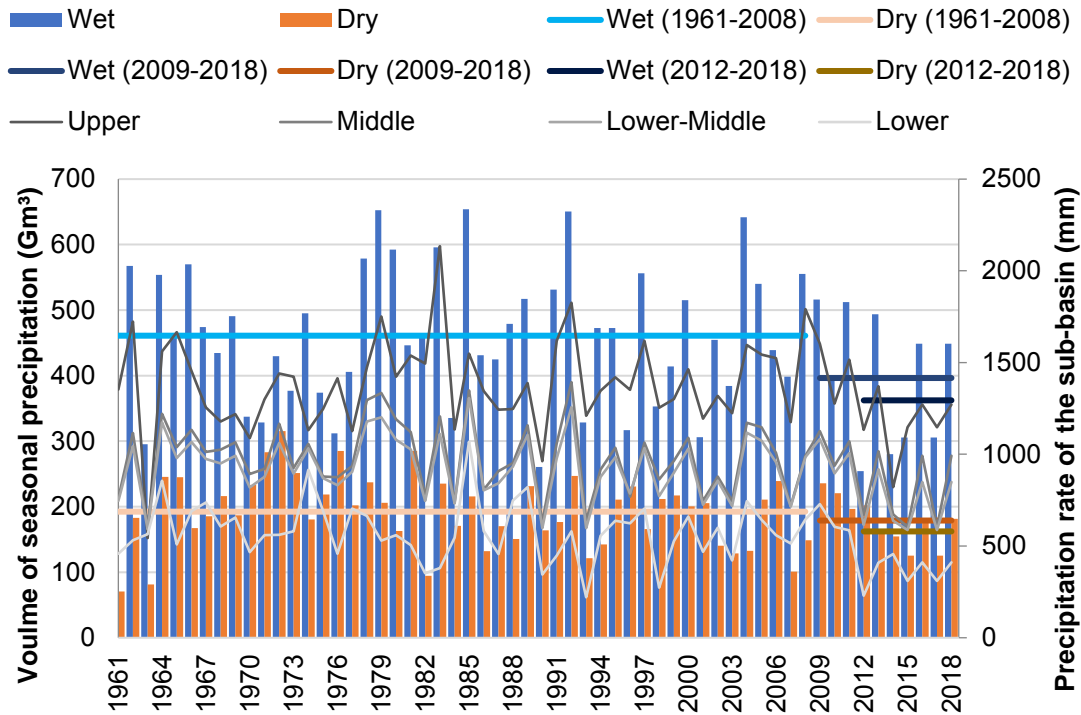


Figure 2.7 - Precipitation at São Francisco Basin: column bars express the seasonal volume of rainfall from 1961 to 2018; horizontal lines express the average values for wet (blue) and dry (orange) season in different periods: 1961-2008 (light color), 2009-2018 (medium-dark color), and 2012-2018 (dark color); the lines with variation express the annual precipitation rate of the four sub-basins (gray colors).



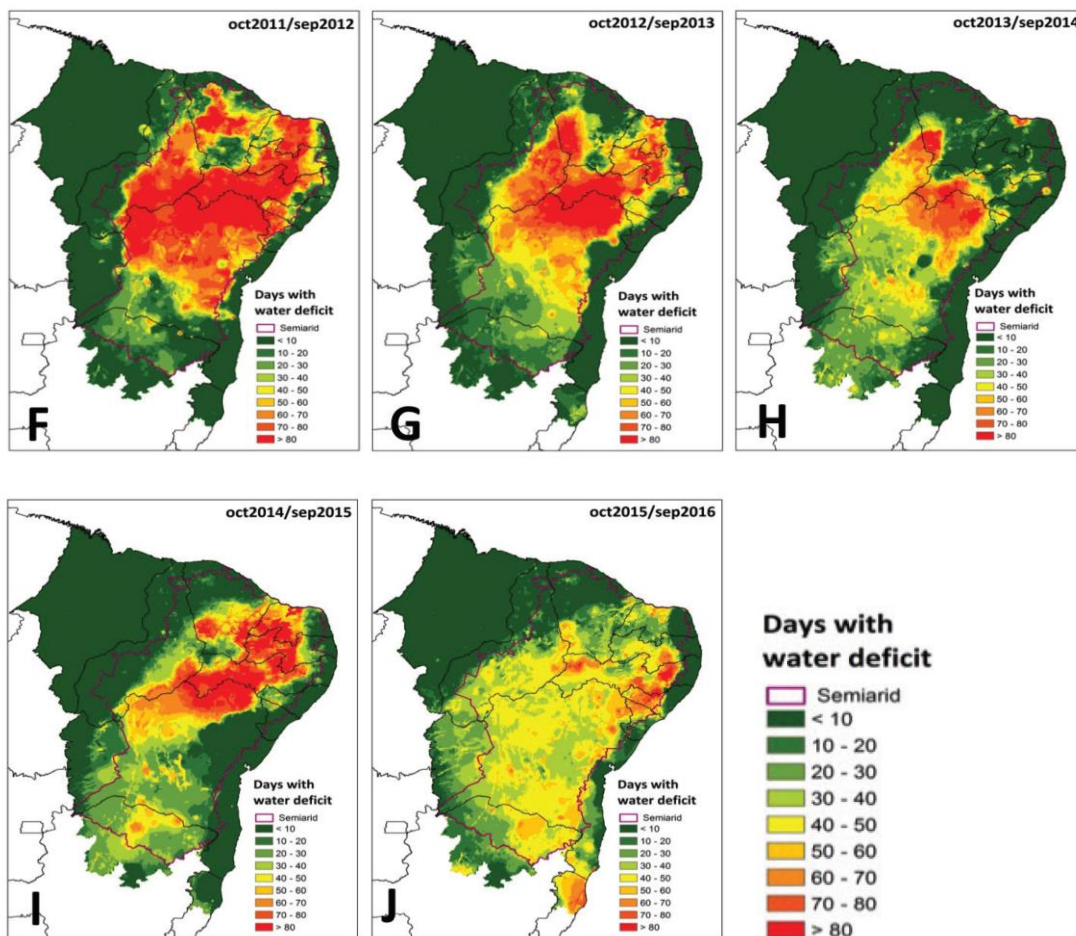
Source: FUNCEME (2020).

MARENGO et al. (2017) identified that the rainfall at the Brazilian Northeast was inferior to typical levels since the middle 1990s based on indicators of drought and meteorological data. **Erro! Fonte de referência não encontrada.** illustrates the frequency of dry days from 2011 to 2016: more than 80 days/year consecutively registered over a significant area of the semi-arid. The author also informed the public spending of more than US\$ 6 billion in adaptation measures to overcome the water shortages in 2012-2015, mostly destined on offering credit to small farmers and bringing water to the region by truck (MARENGO; CUNHA; ALVES, 2016).

Climatological phenomena in global scale, such as the Pacific Decadal Oscillation (PDO) and El Niño Southern Oscillation (ENSO), are mechanisms that can influence the precipitation in some regions of the SFB. SILVA, GALVÍNCIO and NOBREGA (2011) could not indicate evident association between the

phases of ENSO and PDO in the Upper SF as identified in other regions of the Northeastern Brazil. However, a correlation was identified in the Lower-Middle sub-basin, where both positive PDO and ENSO influenced a reduction in precipitation; the opposite effect (increase in precipitation) was verified in negative occurrence for both phenomena. The shift in PDO phase also influenced the values of minimum anomaly for Lower-Middle sub-basin.

Figure 2.8 - Number of days in water deficit in the Brazilian Northeast from 2011-2016.



Source: Marengo et al. (2017).

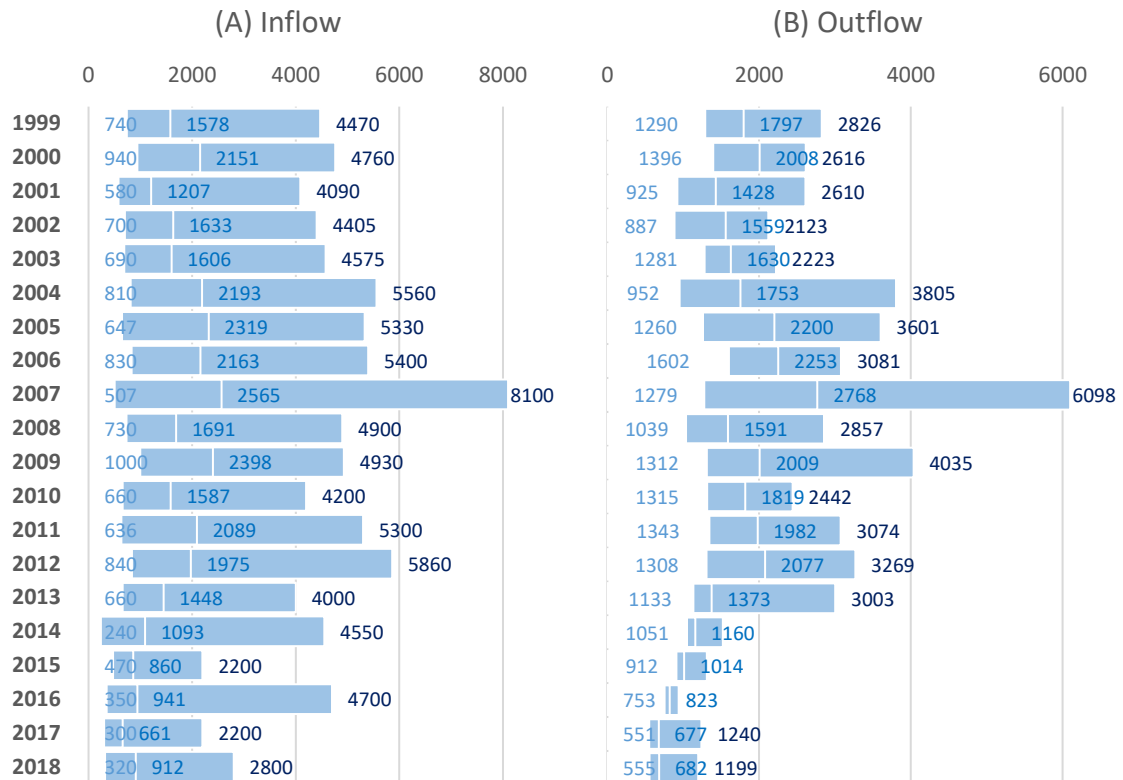
Throughout the severe drought, the streamflow of the SFR was intensively reduced and the operators had to deal with the intense water shortage in the reservoirs. Before the severe drought, the Sobradinho HPP was ruled by an authorized minimum operative outflow of 1,300 m³/s, with the possibility of restriction to 1,100 m³/s in critical climate conditions, under the approval of ANA (ONS, 2011). The sequence of wet seasons with low precipitation occurred

unpredictably and the inflow registered, on average, $<1,100 \text{ m}^3/\text{s}$ in 2014-2018 (ANA, 2019a), decreasing to $661 \text{ m}^3/\text{s}$ in 2017 (Figure 2.9). In the dry season of 2017, the inflow varied in the range of $306\text{-}484 \text{ m}^3/\text{s}$ (ANA, 2019a), or $\sim 15\text{-}24\%$ of the historical average of $2,057 \text{ m}^3/\text{s}$ informed by (ANA, 2020b).

In 2013, the National Water Agency (ANA) created a governance committee composed of regulatory, technical, and environmental bodies to periodically assess the hydrometeorological conditions and the probabilities of precipitation events, to evaluate the basin conditions, and to set the minimum outflow for each reservoir (ANA, 2018b). The governance committee gradually decreased the minimum average outflow at Sobradinho and Xingó to $1,100 \text{ m}^3/\text{s}$ in 2013 (ANA, 2013), $900 \text{ m}^3/\text{s}$ in 2015 (ANA, 2015), $700 \text{ m}^3/\text{s}$ in 2016 (ANA, 2016b), and $550 \text{ m}^3/\text{s}$ in 2017 (ANA, 2017c). As illustrated in Figure 2.9, the outflow at Sobradinho was intensively restricted and presented minor variations starting in 2014. However, at this point, the events of precipitation were not enough to either fill the reservoirs or increase the outflow. In December 2017, the committee also interfered in the demand side by prohibiting irrigation and water withdrawal once a week (River Day), except for human and animal consumption (ANA, 2017d).

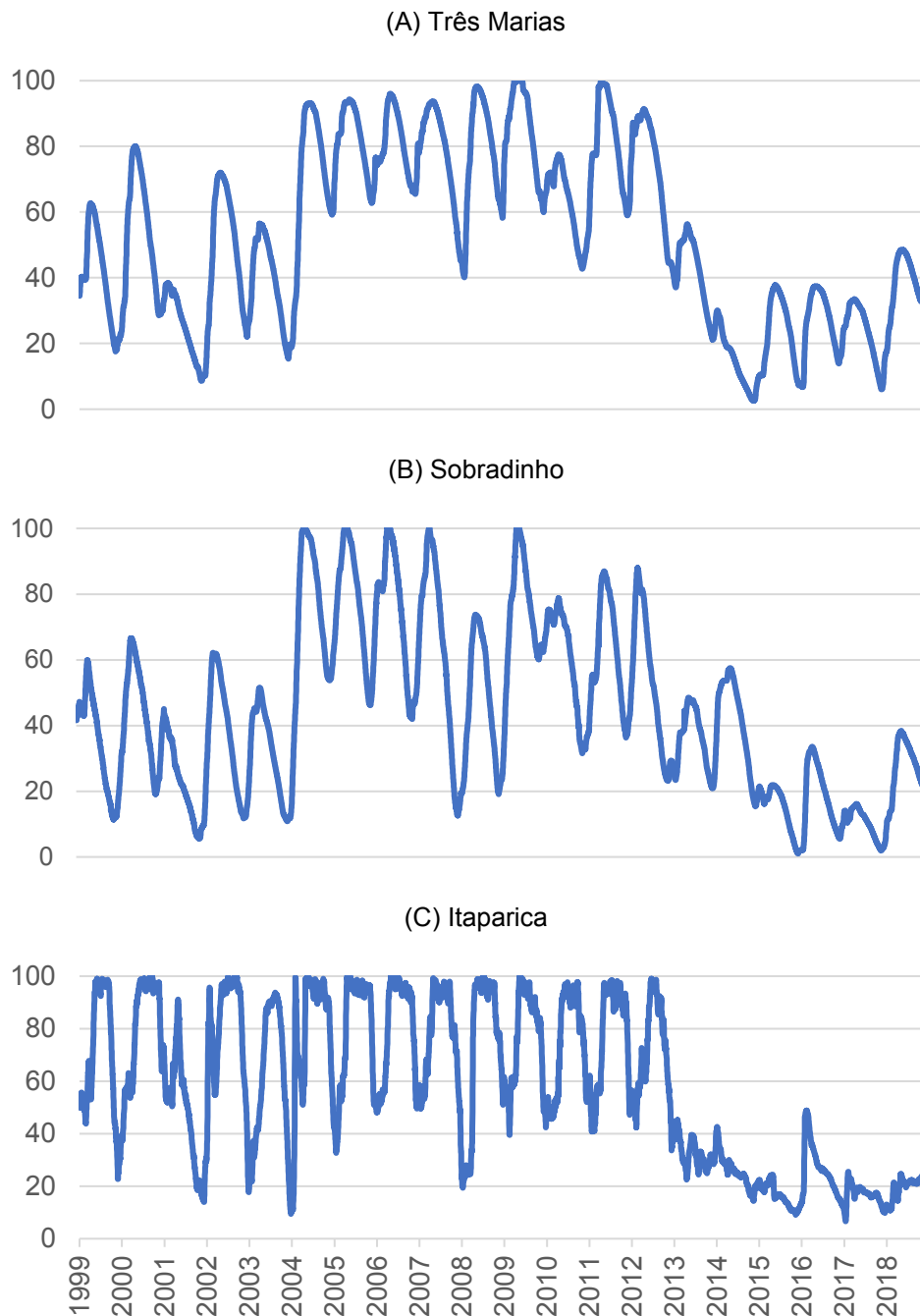
Figure 2.9 also expresses the difference of inflow and outflow of Sobradinho. Generally, the outflow is lower than the inflow to maintain a certain amount of water in the reservoir. This difference is quantified based on the level of water that the operators set to be reached, considering the estimates of seasonal withdrawals and evaporation. Besides, part of the restriction aims to reduce the risks of uncertainties on measuring the actual volume of water inside the reservoir.

Figure 2.9 – (A) Inflow and (B) outflow of the Sobradinho reservoir (m³/s).



The lack of rainfall and the late response of decision-makers – confronted by this unprecedented drought – substantially reduced the water availability in the reservoirs (ONS, 2019a). As illustrated in Figure 2.10, the effective storage at Sobradinho declined below 20% in every dry season from 2014 to 2017, reaching less than 2% in December 2015 and November 2017; Três Marias and Itaparica reached less than 6% and 12%, respectively (ONS, 2019a). Accordingly, power generation and agriculture sectors were significantly affected.

Figure 2.10 – Effective water storage in reservoirs of hydropower plants installed in the São Francisco River from 1999 to 2018: (A) Três Marias, (B) Sobradinho, and (C) Itaparica.

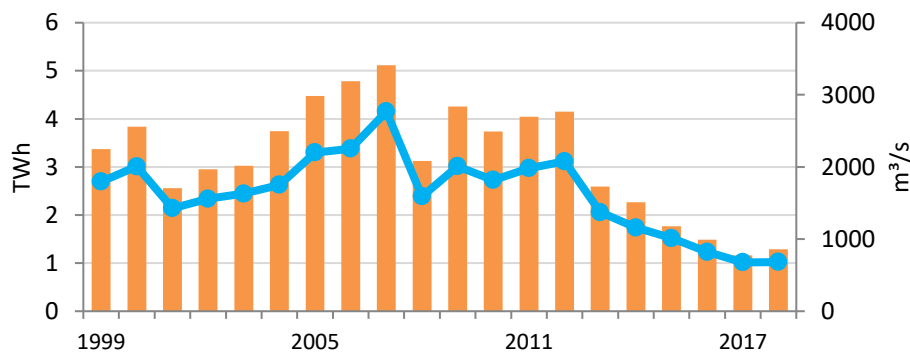


Source: ONS (2019).

On the energy side, hydroelectricity generation was drastically reduced according to the outflow constraint. The electric output of the HPPs installed at SFR declined from 56.5 TWh in 2007 to 14.9 TWh in 2017 (ONS, 2019a), reducing the participation to the SIN from 11.7 to 2.5% (MME/EPE, 2018). Similarly,

Sobradinho HPP declined its generation from 5.11 TWh in 2007 to 1.16 TWh in 2017 (ONS, 2019a), as shown in Figure 2.11. Consequently, the capacity factor dropped from 0.40 in 1999-2008 to 0.29 in 2009-2018 and attained 0.17 in 2014-2018. The shortage of electricity from SFR contributed to a negative impact on the national scale because hydropower source attributes a high share in the Brazilian grid, by 74% of public utility power plants in 2018. The predominance of hydropower turns SIN susceptible to variations in climate conditions (ONS, 2019b). Over these years, the shortage of hydropower had to be overcome using fossil energy in thermal power plants (MME/EPE, 2019).

Figure 2.11 - Hydroelectricity generation (primary axis; orange bars) and average outflow (secondary axis; blue line) at Sobradinho from 1999 to 2018.

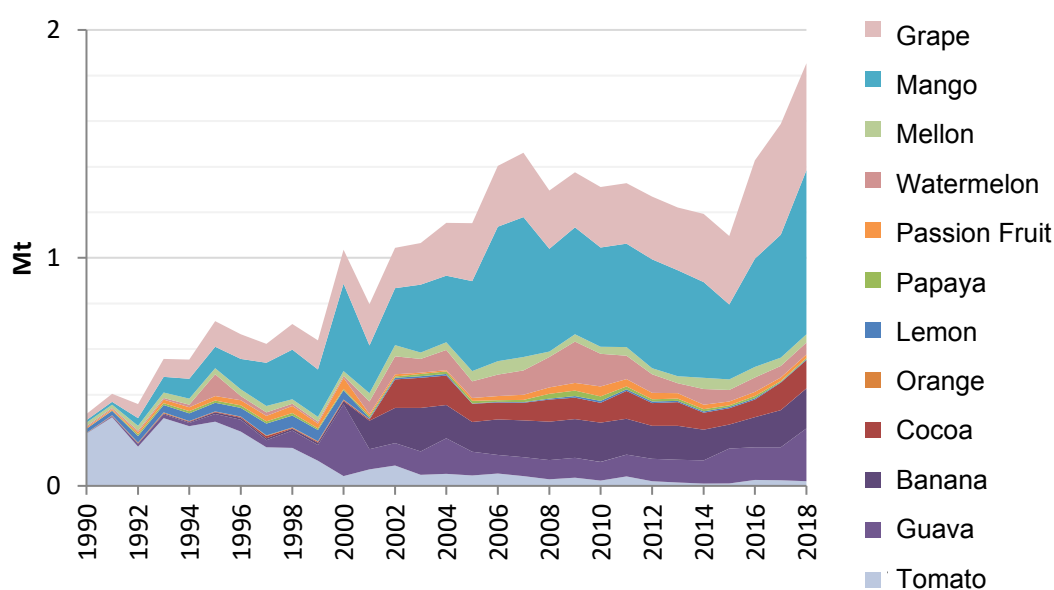


Source: ONS (2019).

Similarly, fruit cultivation was hindered by the water shortages in reservoirs because the crops at semi-arid are dependent on irrigation, especially when it must compensate for the low precipitation (Figure 2.12). The largest fruit producer, Senador Nilo Coelho irrigation district (DINC), directly withdraws water from the Sobradinho reservoir to irrigate 23,486 ha. DINC demanded 78% more water in 2017 (394 Mm³) than in 2011 (221 Mm³), a typical meteorological year (DINC, 2019). Although the water demand of fruit culture was not significant compared to the 28,670 Mm³ effective storage capacity of Sobradinho, in 2017, this annual demand was equivalent to 5% of the average volume in the reservoir.

At this time, the fruit production at the Petrolina microregion⁴, where DINC is located, increased the average production from 0.7 Mt in 2005-2015 to 1.0 Mt in 2017, and 1.28Mt in 2018 (IBGE, 2019). In comparison, the Juazeiro microregion⁵, which is contingent on rainfall and water access from the SFR (harmed by the river level), increased the production over wet years, reaching 0.79Mt in 2007, but declining to 0.36Mt (46%) in 2015 (IBGE, 2019). The diverse responses of Petrolina and Juazeiro microregions (Figure 2.13) can be jointly explained by several factors that reflect productivity: size of the properties, type of cultures, irrigation method, and technological improvements. However, in this period, the opposite change in trends possibly can express the role of the reservoirs. This context revealed the significance of adopting governance and integrated management to balance the multi-purposes and, consequently, guarantee access to water-dependent activities.

Figure 2.12 - Fruit production type of culture at IBGE microregions Petrolina and Juazeiro from 1990 to 2018.

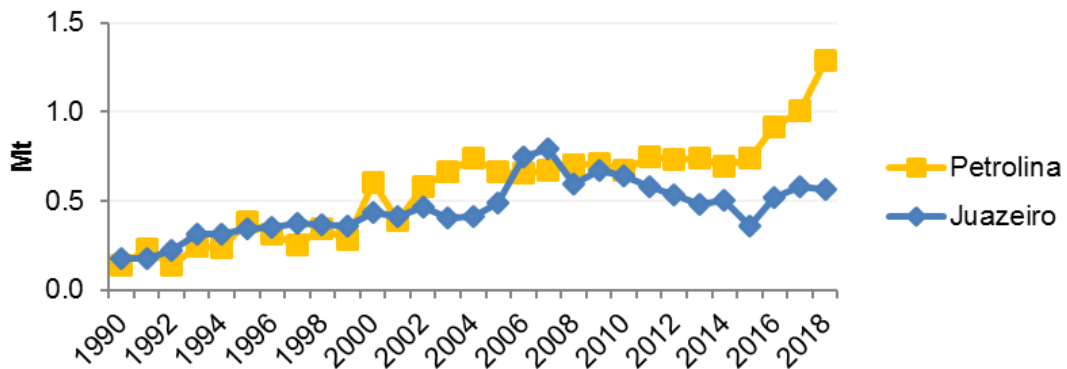


Source: IBGE (2019).

⁴ Municipalities: Afrânio, Cabrobó, Dormentes, Lagoa Grande, Orocó, Petrolina, Santa Maria da Boa Vista, and Terra Nova.

⁵ Municipalities: Campos Alegre de Lourdes, Casa Nova, Curaçá, Juazeiro, Pilão Arcado, Remanso, Sento Sé, and Sobradinho.

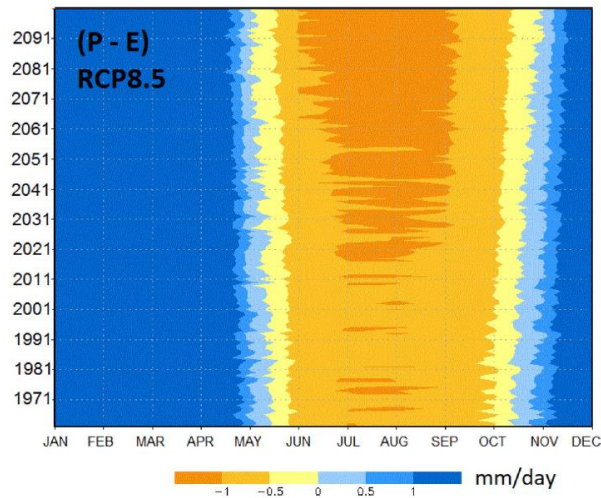
Figure 2.13 - Fruit production of the microregions Petrolina and Juazeiro from 1990 to 2018, in million tons.



Source: IBGE (2019).

Over this century, an increase in temperature, reduction in the volume of precipitation, occurrence of extreme climate events, and long-lasting dry periods are expected for the Brazilian Northeast (MARENGO et al., 2011; MARENGO; TORRES; ALVES, 2017; IPCC, 2018). MARENGO et al. (2012) estimated precipitation reduction in wet season by 3.5 mm/day and annually by 35% by 2100. In another study, MARENGO, TORRES and ALVES (2017) indicated projections of temperature increase between 1 and 5°C - high probability for 4°C (MARENGO et al., 2020). The water deficit during the dry season was predicted to increase in intensity and duration (Figure 2.14), raising the tendency of desertification (MARENGO et al., 2020). Although a reduction in precipitation is predicted to the second part of the wet season (March-May) and dry season at up to 1mm/day, an increase is expected for the first part of the wet season (December – February). The authors estimated an increase in the ensemble mean of multiple climate models from 100 days of consecutive dry conditions in 1901 and projected the occurrence of 140 days in 2100 (MARENGO; TORRES; ALVES, 2017).

Figure 2.14 – Projections in the variation of precipitation minus potential evapotranspiration (mm/day) at Brazilian Northeast from 1970-2100.



Source: Marengo et al. (2020).

Due to the estimated reduction in precipitation and increase in evaporation induced by higher temperatures, the availability of water in the SFR and the energy generation are concomitantly harmed. Besides, land-use change, urbanization, and consumption growth also contribute to the intensification of scarcity and conflicts for the future. Over the next decade, estimates show an increment in consumption by 2.9-5.6% per year for water (ANA, 2016a; CBHSF, 2016) and 3.8% per year for energy (MME/EPE, 2020). Additionally, some studies project critical scenarios for hydrological conditions and energy production in the basin (SCHAEFFER et al., 2012; RIBEIRO NETO et al., 2016; RUFFATO-FERREIRA et al., 2017; DE JONG et al., 2018; MARENGO et al., 2020). These drivers of impact from climate change to the Brazilian semi-arid enhance the role of adopting a Nexus perspective for managing the resources among ecosystem and anthropic activities and investing in alternative energy sources in synergy with hydropower.

3 MATERIALS AND METHODS

3.1 Water-Energy Nexus

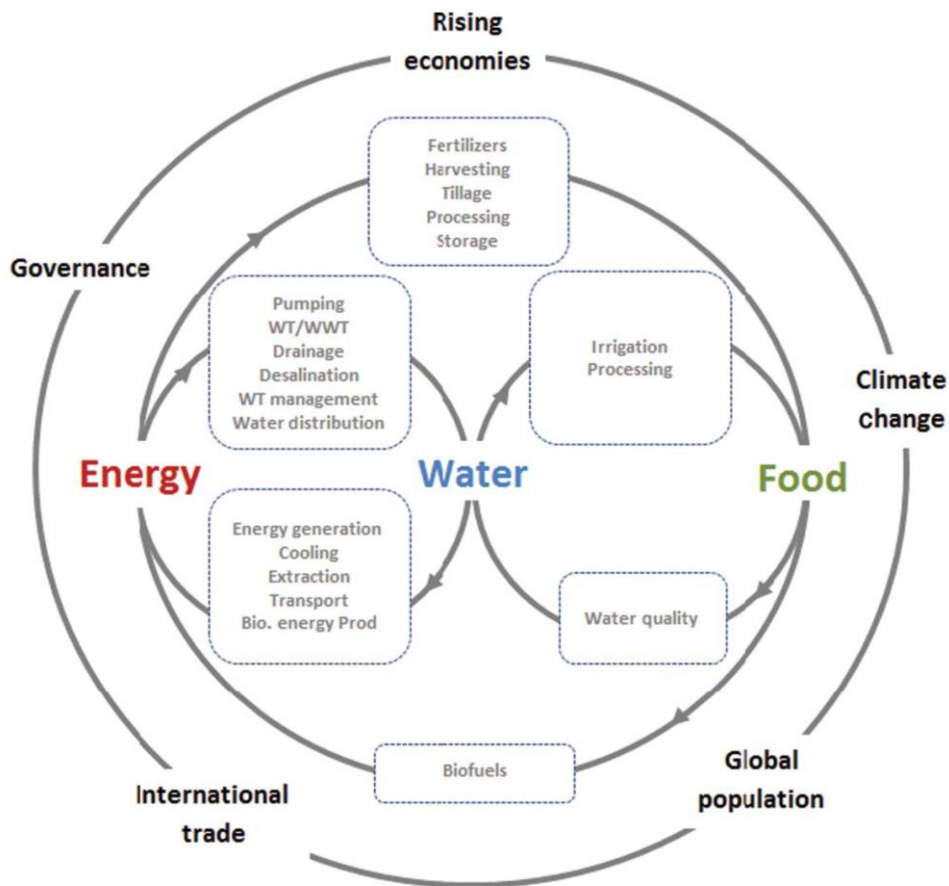
The concept of Nexus was proposed in the context of jointly addressing conservation of the ecosystems, equality in the access of resources, mitigation of climate change, and adaptation of human activities. In environmental sciences, the term was first used in 1983 by the United Nations University, associated with the security in the use of resources (SACHS; SILK, 1990). Recently, Nexus reached relevance in the Bonn Conference 2011, named *Water, Energy, and Food Security Nexus - Solutions for the Green Economy* (HOFF, 2011). Since this meeting, researchers have continuously been working to develop its framework and methodological guidelines.

Conceptually, the coordinated actions towards sustainable development rely on governance capacity, guided by multicriteria assessment (FAO, 2014b). The advances comprehend the definition of the common scientific ground; understanding of the involved systems in human activities; its application on economic sectors; proposal of appropriate indicators, general indexes, and datasets; and the disclose of the results in a transdisciplinary communication that supports governance in creating actions (KURIAN; ARDAKANIAN, 2013; AL-SAIDI; RIBBE, 2017; DARGIN; DAHER; MOHTAR, 2019). The actions for environmental security and ecosystem resilience rely on the assessment of synergies and trade-offs among the systems, which can involve, for instance, water, energy, food, land, or climate. Figure 3.1 illustrates some interactions over water, energy, and food systems.

A consistent proposal towards integrated solutions arises from transdisciplinary knowledge of environmental, social, economic, and political fields (HOFF, 2011; FAO, 2014b; SCOTT; KURIAN; WESCOAT, 2015; TANIGUCHIA et al., 2017; VARIS; KESKINEN; KUMMU, 2017). Methodologically, the appropriate scale and relevant indicators of a study are mainly defined based on the context, diagnosis of critical vulnerabilities, and objectives. The Nexus investigations pursue the overall gains in the dynamics of the systems in several spatial and temporal scales instead of displacing the impacts between systems or achieving the best

performance of separate resources (SCOTT; KURIAN; WESCOAT, 2015; NHAMO et al., 2018). The qualification of appropriate responses will address the objectives in mitigating impacts, being related to processes change, technological update, infrastructure shift, or the introduction of public policies, to be adopted in combination or individually (HAROU et al., 2009; FAO, 2014b; DAHER; MOHTAR, 2015).

Figure 3.1 – Classical schematization of the water-energy-food Nexus.

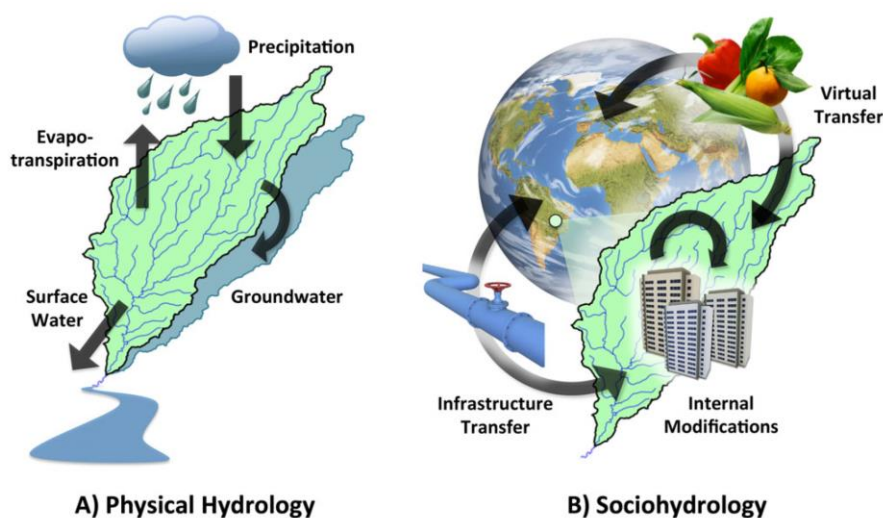


Source: Mohtar and Daher (2012).

An innovative dimension of Nexus is the focus on governance involving multiple sectors (HOFF, 2011; IRENA, 2015; IEA, 2016). The set of information produced in the study has to be oriented to support decision-making by the gather of stakeholders from the scientific community, society, public and economic sectors (FAO, 2014b; SCOTT; KURIAN; WESCOAT, 2015; KURIAN, 2017; SCANLON et al., 2017; RISING, 2020). To meet this goal, the appropriate communication of

the diagnosis and results of the studies is a relevant aspect (Figure 3.2) because uncoordinated decisions can lead to the inefficient use of resources or the adoption of inappropriate strategies in the overall context (HOFF, 2011; IRENA, 2015; IEA, 2016). Accordingly, the capacity to inform the diverse stakeholders on the scientific results (HOWELLS et al., 2013), in an adequate common terminology (BAZILIAN et al., 2011; KURIAN; ARDAKANIAN, 2013; KURIAN, 2017), offers the possibility of identifying synergies and improves the capacity of negotiation. The flow of information among stakeholders, committees, countries, and sectors creates the basis for the design of effective and integrated management programs and policies. For the reason of this conceptual framework, Nexus is considered appropriate for monitoring and advancing the Sustainable Development Goals (FAO, 2014b; BIGGS et al., 2015; SCOTT; KURIAN; WESCOAT, 2015; KURIAN; SUARDI; ARDAKANIAN, 2016).

Figure 3.2 - Conceptual diagrams of different fields of knowledge.



Source: Konar et al. (2016).

Since the São Francisco River presents a territorial concomitance of water scarcity and its essential use for direct consumption, electricity generation, and food production, with asymmetry between availability and demand, the Nexus concept stands as an approach to improve the synergic use of the available resources, taking advantage of the current governance.

3.2 Selected scenarios

The photovoltaic power plant was the designated technology because it responds to relevant issues. Firstly, solar is a renewable source to substitute the use of fossil energy in thermal power plants that feeds the grid during events of water shortages and, consequently, mitigate greenhouse gas emissions. Secondly, the semi-arid portion of the São Francisco basin, where Sobradinho is located, receives high downward surface solar irradiance over the entire year, with potential for photovoltaic production higher than 1,750 kWh/kWp.year (PEREIRA et al., 2017). Thirdly, solar power generation is being promoted by CHESF, the Company of hydroelectricity of São Francisco (CHESF, 2020), and winning a significant share in auctions for the grid expansion with competitive values (MME, 2018; CCEE, 2020a). Fourthly, the installation of PV panels in a floating mechanism is a promising solution because the panels can benefit in production from the cloudiness regime of the lake breeze (GONÇALVES et al., 2020), and in efficiency from the cooling effect of water on the panels surface and local atmosphere (LIU et al., 2017). Alternatively, the floating system can reduce evaporation from the reservoirs by partially covering the lake; and the optimization of solar-hydro complementarity allows to dedicate the water storage for the demand.

We selected converting Sobradinho into a hybrid power plant considering several factors: the relevance of this reservoir for population and economic activities on local and basin scales; the large storage capacity, which allows to conserve more water and assess the consequences of increasing water and energy security; its relative position in the operation of reservoirs in cascade at SFR; and the recent underutilization of this connection to the national electric grid (ONS, 2019a). Besides, a pilot project of 1 MWp FPV is operating at Sobradinho (PLANALTO, 2019a) as part of the Petrolina Solar Energy Reference Center (CHESF, 2018a), which indicates the potential of this solution in this power plant.

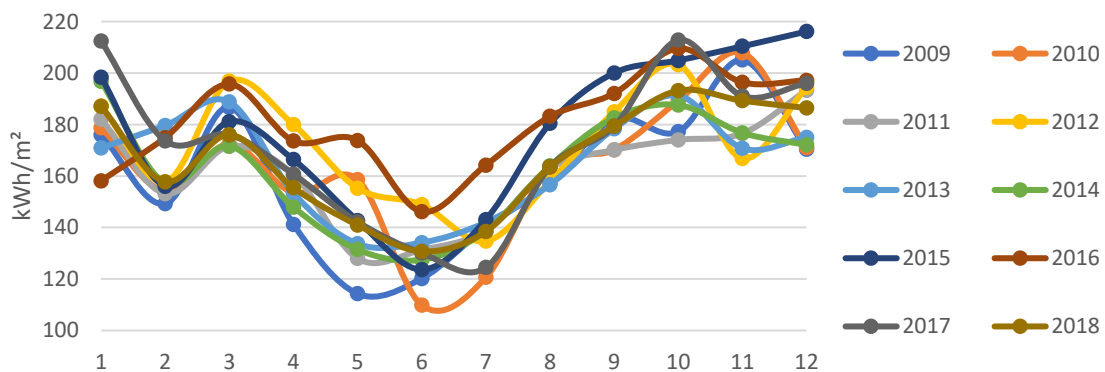
3.2.1 Solar power and solar-water equivalence

To assess the solar power's influence on the allocation of water in the São Francisco River over the severe drought period, we defined a wide range of solar

power scenarios to carry out a sensitivity analysis of the Nexus Water-Energy. We investigated the scenarios of installed PV power capacity at 50, 100, 250, 500, 750, and 1,000 MW. Although the technological solution was selected as the floating PV system, the electricity output was quantified for a ground-mounted system, using characteristics of the polycrystalline silicon cell modules with a panel efficiency of 0.2 currently available in the market (NREL, 2020).

Solar photovoltaic energy is variable, as it depends on the incoming solar radiation at the PV modules, which, in turn, critically depends on the local cloudiness, incidence angle, surface albedo, and operating temperature of the PV modules. The solar electricity output was estimated for the observational ground-measured data of solar irradiation acquired at the BSRN⁶ meteorological station operating at the Petrolina municipality (~70 km from Sobradinho), managed by the SONDA project (PEREIRA et al., 2017; INPE, 2020). The 30-minute global horizontal irradiation (GHI) dataset was converted into monthly averages, resulting in 110-216 kWh/m² for 2009-2018 (Figure 3.3). Data gaps were filled by the average of the specific month. The solar dataset shows a good correlation between high irradiation and years of severe drought, especially for 2015 and 2017. The seasonal complementarity of the energetic sources is expressed in Figure 3.4, showing an increase in solar irradiation concomitant to the low precipitation rate of dry months.

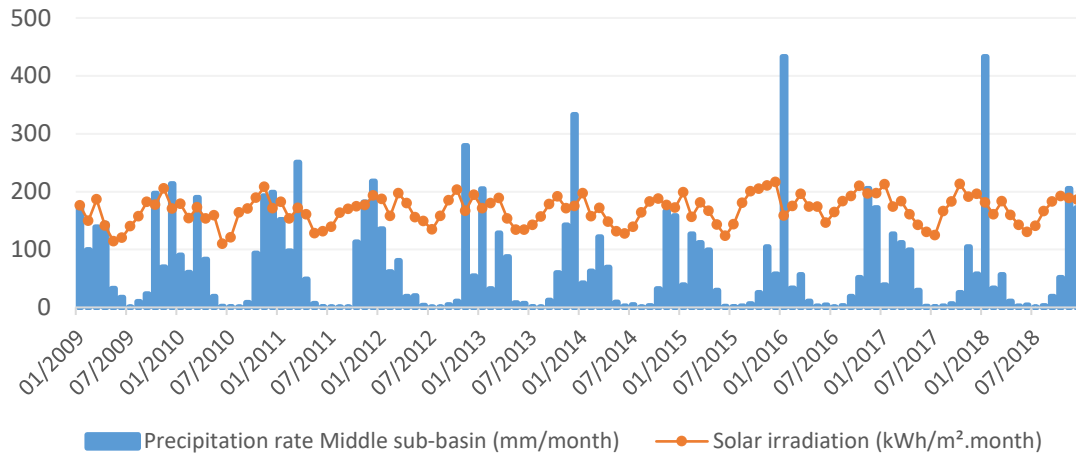
Figure 3.3 - Monthly average irradiation at Petrolina meteorological station (kWh/m²).



Source: INPE (2020).

⁶ World Radiation Monitoring Center (WRMC)/Baseline Surface Radiation Network (BSRN) <https://bsrn.awi.de>

Figure 3.4 – Solar irradiation at Petrolina meteorological station and precipitation rate at Middle sub-basin, on monthly average values.



Source: INPE (2020) and FUNCEME (2020).

The solar irradiation was converted into potential power generation by using Equation 3.1 from LORENZO (2002) for photovoltaic systems connected to the grid:

$$E_{AC} = P \cdot (G_{daeff}/G) \cdot FS \cdot PR \quad (3.1)$$

where

E_{AC} is the electricity produced by the PV system (kWh/month);

P is the nominal power of the PV modules (kWp);

G_{daeff} is the global irradiation that reaches the panel surfaces at the latitude tilted angle (kWh/m².month);

G is the irradiance that determines the nominal power of the modules under standard test conditions (STC), usually 1kW/m² at 25°C;

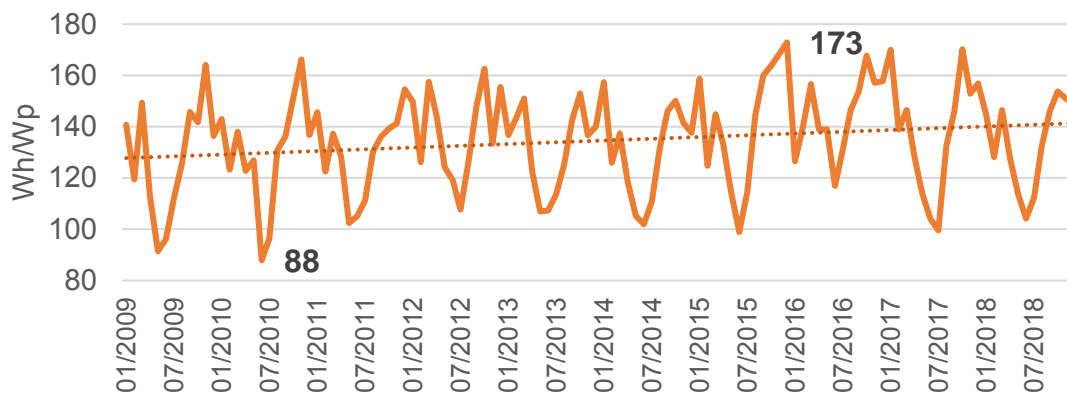
FS is the factor of shading losses due to obstacles (0 for permanently in shadow, and 1 for permanently under light); and

PR is the performance ratio of the PV system, considering optical, thermal, and electrical losses.

In this study, E_{AC} was quantified in monthly time-step. P assumed the solar power range between 50-1,000MW. The monthly average of the solar irradiation observed at the Petrolina station was used for G_{daeff} . For performance ratio (PR), we adopted the 0.8 based on former studies (LIMA; FERREIRA; MORAIS, 2017).

We assumed complete unshaded conditions since the system configuration is for PV panels floating in the reservoir and, therefore, clear of obstacles ($FS = 1$). The potential E_{AC} was estimated in a range of 88-173 Wh/Wp (Figure 3.5). The potential of solar irradiance presented a growing trend, probably explained by the reduction of cloudiness during the days along the study period.

Figure 3.5 - Potential power generation at Petrolina per installed capacity in monthly timestep.



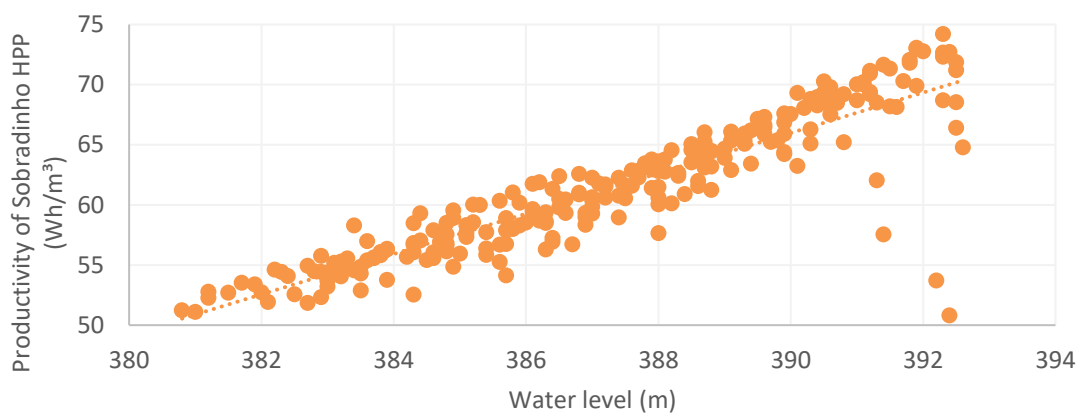
For hydropower simulation, water allocation varied in correlation with the PV installed power capacity. We associated the hydroelectricity output with the turbinated outflow (ONS, 2019a) to estimate the outflow correspondent by the PV operation, which we called saved flow. In a certain condition of water storage, the saved flow required to generate the same quantity of electricity produced by PV was deducted from the historical dataset of Sobradinho (ONS, 2019a), conserving more water in the reservoir.

The saved flow was quantified based on the average productivity factor of the Sobradinho HPP. From 1999 to 2018, Sobradinho generated electricity in a range of 51-74 Wh/m³, on average: 61.4 Wh/m³ (ONS, 2019a). Although the level of the water storage influences the productivity of a hydropower plant (Figure 3.6), as the storage oscillates over the year, it results in some variation for the annual average productivity, as expressed in

Figure 3.7. The dataset for turbinated outflow was only available starting in July 2007; instead, we adopted the dataset for total outflow for the previous period. This assumption resulted in low productivity associated to high levels in some

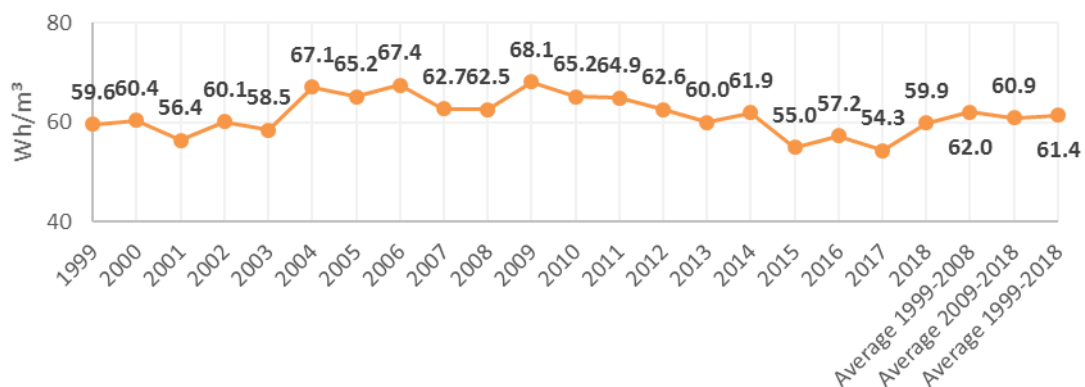
very wet months. The four dots outlying from the linear trend in Figure 3.6 can be explained by this lack of information, which occurred in February and March 2005, January 2006, and March 2007. For the quantification of the saved flow, we adopted the 1999-2018 instead of the 2009-2018 average value to reduce underestimation in productivity. As the FPV increased the storage level, we could achieve higher productivity in the simulated scenarios compared to the values obtained in the severe drought period.

Figure 3.6 - Productivity related to the level of water storage in the Sobradinho reservoir from 1999-2018.



Source: ONS (2019).

Figure 3.7 – Productivity of Sobradinho HPP from 1999-2018.



Source: ONS (2019).

Table 3.1 shows the equivalent water volume and saved flow for each scenario of PV power capacity, which varied from 45 m³/s for the scenario with the

installation of a solar PV of 50 MW to 904 m³/s for the scenario with 1,000 MW, considering 0.2 for panel efficiency.

Table 3.1 - Six scenarios with varying levels of installed power of photovoltaic panels, estimates of annual electricity from the solar source, and the equivalent volume and outflow of water.

Solar intensity scenarios	PV Installed power	Potential annual solar electricity	Equivalence to hydropower ¹	
			Water volume	Outflow (Saved flow)
	MW	MWh	10 ⁶ m ³	m ³ /s
PV-50	50	87,600	1,426	45
PV-100	100	175,200	2,851	90
PV-250	250	438,000	7,129	226
PV-500	500	876,000	14,257	452
PV-750	750	1,314,000	21,386	678
PV-1000	1000	1,752,000	28,515	904

1 - Hydropower productivity at Sobradinho = 61.4 Wh/m³

3.2.2 Operation rules for the reservoirs

In 2017, to avoid future events of reservoir depletion, ANA reviewed the normative of 1,300 m³/s as the minimum operative outflow authorized for Sobradinho (ONS, 2011). The National Water Agency Resolution 2081/2017 (ANA, 2017e) established the outflow values from the reservoirs based on three operational stages - Regular, Attention, and Restriction - classified by the effective storage volume (EV) of Três Marias and Sobradinho. A certain minimum outflow is associated with each operational stage, as expressed in Table 3.2. To create the resolution, several scenarios were analyzed for the critical inflow of 2012-2016 varying three parameters: initial storage in December, outflows of the reservoirs, and effective volume of the operational stages (ONS, 2019c). As projections are not absolute in assuring the climate conditions of the following wet season, the projections of water level embraced a one-year time span (ONS, 2019b). Another relevant aspect to be considered: after a severe meteorological drought, downstream areas face persisting hydrological dry conditions, which usually takes multiple years to recover (VAN OEL et al., 2018). Thus, the

resolution intended to guarantee the water storage above the restriction level at the end of the dry seasons, in November. The rules applied from 2019 onwards.

Table 3.2 - Water Agency Resolution 2081/2017 for the outflow of the reservoirs at São Francisco River related to the effective water storage volume in the reservoir (EV).

Reservoir	Operational stage		
	Regular	Attention	Restriction
Três Marias	EV > 60%	30% < EV < 60%	EV < 30%
Minimum outflow	150 m ³ /s	150 m ³ /s	100 m ³ /s
<i>Maximum outflow</i>	<i>No restriction</i>	<i>To be monthly defined</i>	
Sobradinho	EV > 60%	20% < EV < 60%	EV < 20%
Minimum outflow	Sobradinho 800m ³ /s Xingó 1100 m ³ /s	Both: 800 m ³ /s	Both: 700 m ³ /s
<i>Maximum outflow</i>	<i>No restriction</i>	<i>To be monthly defined Dry period: 1000 m³/s</i>	<i>900 m³/s</i>

Source: ANA (2017).

To make the study adherent to the current operating rules for drought conditions, we combined in the simulated scenarios the historical outflow operation with the Resolution 2081/2017, setting the rules informed in Table 3.3. Some exceptions to the resolution were adopted. For Três Marias, we just set the minimum outflow of 150m³/s, which enabled the allocation of water under the priorities established for the model. For the minimum outflow of Sobradinho in restriction stage, the same limit of alert stage of 800 m³/s was adopted since we intended to avoid low outflows and minimize the most harmful effects that occurred on the ecosystem and water access. For maximum outflow, this rule was substituted by the saved flow instruction aiming to access the positive and negative impacts of the measure.

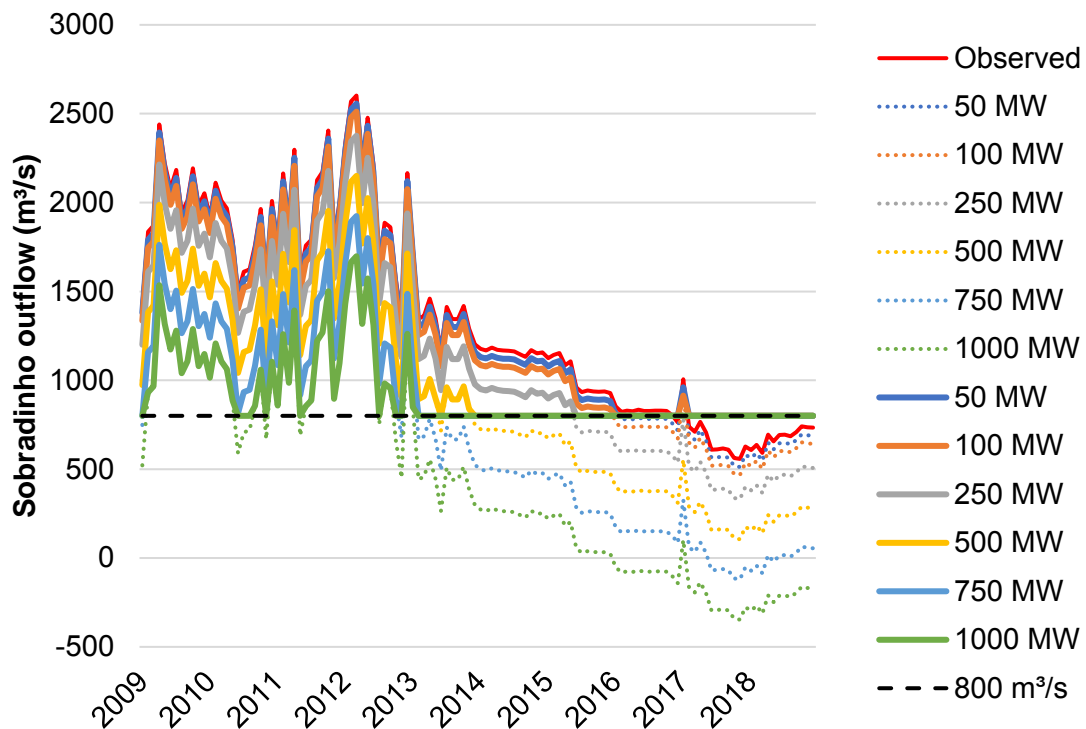
Table 3.3 - Operation rules of water allocation adopted in the simulations.

Reservoir	Operational stage		
	Regular	Attention	Restriction
Três Marias	EV > 60%	30% < EV < 60%	EV < 30%
Minimum outflow	150 m ³ /s		
<i>Maximum outflow</i>	<i>No restriction</i>		
Sobradinho	EV > 60%	20% < EV < 60%	EV < 20%
Minimum outflow at Sobradinho and Xingó	Historical outflow dataset	Historical outflow dataset - saved outflow; limit of 800 m ³ /s	
<i>Maximum outflow</i>	<i>No restriction</i>		

At the alert stage, the saved flow equivalent to generating the electricity added by the PV panels was deducted from the historical dataset respecting the limit of 800m³/s, as illustrated in Figure 3.8. The minimum value was also established to avoid very low streamflow or negative values. These values were applied in the model as the minimum operating outflow for the restriction stage, which means that the simulations could assume higher values when water was available in the system. In addition, the saved flow rule was not applied to the regular stage for one reason: low outflows would not be realistic in high levels of water storage as it leads to the waste of potential electricity when high outflows occurred after filling the reservoir.

The set of the minimum outflow above 800 m³/s mitigates the most harmful impacts of lower streamflow, which reached down 550 m³/s in 2017 (see red line in Figure 3.8), putting into risk water quality, public health, and ecosystem cycles. In the modeling, this adjustment implied a predominance of the rules dividing the study period in two: the first period was directly influenced by the 'saved flow' from PV adding while the second period was ruled by the minimum outflow. It is important to emphasize that the shift of the minimum outflow from 550 m³/s to 800 m³/s was enabled by the PV adding. Every scenario presented an individual extent for each period.

Figure 3.8 – Rules for outflow at Sobradinho at attention stage: quantified for solar scenarios based on saved flow (dashed lines) and adjusted by the minimum outflow of 800 m³/s (solid line).



3.3 Assessment of the scenarios

The scenarios were analyzed in three contexts: water security, water conservancy, and electricity generation. Indicators were quantified regarding water, energy, water-energy, and water-food related to the different components of the SFR system, as described in Table 3.4. The scenarios were considered valid by avoiding water shortage: meeting the demand, conserving water above the minimum operating volume of the reservoirs and sustaining the minimum outflow at Sobradinho and Xingó. The food Nexus was embedded in water security and, therefore, mandatory for the scenario validation. After the validation, indicators were quantified and compared to the observed scenario (modeling of the historical dataset) of 2009-2018.

Table 3.4 – Indicators of assessment of the scenarios.

Indicator	Description	Nexus	Influence	Component	Unit
Water security	Relation of the minimum water volume to the yearly demand	Water, Water-Food	Water storage	Sobradinho	Ratio of the storage to the yearly demand
Solar electricity	PV electricity generated	Energy	Solar radiation	Sobradinho	GWh/month GWh/year
Hydroelectricity	Hydroelectricity generated	Water-Energy	River flow	Sobradinho	GWh/month GWh/year
Capacity factor	Capacity factor of the hybrid power plant	Energy	River flow and PV scale	Sobradinho	Ratio of the transmission line capacity
Electricity output	Total electricity generated (solar + hydro)	Energy	Solar radiation and river flow	Sobradinho SFR HPPs	TWh/year
Water loss by evaporation	Volume of water lost by evaporation from the reservoirs	Water	Water storage	Sobradinho Reservoirs	m ³ /year
Energy loss by evaporation	Potential energy not generated due to water losses by evaporation from the reservoirs	Water-Energy	Water storage	Sobradinho	TWh/year
Energy loss by spilled water	Potential energy lost by outflow higher than the maximum turbinating capacity	Water-Energy	River flow	Sobradinho and HPPs downstream	TWh

3.4 Water and energy system modeling

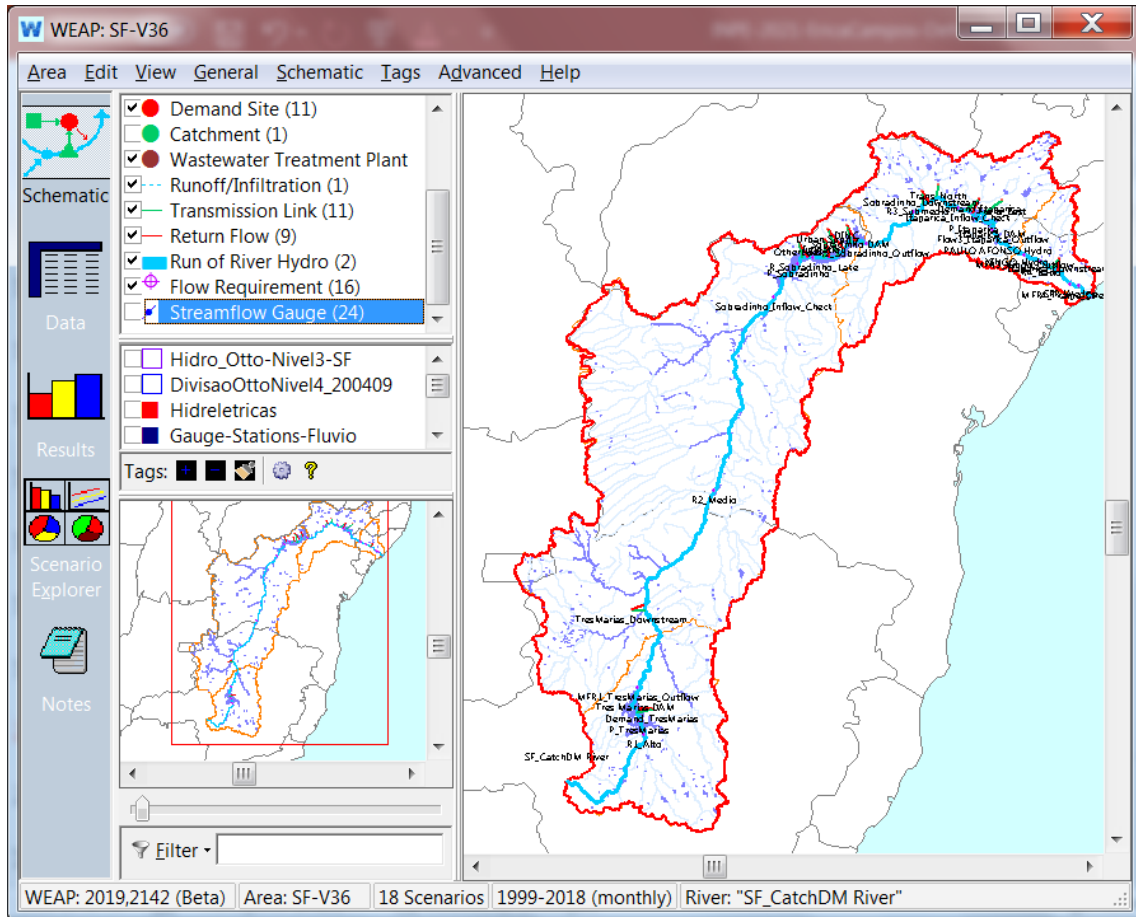
The São Francisco basin water system was modeled using the Water Evaluation and Planning (WEAP) software, version 2019, 2 (SEI, 2015). This integrated platform based on semi-distributed hydrological modeling can incorporate interconnected components such as rivers, reservoirs, HPPs, crops, and multiple demands (YATES et al., 2005). The model configuration can include rules for water allocation among different uses such as agriculture and hydroelectricity.

The program provided the downloading of spatial information on geographic positions, limits of the basin, and the course of the main rivers (Figure 3.9). Hereafter, the elements that made up the model were manually inserted: three HPP with reservoir (Três Marias, Sobradinho, and Itaparica); two run-of-river HPP (PAC and Xingó); the water withdrawals (demand) from the river and reservoirs, and the nodes. Nodes are elements offered by WEAP to input water (reaches) and promote the water allocation among the inserted elements (minimum flow requirements: MFR). The reaches were summed for each sub-basin and the MFRs were inserted next to the reservoirs outflow and at the river mouth. The operation of SFR was designed for the period 1999-2018, and the proposed scenarios were simulated for 2009-2018 as the three reservoirs presented full storage in 2009 (Figure 2.10).

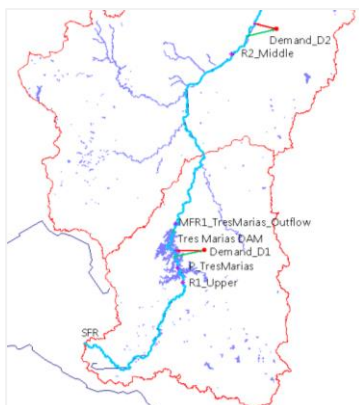
Water allocation and energy generation were designed to reproduce the dataset of the Brazilian governmental agencies ANA and ONS (Brazil's National Grid Operator). We informed data on the physical features of the HPPs and water inputs and outputs from the river and the reservoirs in the study period. The water in the riverbed and the reservoirs fed by the river consists of the available water under management. We did not take into account groundwater because surface water sums 90% of the demand in the basin (CBHSF, 2016).

Figure 3.9 – (A) Schematic interface of WEAP and the elements of modeling São Francisco River at (B) Três Marias region (Upper sub-basin) and (C) Sobradinho and Itaparica region (Lower-Middle and Lower sub-basins).

(A)



(B)



(C)

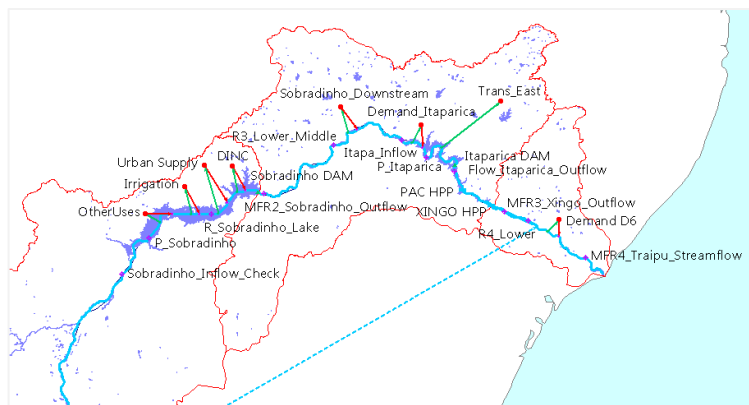
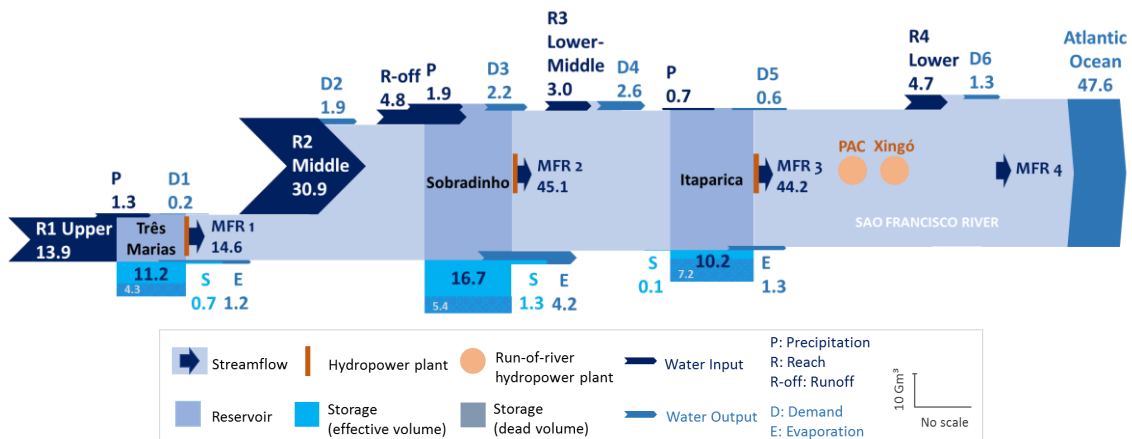


Figure 3.10 illustrates the components of the SFR system and the water flow of inputs and outputs of the water balance with the width of the arrows/flows corresponding to their relative volumes; values in brackets account for the volume

in billion cubic meters for the average of 2009-2018 (y-axis). Water resource was allocated using node elements and a sequence of priority between the components of the model. Four nodes were created to apply the historical dataset and define the minimum flow requirement (MFR) in the simulations: the outflow (ONS, 2019a) of Três Marias (MFR1), Sobradinho (MFR2), and Xingó (MFR3) - located just downstream the HPPs - and the streamflow (ANA, 2019b) at Traipu gauge (MFR4) – located at the river mouth. In the simulations, the MFR nodes were used to set alternative streamflow in these points and consequently modify the water allocation. The priority in delivering water followed the sequence: 1) water demand, 2) minimum flow requirement, 3) storage water at Três Marias, Sobradinho, and Itaparica reservoirs.

Figure 3.10 – Water flow (Sankey diagram) in the components of the San Francisco River model; values in Gm^3 for the average 2009-2018 refer to the y-axis.



3.4.1 Hydropower plants and reservoirs

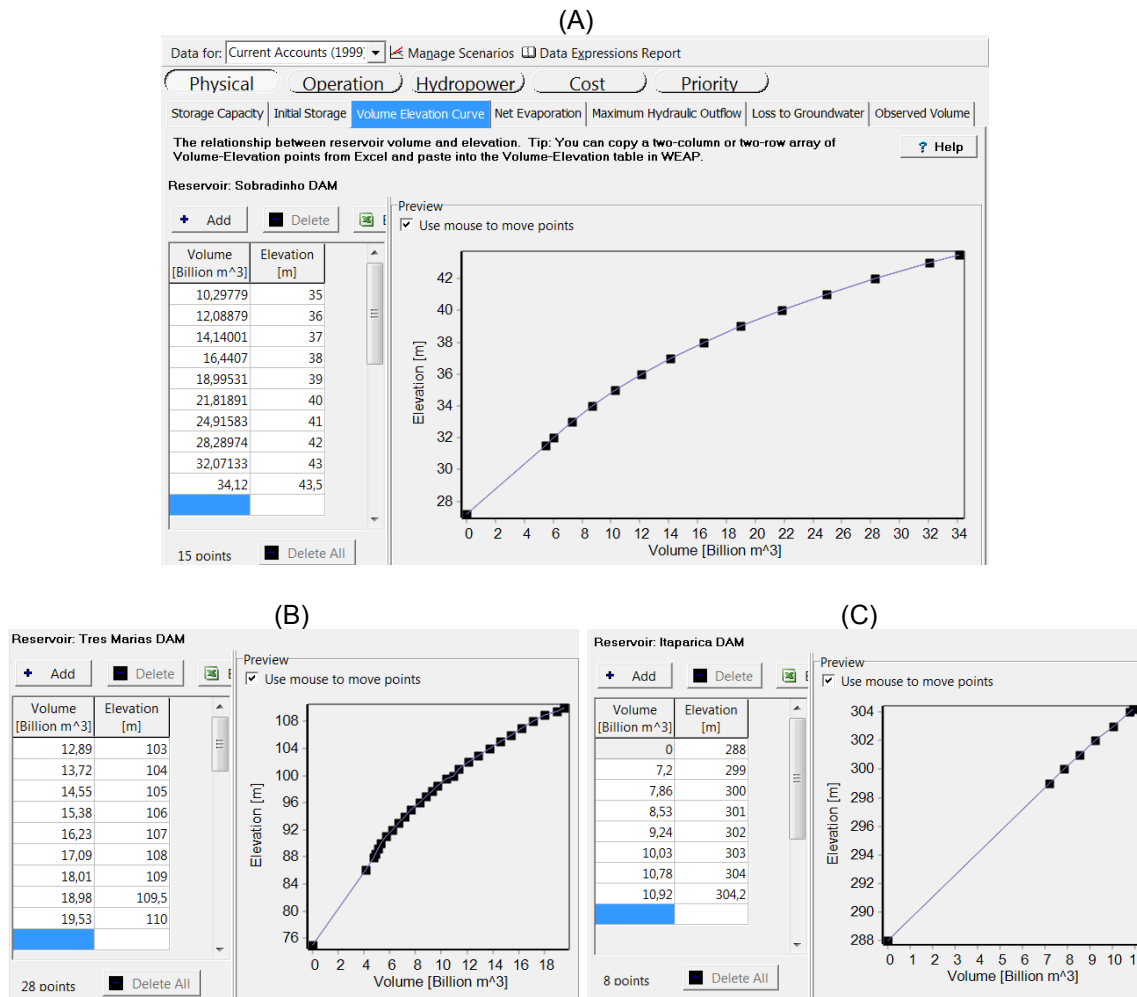
Run-of-river and HPPs with reservoirs were modeled at WEAP. For the reservoir, we informed fixed characteristics (Table 3.5): total storage capacity, effective storage volume, minimum operational volume, volume-elevation curve, maximum hydraulic outflow (ANA, 2020a), maximum turbinated outflow, tailwater elevation, and powerplant efficiency (CHESF, 2018b). For the study period, operational data was included: the water storage for starting the model, defined by the effective volume at 01/01/1999 (ONS, 2019a), and net evaporation (FUNCEME, 2020).

Table 3.5 – Primary information on the hydropower plants and their reservoirs.

Elem.	Characteristics	Unit	Três Marias	Sobradinho	Itaparica	Source
Reservoir	Storage capacity	10 ⁹ m ³	19.53	34.12	10.78	(ANA, 2020a)
	Minimum operating level (Top of inactive)	10 ⁹ m ³	4.25	5.45	7.23	(ANA, 2020a)
	Initial storage (01/01/1999)	10 ⁹ m ³	9.52	18.80	9.14	(ONS, 2019a)
HPP	Maximum turbinating flow	m ³ /s	924	4,260	2,745	(CHESF, 2018b)
	Total turbines	Unit	6	6	6	(CHESF, 2018b)
	Efficiency	%	95	90	92	(CHESF, 2018b)

To quantify hydroelectricity, WEAP combines the water allocation with the inputs of physical information of the reservoirs (Figure 3.11) and characteristics of the power plant (efficiency and maximum turbinating flow). The number of turbines effectively working is not constant and depends on the operational outflow and the maintenance scheme (ONS, 2019d). This implies a variation of the maximum turbinated outflow for the time-steps, whose information was not available. At Sobradinho, each turbine produces electricity using up to 710 m³/s, thus, we adjusted the maximum turbinated outflow for some months by using as reference the turbinated outflow and hydroelectricity output informed by ONS (2019). Besides, Sobradinho has an installed capacity of 1.05 GW (CHESF, 2018b), resulting in a maximum potential output of 9,200 GWh/year, or 767 GWh/month, on average. We assumed this value as the limit for the total dispatches of solar and hydroelectricity into the SIN to take advantage of the existing transmission line capacity already installed at Sobradinho.

Figure 3.11 – Volume-elevation curve of the reservoir (A) Sobradinho, (B) Três Marias and (C) Itaparica (ANA, 2019a).



The run-of-river PAC and Xingó HPPs were included to evaluate the overall impact of the scenarios on the total electricity generated from the SFR. Although we recognize that residual storage may occur upstream of the turbines of a run-of-river HPP, we could not access this information and, therefore, we assumed that the functioning of these power plants did not influence the river flow (SILVÉRIO et al., 2018). These HPPs were added to the model because the water allocation among the reservoirs influences their electric outcomes. Input data for the model was maximum turbine flow and energy efficiency, respectively, 2,310m³/s and 95% at PAC, and 3,000m³/s and 92% at Xingó (CHESF, 2018). Turbines in operation and tailwater elevation were used to adjust the accuracy of the model in the electricity output.

3.4.2 Water input

3.4.2.1 Incremental streamflow

Incremental streamflow expresses the variation of the streamflow between two locations as a result of water inputs and outputs along the river: direct precipitation, runoff, contributing watercourses, withdrawals, evaporation, and transfers with underground water. For the reaches R1-R4⁷ (Figure 3.10), the incremental streamflow was quantified using the inflow and outflow of the three reservoirs (ANA, 2019b; ONS, 2019a) and streamflow of Traipu gauge (ANA, 2019b). Traipu gauge was selected among the gauges located near the river wedge due to its more complete dataset. We assumed for the reaches, respectively, the dataset of Três Marias inflow (R1), the variation from Três Marias outflow to Sobradinho inflow (R2), the variation from Sobradinho outflow to Itaparica inflow (R3), and the variation from Itaparica outflow to Traipu streamflow (R4). To describe the volume of the demand in each section of the river between the reservoirs, this withdrawal was included both as an output and input, included in the corresponding reaches. Water inputs were quantified in cubic meters per second (m³/s) and uploaded in monthly timestep using the 'read from file' tool of WEAP.

Water inputs from the sub-basins associated with Upper (R1) and Middle (R2) contributed to the SFR streamflow more intensely than Lower-Middle (R3) and Lower (R4) because the precipitation rate was higher, as well as the contribution area is larger. Lower-Middle and Lower sub-basins are inserted in semi-arid areas, susceptible to frequent water deficits and more intense rates of water abstractions, transmission losses of the riverbed, and recharge of aquifers that lead to negative variations of the streamflow. Thus, R3 and R4 resulted in negligible or negative values in most of the months. To quantify the water entering the model in months that downstream measurements presented smaller values than the upstream measurements, the negative results were balanced within previous or consecutive months with positive values. For R3, the annual dry

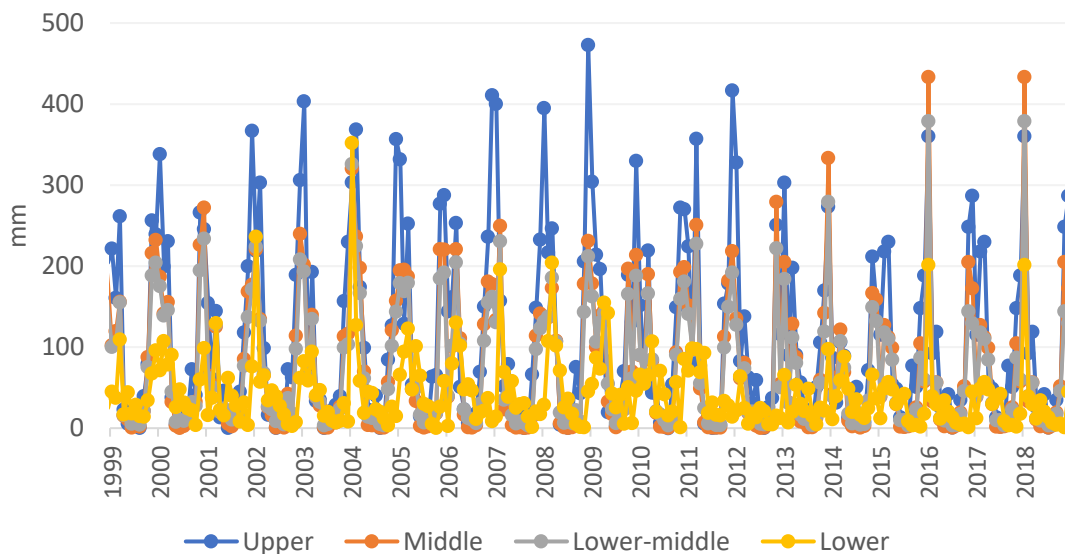
⁷ R1, R2, R3, and R4 corresponds to the four sub-basins of the SFB, as shown in the schematic of Figure 3.10.

seasons and the recent dry years resulted in long sequences of negative numbers. To balance the negative values, we adopted the average result of the dataset for two periods, 1999-2002 and 2003-2018. For R4, we balanced the negative numbers by quantifying an average for the years 2001-2009.

3.4.2.2 Precipitation in the reservoirs

The precipitation in the reservoirs was quantified by multiplying the area of the lake (ANA, 2020a) by the monthly precipitation rate of the sub-basins the reservoirs are located (FUNCEME, 2020). Upper, Middle, and Lower-Middle precipitation rates (Figure 3.12) were adopted for Três Marias, Sobradinho, and Itaparica, respectively.

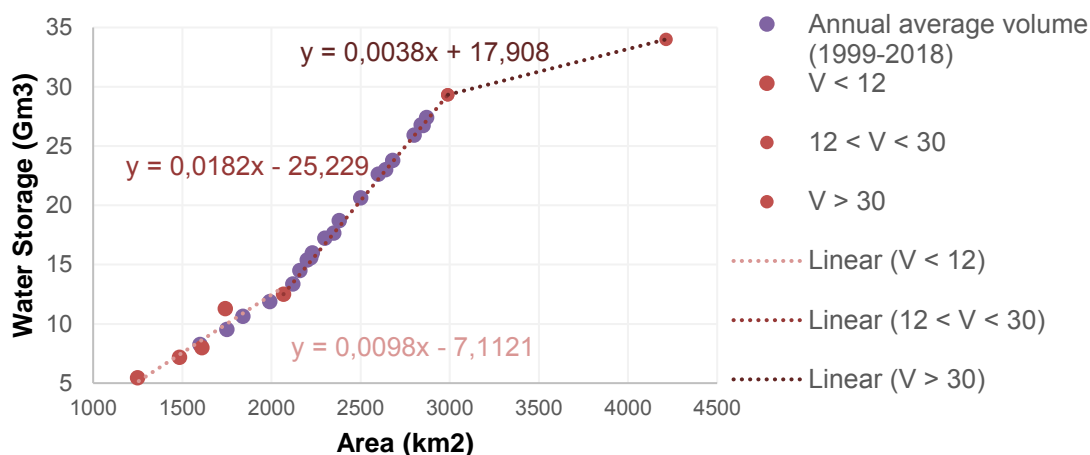
Figure 3.12 – Monthly precipitation rate at the São Francisco sub-basins Upper, Middle, Lower-middle, and Lower.



The maximum flooded area was admitted for Três Marias (1,040 km²) and Itaparica (828 km²). For Sobradinho, we estimated the area from the volume of water in the reservoir by using literature data (AZEVEDO et al., 2018). Based on remote sensing images, the authors measured the area occupied by the Sobradinho reservoir in June (wet month) of 2011, 2015, and 2016, and in October (dry month) of 2015 and 2016. We associated the reservoir's area provided by the authors with the average volume of water stored in the reservoir in the same months (ONS, 2019a). Using this data, we set three linear trends

related to the volume: 1) $V < 12 \text{ Gm}^3$; 2) $12 < V < 30 \text{ Gm}^3$; and 3) $V > 30 \text{ Gm}^3$. Figure 3.13 shows the data used to plot the linear trends (red dots) and the estimative of area for the annual average of water storage (purple dots). To quantify the average water surface area of the Sobradinho reservoir in monthly timestep, we identified the range in which the storage volume was inserted and applied the specific equation of linear correlation; the three equations are expressed in Figure 3.13. Subsequently, to quantify the direct precipitation on the water surface of the Sobradinho reservoir, the estimated surface area was multiplied by the monthly precipitation rate at the associated sub-basin (FUNCEME, 2020).

Figure 3.13 – Correlation of the volume of water at the Sobradinho reservoir and the area of the lake.

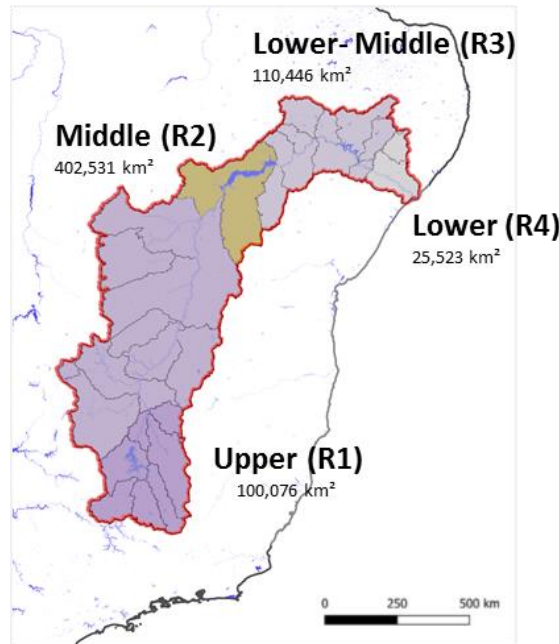


3.4.2.3 Runoff at the Sobradinho reservoir

We quantified the runoff into Sobradinho from the area between the inflow (*Morpará* and *Boqueirão* gauges) and the location of the HPP outflow measurement (~350 km). We estimated the monthly contributing area of both sides of the SF river (SIGEO, 2011), as illustrated in Figure 3.14, taking into account the variation of the Sobradinho lake. The monthly area was multiplied by the monthly precipitation rate of the Middle sub-basin (FUNCEME, 2020) and the runoff coefficient of 8% (MMA, 2006). The total area is estimated to be 69,518 km² with 33,398 km² on the west side and 36,120 km² on the east side. The runoff into the other reservoirs was considered through the physical aspects of the inflow measurement of Três Marias, which includes the input from main

contributors around the boundaries of the reservoir; and the low precipitation rates and runoff coefficient of Itaparica, which were estimated into the incremental streamflow input.

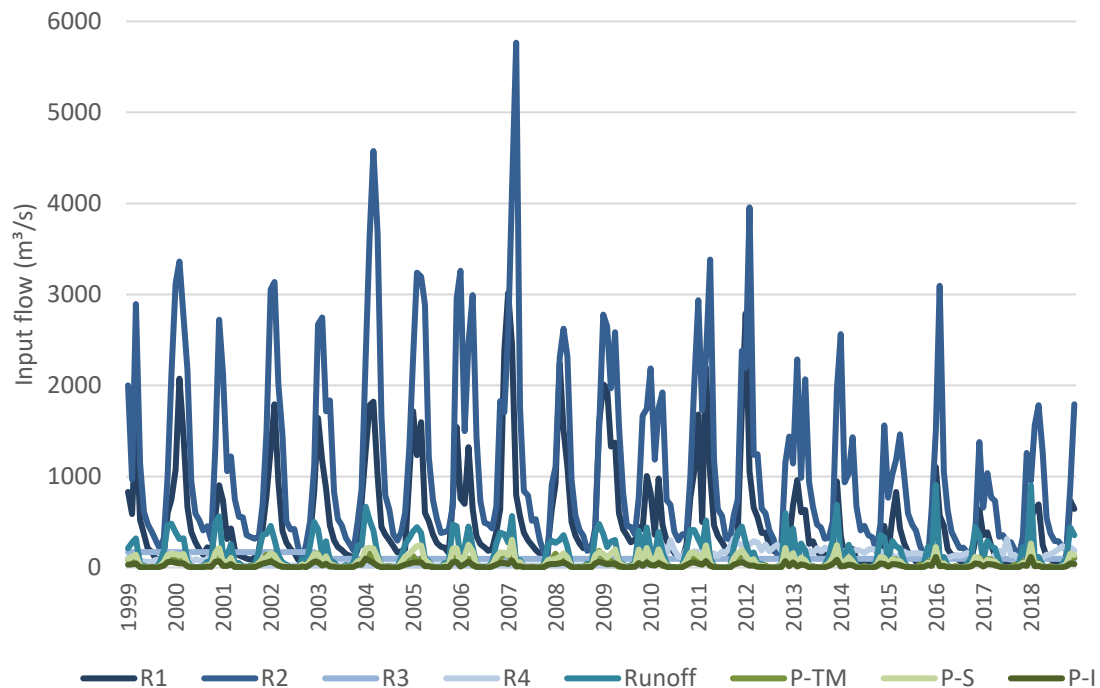
Figure 3.14 – Sub-catchment in the São Francisco reservoir with the contributing area of local runoff to the Sobradinho reservoir (in yellow).



3.4.2.4 Total water input

The input at R2 accounted for the main adding of water in the model (53%, on average for 1999-2018), followed by R1 (25%), local runoff at Sobradinho (7%), R3 (5%), R4 (4%), and the precipitation at Sobradinho (3%), Três Marias (2%), and Itaparica (1%). The monthly inputs are illustrated in Figure 3.15. The precipitation rate is higher at the Upper sub-basin, but the contributing area of the Middle sub-basin makes this region more significant to the water input and, in practice, to the availability of water to downstream sub-basins, which are located in the semi-arid portion of the SFB. The total water input presents a decreasing trend over the study period (dashed line).

Figure 3.15 – Water input (m³/s) in reaches: R1, R2, R3, and R4, local runoff at Sobradinho, precipitation (P) on the three reservoirs, and the linear trend of total input from 1999 to 2018.



3.4.3 Water output

3.4.3.1 Demand

For the demand, we adopted the dataset for ANA’s authorizations of water withdrawal since the São Francisco River is under federal administration. The authorizations can be interpreted as the government's commitment to delivering a certain volume of water to the users, which can be associated with water security. The database is available in GIS format (ANA, 2020c), and includes information on localization, user, volume, data of emission, and validity of the authorization.

The dataset was classified by location – withdrawals from the three reservoirs and SFR - and active authorizations on each year of the 1999-2018 period using the date of emission and validity. The classified authorizations were separated in six different groups: reservoirs and sections of the SFR between the reservoirs: Três Marias (Figure 3.10 – D1), Sobradinho (D3), Itaparica (D5), and the river

downstream of each reservoir (D2, D4, D6). The water demand associated for the six groups was quantified summing the annual volume authorized in each classified declaration.

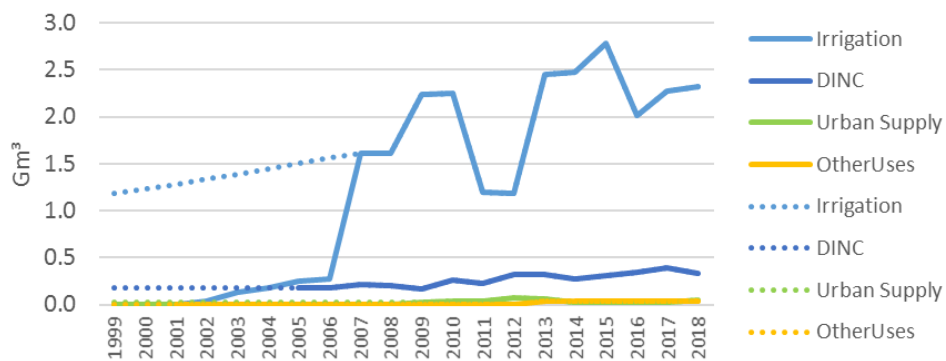
The authorizations for Sobradinho were also classified in urban supply (aggregates public supply and human consumption), Nilo Coelho irrigation district (DINC), irrigation (except DINC), and other uses (aquaculture, livestock, industry, mining, construction, and thermal energy). DINC was specified as this consumer presents 97.5% of the productive area dedicated to fruits (DINC, 2019). An additional demand was ascribed to the Itaparica reservoir: the East Transposition of the SF river (ANA, 2020d), which infers an additional driver of water scarcity. The use of water to produce hydroelectricity at the Brazilian HPPs appears in the database with zero consumption.

The official dataset seems to present some uncertainties. The annual data varied widely throughout the study period, as illustrated in Figure 3.16. This variation is likely related to administrative and practical reasons. First, the authorization started to be organized and delivered in 2001, so there is a lack of information for the years 1999 and 2000. Second, the volume of water increased at a low rate during the first years, but from 2006-2007 onwards it presented high values. Accordingly, the 2007 values probably express a more reliable volume of water being extracted in the preceding period. Third, the authorized volume declined five years later but increased again to the trend level within two years. This oscillation might represent that users registered for an overestimated volume in their first registration; or some five-year permissions got invalid and the users did not immediately renew them - probably as an effect of previous wetter years; or administrative delays concerning database management. The same oscillation occurred five years later, when the authorized volume declined again, possibly due to one of the reasons previously mentioned. Another uncertainty is about its accuracy regarding the authorized volume and effective withdrawals. The authorized volume may not always correspond to the real volume of water that is taken from the watercourse or reservoir. If the user's request for permission does not correspond to the actual water need, it can imply an overestimation. For 2018, the volume of water informed by the consumers related to their effective

consumption (auto-declaration) corresponded to 80% of the authorized volume (ANA, 2019c). The opposite can also happen, and some users may consume more than previously expected when applying for permission. Several penalties in 2018 were associated with disrespect to the authorized volume (29%) or water withdrawals without permission (24%) (ANA, 2019c). In this study, we assumed that factors of under- and overestimation may compensate for each other.

From the primary dataset, we adjusted the values of the first years of the simulation. Figure 3.16 shows the primary data (solid line) and the adjusted values adopted in the study (dashed line). For the main consuming sector, irrigation, the database values from 2007 to 2018 were directly used in the model; for 1999, we adopted the minimum value of the time series (1.19 Mm³ in 2012); while for 2000-2006, we assumed an annual growth rate of 4% to reach the 2007 value. For urban supply, data was available from 2009-2018; we assumed the value of 2009 for 1999-2008. DINC discloses the total withdrawal per year since 2005; this first annual data was repeated from 1999-2004.

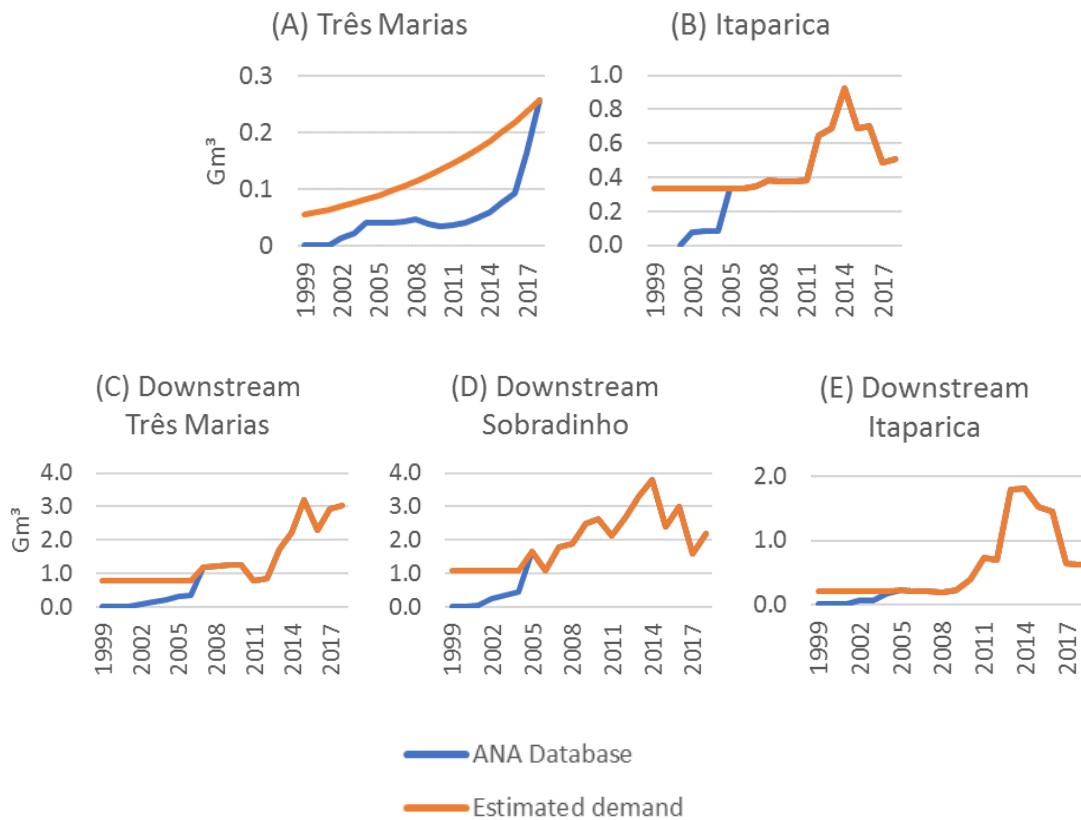
Figure 3.16 – Volume of water of authorized withdrawal from Sobradinho Reservoir for 2001-2018. Primary data by (ANA, 2020c) in solid line; adjusted data incorporated to the model, per user, in dashed line.



The same procedure was adopted to estimate the withdrawals from Três Marias, Itaparica, and SFR sections for the entire period. For Três Marias, data were available for 2002-2018. The average demand was admitted to 1999, and an increasing rate of 8.5% per year was applied to reach the 2018 consumption (Figure 3.17A). For Itaparica, we admitted the primary data for 2005-2018, and the 2005 data as a constant value from 1999-2004 (Figure 3.17B). For the

withdrawals located downstream of each reservoir, in 1999-2006 we assumed the lowest value in the time series, and in 2007-2018 we adopted annual values of the database (Figure 3.17C, D, and E). For 2018 data, the total demand of the SF river (10.2 Gm³) was equivalent to around 20% of the effective water storage at the three reservoirs (47.5 Gm³).

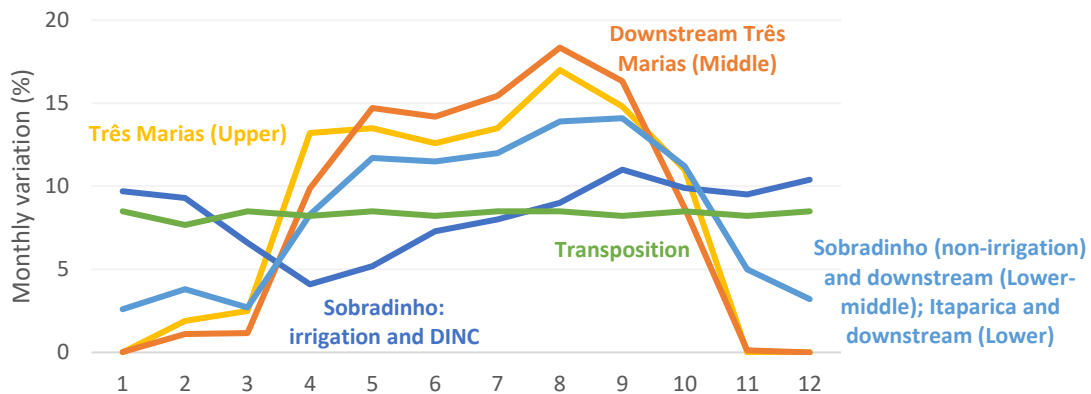
Figure 3.17 – Water demand from the reservoirs Três Marias (A) and Itaparica (B); and from the São Francisco River section downstream Três Marias (C), downstream Sobradinho (D), and downstream Itaparica (E).



The Transposition of the São Francisco River project (ANA, 2020d, 2020e) plans the transfer of water from SFR to its neighboring river basins. Two channels were constructed downstream of Sobradinho to deliver water to the rivers Paraíba do Norte (Transposition East), Jaguaribe, and Piranhas (Transposition North) by the maximum authorized withdrawal of 28 and 99 m³/s (ANA, 2005), respectively. Currently, the testing flow varies around 10.0 and 16.4 m³/s, respectively. Transposition East was the only one that started operating during the study period (March 2017) and was included in the model.

To simulate the seasonality of the demand in dry and wet months (Figure 3.18), we adopted the monthly estimates provided by CBHSF for each sub-basin (CBHSF, 2016), except for DINC and irrigation from Sobradinho reservoir, for which we applied the variation in monthly withdrawal informed by DINC (2019).

Figure 3.18 – Monthly variation of the water consumption from reservoirs and SFR sections.



Source: DINC (2019) and CBHSF (2016).

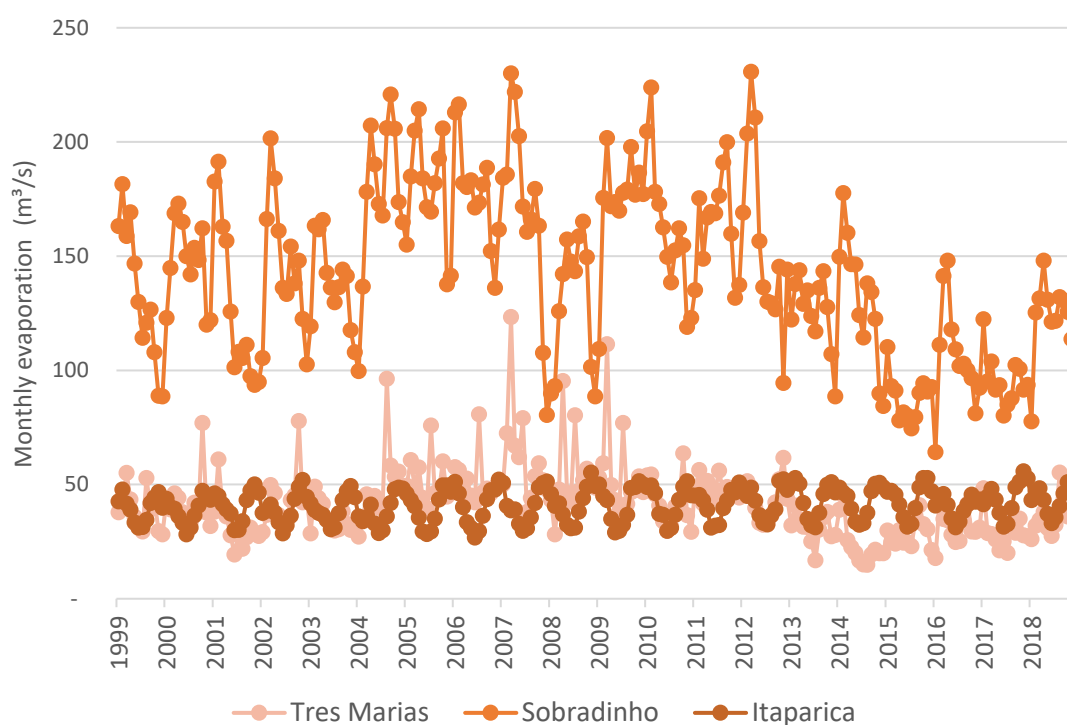
3.4.3.2 Evaporation

WEAP simulates losses of water by evaporation from the reservoirs using a monthly timestep as a function of water storage (and the related reservoir surface area) and evaporation rate. The reservoir surface area is quantified by the software using the volume-elevation curve (ONS, 2019a) and the evaporation rate was informed using the monthly average dataset provided by FUNCEME (2020) for Três Marias, Sobradinho, and Itaparica (Figure 3.12).

The monthly evaporation flow, illustrated in Figure 3.19, resulted in 147 m³/s from the Sobradinho reservoir on the 1999-2018 average. For comparison, we also collected literature data regarding the evaporation from this reservoir. ANA estimated that 110 m³/s are lost from the Sobradinho reservoir, which just considers the flooded areas and neglects the riverbed (ANA, 2017a). PEREIRA et al. (2009) estimated the evaporation of 132 m³/s on average, depending on the methodology: 155 m³/s (Linacre, 1993, based on Penman-Monteith), 140 m³/s (ECA C=0.6), 130 m³/s (Kohler et al., 1955, based on Penman-Monteith) and 120 m³/s (CRLE). VIEIRA et al. (2016) estimated the annual evaporation from

101 m³/s (ECA C=0.4) to 205 m³/s (ECA C=0.8), based on eight quantification methodologies and the average reservoir area of 2,400 km²; if the maximum area was assumed, it would reach 360 m³/s. A recent study estimated the Sobradinho evaporation to be 203 m³/s, using the Penman method (VIEIRA et al., 2018). The higher estimation found in the literature for Sobradinho reached 380 m³/s (MEKONNEN; HOEKSTRA, 2011).

Figure 3.19 – Monthly evaporation rates on Três Marias, Sobradinho, and Itaparica reservoirs from 1999 to 2018, based on the evaporation rate dataset of Funceme (2020).

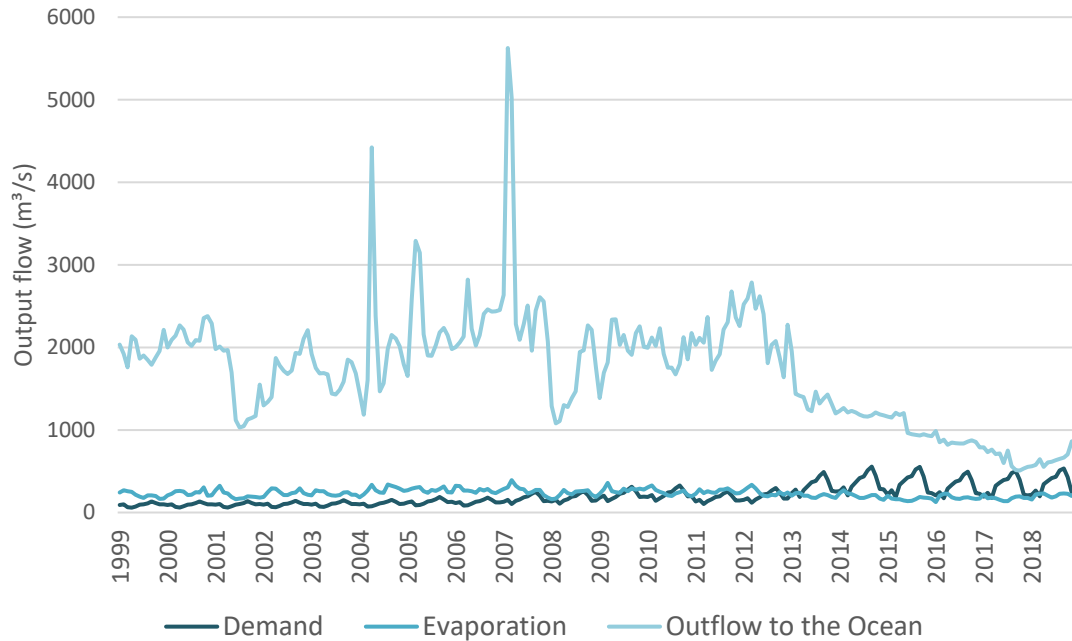


3.4.3.3 Total water output

The outflow to the Atlantic Ocean stands for the main water output of the SFR. On average 1999-2018, 91% of the water followed the natural cycle by being incorporated into the ocean (80%) or the atmosphere by evaporation (11%); the anthropic withdrawal of water sums 9% of the outputs. Figure 3.20 illustrates the outputs expressing the variations of available water, the patterns in the demand, the role of storage in the reservoirs. From 1999-2008, the demand accounted in the range of 2-11% of the output, while the relative participation increased in 2009-2018, reaching 40% in the dry season of 2017. At this period, the

governance committee set the minimum outflow of Sobradinho at 550 m³/s and the reservoirs reached their lowest levels.

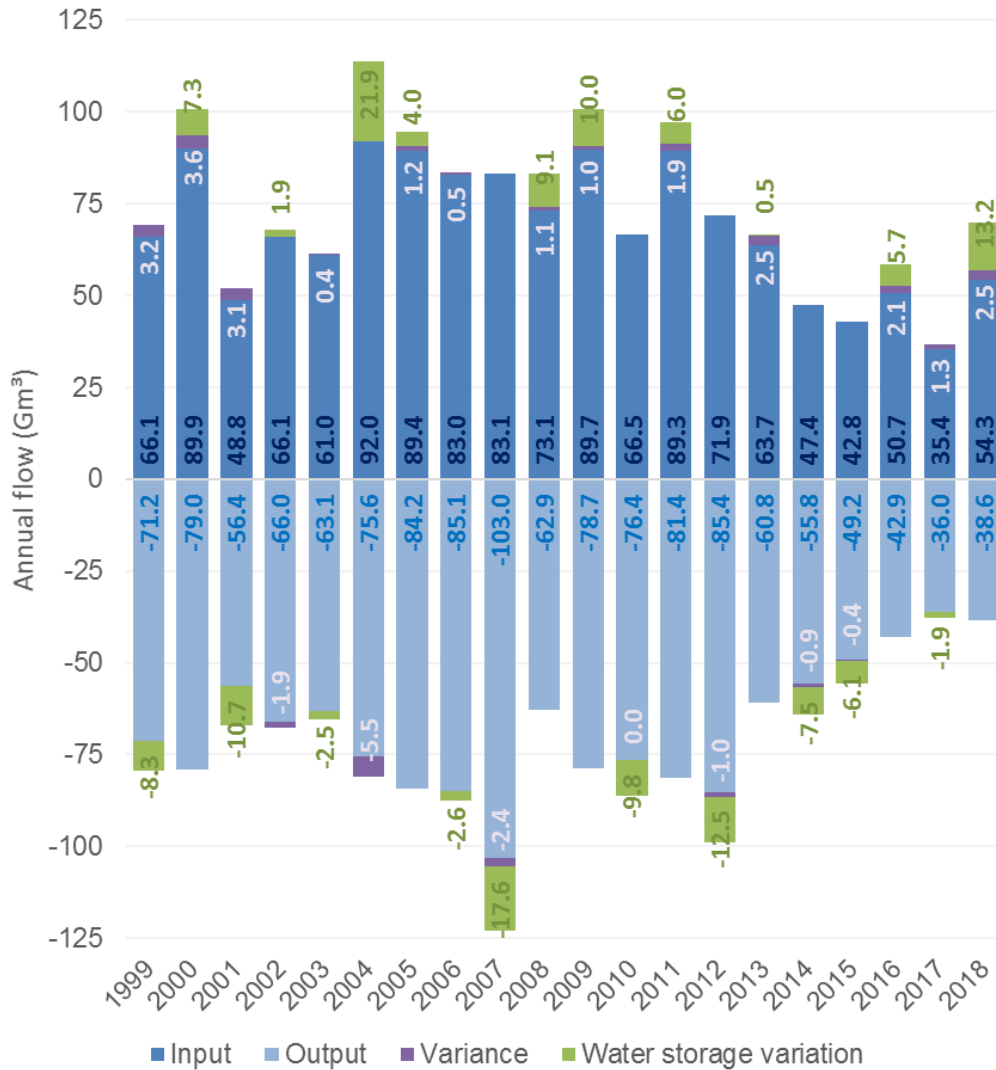
Figure 3.20 - Water output in the model distributed into demand, evaporation from the reservoirs, and outflow to the ocean from 1999 to 2018.



3.4.4 Water balance

The annual water balance is illustrated in Figure 3.21 for the years 1999-2018, expressing the total volume of water in the model as input, output, variation in the total storage of the three reservoirs, and the variance in data. The volume of water annually entering the system - incremental streamflow, precipitation in reservoirs, and runoff - fluctuated from 35.4 to 92.0 Gm³. The volume of water exiting the system - water demand, evaporation from the reservoirs, and outflow into the ocean - summed from 36.0 to 103.0 Gm³. The variation in the storage of water of reservoirs resulted positive or negative, depending on the year: the maximum of 12.5 Gm³ was subtracted in 2012 and 13.2 Gm³ was restored in 2018. The variance in data comprises the uncertainties associated with the values that made up the model, for instance, inflow and outflow of the reservoirs, the quantification of incremental inflow, and the estimates on precipitation, demand, local runoff, and variation in the reservoir storage.

Figure 3.21 – Annual flow of SFR: volume of input, output, variation of water storage in the reservoirs, and variance in data.



3.5 Validation

We used three criteria to verify the correlation of the modeling and the observed dataset in monthly timestep of 1999-2018: 1) water storage at the three reservoirs, 2) streamflow, 3) electricity generation from the HPPs. The Nash-Sutcliffe efficiency (NSE) coefficient was applied to quantify the confidence in the model, defined in Equation 3.2 (NASH; SUTCLIFFE, 1970):

$$NSE = 1 - \frac{\sum_{t=1}^T (Q_m^t - Q_o^t)^2}{\sum_{t=1}^T (Q_o^t - \bar{Q}_o)^2} \quad (3.2)$$

where:

Q_m^t is the modeled value at time t ;

Q_o^t is the observed value at time t ; and

Q_o is the mean of observed values.

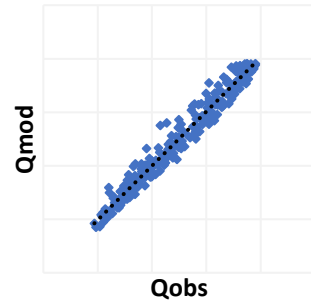
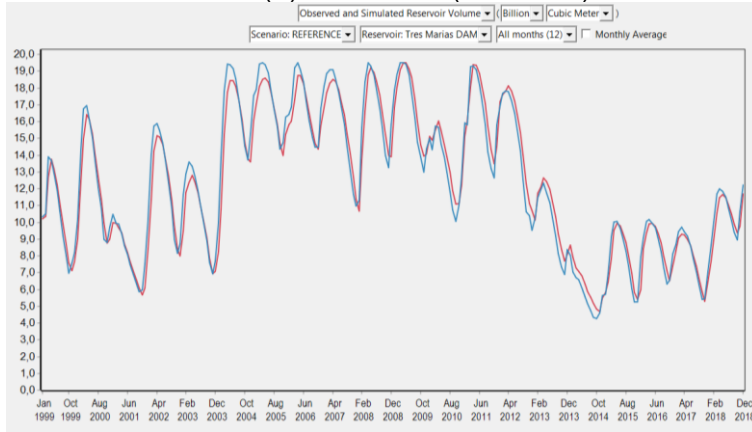
NSE results are classified as 'Fair' for $0.50 < NSE \leq 0.70$, 'Good' for $0.70 < NSE \leq 0.80$, and 'Very good' for $NSE > 0.80$ (MORIASI et al., 2015); a negative NSE means that the residual variance of the model is larger than the observed data variance comparing time-step and mean values.

3.5.1 Model validation 1: reservoirs storage and streamflow

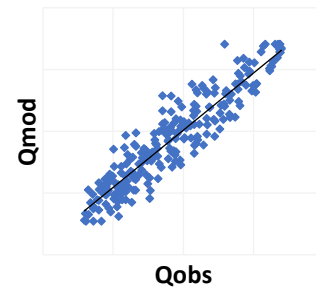
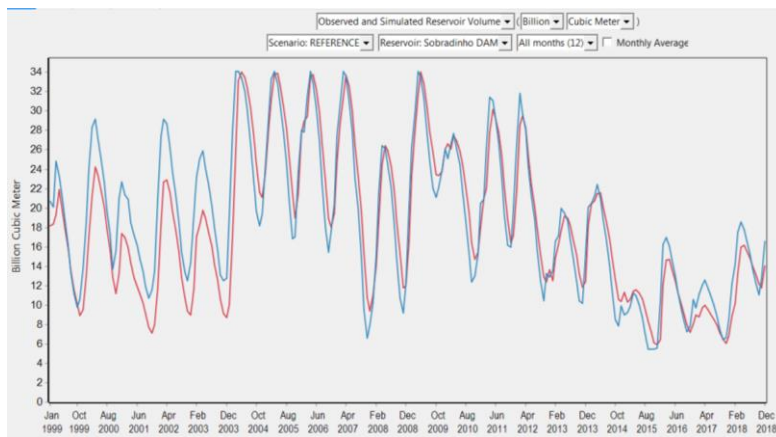
On validation 1, we confronted the modeled water storage with the historical dataset (ANA, 2019a; ONS, 2019a) using the WEAP graphical user interface. NSE resulted in 0.96, 0.86, -0.77, and 0.89, respectively, for Três Marias, Sobradinho, and Itaparica, and the total storage in the three reservoirs (Figure 3.22). The model incorporated the seasonal variations and presented a close relation to the dataset over the study period. At Sobradinho, the simulated storage was higher than the historical dataset in the initial years; one possible explanation is that the adjustments in demand were set at a level lower than the effective consumption. At Itaparica, the simulations performed a higher storage volume during the severe drought period, especially in wet months and after 2012. This can be explained by a larger water deficit, when the lack of precipitation and the dry soil moisture impulse a growth in water withdrawal, probably expressing that the effective consumption was higher than the demand informed by the official dataset.

Figure 3.22 – Volume of water in the modeled reservoirs (A) Três Marias, (B) Sobradinho, and (C) Itaparica (blue line) comparing to the ONS dataset (red line) at left; Nash-Sutcliffe efficiency (NSE) graph for the reservoir at right; and (D) NSE for the total storage in SFR reservoirs.

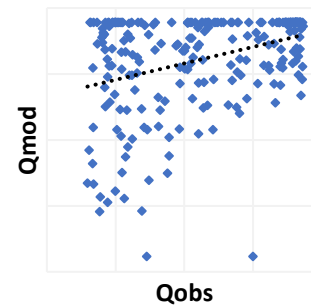
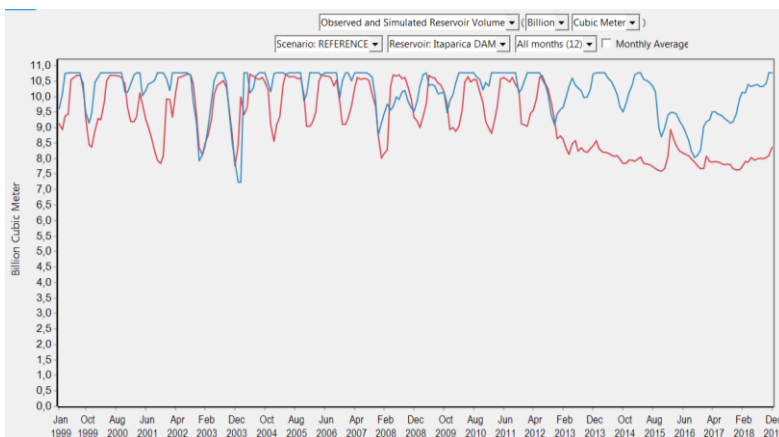
(A) Três Marias (NSE: 0.96)



(B) Sobradinho (NSE: 0.86)



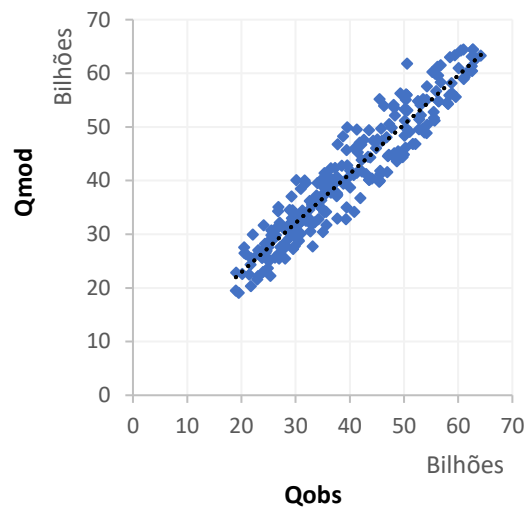
(C) Itaparica (NSE: -0.77)



— Observed Volume
— Storage Volume

(continues)

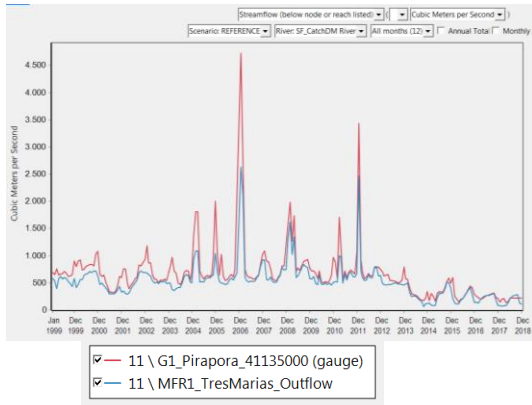
Figure 3.22 - Conclusion.
(D) Total storage (NSE: 0.98)



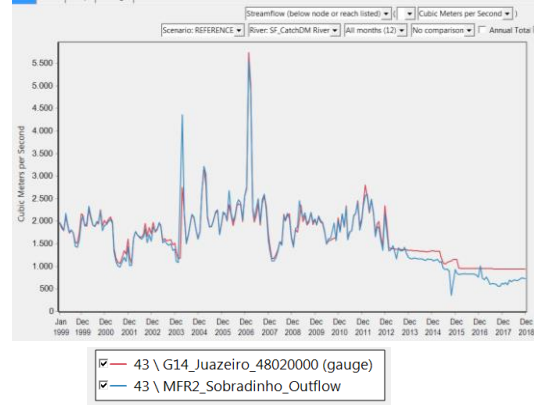
To verify the streamflow, we compared the simulations with the monthly dataset of downstream gauges (ANA, 2019b). We compared the simulated outflows with the following gauges: Três Marias and Pirapora (~150 km distant) (Figure 3.23A); Sobradinho and Juazeiro (~40 km) (Figure 3.23B); Xingó and Piranhas (~5 km) (Figure 3.23C); and the streamflow at the SFR wedge and the Traipu gauge (~100 km) (Figure 3.23D), respectively resulting in NSE 0.68, 0.88, 0.85, 0.84. Xingó was selected instead of Itaparica, as operational rules for SFR (ANA, 2017e) are applied to this HPP. Juazeiro gauge dataset presented a lack of information in several months from 2013 to 2018, which were filled by the average between the previous and next data available. In general, the model simulated the streamflow variations, although some peaks in outflow were less intense, especially at Três Marias. These peaks can be attributed to eventual and rapid shifts in water management, such as water transfer between reservoirs for management reasons, punctual water demands, or events of hydro transportation.

Figure 3.23 – Outflow from the modeled reservoirs and at the wedge streamflow (blue line) comparing with the National Water Agency dataset (red line) at the gauges downstream.

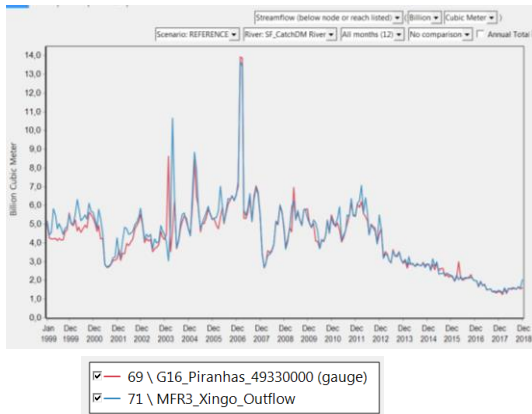
(A) Três Marias x Pirapora (NSE=0.68)



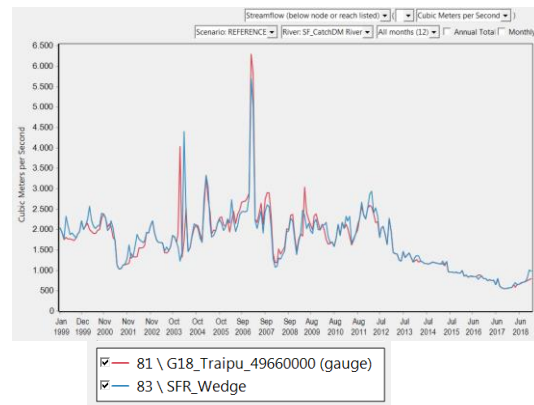
(B) Sobradinho x Juazeiro (NSE=0.88)



(C) Xingó x Piranhas (NSE=0.85)



(D) SFR Wedge x Traipu (NSE=0.84)



3.5.2 Model validation 2: hydroelectricity output

The accuracy of hydroelectricity output in the simulation was verified in comparison to the historical dataset (ONS, 2019a). For 1999-2018, NSE resulted 0.94 for Três Marias (Figure 3.24A), 0.97 for Sobradinho (Figure 3.24B), 0.93 for Itaparica (Figure 3.24C), 0.92 for Paulo Afonso (Figure 3.24D), and 0.94 for Xingó (Figure 3.24E). Considering the total electricity of the five HPP (Figure 3.24D), the NSE resulted in 0.96 for 1999-2018 (Figure 3.25) and 0.98 for the simulating period 2009-2018, demonstrating an adequate level of correlation.

Figure 3.24 – Hydroelectricity output in simulation (blue line) and ONS dataset (red line) for (A) Três Marias, (B) Sobradinho, (C) Itaparica, (D) Paulo Afonso, (E) Xingó, and (F) SFR HPPs, from 1999 to 2018.

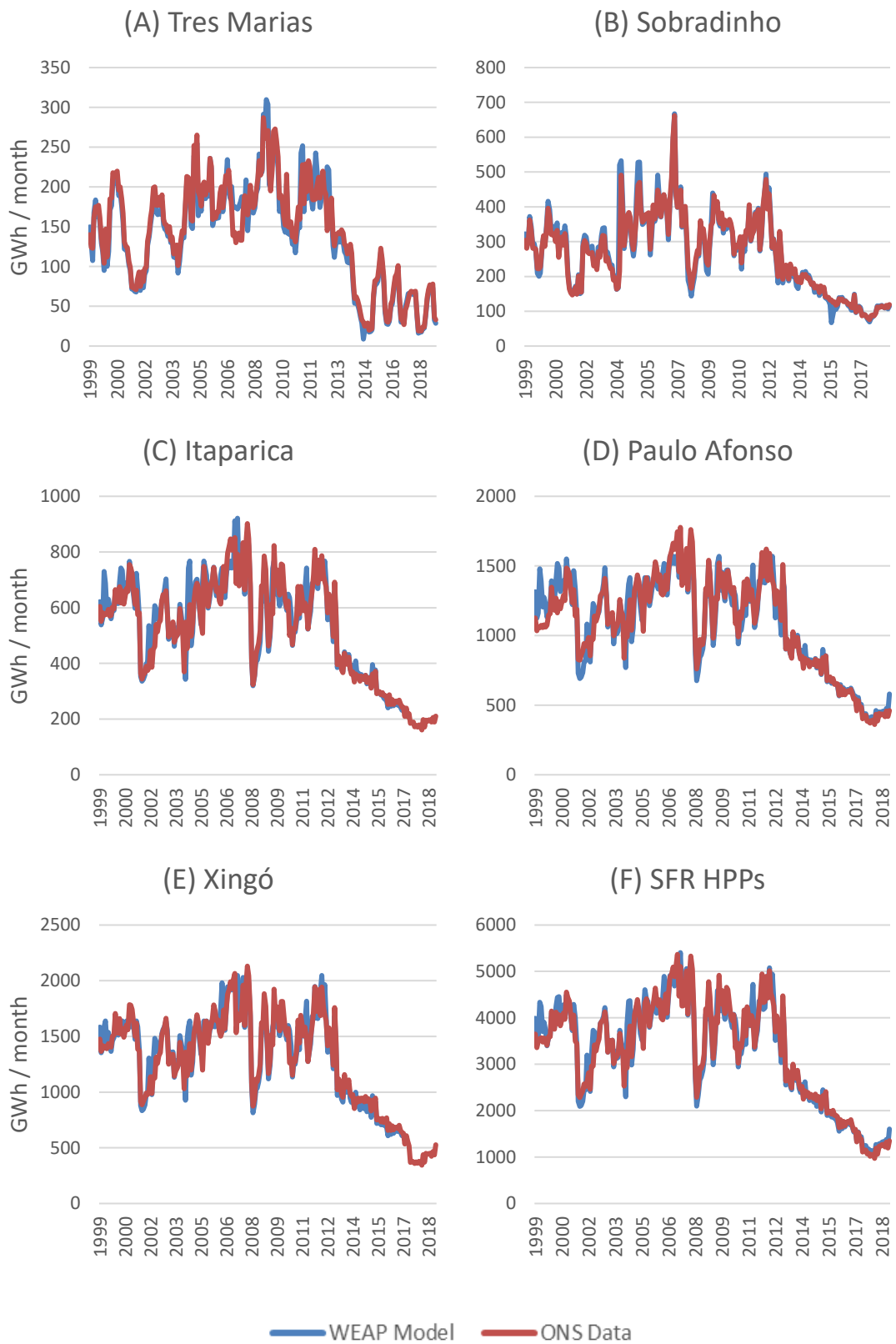
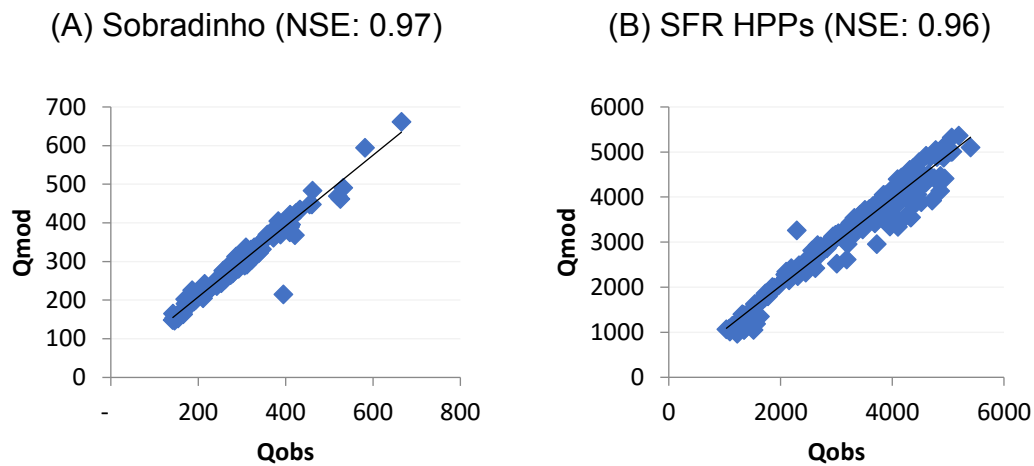


Figure 3.25 - Nash-Sutcliffe efficiency (NSE) of hydroelectricity output comparing ONS dataset and the modeling of (A) Sobradinho and (B) the five hydropower plants installed at São Francisco River.



3.5.3 Model validation 3: water input

In this validation, we analyzed the model regarding the volume of water input. The input was compared with an estimate of runoff in the basin. For each sub-basin, we multiplied the contribution area (CBHSF, 2016), by the monthly precipitation rate of the relative sub-basin (FUNCEME, 2020) and the runoff coefficient. The runoff coefficient was quantified by dividing the streamflow by the volume of precipitation upstream of that location (Table 3.6). We selected four reference points to represent the sub-basins: Três Marias (section 1), between the Três Marias and Sobradinho (section 2), between Sobradinho and Itaparica (section 3), and from Itaparica to the wedge (section 4). For the streamflow (ANA, 2019a), we adopted the inflow at the three reservoirs and the Traipu gauge. To quantify the contribution of each section, the upstream outflow was deducted from the inflow values, except for section 1, which assumed the Três Marias inflow. The runoff at Lower-middle resulted in a negative value as the inflow at Itaparica was lower than the Sobradinho outflow in 73% of the days for 1999-2018. This is coherent to a semi-arid area, where either the rare precipitation events evaporate or infiltrates in soil before reaching the riverbed and the river flow is reduced by withdrawals and evaporation.

Table 3.6 – Calculation of the runoff coefficient.

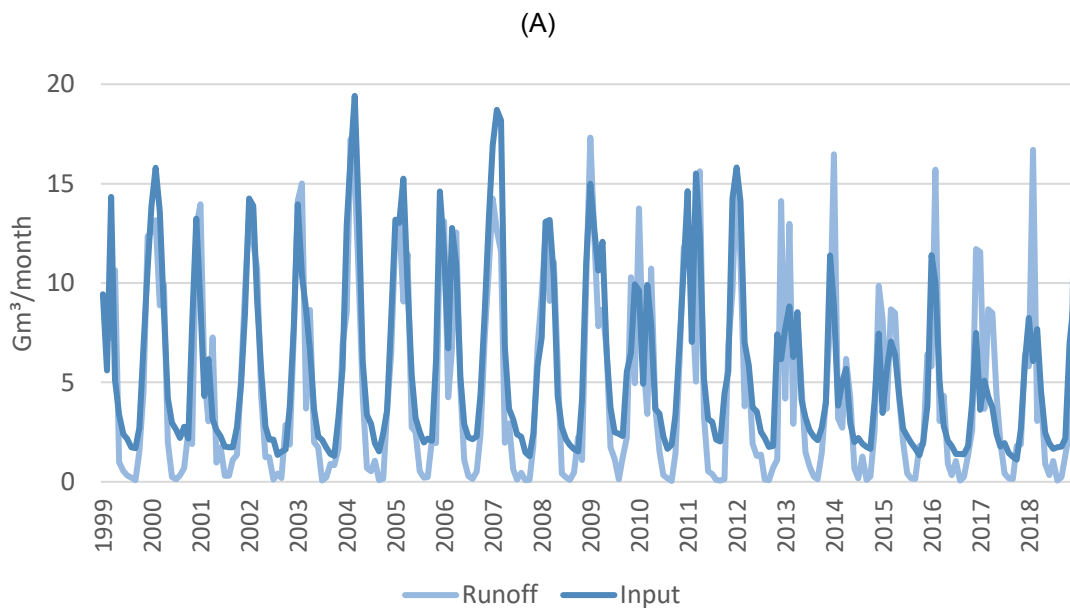
Section	Sub-basin	Streamflow reference point	Average inflow 1999-2018 ¹	Annual volume	Average outflow 1999-2018	Annual volume	Contributing area ²	Precipitation rate ²	Volume of precipitation	Runoff coefficient
			m ³ /s	10 ⁹ m ³	m ³ /s	10 ⁹ m ³				
1	Upper	Três Marias	539	17.0	531	16.7	57,272	1,401	80.2	0.21
2	Middle	Sobradinho	1654	52.1	1630	51.4	375,817	1,194	448.8	0.08
3	Lower-middle	Itaparica	1591	50.2	1589	50.1	146,185	644	94.1	-0.01
4	Lower	Traipu	1720	54.2			59,302	836	49.6	0.08

1 – Source: ONS (2019).

2 – Source: SIGEO (2011).

Figure 3.26 shows the monthly input of water that made up the model compared to the estimated runoff at the São Francisco basin. In general, there is an adequate concordance in the volume of water and seasonal variation. The divergences occurred in dry months because runoff depends on precipitation events and results in zero in dry months, while the input data, which was based on the incremental streamflow, is influenced by the water allocation.

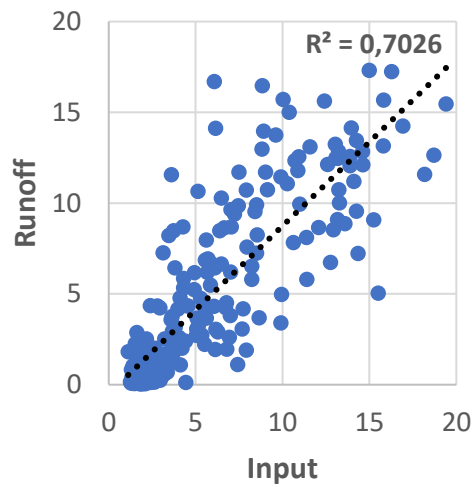
Figure 3.26 – Comparison of the water input in the model and the estimated runoff at São Francisco basin: (A) monthly volume and (B) correlation of the data.



(continues)

Figure 3.26 - Conclusion.

(B)



3.5.4 Variables and uncertainties regarding solar generation

In conclusion of the validation process, the water modeling presented adequate results in most indicators and a very good correlation in hydroelectricity output and storage of water at Sobradinho. For the solar power estimates, the wide variation in the size of the PV power plants expresses a range of possibilities in detriment of the searching for optimized response. Hence, we identified variables and uncertainties related to the results of solar electricity.

3.5.4.1 Performance ratio of the PV system

The performance ratio (PR) considering optical, thermal, and electrical losses ranges in literature by 0.75-0.87 (RÜTHER et al., 2014; CAZZANIGA et al., 2018; QUANSAH; ADARAMOLA, 2019; LOPES et al., 2020). DHIMISH (2020) conducted a study for five years in England, analyzing 8,000 PV crystalline silicon systems, and quantified the PR monthly average on 0.86 (0.84-0.92). LIMA; FERREIRA; and MORAIS (2017) estimated 0.83 for a 1-year study (2013-14) at Brazilian Northeast (Fortaleza). Although values higher than 90% are expected to become regular within some years (REICH et al., 2012), we adopted a more conservative PR of 0.8.

3.5.4.2 Measures of solar irradiance

The output of solar PV electricity was estimated based on the monthly average of solar irradiation acquired from a meteorological station, an observational ground-measured data, operating at the Petrolina municipality (~70 km from Sobradinho). The uncertainties in solar irradiance estimates can be assessed as follows: 1) measurement uncertainty is relatively low, reaching 2% at most for high quality (type A, spectrally flat thermopile) pyranometers as used in this study. Maintenance, redundancy, and quality checks play an important role (SENGUPTA et al., 2021); 2) geographical uncertainty assessed from PEREIRA et al. (2017) show that the Sobradinho reservoir experiences a 4.7% higher level of irradiation compared to the measurement site. Moreover, the validation presented in this Solar Atlas shows an uncertainty range of -4.8% to +5.1% for the Petrolina region; 3) microclimate effects due to lake breeze may also improve irradiance inside the lake to a level still unveiled. Past studies found a 1.7% improvement for another reservoir in Brazil GONÇALVES et al. (2020); 4) conversion to plane-of-array (POA) irradiance inputs other uncertainties. In this study, the global horizontal irradiation was the input for power conversion. Tilt optimization implies in small effect of ~1% in the low latitudes of Sobradinho (Lat ~9° S), as shown in (NICOLÁS-MARTÍN et al., 2020). The combination of the uncertainties mentioned above ranges from -0.4% to +13.5%, confirming the conservative approach adopted in this study.

3.5.4.3 Solar panel efficiency

We adopted the rate of 20% for solar panel efficiency. Other solar technologies can attain an efficient rate of 12.6 to 47%, while polycrystalline silicon cell modules can reach 23.3%, increasing by 15% the solar generation and, consequently, the saved flow. More efficient panels can reduce area but imply additional costs to the system.

3.5.4.4 Technical uncertainties

Additionally, there are uncertainties regarding the functionality of the floating PV system in producing electricity such as gains from temperature stability and lower dusting due to the presence of water, or variation from the engineering project such as panels characteristics, distribution, floating components, and materials;

angle and position over the lake; the presence of solar tracking or water veil-cooling, among others. Gains from temperature stability is subject to several recent studies and number vary from 0,7% to 15,5%, assuming an average value of 12% according to literature (RANJBARAN et al., 2019; GONZALEZ SANCHEZ et al., 2021).

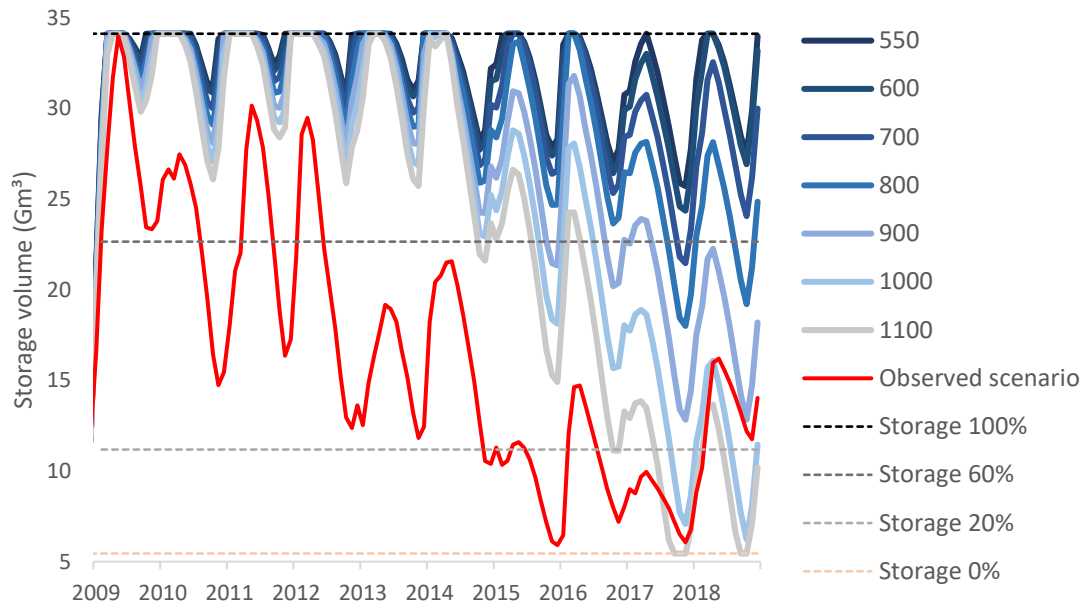
4 RESULTS

The simulated scenarios were analyzed in terms of water allocation and energy output under the solar power adding and alternative operative rules set for the reservoirs in cascade. We classified as valid the scenarios that met the water demand, maintained the water storage above the minimum operational level, and sustained the river flow above 800 m³/s. Next, we quantified indicators of the valid scenarios for local and regional scale: for Sobradinho – water security, electricity generated by solar and hydropower, and capacity factor as a hybrid powerplant; and for the SFR system – hydro and total electricity generated, water and potential energy losses.

4.1 Limits for water allocation

We started the simulations by analyzing theoretical scenarios of outflow from Sobradinho HPP to estimate the maximum value that the water in the SF system would sustain without depleting the reservoir. To access this limit, we adopted the minimum outflow in a range of 550 to 1,100 m³/s over 2009-2018 (Figure 4.1); the rules related to PV adding (saved flow) or storage level were not applied in this first analysis. Figure 4.1 shows the results for each simulation and demonstrates that even if applied since 2009, values of minimum outflow higher than 1,000 m³/s would lead to the reservoir's depletion. Thus, the ecological streamflow of 1,300 m³/s was not feasible to be achieved in these conditions of meteorological drought, and effective gains in water security were only achieved by adopting low outflow values in the operation of the Sobradinho reservoir.

Figure 4.1 – Water storage at Sobradinho reservoir using minimum streamflow from 550 to 1,100 m³/s in the period 2009-2018.



4.2 Effect of solar power generation on water conditions

The simulated scenarios of solar power positively impacted the water availability at the Sobradinho HPP during the years of severe drought. The volume of water kept in the reservoir by the constraint to outflow increased the water security for Scenarios PV-250, PV-500, PV-750, and PV-1000 (Figure 4.2 and Figure 4.3). For Scenarios PV-50 and PV-100, the reservoir volume dropped to zero and, therefore, these scenarios were classified as invalid.

Water storage for the valid scenarios was maintained at EV>20% for the entire period, except for PV-250, which crossed this level for four consecutive months (September-December) during the dry season of 2017. After 2014, scenarios PV-750 and PV-1000 presented the same water storage due to climatic conditions when the lack of precipitation limited the influence of adding solar power. The storage was not completely recovered and fluctuated by 40-70% in 2017-2018 in both scenarios. Thus, after several years of severe drought, the available water proved to be insufficient to maintain the minimum streamflow of the SFR and conserve high levels of water in the reservoirs. When the lack of precipitation went critical, the stored water was applied to sustain the outflow above 800m³/s, reducing the reservoirs' water level.

Figure 4.2 - Water storage at Sobradinho for PV scenarios ranging from 50-1,000 MW: valid scenarios (blue line), invalid scenarios (orange line), and observed scenario (red line).

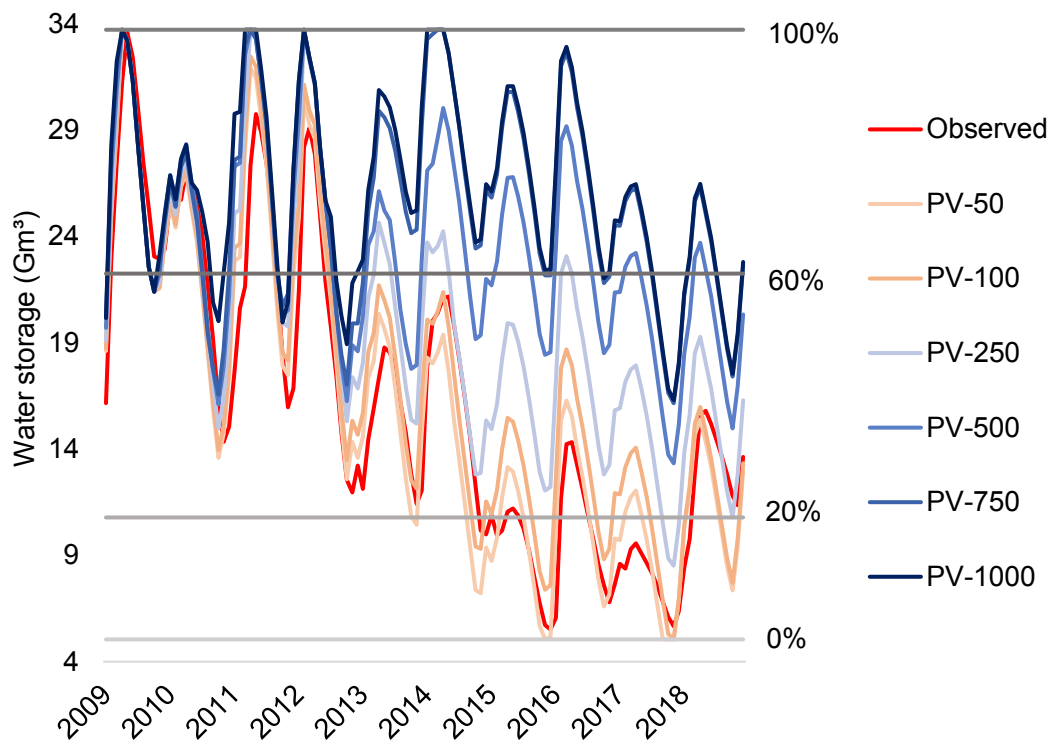
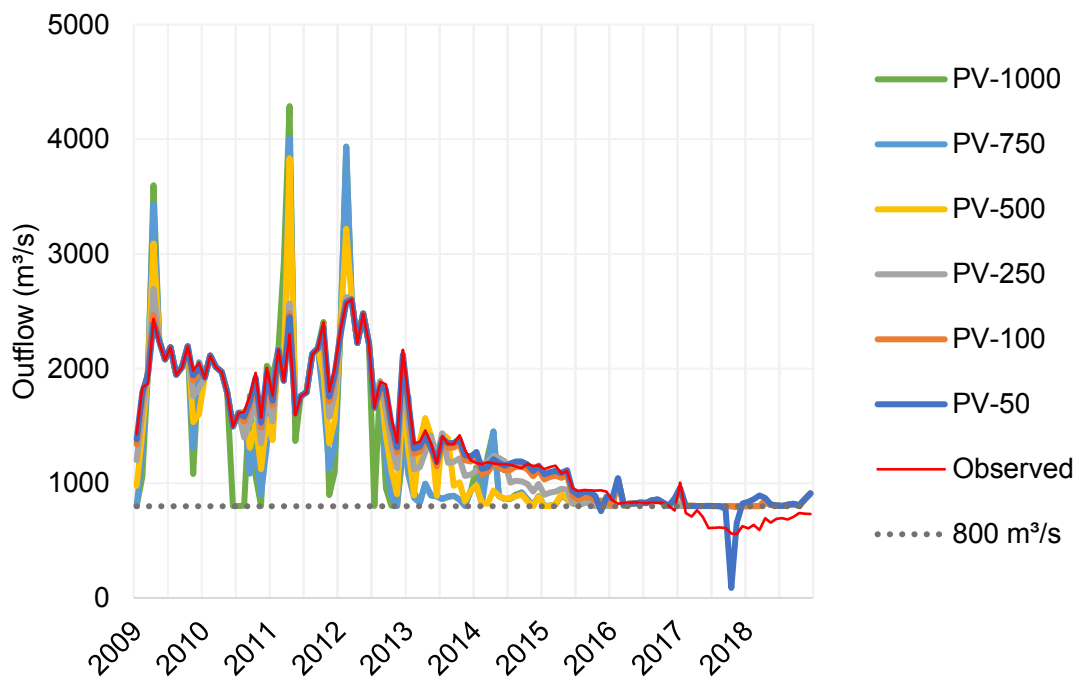


Figure 4.3 – Outflow from Sobradinho reservoir in valid and observed scenarios.



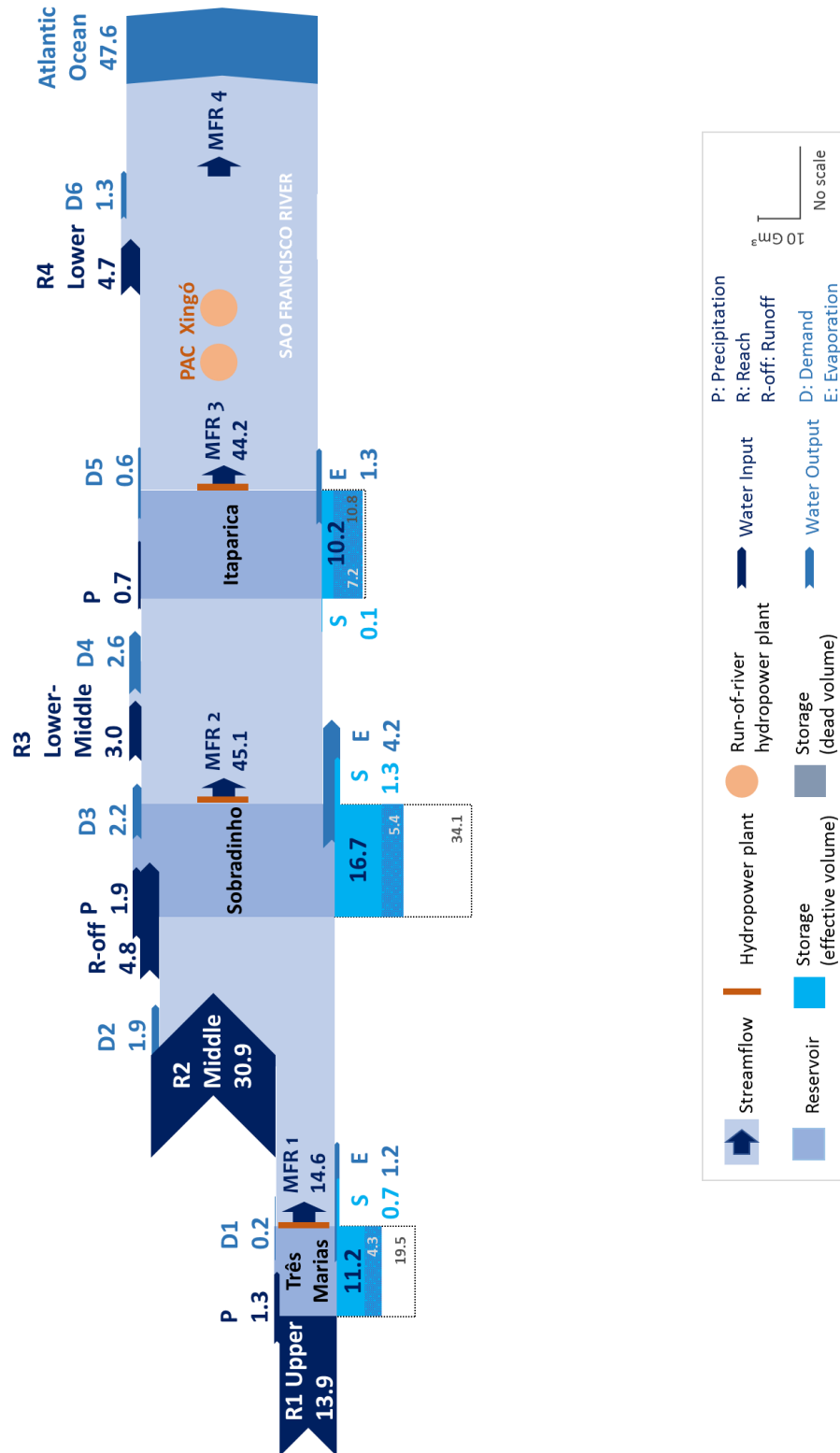
Although the operating rules were supposed to constraint the outflow depending on the PV installed power, Sobradinho predominantly assumed an outflow close to the minimum, starting in 03/2013 for PV-750-1000, 11/2013 for PV-500, and 06/2015 for PV-250 (Figure 4.3). The saved flow rule for the largest PV power plants led rapidly to the adoption of the minimum outflow, as illustrated in Figure 3.8. The wet season of 2009, 2011, and 2012 achieved the maximum water storage level and required the release of the exceeding volume. All scenarios assumed similar outflow values from 07/2015 until the end of the simulation period, operating close to the minimum, with some episodic increases to allocate water between the reservoirs.

The average water flows in the components of the São Francisco River model are illustrated as a Sankey diagram in Figure 4.4 for the observed scenario in average data 2009-2018 (A), the year 2017 (B), the scenarios PV-250 (C), and PV-1000 (D). The relative volume of water of the components is illustrated with the width of the arrows (y-axis). The data on the upper side of the diagram represents the fixed inputs of incremental streamflow (R), precipitation (P) and run-off (R-off), and the output of demand (D). The data on the lower side represents the reservoirs on the average storage of water, dead volume, and the output of evaporation from the lake (E). The installed HPPs are represented by the orange components connected to the reservoirs and at the riverbed. The average volume of water conserved in the Sobradinho reservoir increased with the more adding of solar PV: from 16.7 Gm³ in for the observed scenario to 20.5 Gm³ for PV-250 and 26.6 Gm³ for PV-1000.

Regarding the analysis of the São Francisco River, the comparison of the Figure 4.4-A and Figure 4.4-B demonstrate the relevance of the water input at Upper and Middle sub-basins to the availability of water downstream. Since the average annual precipitation at Middle sub-basin (30.9 billion m³ for 2009-2018) is similar to the storage capacity of Sobradinho (34,1 billion m³), years of low precipitation jeopardize water security (Figure 4.4-C and Figure 4.4-D). Thus, during a sequence of dry years, the capacity of managing the water in the reservoirs to address water security and ecological streamflow is limited - even with the high storage capacity of Sobradinho.

Figure 4.4 – Water flow in the components of the San Francisco River model: (A) Observed scenario for average 2009-2018, (B) Observed scenario in 2017, (C) Scenario PV-250, and (D) Scenario PV-1000. Values in billion cubic meters in the y-axis.

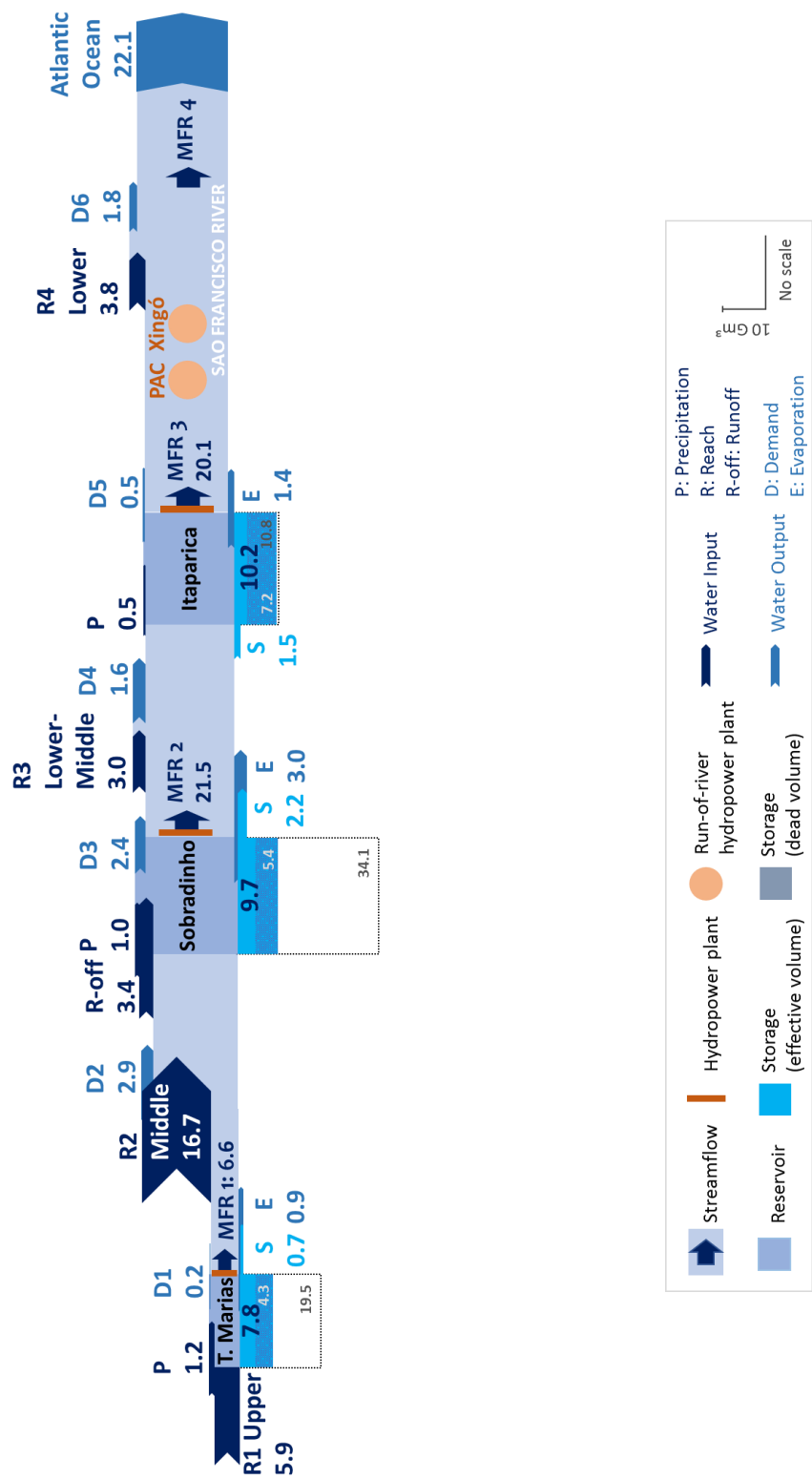
(A) Observed scenario – Average 2009-2018



(continues)

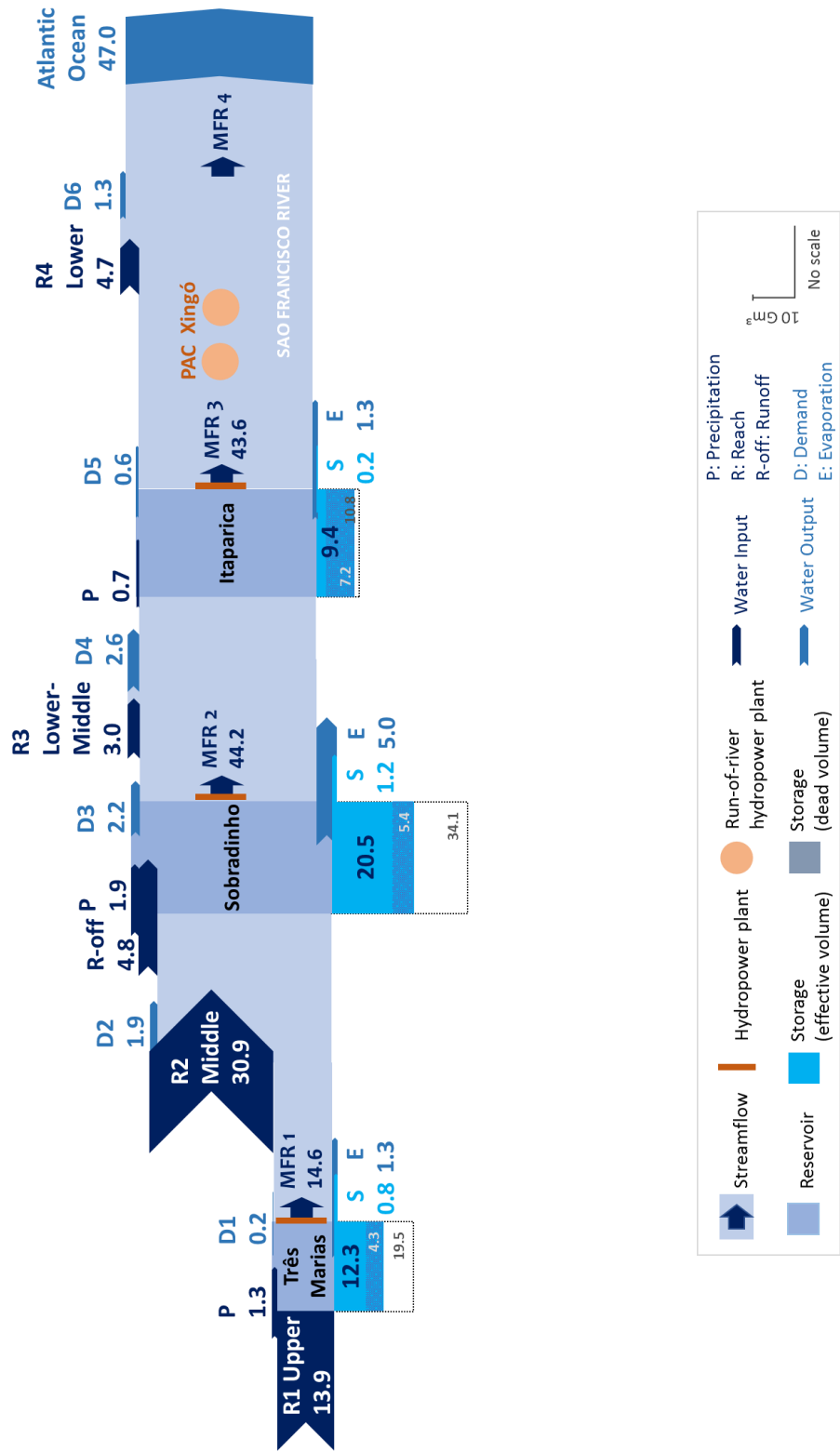
Figure 4.4 – Continuation.

(B) Observed scenario – 2017 (very dry year)



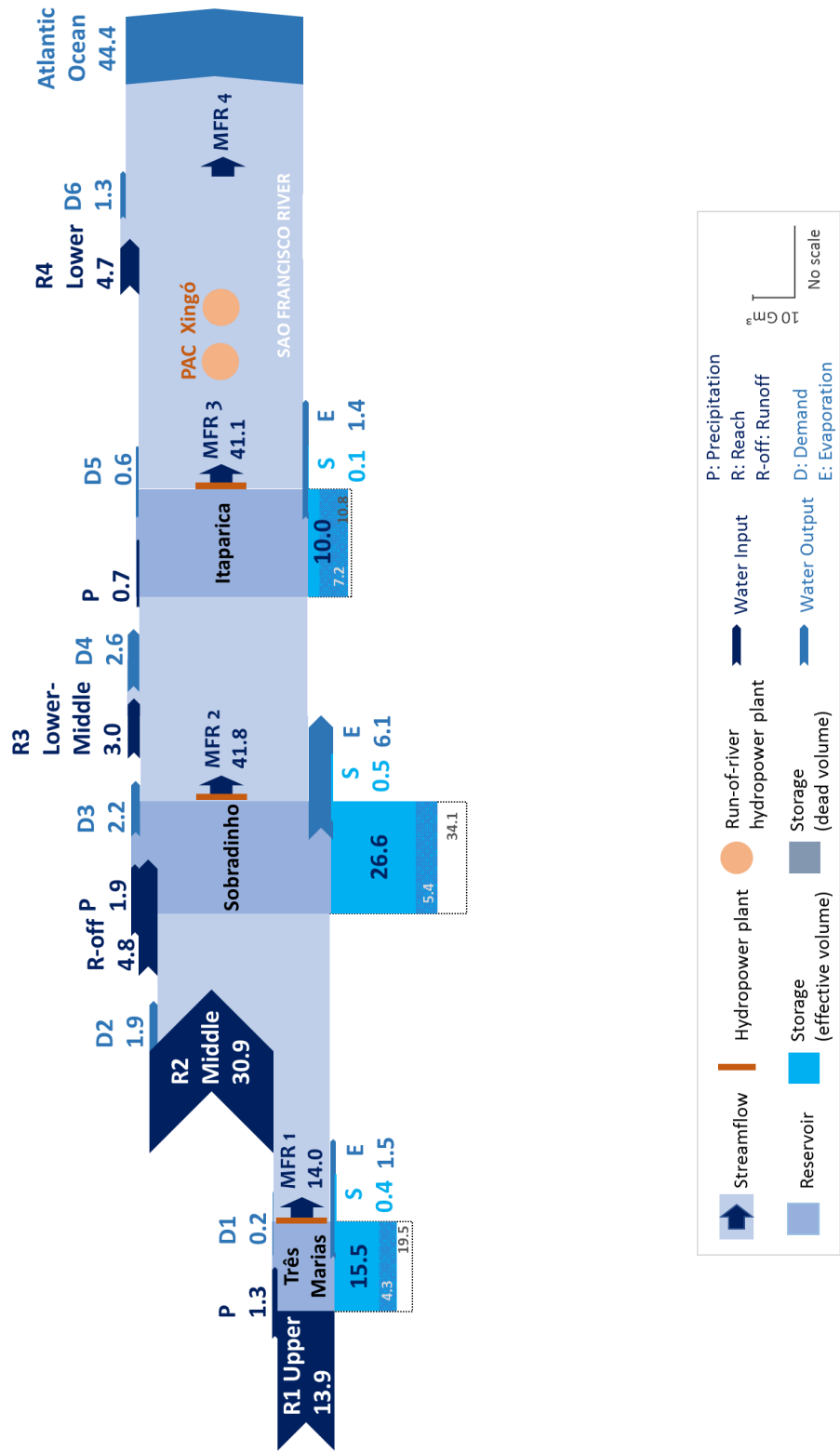
(continues)

Figure 4.4 – Continuation.
 (C) Scenario PV-250



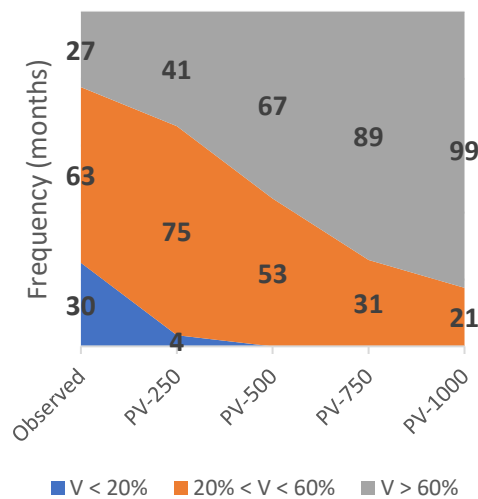
(continues)

Figure 4.4 – Conclusion.
(D) Scenario PV-1000



On the energy side, for the operation of the hydropower plants, conditions of water storage above 60% of the capacity and constant outflows contribute to increasing the predictability and the control in dispatching electricity, consequently increasing the energy security. These two conditions are even more relevant in systems such as the Brazilian electric grid, in which the dispatches involve several connected power plants. The frequency of months with storage levels above 60% has significantly increased following the installed PV. Scenarios PV-500 to PV-1000 kept the water storage above 20% of the capacity during the entire period, and above 60% in the majority of the months (Figure 4.5).

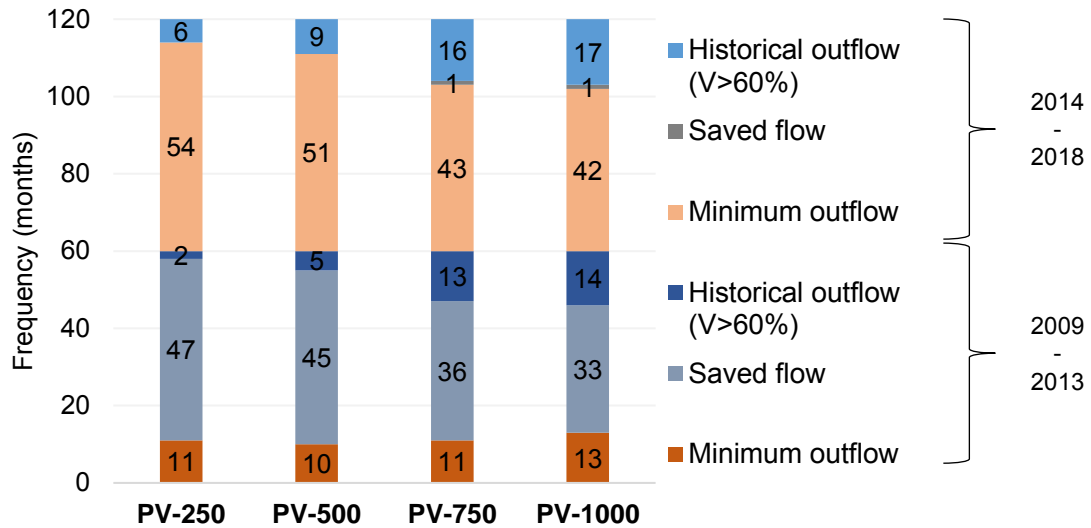
Figure 4.5 – Frequency of months with water storage in the three operation stages defined by the National Water Agency (ANA).



Nevertheless, the prevalence of the operating rules modeling the water allocation depended not only on the water storage of Sobradinho but also on the variation of the historical outflow produced by the saved flow value. Applied to water storage above 60%, the rule of adopting the historical outflow occurred more frequently according to scenarios of higher PV installed. In fact, the simulations responded differently comparing the two halves of the study period: 2009-2013 and 2014-2018, as illustrated in Figure 4.6. The prevalence occurred for the saved flow rule in the first years of the simulation while the minimum outflow ruled

most months over the critical years in reason of the low outflows put into practice in the historical dataset.

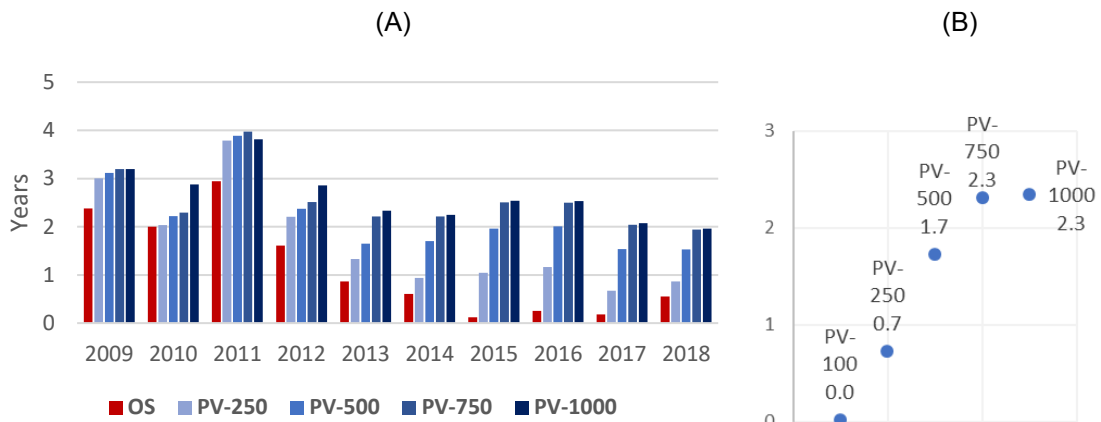
Figure 4.6 - Frequency of the operating rule in prevalence in the simulated scenarios for the period 2009-2013 and 2014-2018.



4.3 Water security

The increase of water storage in the PV scenarios compared to the observed scenario reflected improvements in water security for PV-250 to PV-1000 during the study period (Figure 4.7). Over the dry season in 2017, the lowest storage volume at Sobradinho corresponded to the water demand from the reservoir (D3 - Figure 3.10) and the river between Sobradinho and Itaparica (D4) by 0.7, 1.7, and 2.3 years, respectively, for PV-250, PV-500, and PV-750-1000. The performance was restricted to Scenario PV-750, as PV-1000 resulted similarly in stored volume due to the lack of water to both maintain the streamflow and reserve more water, as explained in the previous section. Considering the lowest level of water storage in the three reservoirs related to the annual demand from the SF river, the ratio resulted in 0.6 years of the demand for PV-250 and 2.0 years for PV-1000.

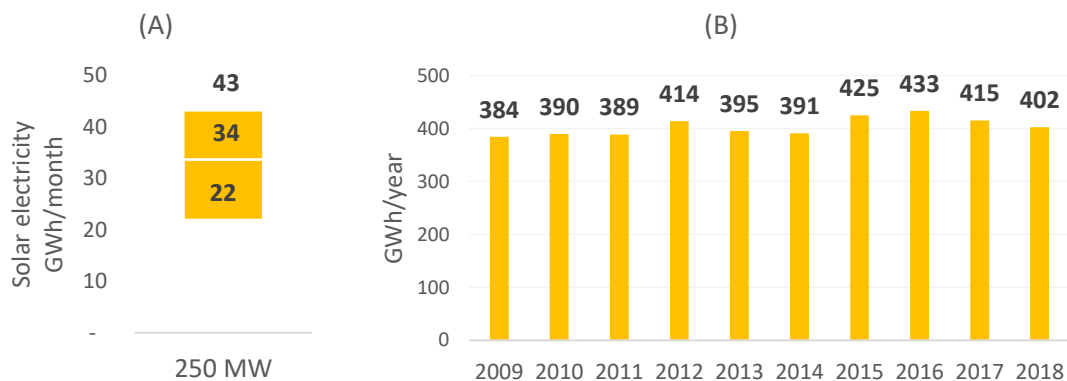
Figure 4.7 – (A) Ratio of the lowest level of water storage in Sobradinho and the yearly water withdrawal from the reservoir (D3) and between Sobradinho and Itaparica (D4); (B) result for 2017.



4.4 Solar electricity

If we now turn to solar power generation, we estimated the monthly production by 22 to 43 GWh, on average 34 GWh, for each 250MW of PV installed at Sobradinho (Figure 4.8-A). The annual output ranged from 384 to 433 GWh/year (Figure 4.8-B). Despite the monthly seasonality, PV annual generation stood constant along the study period, showing a slight increase in generation in dry years. The Scenarios PV-250 to PV-1000 generated annually from 404 to 1,615 GWh, on average.

Figure 4.8 - Range of (A) monthly and (B) annual electricity generation of a PV installed power of 250MW located at the Sobradinho reservoir.



4.5 Hydroelectricity

The hydroelectricity monthly generated by Sobradinho in the simulated scenarios ranged between 110-503 GWh in PV-250 and 128-665 GWh in the PV-1000, on the average 228 GWh/month. The historical dataset registered that 76-479 GWh/month were dispatched to SIN over the years 2009-2018 (ONS, 2019a). Figure 4.9 shows the results for scenarios PV-250 (Figure 4.9-A), PV-500 (Figure 4.9-B), PV-750 (Figure 4.9-C), and PV-1000 (Figure 4.9-D). The more intense the solar adding, the more diverse was the reservoir operation from the practices adopted by ONS. Although the rule of saved flow was set to directly compensate the constrained outflow by solar source, the water allocation did not respond linearly because the other rules (apply historical outflow for $V < 60\%$ and minimum outflow of $800 \text{ m}^3/\text{s}$) concomitantly influenced the simulations.

The hydroelectricity output presented trade-offs in the short (seasonal) and long term (interannual). Seasonally, higher PV scenarios presented more monthly variation, with increases in wet months led by the outflow of exceedance water in the reservoirs or the prevalence of the operative rule to the historical outflow. Interannually, the additional water stored in the first years was applied in maintaining an outflow higher than $800 \text{ m}^3/\text{s}$ starting from 2013, consequently generating more electricity than the observed scenario. These dispatches could have meant a significant increment of the renewable source to the SIN over the critical years of drought. In fact, the solar PV surpassed the quantity of electricity provided by the Sobradinho HPP during the critical dry months of 2017 starting from Scenario PV-500; and from August 2015 to December 2018 in the PV-1000. These trade-offs can be verified in Figure 4.9 and Figure 4.10 by comparing the results for the PV scenarios to the observed dataset. The annual generation of Sobradinho HPP resulted similarly among the simulated scenarios. The variations were more significant comparing 2009-2012, which resulted in the range of 3.1 to 4.4 TWh/year, and 2013-2018, when the output diminished to 1.7 to 2.3 TWh/year, as illustrated in Figure 4.10.

Figure 4.9 – Scenarios of monthly electricity output from Sobradinho hybrid power plant per energy source: (A) PV-250, (B) PV-500, (C) PV-750, and (D) PV-1000, compared to the historical time-series 2009-2018 (red bold line).

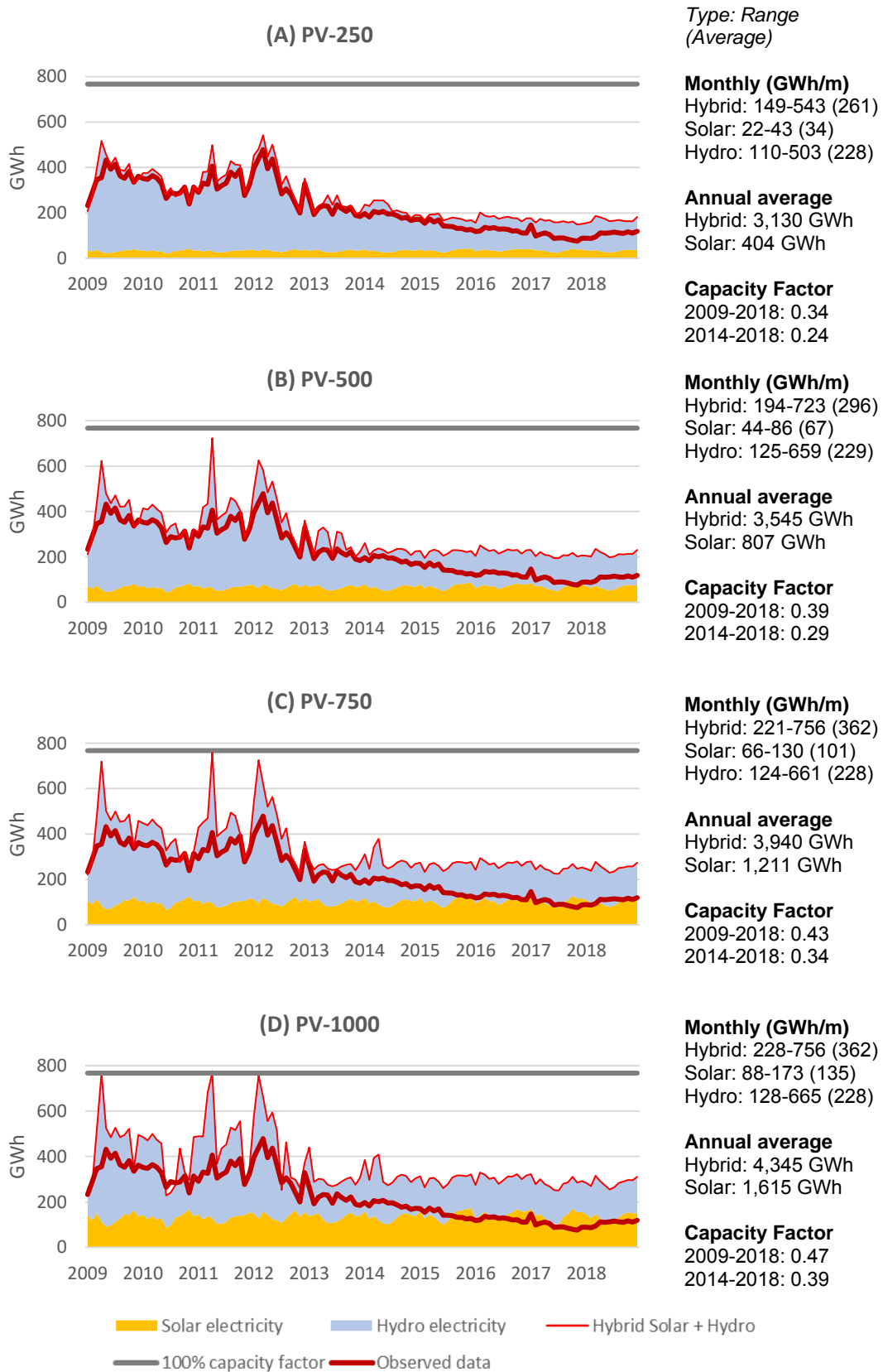
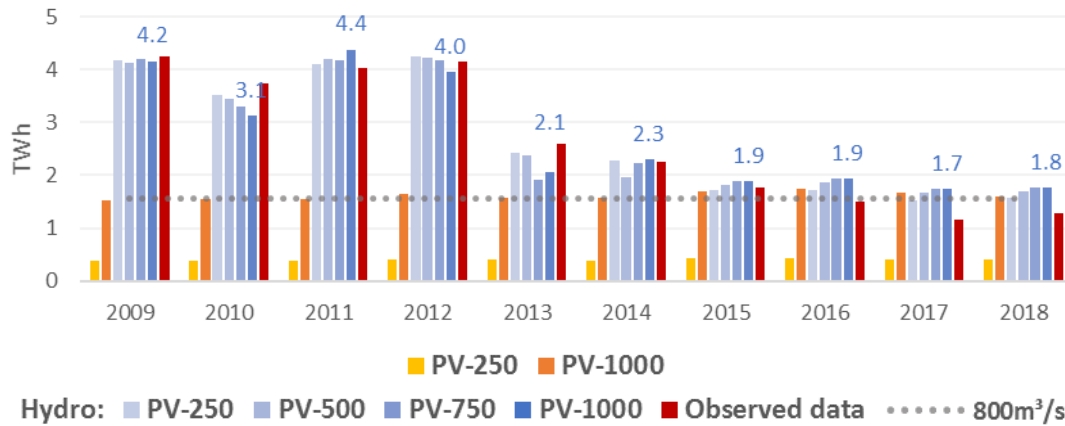


Figure 4.10 – Annual electricity generation for PV scenarios in Sobradinho: PV-250 (yellow), PV-1000 (orange), hydroelectricity outputs of the simulated scenarios (blue), the observed dataset from ONS (red), and the equivalent generation for HPP outflow of 800 m³/s.



4.6 Capacity factor of Sobradinho

The capacity factor of Sobradinho increased from 0.29 of the historical time-series 2009-2018 to 0.34 in PV-250, 0.39 in PV-500, 0.43 in PV-750, and 0.47 in PV-1000, optimizing the existing infrastructure to transport electricity to the grid. Analyzing the Sobradinho infrastructure, the average restrains of 767 GWh/month was only achieved once, in PV-1000, in April 2011. Thus, in either scenario, energy curtailment was not necessary throughout the study.

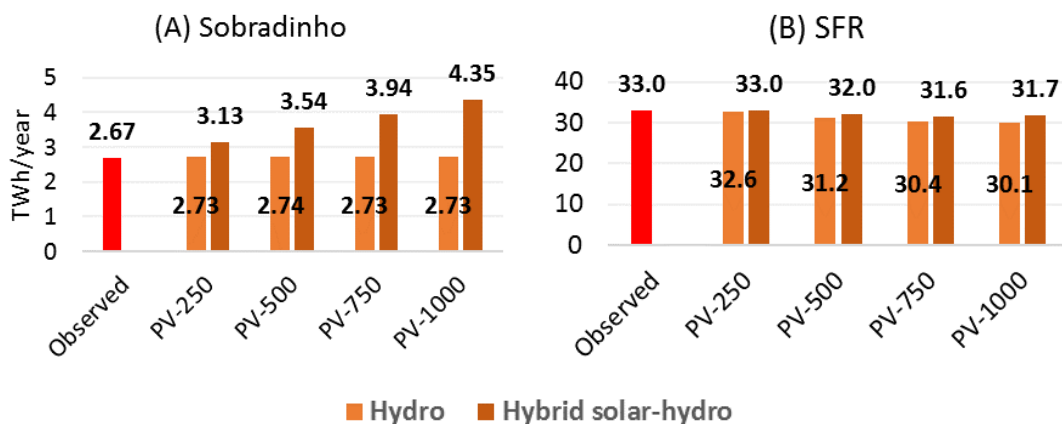
The present study was focused on quantifying monthly and annual results; however, we additionally analyzed the occurrence of energy losses in terms of hourly generation at Sobradinho. The highest irradiation data at Petrolina was registered at $GHI = 1,124 \text{ W/m}^2$ on 07/02/2011 at 3 p.m. (INPE, 2020). Using Equation 1, the solar generation resulted in 225 and 899 MWh for PV-250 and PV-1000, respectively, the equivalent to 21 and 86% of the Sobradinho installed capacity of 1,050 MW to dispatch electricity. Thus, complementary to solar at this hourly condition, the outflow at Sobradinho HPP can be estimated by 3,730 m³/s for PV-250 and 682 m³/s for PV-1000 without losing energetic resources. Assuming that the integrated operation of a hybrid power plant is managed to vary the reservoir's outflow over the 24h and predominantly dispatch solar power during the day and hydropower during the night, the highest hourly PV power generation is attainable of proper management to avoid energy losses.

Accordingly, the hybrid plant can bring additional gains in the use of renewable energy resources, beyond the benefits of two separated plants.

4.7 Electricity output from Sobradinho and SFR system

The simulations of a hybrid Sobradinho power plant combining solar and hydro sources resulted in more electricity to the SIN in all scenarios compared to the time-series 2009-2018 of 2.67 TWh/year. The scenarios achieved, on average: 3.13 (117%), 3.54 (133%), 3.94 (147%), and 4.35 TWh/year (162%), respectively, for PV-250, PV-500, PV-750, and PV-1000 (Figure 4.11-A). Simultaneously, shifting the spatial scale of the analysis, the five HPPs installed at the SFR presented a slight reduction in the simulated scenarios compared to the observed scenario, up to 9% less hydroelectricity. This reduction was inversely proportional to the solar power intensity, as illustrated in Figure 4.11-B.

Figure 4.11 – Average electricity output in historical dataset 2009-2018 and simulated PV scenarios at (A) Sobradinho and (B) five HPPs at SFR.



This outcome can be explained by three factors associated with the HPPs working in cascade. First, as more water was kept in the reservoirs, the loss of water by evaporation led to a loss of potential energy in correlation to the solar intensity and its saved outflow value. Second, the high river flow in wet months exceeded the maximum turbinating outflow in HPP downstream Sobradinho and induced events of water being released without generating electricity (spilled water). These two events are detailed in the coming section. A third factor is associated with the variance in the modeling of Itaparica as the exceedance of

water retained in this reservoir compared to the observed dataset diminished the results by 0.13 TWh/year, equivalent to 0.4% of the total output. The hydroelectricity loss between the simulated and observed scenarios was partially compensated by the solar adding at Sobradinho. The average electricity output of the observed scenario was 33.0 TWh/year, which was nearly maintained for Scenario PV-250 (99.8%) and resulted in 32.0 for PV-500 (97.0%), 31.6 for PV-750 (95.6%), and 31.7 TWh for PV-1000 (96.0%). Compared to the observed scenario, the incremental evaporation and spilled water resulted in a loss of potential energy by 0.1 and 1.3 TWh/year, respectively, for PV-250 and PV-1000.

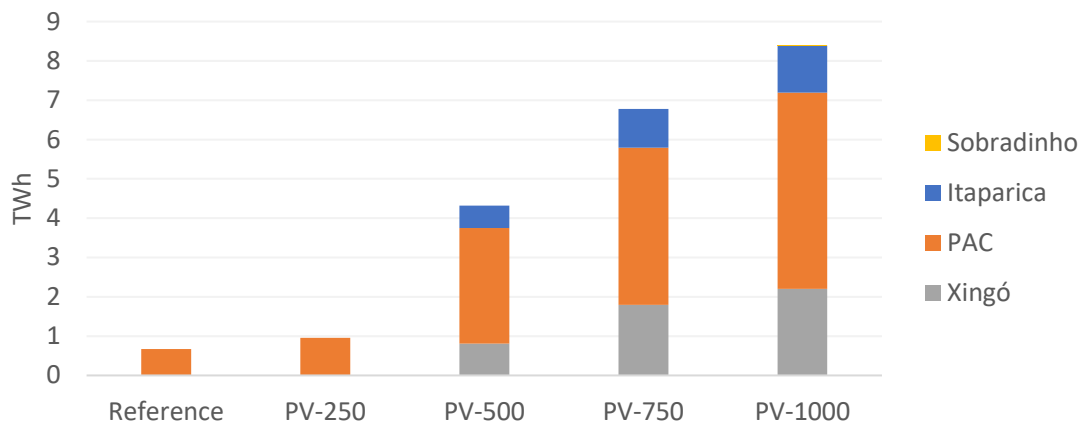
4.8 Loss of water and potential energy

4.8.1 Spilled water

Spilled water occurs if the outflow is higher than the maximum turbinating outflow of the HPP. In this condition, water is released into the river without generating electricity, which we considered a loss of potential energy. In addition, the energy loss of spilled water is enhanced by the individual productivity of the plant. Sobradinho can harness 4,260 m³/s, producing 61.4 Wh/m³, while the HPPs downstream present either lower values of maximum turbinated outflow and higher productivity factor, respectively: 2,745 m³/s and 126 Wh/m³ at Itaparica; 2,310 m³/s and 319 Wh/m³ at PAC; 3,000 m³/s and 305 Wh/m³ at Xingó.

The loss of potential energy also occurred in the observed scenario at 0.7 TWh for the 2009-2018 time-series; in the simulated scenarios, it summed 1.0, 4.3, 6.8, and 8.4 TWh, respectively for PV-250, PV-500, PV-750, and PV-1000. Spilled water was registered at the end of the wet season of 2009, 2011, and 2012, occurring in multiple HPPs depending on the scenario, as illustrated in Figure 4.12. Sobradinho only registered this type of loss in Scenario PV-1000, and in one month (April 2011). Scenario PV-250 only registered losses at PAC, while starting from PV-500 it occurred in every HPPs downstream Sobradinho.

Figure 4.12 - Loss of potential energy by spilled water at the hydropower plants Sobradinho, Itaparica, PAC, and Xingó for observed scenario, PV-250, PV-500, PV-750, and PV-1000.



4.8.2 Evaporation from the reservoirs

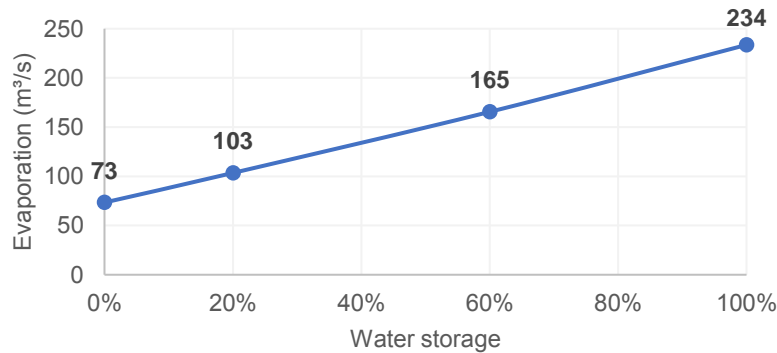
Evaporation is a collateral effect of reserving water, especially in areas characterized by climate conditions of water deficit. In the observed scenario, the volume of 6.7 Gm³/year evaporated from the three reservoirs on the average 2009-2018; of which 4.2 Gm³/year from Sobradinho. In this reservoir, the evaporation was equivalent to the average water storage volume by 21% in 2009 and 37% in 2017. Although it represents a high amount, this volume of evaporation associates with an undesirable storage level, which stood insufficient to provide water security. The simulated scenarios have retained more water in the reservoirs, increasing the surface area of the lake and, therefore, inducing incremental evaporation compared to the observed scenario.

The incremental evaporation is a hypothesis of the study, considering that the water was effectively maintained in the reservoirs for water security, which eventually could have had other destinations of water demand or allocation in reservoirs operation, such as direct consumption, water transfer, or streamflow increase. Considering the evaporation from Três Marias, Sobradinho, and Itaparica, scenarios PV-250, PV-500, PV-750, and PV-1000, respectively, resulted in the total evaporation of 7.6, 8.3, 8.8, and 8.9 Gm³/year, on average. Thus, as more solar PV was added, the increase in water storage resulted in more evaporation from the reservoirs. Sobradinho responded to about 70% of the

total evaporation due to the lake's geometry and the largest increase in water storage compared to the other reservoirs.

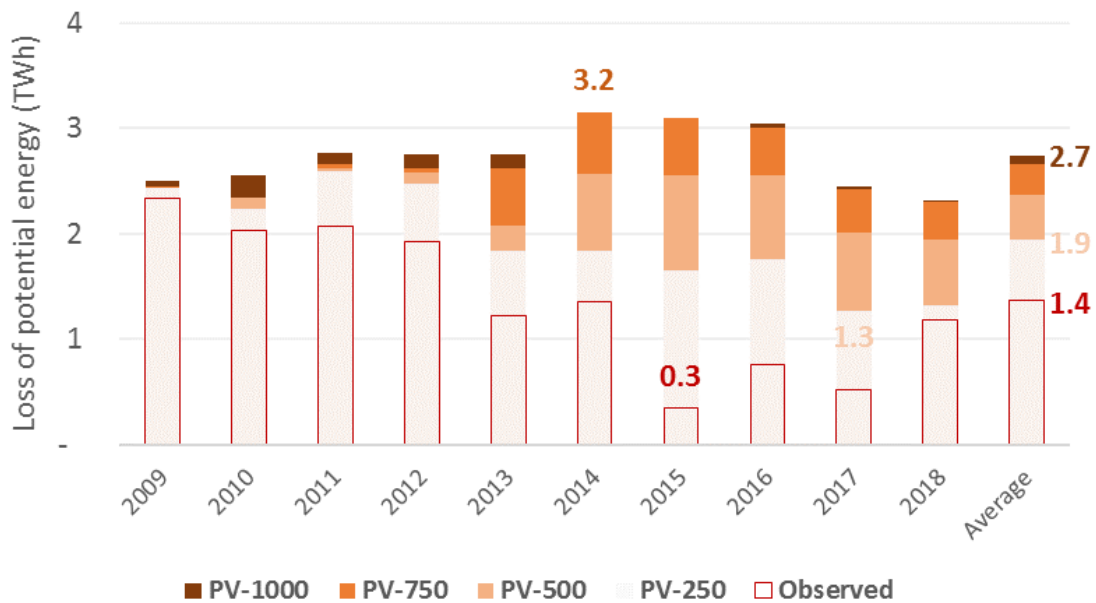
The evaporation from Sobradinho can assume the range of 73 m³/s for effective volume 0% to 234 m³/s for 100% (Figure 4.13). Provided that, part of the saved flow was turned into incremental evaporation, estimated at a rate of 17%. Considering that the downstream HPPs produce hydroelectricity in cascade, we assumed the incremental evaporation at Sobradinho as a loss of potential energy from the SF electric system. For each cubic meter released from Sobradinho, the productivity of this and the next HPPs was estimated by 729 Wh/m³, on average.

Figure 4.13 – Range of evaporation from Sobradinho reservoir related to the water storage.



The loss of potential energy depends on the baseline for evaporation used in the analysis. The comparison of the PV scenarios with the observed scenario resulted in a large increase in evaporation. Nevertheless, the flows of evaporation in the observed scenario were associated with low water storage levels, which stood as inappropriate for the purpose of the reservoir. Compared to the observed scenario, the incremental loss resulted in 0.6 (PV-250) to 1.4 TWh/year (PV-1000), on average, although it varied along the study period, as illustrated in Figure 4.14.

Figure 4.14 – Loss of potential energy by evaporation from Sobradinho reservoir for the simulated scenarios compared to the observed scenario, excepting the evaporation of dead volume condition.



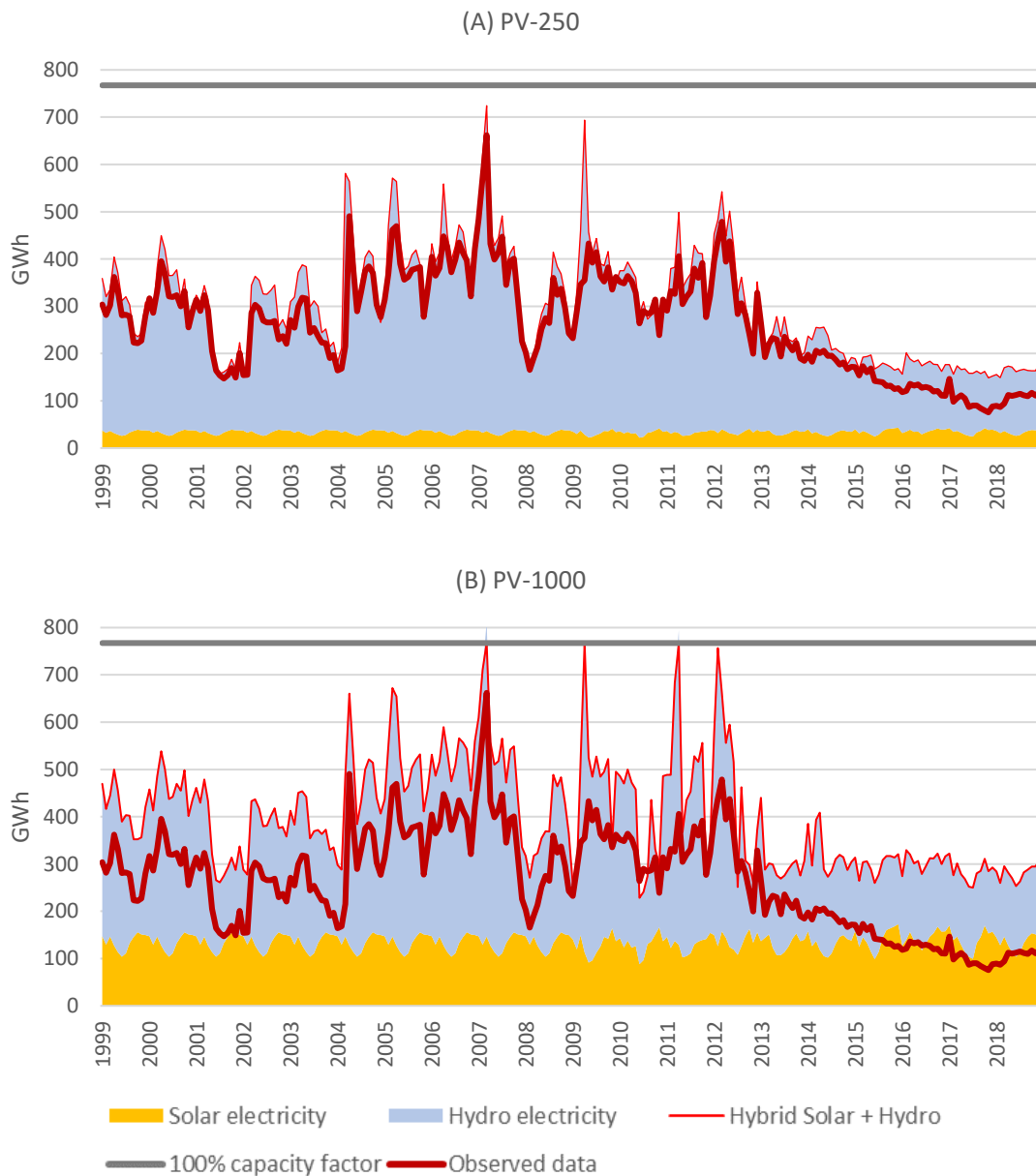
The estimated loss of potential energy explains the reduction in electricity outputs of the PV scenarios compared to the observed scenario (Figure 4.11-B). However, these indicators of energy loss should not represent the main result for decision-making or an aspect of disadvantage for adding solar power in the system as these results are related to years of water shortage. The spilled water occurred in conditions of water exceedance at Sobradinho reservoir, when the water storage was complete and the outflow was necessary. The evaporation needs to be particularly evaluated by studies on the optimization of water storage regarding the loss of potential energy from the SF system. Moreover, evaporation comprises the water cycle and implies ecological and local climate benefits, which were not approached in this study but can bring different perspectives for analyzing the results.

4.9 Effects of solar PV in typical and wet periods

As the study was carried out in a period of water scarcity, we also simulated the adoption of PV-250 and PV-1000 for the years 1999-2008 in order to identify the occurrence of potential energy losses by spilled water in typical and wet hydrologic conditions (Figure 4.15). Solar and hydropower were completely

harnessed, except in April 2007 for Scenario PV-1000, when spilled water was registered. The capacity factor of Sobradinho was improved from 0.40 in historical time series to 0.44 and 0.57, respectively for PV-250 and PV-1000, which expresses the potential gains of solar PV adding in periods not affected by drought. Solar sources can play a role in complementing the hydropower efficiency and the reduction in water availability at the São Francisco basin that occurred in the last decades.

Figure 4.15 - Monthly electricity output of Sobradinho hybrid power plant per energy source in scenario (A) PV-250 and (B) PV-1000 from 1999 to 2018 compared to the historical time-series (red bold line).



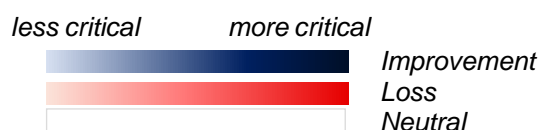
5 DISCUSSION

We simulated the use of solar power in the range of 50-1,000 MW to partially replace the hydropower generation and manage the water allocation among three large-scale reservoirs in cascade aiming to reduce water shortage over a severe drought in the semi-arid region of Brazil. The simulations revealed the potential influence of PV systems on water and energy resources at Sobradinho and São Francisco River in 2009-2018. The study was focused on analyzing the synergies and trade-offs on water and energy outputs, in local and regional spatial scales, instead of recommending a specific size of the PV power plant to solve resources shortages at the São Francisco River. The research framework was defined in the severe drought to provide information for stakeholders to better prepare for future climate conditions at semi-arid areas since projections point to an intensification of dry periods (IPCC, 2018). Nevertheless, the results must be interpreted as related to severe droughts, and their application for typical climatic periods needs to be properly balanced.

In the critical climatic conditions experienced in the period under investigation, clear benefits for water allocation could be identified by adding solar power, making this an advantageous strategy for human consumption, economic activities, and aquatic ecosystems. For those years, benefits were identified in the range of 250 to 1000 MW of installed power (Table 5.1); scenarios of PV systems with less installed power were insufficient to improve water security. Although water security was effectively improved by adding PV, it got limited by the total volume of available water in the system. The lack of precipitation was intense over the study timeframe and the reservoirs got depleted at Sobradinho by applying a constant outflow higher than 1,000 m³/s in the simulations. This value is equivalent to about half the historical average outflow. Consequently, the resolution established by the National Water Agency at 800 m³/s showed to be a necessary limitation, therefore, it was adopted as the minimum outflow to mitigate the most harmful ecological impacts.

Table 5.1 – Qualitative summary of indicators for the simulated PV scenarios. The colors express improvement (blue) or loss (red) compared to the observed scenario. The gradient expresses the intensity of the change.

Item	Indicator	PV			
		250	500	750	1000
1	Water security	+	++	+++	+++
2	Solar electricity	+	++	+++	++++
3	Hydroelectricity Sobradinho	o	o	o	o
	Hydroelectricity SFR	-	--	---	----
4	Sobradinho capacity factor	+	++	+++	++++
5	Total electricity Sobradinho	+	++	+++	++++
	Total electricity SFR	o	-	--	--
6	Water loss by evaporation	-	--	---	----
7	Energy loss by evaporation	-	--	---	----
8	Energy loss by spilled water	-	--	---	----



In the simulated scenarios, photovoltaic power plants at Sobradinho in the range of 250 to 1,000 MW achieved water storage levels higher than 40% of the effective volume during the driest years. The water storage increased from 0.1 years of the demand in the observed scenario to 0.7-2.3 years in the dry season of 2017, increasing the water security. It is important to note that the alleviation in supply conditions and the perception of water security during a drought period can also bring collateral effects (VAN OEL et al., 2018). The constant increase in the supply capacity creates a false perception of security in the use of water and offers for the demand side conditions to increase carelessly. Instead, the resources management needs to be jointly addressed on supply and demand sides by those responsible for water governance.

Besides the increase in storage of water to meet future demand, the shifts in water management could be associated with social, environmental, and economic aspects. The replacement of the lowest outflow of the historical dataset (550 m³/s) by a minimum of 800 m³/s would have allowed to: 1) maintain the

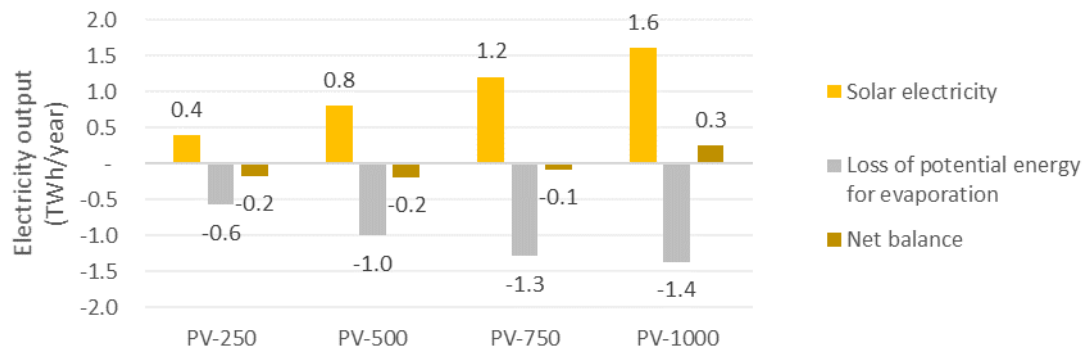
access of water downstream Sobradinho, since the infrastructure for withdrawals became inoperative when the riverbed reached low levels and 2) minimize the most harmful impacts in water quality and ecosystem conservancy (ANA, 2018b). First, the expending of the public sector on construction to provide water access reached ~US\$ 5.6 million in 2017, mainly for the reparation of the riverbed and reallocation of withdrawal equipment (CBHSF, 2020). Second, the negative impacts on the ecosystem involved higher salinity concentration, especially at the river mouth. FONSECA et al. (2020) and CAVALCANTE et al. (2020) analyzed the saline wedge at SFR, concluding that the salt concentration presented less amplitude over the tides and reached more than 10 km beyond the mouth of the river. The authors characterized the river flow pattern as unable to either avoid the estuarine plume or carry sediments from runoff and upstream. The negative impacts on water quality are probably long-lasting and cumulative in affecting human health, disturbing irrigated agriculture and pasture, and substituting aquatic communities and loss of species (VASCO; AGUIAR NETTO; SILVA, 2019). Although the four valid PV scenarios achieved increases in the river flow downstream Sobradinho, the pattern of water allocation responded differently in each scenario. There was a predominance of low values in dry seasons and high values in wet seasons when adopting the largest PV plants (Figure 4.3). The wide range in the streamflow influences the pattern of electricity dispatches and makes the HPPs operation more complex, compromising the energy security.

The electricity dispatches demonstrated the importance of assessing the system on different scales. At the local scale (Sobradinho), the PV scenarios increased the electricity output by 17-62% (Figure 4.11-A). At the regional scale (SFR), we identified up to 4.4% less electricity (Figure 4.11-B) lost by spilled water and incremental evaporation. Evaporation is the main factor of potential energy loss compared to the observed scenario: 86% in PV 250, 70% in PV-500, 65% in PV-750, and 62% in PV-1000. Although average results showed this loss of potential energy, more electricity was produced over the most critical years of the severe drought, from 2013-2018 (Figure 4.10). In those years, the solar adding would have maintained the prevalence of the renewable share and improved the energy security of the national electric grid.

In that period, Brazil experienced water scarcity in many HPPs leading to the use of thermal power to compensate for the hydropower shortages. The share of non-renewable energy increased from 14.5% in 2012 to 24.3% in 2014 (MME, 2019a). The dependence on thermal energy to meet the electricity demand implied two additional outcomes: socioeconomic implication, since incremental costs were transferred to the consumers (ANEEL, 2013), and environmental implication, as GHG emissions of the Brazilian electricity reached 0.136 tCO₂/MWh (71.0 MtCO₂) in 2014 (MCTI, 2020). Before, the GHG factor was registered by 0.025 tCO₂/MWh in 2009 and 0.065 tCO₂/MWh in 2012 (MCTI, 2020). In this aspect, the predominance of renewable energy and reduction of GHG emissions play a role in the international context as both collaborate on the Sustainable Development Goals (ONU, 2015) and Paris Agreement (MMA, 2017). Regarding the last one, the Brazilian Nationally Determined Contribution (NDC) committed to reducing emissions by 37% until 2025 and by 43% until 2030 based on the 2015 level (FED. REP. BRASIL, 2016).

Still in the approach of the energy side, we analyzed the net balance by comparing the electricity obtained from the PV panels with the loss of potential energy by incremental evaporation. For this estimate, we assumed that the additional water evaporated from the Sobradinho reservoir compared to the observed scenario would be turbinated at the HPPs Sobradinho, Itaparica, PAC, and Xingó. Scenario PV-1000 achieved additional gains of 0.3 TWh/year on the electric output, while the other scenarios presented an equivalence (Figure 5.1). Since the storage of water got limited and the evaporation of PV-750 and PV-1000 is comparable, this explains the gains in net balance of the last scenario.

Figure 5.1 – Net balance of solar electricity output considering the loss of potential energy for evaporation.



Although the loss of potential energy associated with evaporation from the Sobradinho reservoir implied an offset of solar adding in some scenarios, the hypothesis of this study is attached to improvements in water storage, turning the increase of evaporation into an intrinsic collateral effect. For comparison, the average evaporation from Sobradinho (excluding evaporation of inactive volume) in observed scenario and PV-1000 was comparable to the water demand from the reservoir, respectively, by 80% and 150%. The characteristics inherent to the semi-arid, the geometry of the lake, and the current engineering technology led to this outcome, which is complicated to avoid in the short term.

Alternatives to reduce evaporation are associated with controlling water storage. Several aspects need to be considered to optimize the reservoir and avoid losses by evaporation, for instance, the projection for demands and hydrological conditions of the basin in the long-term, or the productivity of the HPP and the associated evaporation based on different operative water levels. The restrictions in water storage possibly provide more energy by turbinating this amount of water instead of losing it by evaporation. Some studies investigated this type of water-energy trade-off: Basheer and Elagib (2018) quantified the ratio of energy generation and evaporation volume for several scenarios of maximum and minimum operation level for the Jebel Aulia reservoir, in Sudan, identifying an optimum operating level based on 1980-2009 dataset. CHARMCHI, IFAEI and YOO (2021) proposed a hydropower pinch point, which is a targeted level of water periodically set based on the projections for the water inputs and outputs.

Here, the PV contribution to the Sobradinho HPP can eventually enable the definition of an optimized operating level that concomitantly reduces evaporation.

Another opportunity for reducing evaporation is associated with the installation of the floating solar panels over the reservoirs by shadowing the water surface and shifting the water-atmosphere interface (SAHU; YADAV; SUDHAKAR, 2016; ROSA-CLOT; TINA, 2018). In this study, although the modules stand as a technical option to reduce evaporation, the proposed PV plants corresponded to a small portion of the Sobradinho's lake, which were admitted as neglectable. Alternatively, PV panels located in another reservoir in the SF cascade system or a diverse composition of HPPs would result differently. Moreover, the effect of local climatic conditions and the heat transfer between lake and solar panel needs to be measured to confirm the gains and losses in water balance.

Additionally, the intensification of water scarcity in semi-arid areas will probably evolve into negative effects on the energy sector (SCHAEFFER et al., 2012) since drought events are expected to become more frequent and severe due to global climate changes (IPCC, 2018). The HPPs consist of vast opportunities to optimize existing infrastructures and connect systems, exploring the complementarity of different sources into the energy supply. In this context, solar PV technology reduces the dependence on water and increases the diversification of energetic sources on the national grid. Moreover, converting HPPs into hybrid power plants by adding solar power can bring additional benefits and contributes to the route for sustainability pathways due to the presence of high irradiation in months of low cloudiness and, therefore, low precipitation; and by the management of available water under rules of governance that equalizes the multiple demands.

5.1 Opportunities and limitations for hybrid solar-hydro powerplants

Hybrid power plants combining solar and hydro resources are expected to bring benefits in three aspects: synergy in electricity generation, security for power intermittence, and optimization of existing infrastructure. In the first aspect, solar and hydro are complementary in hourly and seasonal management (BELUCO; KROEFF DE SOUZA; KRENZINGER, 2012; KOUGIAS et al., 2016). While PV

provides electricity during the day, the outflow can be restricted in this period, saving water to be harnessed during the night. This trade-off is relevant in Brazil because, since 2016, the peak-hour in electric consumption has been registered at 3 pm, when the incoming solar irradiance is the highest (PEREIRA et al., 2017). The trade-off is also found in seasonal variation, as irradiation presents a slight increase at the end of the dry season (PEREIRA et al., 2017), while the water storage in reservoirs is declining (ANA, 2019a). Furthermore, the role of solar power might be enhanced by climate change conditions in the Brazilian Northeastern region. Here, the presence of solar power to generate electricity is more certain than the presence of proper hydrologic conditions (MARENGO; BERNASCONI, 2014; ALVES et al., 2020).

The second aspect of intermittence remains an obstacle to the extensive adding of renewable sources such as solar, wind, and run-of-river HPPs into the electric systems. The low predictability of these energy resources increases the complexity of operating the grid (ONS, 2019b). Simultaneously, HPPs with reservoirs provide operation control by the characteristics of safe and rapid response (MME, 2018; SILVÉRIO et al., 2018). Thus, maintaining appropriate water levels in the reservoirs turns the HPPs into natural batteries to overcome the instant lack of generation from the solar source. The potential energy of HPPs creates the conditions to optimize the electric supply system, improve energy security, and reduce operational costs (DAVID; MOROMISATO, 2012). Therefore, the management of the existing reservoirs comes to be necessary under the growing share of renewable in the national grid and the uncertainties regarding hydropower plants to provide the historical amount of hydroelectricity under the conditions imposed by the global climate changes.

The third aspect is related to optimizing the existing infrastructure and avoiding socio-environmental impacts. One relevant aspect for the optimized HPP in Brazil is the fact that the potential sites for the construction of novel plants with reservoirs infers harmful socio-environmental impacts as these areas of interest are mostly environmentally protected or indigenous lands (MME, 2018). The land-use change by flooding vast areas and the collateral effects of the reservoirs in the ecosystem and social interactions of these protected regions enhance the

relevance of carefully managing the existing ones (PRADO JR et al., 2016). The recent expansion of the electric system focused on implementing run-of-river HPP, whose electricity needs to be immediately dispatched, similarly to solar and wind power. The conversion of existing infrastructure into hybrid power plants also benefits from economic and legal aspects regarding land property, settlements reallocation, and mitigation of socioenvironmental impacts. These aspects are estimated to participate in the construction cost of a power plant by 4-15% for conventional HPPs and by 0.4-1.9% for ground-mounted PV plants (MME, 2018). The floating PV systems may vary these percentual costs because, although land is already guaranteed, the floating system and the security of materials and components implies additional costs.

Another aspect is the sharing of the transmission lines, taking advantage of the seasonal generation and complementarity of hydro and solar power. In the observed scenario, the capacity factor of Sobradinho in the periods of highest hydroelectricity production was, on average, 0.55 in 2007 (ONS, 2019a), reaching 0.74 and 0.86, respectively in February and March (ONS, 2019a). In the PV scenarios, the capacity factor was improved by ~0.04 for every 250 MW. These values denote that the existing transmission lines were not an aspect of limitation for the size of PV plants simulated in this study. Instead, the solar electricity occupied the underused infrastructure to increment the regional power supply, consequently, avoiding additional losses of electricity transportation from other regions (MME, 2019a).

In the Brazilian electric grid, energy losses associated with electric power distribution reach ~20% and contribute to harm energy security (MME, 2020). Due to the size of the country, the origin and destiny of electricity dispatches can assume long distances, taking advantage of the integrated distribution system covering most of the national territory. The origin of the dispatches varies in time and space to prioritize the costs of electricity production (GODINHO; LIMA, 2020). Hence, the electricity generated in one region can be transmitted to another depending on the price of the electricity, the intensity of consumption, and the capacity of regional power plants to meet the demand. In the annual balance of 2011 to 2016, production was lower than consumption at the Brazilian

Northeast, and the region prevailed receiving electricity from North and Southeast. In 2013, for instance, the dispatches to the Northeastern region summed 28.7 GW (MME, 2019a). In this context, the predominance of regional transmissions can improve the performance of the electric grid.

5.2 Opportunities and limitations for large-scale PV power plant

The installation of solar PV is growing fast worldwide due to policy support, technological evolution, and the reduction of costs (IEA, 2020). In Brazil, the largest PV plant in operation is Pirapora Solar Complex, a 399 MW ground-mounted plant located at one side of SFR, 150 km downstream of Três Marias (IRENA, 2019). To provide a comparison, the wind power plants Pedra do Reino I and III, located near Sobradinho, started operating in 2015 with an installed capacity of 48 MW, producing 180 GWh/year, on average. Several aspects contribute to sorting the type of energy power, as availability of the energy source, availability of the technology, affordability, local climate pattern, efficiency, or jobs creation (IRENA, 2015; MME, 2018). At the SF basin, solar power represents an appropriate candidate due to the abundant solar irradiation and the social-driver potential of creating jobs that can advance the economic activities in the region. These jobs are focused on the assembling of the panels, construction, installation, and maintenance of the system (IRENA, 2019; ABSOLAR, 2020).

Regarding the financial feasibility of the simulated scenarios, a PV plant of 250 MW consisted of the minimum necessary to avoid water shortages in 2017. The investments for this plant would start at US\$ 0.43 billion, considering the average installation cost of 1.7 US\$/Wp (WB/ESMAP/SERIS, 2019). The Brazilian studies for energy expansion project the centralized PV to increase by 5,600 to 11,117 MW until 2029, with investments by the range of US\$ 3.7-5.0 billion (0.45-0.65 US\$/Wp) only at the Brazilian Northeastern region (MME/EPE, 2020). The costs for implementing the Belo Monte Hydropower, concluded in 2019, reached around US\$ 7.8 billion (PLANALTO, 2019b) for the installed capacity of 11,788 MW (0.7 US\$/Wp), and assured energy of 4,500 MW (1.7 US\$/Wp). Belo Monte Hydropower is composed of a 478 km² reservoir located inside the Amazon rainforest, at the Xingu River (Altamira city – Pará state). Another recent

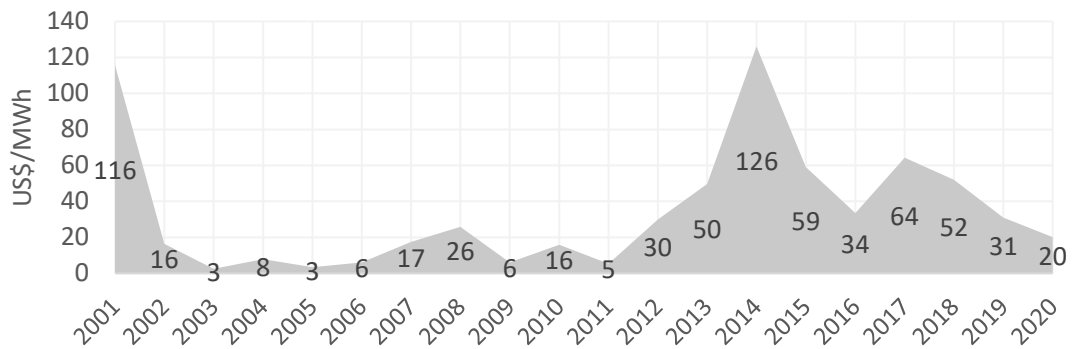
initiative was Santo Antonio HPP, a 546 km² reservoir installed at Madeira river (Porto Velho city – Rondônia state) with costs of US\$ 3.7 billion for the installed capacity of 3,568 MW (1.0 US\$/Wp), and assured energy of 2,424 MW (1.5 US\$/Wp) (FOLHA, 2021). Beyond the financial comparison, the electric expansion built on large-scale reservoirs brings a wide diversity of social and ecological consequences that must be embraced in future studies (PRADO JR et al., 2016; ATKINS, 2020).

If we now consider the correspondent investment in solar PV is dedicated to initiatives for controlling the demand, such as water use efficiency, water treatment, reuse technologies, and equipment to access groundwater, PV would probably benefit the served population. However, the existing infrastructure (for instance, DINC canals comprise ~900km and 39 pumping stations) is currently necessary to provide broad access to water, and it will take time to be replaced. Some scientists defend the deconstruction of some existing reservoirs (HOENKE; KUMAR; BATT, 2014; FOX; MAGILLIGAN; SNEDDON, 2016; O'HANLEY et al., 2020). However, the reservoirs of HPP are designed to minimize the effects of hydrological seasonality and absorb the potential conditions of the river flow for both water and energy supplies. One possibility to be investigated is the predominant use of PV, conducting a re-dimension of the water storage to operate dedicated to the water supply. Currently, if the investment is only dedicated to water management, the energy security would not be jointly improved, which is critically necessary as the demand for electricity in Brazil is estimated to increase by 3.8%/year for 2020-2029 (MME/EPE, 2020), and hydropower is not a warranted source in the future (DE JONG et al., 2018). Therefore, there is a need to optimize the existing supply services while implementing measurements on both supply and demand sides towards the shift to a sustainable pathway.

The electricity market is also an economic perspective that justifies the spending on solar power. However, the trade-offs from electricity costs were not approached in this study because the regulations on selling prices of electricity from hybrid systems are currently evolving in Brazil (ANEEL, 2020). Instead, we identified the existence of incremental costs of electricity over the severe drought

led by the powering of thermal power plants. In 2012-2018, the commercial value of the Northeastern sub-system resulted higher than 30 US\$/MWh, on an annual average, achieving 126 US\$/MWh in 2014 (Figure 5.2). Previously, this value only occurred in 2001, in a similar electric crisis in reason of water shortages in hydropower plants. The price reached ~100 US\$/MWh in 69 weeks, attaining the maximum value of ~150 US\$/MWh in 19 weeks (CCEE, 2020b).

Figure 5.2 – Commercial value⁸ of the electricity of the Northeastern sub-system.



Source: CCEE (2020).

The estimate of the electricity production cost in the life cycle of 25 years presumed for a 250 MW FPV plant resulted in 59 US\$/MWh, as detailed in Table 5.2. We considered an installation investment of US\$ 428 million, the average generation of 404 GW/year for the 25 years, and an annual cost ratio of 1,6% of the installation cost for operation and maintenance.

Table 5.2 - Installation and electricity production cost of the PV system in the simulated scenarios PV-250 and PV-1000.

Installed capacity	Intallation cost	O&M annual (1,6%)	Total cost (25 years life span)	Total energy in 25 years	Electricity production cost
MW	Million US\$	Million US\$	Million US\$	TWh	US\$/kWh
250	428	7	599	10.1	0.059
1000	1,711	27	2,395	40.4	

⁸ 1 US\$ = R\$ 5.35 (02/02/2021)

GODINHO and LIMA (2020) estimated that the adoption of thermal energy to provide electricity to the grid cost an additional US\$ 2.7 billion in the period 2013-2019, equivalent to the installation cost of ~1,500 MW in FPV. In a perspective of fuel expenses, natural gas was used in the public utility power plants to produce 424 TWh over 2009-2018, estimated to consume ~37 billion m³ of gas⁹ - from a consumption range of 706 Gm³ in 2009 to 6,093 Gm³ in 2014 - at a total cost¹⁰ of ~US\$ 19.7 billion. Considering the preceding installation of a 250 MW PV power plant, the total generation of ~4 TWh by solar source could have substituted ~1% of the natural gas. Assuming that, the spending on natural gas to generate the same amount of electricity of 250 MW is equivalent to ~43% of the PV installation cost while the potential benefits could have extended for additional 15 years. Besides, the shift of energy source could have mitigated the greenhouse gases (GHG) emissions by more than 580,000 tCO₂.

Accordingly, the technical and economic potential of the proposed solution is demonstrated by some aspects: the existence of a floating power plant currently in operational test at Sobradinho, the feasibility of the PV power plants at the range of 250-1000 MW, the adherent cost to the Brazilian projections to invest in the electric grid and the incremental costs for the electric sector caused by the incidence of severe droughts. Other technical solutions should be alternatively analyzed in terms of synergies and trade-offs such as the installation of distributed solar power plants. This PV category is rapidly evolving in the Brazilian electric market and the coordinated incentive can stand as a strategy to conserve more water in the existing reservoirs.

5.3 Opportunities and limitations for floating PV systems

The floating PV power plant is a technology emerging in scale since 2007. Some studies qualitatively accessed the potential advantages and disadvantages of the FPV to the water system and solar electricity output, which are listed in Table 5.3.

⁹ 11.55 MWh/10³m³

¹⁰ Annual average cost ranged from 411 to 625 US\$/10³m³ for 2009-2018 (MME, 2019b).

Table 5.3 – Potential advantages and disadvantages of the floating photovoltaic technology (FPV).

Potential advantages	<ul style="list-style-type: none"> • panels efficiency: the cooling effect of water surface increases the efficiency by ~12.5% (CHOI, 2014; SACRAMENTO et al., 2015; CAZZANIGA et al., 2018; LIU et al., 2018). PV systems perform better at lower and constant temperatures, and the losses in electricity production can be associated with 0.4–0.45%/°C for silicon crystalline, and 0.2%/°C for a-Si (CAZZANIGA et al., 2018). Sacramento et al. (2015) carried out an experiment with floating panels in a water tank at Brazilian Northeast (Ceará) and estimated differences in temperature from 14-22°C in the front and 17-24°C in the backside on the panels (air temperature ~31°C), leading to an increase in electricity generation by 9.5-14.5%; • maintenance: it reduces water withdrawals for cleaning panels, exempts clearing the vegetation of grounded areas, and the presence of water around reduces the dust deposition over the glasses (SAHU; YADAV; SUDHAKAR, 2016); • land-use change: it overlaps the water storage occupation and avoids the additional land use; • shadow: reduces the possibility of nearby landscape or built structures to compromise the light incidence (LIU et al., 2018); • evaporation: reduced under the PV modules area (50-90%), as the panels transform the interface water-atmosphere by shadowing the water, blocking the wind effect, and creating a convective air (vapor-saturated) around the system (SAHU; YADAV; SUDHAKAR, 2016; ROSA-CLOT; TINA, 2018). <p style="text-align: right;">(continues)</p>
-----------------------------	--

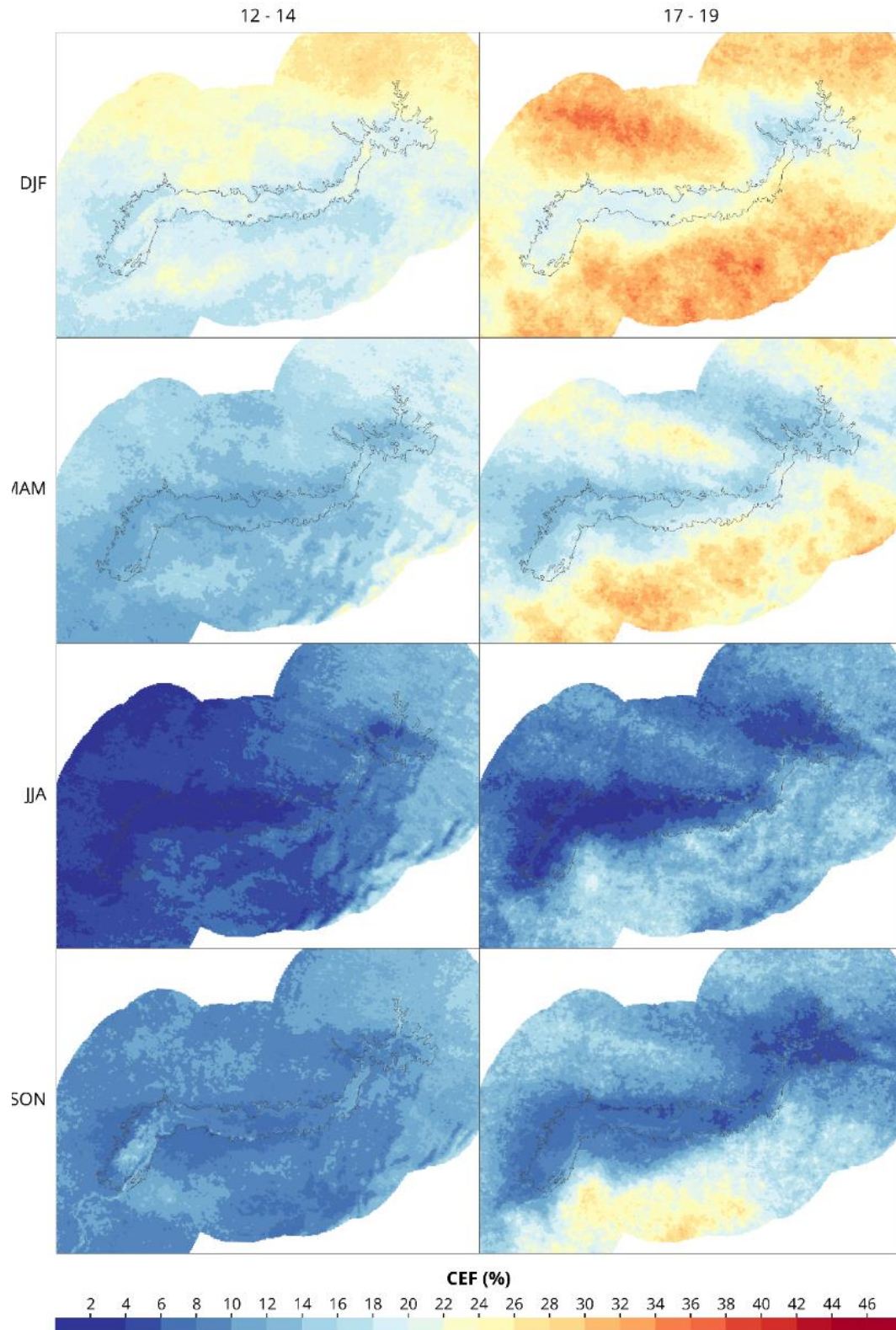
Table 5.3 – Conclusion.

Potential disadvantages	<ul style="list-style-type: none"> • lifetime of panels due to corrosion of metal parts in contact with water, ultraviolet exposure of floating structure (LIU et al., 2018), • panels break from thermal shocks (CAZZANIGA et al., 2018); • effect of moisture to the panel (SAHU; YADAV; SUDHAKAR, 2016); • fissure caused by vibration from water waves (SAHU; YADAV; SUDHAKAR, 2016); • installation and maintenance costs (SAHU; YADAV; SUDHAKAR, 2016), whereas additional components and security materials are demanded, such as floats, moorings, water-resistant electrical cables, and connectors (STIUBIENER et al., 2020), incrementing by 25-30% (FERRER-GISBERT et al., 2013; GORJIAN et al., 2020); R\$ 56 million were invested in the 2,5MWp FPV in test at Sobradinho (CHESF, 2020a); • Adoption of active mooring systems to adjust to water level changes along the year; • safety from electrical accidents or transmitting the power through the water body (SAHU; YADAV; SUDHAKAR, 2016); • disturbance on water quality, aquatic ecosystem, and biodiversity (SAHU; YADAV; SUDHAKAR, 2016); • contamination of water by chemical elements produced by PV modules degradation (LIU et al., 2018); • negative impacts on navigation, tourism, and landscape (STIUBIENER et al., 2020).
--------------------------------	---

FPV was conceptually selected because it responds to relevant issues of the region, which are discussed as follows. However, we did not quantify the effects of the presence of water on the solar output because the mutual influence of the panels and floating structure inside a reservoir still needs to be measured for specific climate conditions, equipment characteristics, and lake scale.

PV systems located inside the reservoirs are a promising solution for warm weather because the panels might benefit from the water-cooling effect and the reduced cloudiness over the lake. The influence of water bodies on the local environment, reducing the cloudiness and consequently increasing the irradiation over the water surface, was investigated for the Serra da Mesa reservoir, in Brazil (distant ~1,000 km from Sobradinho) (GONÇALVES et al., 2020). The authors quantified a reduction of 5.7% in cloudiness, with an average increase of solar irradiance by 1.73%. Preliminary satellite images of Sobradinho visually indicate differences between the effective cloud cover index (CEF) of the reservoir area and the surrounding dry land, as illustrated in Figure 5.3. This influencing factor needs to be evaluated and properly quantified for Sobradinho.

Figure 5.3 – Estimates of average cloud cover index (CEF) over the Sobradinho reservoir region for the two periods of the day (early and late afternoon) and season of the year [December, January, February (DJF); March, April, May (MAM); June, July, August (JJA); and September, October, November (SON)].



Source: INPE (2020).

Another advantage: PV panels can reduce water evaporation in the covered area (GONZALEZ SANCHEZ et al., 2021). In the case of Sobradinho, our preliminary analysis showed a negligible influence due to the small area covered by the simulated PV modules and floating system compared to the water surface of Sobradinho. Our estimate indicated that a PV system with the installed power capacity of 250 MW (~770,000 panels) occupies ~3.2 km², considering panel potential of 325 Wp, panel area of 2.0 m², and maintenance space between panels of 2.2 m² for each panel. Sobradinho reservoir has a minimum lake area of 1,250 km² when the effective storage is dried out (V=0%) and extends for 4,214 km² in full reservoir conditions (V=100%). Based on these values, the scenario of PV-250 would occupy around 0.25% of the minimum area or 0.075% of the complete lake. Table 5.4 details the estimate for the coverage area of Sobradinho lake and Figure 5.4 illustrates the insertion of the simulated floating PV power plants of 250 and 1000 MW over the Sobradinho lake in wet (2011) and dry years (2015 and 2016).

Table 5.4 – Size of the PV system for the simulated scenarios and the covering area of Sobradinho lake.

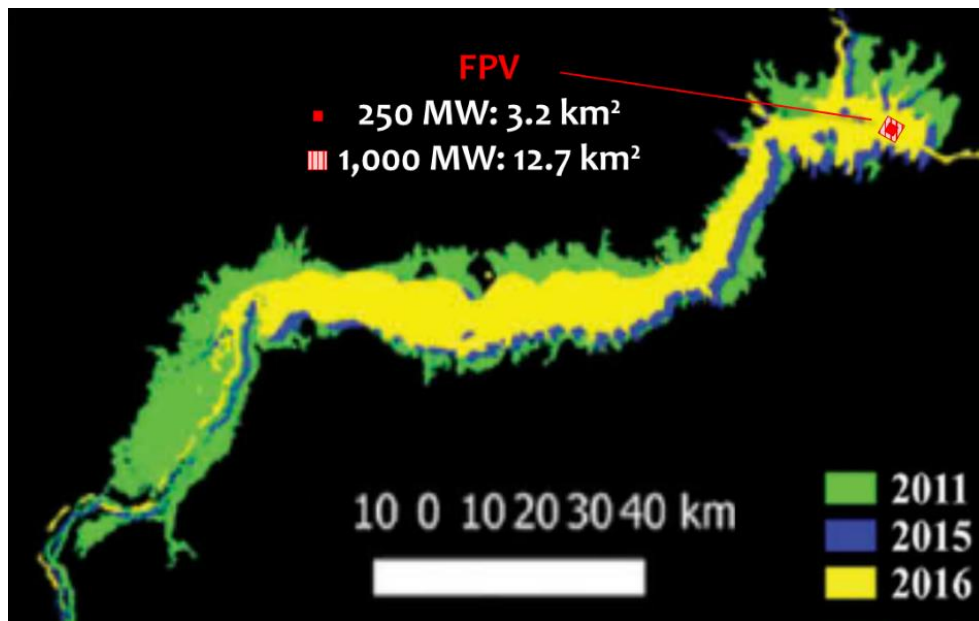
Installed capacity	Number of panels (325 Wp ¹)	PV system area ^{2,3}	Ratio of Sobradinho lake area	
			EV 0%	EV 100%
MW	Units	km ²		
250	769,231	3.2	0.25%	0.075%
500	1,538,462	6.4	0.51%	0.151%
750	2,307,692	9.5	0.76%	0.226%
1000	3,076,923	12.7	1.02%	0.302%

1 - Canadian Solar CS3U-325P - STC 325W PTC 300W - multi-c Si.

2 – Panel area: 2.0 m².

3 – Maintenance space between panels: 2.2 m²/panel.

Figure 5.4 - Size of the floating PV power plants with an installed capacity of 250 and 1,000 MW in simulated insertion at the Sobradinho lake for the relative area in October 2011, 2015, and 2016.



Source: Adapted from Azevedo et al. (2018).

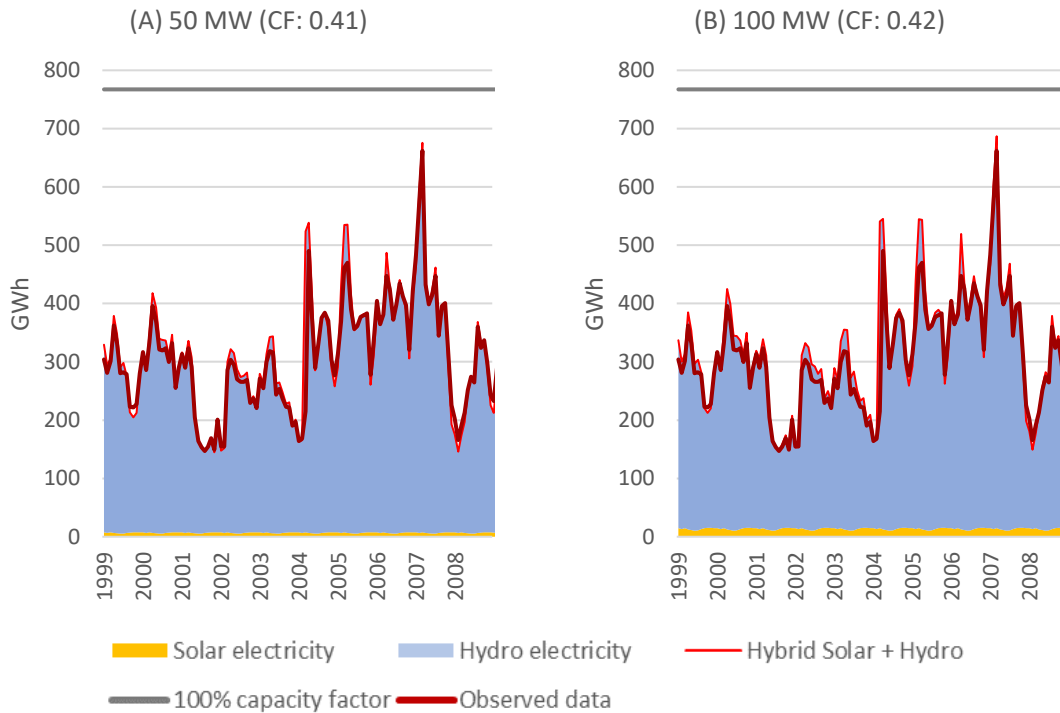
Hence, the area of the Sobradinho lake was not considered a limiting aspect for the proposed scenarios, although we acknowledge the necessity to assess the ecological impacts of panels, floats, and electrical cables for the ecosystem, aquatic life, and quality of water. The precise area of a PV system depends on an engineering project that specifies panels, their distribution, floating components, and materials; angle and position over the lake; presence of solar tracking or water veil-cooling, among other technical characteristics.

5.4 Opportunities and limitations for small-scale PV power plant

PV power plants with an installed capacity lower than 100 MW resulted insufficient to promote water security over the study period. However, it represents an opportunity to improve energy security in less intense dry seasons. To analyze the eventual gains, we simulated the adoption of the scenarios PV-50 and PV-100 from 1999 to 2008 (Figure 5.5). These PV plants generated 80 GWh/year for each 50 MW and produced, respectively, an additional 145 and 218 GWh/year summing solar and hydropower. The capacity factor increased from 0.40 in the observed scenario to 0.41 for PV-50 and 0.42 for PV-100. Losses

of potential energy by spilled water were not registered. Therefore, hybrid plants with small-scale solar PV bring the opportunity to increment electricity dispatches, optimize the HPP, and increase water allocation control.

Figure 5.5 - Monthly electricity output of Sobradinho hybrid power plant per energy source in scenario (A) PV-50 and (B) PV-100 from 1999 to 2008 compared to the historical time-series (red bold line).



5.5 Final remarks

Accordingly, Nexus studies provide information for managers, policymakers, scientific community, and the diversity of actors involved in the decision-making. The definition of the appropriate scenario is contingent upon the historical conditions of the basin and the expected goals. The simulated scenarios implied positive and negative impacts on water and energy securities, with secondary effects on social, environmental, and economic aspects. In addition to the results of the present study, the decisions need to be confronted with a broad series of supplementary information, for instance: trends in population, economic activities, and climatology; international commitments of sustainable development; governance structure; active policies that interfere in the use of resources; local, regional and national existing programs for water and energy

supply, and current measures to control water and energy demand. The pursuit of mutualism and synergies among sectors in the use of resources depends on the constant monitoring and evaluation – on multiple scales – of the conditions, actions, responses, and rebound effects.

5.6 Recommendations for future researches

This study presents an approach for integrated management of water and energy resources in scarce conditions by placing additional renewable energy sources in the existent infrastructure and changing the management of its capacity. Future studies can bring important contributions by advancing the investigation on:

- i. Quantify the optimal solar production in a range of projected climate and hydrological conditions under the influence of global environmental changes;
- ii. Measure the gains and losses in electricity generation of the floating PV system located inside the Sobradinho reservoir;
- iii. Analyze the viability and the water and energy outcomes of additionally adding the FPV power plant in the Três Marias and Itaparica reservoirs at São Francisco River;
- iv. Analyze scenarios for the hybrid power plant investigating the complementarity in the harness of hydro and solar energy sources, and minimizing water and energy losses by spilled water and evaporation;
- v. Assess the optimized operating level of Sobradinho reservoir that concomitantly guarantees the water security of the projected demand in the long-term and reduces losses by evaporation;
- vi. Analyze the potential gains of changing the water allocation based on the installation of distributed generation from PV power plants located in urban areas.

6 CONCLUSIONS

This study presents a scenario-based analysis of partly replacing hydroelectricity generation using solar power aiming to improve the water and energy management strategies for reservoirs operating in cascade at the São Francisco River, partially inserted in the Brazilian semi-arid region. This river provides water for human activities at the semi-arid portion of the basin, while the reservoirs that the river feeds represent ~15% of the water storage capacity of the national electric grid. Here, the recent events of drought and the climate projections indicate that the typical management of water and energy leads to sub-optimal outcomes. Hence, synergetic measurements of resources management need to be rapidly embraced to prepare for the future and minimize the most harmful social, environmental, and economic impacts, contributing to improvements on the Sustainable Development Goals, particularly SDG 6 and SDG 7.

The severity of the drought in the 2010s decade restricted the capacity to management the water of SFR. We estimated at 1,000 m³/s the maximum outflow from the Sobradinho reservoir to maintain water security as higher outflow values would deplete the effective water storage. This value is considerably lower than the authorized minimum operative outflow (ecological streamflow) of 1,300 m³/s that regulated the reservoir's operation before this severe drought. Considering that limit for the water availability, the operative rule of minimum outflow at 800 m³/s set by the National Water Agency was adopted in the scenarios under investigation because it enabled the increasing on water security in the critical climatic conditions of 2015 and 2017.

In this context, solar power stands as an alternative for saving water in reservoirs and reducing its use to produce energy. To carry out a sensitivity analysis on the adoption of solar power into a hydropower plant during a drought period, the solar FPV scenarios were proposed in the range of 50 to 1,000 MW of installed power and simulated for the years 2009 to 2018. The scenarios of 50 and 100 MW were insufficient to increase the water storage of Sobradinho and were classified as

invalid, while scenarios PV-250, PV-500, PV-750, and PV-1000 achieved benefits in water and energy security.

We adopted a solar-water equivalence to set the saved flow (Sobradinho outflow restriction) of the simulated scenarios. Based on the Sobradinho average productivity of 61.4 Wh/m^3 , the saved flow varied from $226 \text{ m}^3/\text{s}$ for the PV-250 to $904 \text{ m}^3/\text{s}$ for PV-1000 MW, respectively substituting 404 to 1,615 GWh, on average every year. The gains and losses of generating electricity by floating systems need to be properly quantified and were qualitatively discussed in this study.

The study demonstrated that the PV power plants could have played a significant role in water and energy security in this high-dependent water demand area during a severe drought event. Water security was improved at the Sobradinho reservoir by adopting PV power plants in the range of 250 to 1,000 MW, achieving 0.7-2.3 years of the water demand in the most critical year while electricity dispatches increased by 17-63%, on average. The largest simulated scenario occupied less than 1% of the Sobradinho lake area in a condition of absence of water.

Besides the local security in water and energy, the measure could produce collateral improvements in social, environmental, and economic aspects such as in-river water quality, ecological conservation, jobs and income creation, and the optimization of the existing infrastructure of water and energy supply. However, on a regional scale, as Sobradinho is part of a five-hydropower plant system in cascade, the total electricity output was maintained for the PV scenario of 250 MW but reduced by 4.4% for the scenario of 1000 MW. In scenarios higher than 500 MW, the solar power output was partially offset. These losses of water and potential energy are related to evaporation from the reservoirs and spilled water in the hydropower plants downstream Sobradinho. Despite this overall loss, a power generation increment was quantified in the critical years of the prolonged drought, which would have contributed to increase the renewable share of the grid. In fact, scenarios higher than 500 MW surpassed the hydroelectricity provided by Sobradinho in the critical dry months. This increase in energy output

over the severe drought follows the higher streamflow of the São Francisco River, attained by the release of water flow that was conserved in the reservoirs in the first years of the simulation. The higher streamflow is a required condition to mitigate the verified impacts in social, environmental, and economic aspects.

The most harmful impacts of electricity shortages in the grid would have been avoided by adding the solar PV system into Sobradinho HPP. The discussion section brings the opportunities of combining solar and hydro power regarding daily and seasonal complementarity. The control in the operation of the national grid provided by the water reserve, especially with the increase of renewable resources with characteristics of intermittance in producing electricity being introduced to the grid. Other aspect of discussion was focused on the optimization of the existing infrastructure for generating and transmitting electricity and, consequently, avoiding socio-environmental impacts related to the installation of new infrastructure.

On the economic side, the investments for each 250 MW of solar PV power plant costs around US\$ 0.43 billion. The Brazilian study for expanding the centralized PV proposes the installation of 1,000 MW/year in the years 2019-2029, with investments of US\$ 3.7-5.0 billion at the Brazilian Northeastern region. Therefore, the simulated scenarios show feasibility and adherence to the national plans for the Brazilian electric sector regarding both costs and installed power.

Moreover, solar PV was associated to a compensation on the emergency spending over the period of drought. For instance, the spending made on natural gas from 2009-2018 to generate electricity equivalent to the PV-250 MW summed ~43% of the installation cost. This shift in energetic source was able to mitigate greenhouse gases (GHG) emissions by more than 580,000 tCO₂.

Accordingly, as the potential complementarity of solar and hydropower is expected to be enhanced under future climatic conditions, the research provides information for actors responsible for the management of water and energy supply systems. The results subsidize these actors in comprehending the opportunities, limitations, and interlinkages across sectors towards the integrated governance and the development of appropriate public policies.

REFERENCES

ABSOLAR. **Energia solar vai gerar mais de 120 mil empregos no Brasil em 2020**. Available from: <<http://www.absolar.org.br/noticia/noticias-externas/energia-solar-vai-gerar-mais-de-120-mil-empregos-no-brasil-em-2020-projeta-absolar.html>>. Access on: 21 Jan. 2021.

AGÊNCIA NACIONAL DE ÁGUAS - ANA. **Resolução no 411 de 22 de setembro de 2005**. Available from: <<https://arquivos.ana.gov.br/resolucoes/2005/411-2005.pdf>>. Access on: 20 Mar. 2020

AGÊNCIA NACIONAL DE ÁGUAS - ANA. **Resolução nº 442, de 08 de abril de 2013**: dispõe sobre a redução temporária da descarga mínima defluente dos reservatórios de Sobradinho e Xingó, no rio São Francisco. 2013. Available from: <<http://arquivos.ana.gov.br/resolucoes/2013/442-2013.pdf>>. Access on: 13 Aug. 2020

AGÊNCIA NACIONAL DE ÁGUAS - ANA. **Resolução no 713, de 29 de junho de 2015**. 2015. Available from: <<https://arquivos.ana.gov.br/resolucoes/2015/713-2015.pdf>>. Access on: 6 Nov. 2020

AGÊNCIA NACIONAL DE ÁGUAS - ANA. **Demandas hídricas consuntivas**. Available from: <<http://metadados.ana.gov.br/geonetwork/srv/pt/main.home?uuid=4b9960a4-6436-43d7-9beb-bad256f090fc>>. Access on: 9 Aug. 2018a.

AGÊNCIA NACIONAL DE ÁGUAS - ANA. **Resolução no 1.283, de 31 de outubro de 2016**: dispõe sobre a redução temporária da descarga mínima defluente dos reservatórios de Sobradinho e Xingó, no rio São Francisco. 2016b. Available from: <<https://arquivos.ana.gov.br/resolucoes/2016/1283-2016.pdf>>. Access on: 6 Nov. 2020

AGÊNCIA NACIONAL DE ÁGUAS - ANA. **Conjuntura dos recursos hídricos no Brasil 2017: relatório pleno**. Brasília, 2017a. Available from:

<<http://www.snirh.gov.br/portal/snirh/centrais-de-conteudos/conjuntura-dos-recursos-hidricos>>.

AGÊNCIA NACIONAL DE ÁGUAS - ANA. **Atlas irrigação**: uso da água na agricultura irrigada. Brasília. 2017b. Available from:

<<http://atlasirrigacao.ana.gov.br/>>. Access on: 27 Apr. 2018.

AGÊNCIA NACIONAL DE ÁGUAS - ANA. **Resolução nº 1.291, de 17 de julho de 2017**. 2017c. Available from:

<<http://arquivos.ana.gov.br/resolucoes/2017/1291-2017.pdf>>. Access on: 13 Aug. 2020.

AGÊNCIA NACIONAL DE ÁGUAS - ANA. **Resolução nº 2.219, de 11 de dezembro de 2017 (Dia do Rio)**. Brasília, 2017d. Available from:

<<http://arquivos.ana.gov.br/resolucoes/2017/2219-2017.pdf?104339>>. Access on: 24 Feb. 2020.

AGÊNCIA NACIONAL DE ÁGUAS - ANA. **Resolução nº 2.081, de 04 de dezembro de 2017**: dispõe sobre as condições para a operação do Sistema Hídrico do Rio São Francisco, que compreende os reservatórios de Três Marias, Sobradinho, Itaparica (Luiz Gonzaga), Moxotó, Paulo Afonso I, II, III, IV e Xingó. 2017e. Available from:

<<http://arquivos.ana.gov.br/resolucoes/2017/2081-2017.pdf>>. Access on: 31 July 2020

AGÊNCIA NACIONAL DE ÁGUAS - ANA. **Sala de situação**: São Francisco.

Available from: <<https://www.ana.gov.br/sala-de-situacao/sao-francisco>>.

Access on: 1 May 2018a.

AGÊNCIA NACIONAL DE ÁGUAS - ANA. **Reunião de avaliação da bacia do rio São Francisco**. Available from: <www.youtube.com/user/anagovbr/videos>.

Access on: 1 May 2018b.

AGÊNCIA NACIONAL DE ÁGUAS - ANA. **HIDROWEB**: sistema de informações hidrológicas. Available from:

<http://www.snirh.gov.br/hidroweb/publico/mapa_hidroweb.jsf>. Access on: 21 Feb. 2019a.

AGÊNCIA NACIONAL DE ÁGUAS - ANA. **SAR - Sistema de Acompanhamento de Reservatórios**. Available from: <<http://sar.ana.gov.br/MedicaoSin>>. Access on: 21 Feb. 2019b.

AGÊNCIA NACIONAL DE ÁGUAS - ANA. **Conjuntura dos recursos hídricos no Brasil 2019**. Brasília. 2019c. Available from: <<http://conjuntura.ana.gov.br/>>. Access on: 18 Feb. 2020.

AGÊNCIA NACIONAL DE ÁGUAS - ANA. **Boletim de monitoramento dos reservatórios do Rio São Francisco**. 2020a. Available from: <<http://www3.ana.gov.br/portal/ANA/sala-de-situacao/sao-francisco/sao-francisco-boletim-mensal>>. Access on: 21 Nov. 2020.

AGÊNCIA NACIONAL DE ÁGUAS - ANA. **Conjuntura dos recursos hídricos no Brasil 2020**: informe anual. Brasília, 2020b. Available from: <<http://www3.snirh.gov.br/portal/snirh/centrais-de-conteudos/conjuntura-dos-recursos-hidricos/conjuntura-2020>>.

AGÊNCIA NACIONAL DE ÁGUAS - ANA. **Outorgas de direito de uso de recursos hídricos**. Available from: <<http://www3.ana.gov.br/portal/ANA/gestao-da-agua/outorga-e-fiscalizacao/principais-servicos/outorgas-emitidas/outorgas-emitidas>>. Access on: 20 Jan. 2020c.

AGÊNCIA NACIONAL DE ÁGUAS - ANA. **Projeto de Integração do rio São Francisco (PISF)**. Available from: <<https://www.gov.br/ana/pt-br/assuntos/seguranca-hidrica/pisf>>. Access on: 28 Nov. 2020d.

AGÊNCIA NACIONAL DE ÁGUAS - ANA. **Plano de Gestão Anual (PGA) do projeto de integração do rio São Francisco (PISF)**. Available from: <<https://www.ana.gov.br/regulacao/outorga-e-fiscalizacao/pisf/pga-pisf>>. Access on: 28 Nov. 2020e.

AGÊNCIA NACIONAL DE ENERGIA ELÉTRICA - ANEEL. **Resolução normativa nº 547, de 16 de abril de 2013**: estabelece os procedimentos comerciais para aplicação do sistema bandeiras tarifárias. ANEEL, 2013. Available from: <www.aneel.gov.br>. Access on: 17 Nov. 2020

AGÊNCIA NACIONAL DE ENERGIA ELÉTRICA - ANEEL. **Tratamento**

regulatório para implantação de usinas híbridas: consulta 061/2020. 2020. Available from: <<https://www.aneel.gov.br/consultas-publicas>>. Access on: 22 Jan. 2021.

AL-SAIDI, M.; RIBBE, L. **Nexus outlook:** assessing resource use challenges in the water, energy and food nexus. 2017. Available from: <www.water-energy-food.org/fileadmin/user_upload/files/documents/others/Outlook-Nexus_Assessing_Resource_Use_Challenges.pdf>.

ALVALÁ, R. C. S.; CUNHA, A. P. M. A.; BRITO, S. S. B.; SELUCHI, M. E.; MARENGO, J. A.; MORAES, O. L. L.; CARVALHO, M. A. Drought monitoring in the Brazilian Semiarid region. **Anais da Academia Brasileira de Ciências**, v. 91, Supp. 1, 2017.

ALVES, L. M.; CHADWICK, R.; MOISE, A.; BROWN, J.; MARENGO, J. A. Assessment of rainfall variability and future change in Brazil across multiple timescales. **International Journal of Climatology**, v. 41, n.S1, e 6818, 2020.

ATKINS, E. Contesting the 'greening' of hydropower in the Brazilian Amazon. **Political Geography**, v. 80, e102179, 2020.

AZEVEDO, S. C.; CARDIM, G. P.; PUGA, F.; SINGH, R. P.; SILVA, E. A. Analysis of the 2012-2016 drought in the northeast Brazil and its impacts on the Sobradinho water reservoir. **Remote Sensing Letters**, v. 9, n. 5, p. 438–446, 2018.

BAHRI, M. Analysis of the water, energy, food and land nexus using the system archetypes: a case study in the Jatiluhur reservoir, West Java, Indonesia. **Science of the Total Environment**, v. 716, e137025, 2020.

BASHEER, M.; ELAGIB, N. A. Sensitivity of water-energy nexus to dam operation: a water-energy productivity concept. **Science of the Total Environment**, v. 616–617, p. 918–926, 2018.

BASTO, I. D. R. G.; FONTES, A. S.; MEDEIROS, Y. D. P. Effects of an outflow regime adoption of the São Francisco river reservoir system to meet water demands for multiple uses. **Revista Brasileira de Recursos Hídricos**, v. 25, p. 1–22, 2020.

BAZILIAN, M.; ROGNER, H.; HOWELLS, M.; HERMANN, S.; ARENT, D.; GIELEN, D.; STEDUTO, P.; MUELLER, A.; KOMOR, P.; TOL, R. S. J.; YUMKELLA, K. K. Considering the energy, water and food nexus: towards an integrated modelling approach. **Energy Policy**, v. 39, n. 12, p. 7896–7906, 2011.

BELUCO, A.; KROEFF DE SOUZA, P.; KRENZINGER, A. A method to evaluate the effect of complementarity in time between hydro and solar energy on the performance of hybrid hydro PV generating plants. **Renewable Energy**, v. 45, p. 24–30, 2012.

BEZERRA, B. G.; SILVA, L. L.; SANTOS E SILVA, C. M.; DE CARVALHO, G. G. Changes of precipitation extremes indices in São Francisco River Basin, Brazil from 1947 to 2012. **Theoretical and Applied Climatology**, v. 135, n. 1–2, p. 565–576, 2019.

BIGGS, E. M.; BRUCE, E.; BORUFF, B.; DUNCAN, J. M. A.; HORSLEY, J.; PAULI, N.; MCNEILL, K.; NEEF, A.; VAN OGTROP, F.; CURNOW, J.; HAWORTH, B.; DUCE, S.; IMANARI, Y. Sustainable development and the water–energy–food nexus: a perspective on livelihoods. **Environmental Science & Policy**, v. 54, p. 389–397, 2015.

BRAMBILLA, M.; FONTES, A. S.; MEDEIROS, Y. D. P. Cost-benefit analysis of reservoir operation scenarios considering environmental flows for the lower stretch of the São Francisco River (Brazil). **Brazilian Journal of Water Resources**, v. 22, 2017.

BRASIL. FEDERATIVE REPUBLIC. **Intended nationally determined contribution**: towards achieving the objective of the United Nations framework convention on climate change. 2016. Available from: <https://www4.unfccc.int/sites/ndcstaging/PublishedDocuments/Brazil%20First/BRAZIL%20iNDC%20english%20FINAL.pdf>.

BRASIL. MINISTÉRIO DA AGRICULTURA, PECUÁRIA E ABASTECIMENTO - MAPA. **Plano nacional de desenvolvimento da fruticultura**. Brasília, 2018. Available from: <<http://www.agricultura.gov.br/noticias/mapa-lanca-plano-de-fruticultura-em-parceria-com-o-setor->

privado/PlanoNacionaldeDesenvolvimentodaFruticulturaMapa.pdf>. Access on: 8 Oct. 2018.

BRASIL. MINISTÉRIO DA CIÊNCIA, TECNOLOGIA E INOVAÇÃO - MCTI.

Fator médio: inventários corporativos. Available from:

<http://antigo.mctic.gov.br/mctic/opencms/ciencia/SEPED/clima/textogeral/emissao_corporativos.html>. Access on: 12 Nov. 2020.

BRASIL. MINISTÉRIO DE MINAS E ENERGIA - MME. **Anuário estatístico de energia elétrica 2018 - ano base 2017**. 2018. Available from

<<http://www.epe.gov.br/pt/publicacoes-dados-abertos/publicacoes/anuario-estatistico-de-energia-eletrica>>. Access on: 14 Jan. 2019.

BRASIL. MINISTÉRIO DE MINAS E ENERGIA - MME. **Balanco energético nacional 2019**. 2019. Available from:

<<http://www.epe.gov.br/pt/publicacoes-dados-abertos/publicacoes/balanco-energetico-nacional-2019>>. Access on: 31 July 2019.

BRASIL. MINISTÉRIO DE MINAS E ENERGIA - MME. **Plano decenal de expansão de energia 2029**. 2020. Available from:

<<https://www.epe.gov.br/pt/publicacoes-dados-abertos/publicacoes/plano-decenal-de-expansao-de-energia-2029>>. Access on: 3 dez. 2020.

BRASIL. MINISTÉRIO DE MINAS E ENERGIA - MME. **Plano nacional de energia 2050**. Brasília, 2018. Available from:

<http://www.mme.gov.br/secretarias/planejamento-e-desenvolvimento-energetico/publicacoes/relatorio-do-pne-2050/-/document_library_display/bGHIG0XSkBz4/recent?p_r_p_564233524_categoryId=&p_r_p_564233524_tag=>>. Access on: 27 Oct. 2020.

BRASIL. MINISTÉRIO DE MINAS E ENERGIA - MME. **Anuário estatístico de energia elétrica 2019 - ano base 2018**. Brasília, 2019a. Available from:

<https://www.epe.gov.br/sites-pt/publicacoes-dados-abertos/publicacoes/PublicacoesArquivos/publicacao-160/topico-168/Anuario_2019_WEB_alterado.pdf>. Access on: 27 Oct. 2020.

BRASIL. MINISTÉRIO DE MINAS E ENERGIA - MME. **Balanco energético**

nacional 2019 - ano base 2018. Brasília: MME, 2019b.

BRASIL. MINISTÉRIO DE MINAS E ENERGIA - MME. **Anuário estatístico de energia elétrica 2020 - ano base 2019**. Brasília, 2020. Available from: <[https://www.epe.gov.br/sites-pt/publicacoes-dados-abertos/publicacoes/PublicacoesArquivos/publicacao-160/topico-168/Anuário Estatístico de Energia Elétrica 2020.pdf](https://www.epe.gov.br/sites-pt/publicacoes-dados-abertos/publicacoes/PublicacoesArquivos/publicacao-160/topico-168/Anuário%20Estatístico%20de%20Energia%20Elétrica%202020.pdf)>. Access on: 27 Oct. 2020.

BRASIL. MINISTÉRIO DO MEIO AMBIENTE - MMA. **Caderno da região hidrográfica do São Francisco**. Brasília. 2006. Available from: <www.mma.gov.br/estruturas/161/_publicacao/161_publicacao03032011023538.pdf>. Access on: 17 Feb. 2020.

BRASIL. MINISTÉRIO DO MEIO AMBIENTE - MMA. **Acordo de Paris**. Available from: <<https://www.mma.gov.br/clima/convencao-das-nacoes-unidas/acordo-de-paris.html>>. Access on: 12 Nov. 2020.

BRASIL. PLANALTO. **Presidente aciona usina solar flutuante no Nordeste (Brasil)**. Available from: <<https://www.gov.br/planalto/pt-br/acompanhe-o-planalto/noticias/2019/08/presidente-aciona-usina-solar-flutuante-no-nordeste>>. Access on: 9 Oct. 2020a.

BRASIL. PLANALTO. **Governo aciona Belo Monte, a maior geradora de energia do Brasil**. Available from: <<https://www.gov.br/pt-br/noticias/energia-minerais-e-combustiveis/2019/07/governo-aciona-belo-monte-a-maior-geradora-de-energia-do-brasil>>. Access on: 19 July 2019b.

BRITO, S. S. B.; CUNHA, A. P. M. A.; CUNNINGHAM, C. C.; ALVALÁ, R. C.; MARENGO, J. A.; CARVALHO, M. A. Frequency, duration and severity of drought in the Semiarid Northeast Brazil region. **International Journal of Climatology**, v. 38, n. 2, p. 517–529, 2018.

CÂMARA DE COMERCIALIZAÇÃO DE ENERGIA ELÉTRICA - CCEE. **Leilões**. Available from: <https://www.ccee.org.br/portal/faces/oquefazemos_menu_lateral/leiloes?_adf.ctrl-state=7pdrtdqkbz_1&_afLoop=568310366034078#!%40%40%3F_afLoop%3D5>

68310366034078%26_adf.ctrl-state%3D7pdrtkbz_5%40collapseExampleCCEE_657102>. Access on: 26 Oct. 2020a.

CÂMARA DE COMERCIALIZAÇÃO DE ENERGIA ELÉTRICA - CCEE.

Informações ao mercado. Available from:

<[https://www.ccee.org.br/portal/faces/pages_publico/o-que-fazemos/infomercado?_adf.ctrl-](https://www.ccee.org.br/portal/faces/pages_publico/o-que-fazemos/infomercado?_adf.ctrl-state=13oc7b6en8_27&_afLoop=105788396253003#!)

[state=13oc7b6en8_27&_afLoop=105788396253003#!](https://www.ccee.org.br/portal/faces/pages_publico/o-que-fazemos/infomercado?_adf.ctrl-state=13oc7b6en8_27&_afLoop=105788396253003#!)>. Access on: 7 Apr. 2020b.

CARVALHO, C.; KIST, B. B.; BELING, R. R. **Anuário brasileiro de horti & fruti 2020**. Santa Cruz do Sul: Gazeta, 2020.

CAVALCANTE, G.; VIEIRA, F.; CAMPOS, E.; BRANDINI, N.; MEDEIROS, P. R. P. Temporal streamflow reduction and impact on the salt dynamics of the São Francisco River Estuary and adjacent coastal zone (NE/Brazil). **Regional Studies in Marine Science**, v. 38, e101363, 2020.

CAZZANIGA, R.; CICU, M.; ROSA-CLOT, M.; ROSA-CLOT, P.; TINA, G. M.; VENTURA, C. **Floating photovoltaic plants: performance analysis and design solutions: renewable and sustainable energy reviews**. [S.I.]: Elsevier, 2018.

CENTRO DE ESTUDOS AVANÇADOS EM ECONOMIA APLICADA - CEPEA. **Anuário 2019-2020: retrospectiva 2019 & perspectivas 2020**. [S.I.]: HF Brasil, 2020.

CHARMCHI, A. S. T.; IFAEI, P.; YOO, C. Smart supply-side management of optimal hydro reservoirs using the water/energy nexus concept: a hydropower pinch analysis. **Applied Energy**, v. 281, e116136, 2021.

CHOI, Y. K. A study on power generation analysis of floating PV system considering environmental impact. **International Journal of Software Engineering and its Applications**, v. 8, n. 1, p. 75–84, 2014.

COMITÊ DA BACIA HIDROGRÁFICA DO RIO SÃO FRANCISCO - CBHSF. **Deliberação CBHSF Nº 08, de 29 de julho de 2004**: define a disponibilidade hídrica, vazão máxima de consumo alocável, as vazões remanescentes média

e mínima ecológica na foz como parte integrante do Plano de Recursos Hídricos da Bacia Hidrográfica do Rio São Francisco. Available from: <<https://cbhsaofrancisco.org.br/documentacao/deliberacoes/>>. Access on: 24 Nov. 2020.

COMITÊ DA BACIA HIDROGRÁFICA DO RIO SÃO FRANCISCO - CBHSF. **Plano de recursos hídricos da Bacia Hidrográfica do Rio São Francisco 2016-2025**. Alagoas, 2016. Available from: <<http://cbhsaofrancisco.org.br/planoderecursoshidricos/relatorios/>>. Access on: 11 Sept. 2018.

COMITÊ DA BACIA HIDROGRÁFICA DO RIO SÃO FRANCISCO - CBHSF. **Projetos de recuperação hidroambiental do Comitê da Bacia Hidrográfica do Rio São Francisco (CBHSF)**. Available from: <<https://cbhsaofrancisco.org.br/acoes-e-projetos-do-cbhsf/projetos-de-recuperacao-hidroambiental-do-comite-do-sao-francisco/>>. Access on: 19 Sept. 2020.

COMPANHIA DE DESENVOLVIMENTO DOS VALES DO SÃO FRANCISCO E DO PARNAÍBA - CODEVASF. **Irrigação**. Available from: <<https://www.codevasf.gov.br/linhas-de-negocio/irrigacao>>. Access on: 5 Nov. 2020.

COMPANHIA HIDRO ELÉTRICA DO SÃO FRANCISCO - CHESF. **Usina solar flutuante de Sobradinho**. Available from: <<https://www.chesf.gov.br/pdi/Documents/Usina Solar Flutuante.pdf>>. Access on: 29 Oct. 2020a.

COMPANHIA HIDRO ELÉTRICA DO SÃO FRANCISCO - CHESF. **Sistema Chesf sistemas de geração**. Available from: <<https://www.chesf.gov.br/SistemaChesf/Pages/SistemaGeracao/SistemasGeracao.aspx>>. Access on: 6 Oct. 2018b.

COMPANHIA HIDRO ELÉTRICA DO SÃO FRANCISCO - CHESF. **Chesf energiza usina solar flutuante**. Available from: <https://www.chesf.gov.br/_layouts/15/chesf_noticias_farm/noticia.aspx?idnoticia=373>. Access on: 29 Oct. 2020.

COMPANHIA HIDRO ELÉTRICA DO SÃO FRANCISCO - CHESF. **Centro de referência em energia solar de Petrolina**. Petrolina. 2020. Available from: <https://www.chesf.gov.br/ImagensNoticias/Material_Institucional_CRESP.pdf>. Access on: 23 Apr. 2021.

CORREIA, M. F.; DA SILVA DIAS, M. A. F.; DA SILVA ARAGÃO, M. R. Soil occupation and atmospheric variations over Sobradinho Lake area. Part one: an observational analysis. **Meteorology and Atmospheric Physics**, v. 94, n. 1/4, p. 103–113, 2006.

CROOK, J. A.; JONES, L. A.; FORSTER, P. M.; CROOK, R. Climate change impacts on future photovoltaic and concentrated solar power energy output. **Energy and Environmental Science**, v. 4, n. 9, p. 3101–3109, 2011.

DAHER, B. T.; MOHTAR, R. H. Water–Energy–Food (WEF) nexus tool 2.0: guiding integrative resource planning and decision-making. **Water International**, v. 40, n. 5–6, p. 748–771, 2015.

DARGIN, J.; DAHER, B.; MOHTAR, R. H. Complexity versus simplicity in Water Energy Food nexus (WEF) assessment tools. **Science of the Total Environment**, v. 650, p. 1566–1575, 2019.

DAVID, G.; MOROMISATO, Y. **Programação dinâmica aplicada ao cálculo da energia firme de usinas hidrelétricas**. 2012. Available from: <<https://repositorio.ufjf.br/jspui/handle/ufjf/1931>>. Access on: 29 July 2020.

DE JONG, P.; TANAJURA, C. A. S.; SÁNCHEZ, A. S.; DARGAVILLE, R.; KIPERSTOK, A.; TORRES, E. A. Hydroelectric production from Brazil's São Francisco River could cease due to climate change and inter-annual variability. **Science of The Total Environment**, v. 634, p. 1540–1553, 2018.

DHIMISH, M. Thermal impact on the performance ratio of photovoltaic systems: a case study of 8000 photovoltaic installations. **Case Studies in Thermal Engineering**, v. 21, e100693, 2020.

DISTRITO DE IRRIGAÇÃO NICO COELHO - DINC. **Distrito de Irrigação Nilo Coelho**. Available from: <<https://www.dinc.org.br/>>. Access on: 18 Nov. 2019.

EMPRESA BRASILEIRA DE PESQUISA AGROPECUÁRIA - EMBRAPA.

Balanço hídrico do Submédio São Francisco. Available from: <<http://www.cpatsa.embrapa.br:8080/bhsf/index.php?opcao=precipitacao>>. Access on: 17 Feb. 2020.

FOOD AND AGRICULTURE ORGANIZATION - FAO. **The Water-Energy-Food nexus:** a new approach in support of food security and sustainable agriculture. Rome, 2014a. Available from: <www.fao.org/policy-support/resources/resources-details/en/c/421718/>. Access on: 30 Apr. 2018.

FOOD AND AGRICULTURE ORGANIZATION - FAO. **Walking the Nexus Talk:** assessing the Water-Energy-Food nexus in the context of the sustainable energy for all initiative. Rome, 2014b. Available from: <www.fao.org/3/a-i3959e.pdf>.

FERRER-GISBERT, C.; FERRÁN-GOZÁLVEZ, J. J.; REDÓN-SANTAFÉ, M.; FERRER-GISBERT, P.; SÁNCHEZ-ROMERO, F. J.; TORREGROSA-SOLER, J. B. A new photovoltaic floating cover system for water reservoirs. **Renewable Energy**, v. 60, p. 63–70, 2013.

FOLHA DE SÃO PAULO. Seca reduz água nas usinas, e custo para evitar apagão pode chegar a R\$ 6 bi. **A Folha de São Paulo**, 13 maio 2021. Available from: <https://www1.folha.uol.com.br/mercado/2021/03/seca-reduz-agua-nas-usinas-e-custo-para-evitar-apagao-chegaria-a-r-6-bi.shtml>.

FONSECA, S. L. M.; MAGALHÃES, A. A. J.; CAMPOS, V. P.; MEDEIROS, Y. D. P. Effect of the reduction of the outflow restriction discharge from the Xingó dam on water salinity in the lower stretch of the São Francisco River. **Revista Brasileira de Recursos Hídricos**, v. 25, 2020.

FOX, C. A.; MAGILLIGAN, F. J.; SNEDDON, C. S. “You kill the dam, you are killing a part of me”: dam removal and the environmental politics of river restoration. **Geoforum**, v. 70, p. 93–104, 2016.

FUNDAÇÃO CEARENSE DE METEOROLOGIA E RECURSOS HÍDRICOS - FUNCEME. **Fundação Cearense de Meteorologia e Recursos Hídricos**. Available from: <<http://www.funceme.br/>>.

GARCIA, M.; RIDOLFI, E.; DI BALDASSARRE, G. The interplay between

reservoir storage and operating rules under evolving conditions. **Journal of Hydrology**, v. 590, 2020.

GODINHO, G. C.; LIMA, D. A. Security of power supply in hydrothermal systems: assessing minimum storage requisites for hydroelectric plants. **Electric Power Systems Research**, v. 188, e106523, 2020.

GONÇALVES, A. R.; ASSIREU, A. T.; MARTINS, F. R.; CASAGRANDE, M. S. G.; MATTOS, E. V.; COSTA, R. S.; PASSOS, R. B.; PEREIRA, S. V.; PES, M. P.; LIMA, F. J. L.; PEREIRA, E. B. Enhancement of cloudless skies frequency over a large tropical reservoir in Brazil. **Remote Sensing**, v. 12, n. 17, e2793, 2020.

GONZALEZ SANCHEZ, R.; KOUGIAS, I.; MONER-GIRONA, M.; FAHL, F.; JÄGER-WALDAU, A. Assessment of floating solar photovoltaics potential in existing hydropower reservoirs in Africa. **Renewable Energy**, v. 169, p. 687–699, 2021.

GORJIAN, S.; SHARON, H.; EBADI, H.; KANT, K.; SCAVO, F. B.; TINA, G. M. Recent technical advancements, economics and environmental impacts of floating photovoltaic solar energy conversion systems. **Journal of Cleaner Production**, v. 278, e124285, 2020.

HAROU, J. J.; PULIDO-VELAZQUEZ, M.; ROSENBERG, D. E.; MEDELLÍN-AZUARA, J.; LUND, J. R.; HOWITT, R. E. Hydro-economic models: concepts, design, applications, and future prospects. **Journal of Hydrology**, v. 375, n. 3–4, p. 627–643, 2009.

HOENKE, K. M.; KUMAR, M.; BATT, L. A GIS based approach for prioritizing dams for potential removal. **Ecological Engineering**, v. 64, p. 27–36, 2014.

HOFF, H. **Understanding the nexus**. Stockholm, 2011. Available from: <http://wef-conference.gwsp.org/fileadmin/documents_news/understanding_the_nexus.pdf>.

HOWELLS, M.; HERMANN, S.; WELSCH, M.; BAZILIAN, M.; SEGERSTRÖM, R.; ALFSTAD, T.; GIELEN, D.; ROGNER, H.; FISCHER, G.; VAN

VELTHUIZEN, H.; WIBERG, D.; YOUNG, C.; ROEHRL, R. A.; MUELLER, A.; STEDUTO, P.; RAMMA, I. Integrated analysis of climate change, land-use, energy and water strategies. **Nature Climate Change**, v. 3, n. 7, p. 621–626, 2013.

HUANG, T.; YU, D.; CAO, Q.; QIAO, J. Impacts of meteorological factors and land use pattern on hydrological elements in a semi-arid basin. **Science of the Total Environment**, v. 690, p. 932–943, 2019.

HUNT, J. D.; BYERS, E.; RIAHI, K.; LANGAN, S. Comparison between seasonal pumped-storage and conventional reservoir dams from the water, energy and land nexus perspective. **Energy Conversion and Management**, v. 166, p. 385–401, 2018.

INSTITUTO BRASILEIRO DE GEOGRAFIA E ESTATÍSTICA - IBGE. **Produção agrícola municipal**. Available from: <<https://sidra.ibge.gov.br/>>. Access on: 30 Sept. 2019.

INSTITUTO NACIONAL DE METEOROLOGIA - INMET. **Clima no Brasil**. Available from: <<https://clima.inmet.gov.br/>>. Access on: 24 Feb. 2021.

INSTITUTO NACIONAL DE PESQUISAS ESPACIAIS - INPE. **SONDA - Sistema Nacional de Organização de Dados Ambientais**. Available from: <<http://sonda.ccst.inpe.br/>>. Access on: 7 Oct. 2020.

INTERNATIONAL ENERGY AGENCY - IEA. **World energy outlook 2016: excerpt - water-energy nexus**. 2016. Available from: <www.iea.org/publications/freepublications/publication/WorldEnergyOutlook2016ExcerptWaterEnergyNexus.pdf>. Access on: 20 Apr. 2018.

INTERGOVERNMENTAL PANEL ON CLIMATE CHANGE - IPCC. Impacts of 1.5°C Global Warming on Natural and Human Systems. In: HOEGH-GULDBERG, D.; JACOB, M.; TAYLOR, M.; BINDI, S.; BROWN, I.; CAMILLONI, A.; DIEDHIOU, R.; DJALANTE, K.; EBI, F.; ENGELBRECHT, J. G.; HIJIOKA, S.; MEHROTRA, A.; PAYNE, S. I.; SENEVIRATNE, A.; THOMAS, R.; WARREN, G. Z.; MASSON-DELMOTTE, V.; ZHAI, H. O.; PÖRTNER, D.; ROBERTS, J.; SKEA, P.R.; SHUKLA, A.; PIRANI, W.; MOUFOUMA-OKIA, C.;

PÉAN, R.; PIDCOCK, S.; CONNORS, J. B. R.; MATTHEWS, Y.; CHEN, X.; ZHOU, M. I.; GOMIS, E.; LONNOY, T.; MAYCOCK, M.; TIGNOR, T. W. (Ed.). **IPCC special report on the impacts of global warming of 1.5°C above pre-industrial levels and related global greenhouse gas emission pathways**. [S.l.]: IPCC, 2018.

INTERNATIONAL ENERGY AGENCY - IEA. **Renewables 2020: analysis and forecast to 2025**. 2020. Available from:

<<https://www.iea.org/reports/renewables-2020>>. Access on: 10 Nov. 2020.

INTERNATIONAL RENEWABLE ENERGY AGENCY - IRENA. **Renewable energy in the water, energy and food nexus**. 2015. Available from:

<<http://www.irena.org/publications/2015/Jan/Renewable-Energy-in-the-Water-Energy--Food-Nexus>>. Access on: 19 Apr. 2018.

INTERNATIONAL RENEWABLE ENERGY AGENCY - IRENA. **Renewable energy and jobs: annual review 2019**. 2019. Available from:

</publications/2019/Jun/Renewable-Energy-and-Jobs-Annual-Review-2019>. Access on: 21 Jan. 2021.

KONAR, M.; EVANS, T. P.; LEVY, M.; SCOTT, C. A.; TROY, T. J.; VÖRÖSMARTY, C. J.; SIVAPALAN, M. Water resources sustainability in a globalizing world: who uses the water? **Hydrological Processes**, v. 30, n. 18, p. 3330–3336, 2016.

KOUGIAS, I.; BÓDIS, K.; JÄGER-WALDAU, A.; MONFORTI-FERRARIO, F.; SZABÓ, S. Exploiting existing dams for solar PV system installations. **Progress in Photovoltaics: Research and Applications**, v. 24, n. 2, p. 229–239, 2015.

KOUGIAS, I.; SZABÓ, S.; MONFORTI-FERRARIO, F.; HULD, T.; BÓDIS, K. A methodology for optimization of the complementarity between small-hydropower plants and solar PV systems. **Renewable Energy**, v. 87, p. 1023–1030, 2016.

KURIAN, M. The water-energy-food nexus: trade-offs, thresholds and transdisciplinary approaches to sustainable development. **Environmental Science & Policy**, v. 68, p. 97–106, 2017.

KURIAN, M.; ARDAKANIAN, R. Institutional arrangements and governance

structures that advance the nexus approach to management of environmental resources. In: HÜLSMANN, S.; ARDAKANI, R. (Ed.). **Advancing a nexus approach to sustainable management of water, soil and waste: draft white book**. Switzerland: United Nations University (ONU-Flores), 2013.

KURIAN, M.; SUARDI, M.; ARDAKANI, R. **Nexus planning primer: lessons from case studies**. 2016. Available from: <<https://collections.unu.edu/view/UNU:3374#viewMetadata>>. Access on: 24 Apr. 2018.

LIMA, A. A. B.; ABREU, F. Sobradinho Reservoir: governance and stakeholders. In: TORTAJADA, C. (Ed.). **Increasing resilience to climate variability and change**. Singapore: Springer, 2016. p. 157–177.

LIMA, L. C.; FERREIRA, L. A.; MORAIS, F. H. B. L. Performance analysis of a grid connected photovoltaic system in northeastern Brazil. **Energy for Sustainable Development**, v. 37, p. 79–85, 2017.

LINK, P. M.; SCHEFFRAN, J.; IDE, T. Conflict and cooperation in the water-security nexus: a global comparative analysis of river basins under climate change. **Wiley Interdisciplinary Reviews: Water**, v. 3, n. 4, p. 495–515, 2016.

LIU, H.; KRISHNA, V.; LUN LEUNG, J.; REINDL, T.; ZHAO, L. Field experience and performance analysis of floating PV technologies in the tropics. **Progress in Photovoltaics: Research and Applications**, v. 26, n. 12, p. 957–967, 2018.

LIU, L.; WANG, Q.; LIN, H.; LI, H.; SUN, Q.; WENNERSTEN, R. Power generation efficiency and prospects of floating photovoltaic systems. In: ENERGY PROCEDIA, 2017. **Proceedings...** Elsevier, 2017.

LOPES, M. P. C.; ANDRADE NETO, S.; CASTELO BRANCO, D.; FREITAS, M. A. V.; FIDELIS, N. S. Water-energy nexus: floating photovoltaic systems promoting water security and energy generation in the semiarid region of Brazil. **Journal of Cleaner Production**, v. 273, p. 122010, 2020.

LORENZO, E. La energía que producen los sistemas fotovoltaicos conectados a la red: el mito del 1300 y “el cascabel del gato”. **Revista Era Solar**, n. 107, p. 22–28, 2002.

MANETA, M. P.; TORRES, M.; WALLENDER, W. W.; VOSTI, S.; KIRBY, M.; BASSOI, L. H.; RODRIGUES, L. N. Water demand and flows in the São Francisco River Basin (Brazil) with increased irrigation. **Agricultural Water Management**, v. 96, n. 8, p. 1191–1200, 2009.

MANNAN, M.; AL-ANSARI, T.; MACKEY, H. R.; AL-GHAMDI, S. G. Quantifying the energy, water and food nexus: a review of the latest developments based on life-cycle assessment. **Journal of Cleaner Production**, v.193, p.300-314, 2018.

MARENGO, J. A.; ALVES, L. M.; BESERRA, E. A.; LACERDA, F. F. **Variabilidade e mudanças climáticas no semiárido brasileiro: recursos hídricos em regiões áridas e semiáridas**. Campina Grande: Instituto Nacional do Semiárido, 2011. ISBN 978-85-64265-01-1.

MARENGO, J. A.; BERNASCONI, M. Regional differences in aridity/drought conditions over Northeast Brazil: present state and future projections. **Climatic Change**, v. 129, n. 1–2, p. 103–115, 2014.

MARENGO, J. A.; CHOU, S. C.; KAY, G.; ALVES, L. M.; PESQUERO, J. F.; SOARES, W. R.; SANTOS, D. C.; LYRA, A. A.; SUEIRO, G.; BETTS, R.; CHAGAS, D. J.; GOMES, J. L.; BUSTAMANTE, J. F.; TAVARES, P. Development of regional future climate change scenarios in South America using the Eta CPTEC/HadCM3 climate change projections: climatology and regional analyses for the Amazon, São Francisco and the Paraná River basins. **Climate Dynamics**, v. 38, n. 9–10, p. 1829–1848, 2012.

MARENGO, J. A.; CUNHA, A. P.; ALVES, L. M. A seca de 2012-15 no semiárido do Nordeste do Brasil no contexto histórico. **Climanálise**, 2016.

MARENGO, J. A.; CUNHA, A. P. M. A.; NOBRE, C. A.; RIBEIRO NETO, G. G.; MAGALHAES, A. R.; TORRES, R. R.; SAMPAIO, G.; ALEXANDRE, F.; ALVES, L. M.; CUARTAS, L. A.; DEUSDARÁ, K. R. L.; ÁLVALA, R. C. S. Assessing drought in the drylands of northeast Brazil under regional warming exceeding 4 °C. **Natural Hazards**, v. 103, n. 2, p. 2589–2611, 2020.

MARENGO, J. A.; TORRES, R. R.; ALVES, L. M. Drought in Northeast Brazil—

past, present, and future. **Theoretical and Applied Climatology**, v. 129, n. 3–4, p. 1189–1200, 2017.

MARENGO, J.; ALVES, L.; ALVALA, R.; CUNHA, A. P.; BRITO, S.; MORAES, O. Climatic characteristics of the 2010-2016 drought in the semiarid Northeast Brazil region. **Anais da Academia Brasileira de Ciências**, v.90, Supp.1, 2017.

MAUÉS, J. A. Floating solar PV-hydroelectric power plants in Brazil: energy storage solution with great application potential. **International Journal of Energy Production and Management**, v. 4, n. 1, p. 40–52, 2019.

MEKONNEN, M. M.; HOEKSTRA, A. Y. **Value of water research: the water footprint of electricity from hydropower** Value of Water. [S.l.: s.n.], 2011.

MOHTAR, R. H.; DAHER, B. Water, energy, and food: the ultimate nexus. In: LOGAN JUNIOR, E.; HELDMAN, D.R.; MORARU, C. I. (Ed.). **Encyclopedia of agricultural, food, and biological engineering**. 2.ed. New York: Taylor and Francis, 2012.

MORIASI, D. N.; GITAU, M. W.; PAI, N.; DAGGUPATI, P. Hydrologic and water quality models: performance measures and evaluation criteria. **Transactions of the ASABE**, v. 58, n. 6, p. 1763–1785, 2015.

NASH, J.E.; SUTCLIFFE, J.V. River flow forecasting through conceptual models part I: a discussion of principles. **Journal of Hydrology**, v. 10, n. 3, p. 282-290, 1970.

NATIONAL DROUGHT MITIGATION CENTER - NDMC. **SPI generator**.

University of Nebraska-Lincoln, 2020. Available from:

<<https://drought.unl.edu/droughtmonitoring/SPI/SPIProgram.aspx>>.

NHAMO, L.; NDLELA, B.; NHEMACHENA, C.; MABHAUDHI, T.; MPANDELI, S.; MATCHAYA, G.; NHAMO, L.; NDLELA, B.; NHEMACHENA, C.; MABHAUDHI, T.; MPANDELI, S.; MATCHAYA, G. The water-energy-food nexus: climate risks and opportunities in Southern Africa. **Water**, v. 10, n. 5, p. 567, 2018.

NICOLÁS-MARTÍN, C.; SANTOS-MARTÍN, D.; CHINCHILLA-SÁNCHEZ, M.; LEMON, S. A global annual optimum tilt angle model for photovoltaic generation

to use in the absence of local meteorological data. **Renewable Energy**, v. 161, p. 722–735, 2020.

O'HANLEY, J. R.; POMPEU, P. S.; LOUZADA, M.; ZAMBALDI, L. P.; KEMP, P. S. Optimizing hydropower dam location and removal in the São Francisco river basin, Brazil to balance hydropower and river biodiversity tradeoffs. **Landscape and Urban Planning**, v. 195, p. 103725, 2020.

OPERADOR NACIONAL DO SISTEMA ELÉTRICO - ONS. **Plano anual da operação energética (PEN 2011)**: volume I - relatório executivo. 2011. Available from: <<http://www.ons.org.br/paginas/conhecimento/acervo-digital/documentos-e-publicacoes?categoria=Relatório+PEL>>. Access on: 18 Sept. 2020.

OPERADOR NACIONAL DO SISTEMA ELÉTRICO - ONS. **Histórico da operação do Sistema interligado Nacional (SIN)**. Available from: <<http://www.ons.org.br/paginas/resultados-da-operacao/historico-da-operacao>>. Access em: 18 Feb. 2019a.

OPERADOR NACIONAL DO SISTEMA ELÉTRICO - ONS. **Plano da operação energética 2019/2023 - PEN 2019**. 2019b. Available from: <[http://www.ons.org.br/AcervoDigitalDocumentosEPublicacoes/PEN_Executivo_2019-2023.pdf#search=PEN 2019 - Sumário Executivo](http://www.ons.org.br/AcervoDigitalDocumentosEPublicacoes/PEN_Executivo_2019-2023.pdf#search=PEN%2019%20-%20Sum%C3%A1rio%20Executivo)>. Access on: 12 Nov. 2020.

OPERADOR NACIONAL DO SISTEMA ELÉTRICO - ONS. **Geração de energia**. Available from: <http://ons.org.br/Paginas/resultados-da-operacao/historico-da-operacao/geracao_energia.aspx>. Access on: 30 Sept. 2018c.

OPERADOR NACIONAL DO SISTEMA ELÉTRICO - ONS. **Personal communication** (field work). 2019d.

ORGANIZAÇÃO DAS NAÇÕES UNIDAS - ONU. **Sustainable development goals: 17 goals to transform our world**. Available from: <www.un.org/sustainabledevelopment/>. Access on: 26 Apr. 2018.

PEREIRA, B.; MEDEIROS, P.; FRANCKE, T.; RAMALHO, G.; FOERSTER, S.;

DE ARAÚJO, J. C. Assessment of the geometry and volumes of small surface water reservoirs by remote sensing in a semi-arid region with high reservoir density. **Hydrological Sciences Journal**, v. 64, n. 1, p. 66–79, 2019.

PEREIRA, E. B.; MARTINS, F. R.; GONÇALVES, A. R.; COSTA, R. S.; LIMA, F. J. L.; RÜTHER, R.; ABREU, S. L.; TIEPOLO, G. M.; PEREIRA, S. V.; SOUZA, J. G. **Atlas Brasileiro de Energia Solar**. São José dos Campos: [s.n.], 2017.

PEREIRA, S. B.; PRUSKI, F. F.; SILVA, D. D.; RAMOS, M. M. Evaporação líquida no lago de Sobradinho e impactos no escoamento devido à construção do reservatório. **Revista Brasileira de Engenharia Agrícola e Ambiental**, v. 13, n. 3, p. 346–352, 2009.

PRADO JUNIOR, F. A.; ATHAYDE, S.; MOSSA, J.; BOHLMAN, S.; LEITE, F.; OLIVER-SMITH, A. How much is enough? an integrated examination of energy security, economic growth and climate change related to hydropower expansion in Brazil. **Renewable and Sustainable Energy Reviews**, v.6, p.1132-1136, 2016.

QUANSAH, D. A.; ADARAMOLA, M. S. Assessment of early degradation and performance loss in five co-located solar photovoltaic module technologies installed in Ghana using performance ratio time-series regression. **Renewable Energy**, v. 131, p. 900–910, 2019.

RANJBARAN, P.; YOUSEFI, H.; GHAREHPETIAN, G. B.; ASTARAEI, F. R. A review on floating photovoltaic (FPV) power generation units. **Renewable and Sustainable Energy Reviews**, v.110, p.332-347, 2019.

REICH, N. H.; MUELLER, B.; ARMBRUSTER, A.; VAN SARK, W. G. J. H. M.; KIEFER, K.; REISE, C. Performance ratio revisited: Is PR > 90% realistic? In: **PROGRESS IN PHOTOVOLTAICS: RESEARCH AND APPLICATIONS**, 2012. **Proceedings...** John Wiley & Sons, 2012. Available from: <<https://onlinelibrary.wiley.com/doi/full/10.1002/pip.1219>>. Access on: 7 Oct. 2020

RIBEIRO NETO, A.; DA PAZ, A. R.; MARENGO, A. R.; CHOU, J. A.

Hydrological processes and climate change in hydrographic regions of Brazil. **Journal of Water Resource and Protection**, v. 8, p. 1103–1127, 2016.

RISING, J. Decision-making and integrated assessment models of the water-energy-food nexus. **Water Security**, v. 9, 2020.

ROSA-CLOT, M.; TINA, G. M. Floating plants and environmental aspects. In: _____ (Ed.). **Submerged and floating photovoltaic systems**. [S.l.]: Elsevier, 2018. p. 185–212.

RUFFATO-FERREIRA, V.; DA COSTA BARRETO, R.; OSCAR JÚNIOR, A.; SILVA, W. L.; DE BERRÊDO VIANA, D.; DO NASCIMENTO, J. A. S.; DE FREITAS, M. A. V. A foundation for the strategic long-term planning of the renewable energy sector in Brazil: hydroelectricity and wind energy in the face of climate change scenarios. **Renewable and Sustainable Energy Reviews**, v. 72, p. 1124–1137, 2017.

RÜTHER, R.; REINDL, T.; NOBRE, A. M.; ANTONIOLLI, A. F. A Review on grid-connected PV systems in Brazil including system performance. In: EUROPEAN PHOTOVOLTAIC SOLAR ENERGY CONFERENCE AND EXHIBITION, 29., 2014. **Proceedings...** 2014. p. 2747–2752.

SACHS, I.; SILK, D. **Food and energy**: strategies for sustainable development. Food-Energy Nexus Programme. Tokyo: United Nations University, 1990. 83 p.

SACRAMENTO, E. M.; CARVALHO, P. C. M.; DE ARAÚJO, J. C.; RIFFEL, D. B.; CORRÊA, R. M. C.; PINHEIRO NETO, J. S. Scenarios for use of floating photovoltaic plants in Brazilian reservoirs. **IET Renewable Power Generation**, v. 9, n. 8, p. 1019–1024, 2015.

SAHU, A.; YADAV, N.; SUDHAKAR, K. Floating photovoltaic power plant: a review. **Renewable and Sustainable Energy Reviews**, v.66, p.815-824, 2016.

SANTOS, J. A. F. A.; DE JONG, P.; ALVES DA COSTA, C.; TORRES, E. A. Combining wind and solar energy sources: potential for hybrid power generation in Brazil. **Utilities Policy**, v. 67, p. 101084, 2020.

SCANLON, B. R.; RUDELL, B. L.; REED, P. M.; HOOK, R. I.; ZHENG, C.; TIDWELL, V. C.; SIEBERT, S. The food-energy-water nexus: transforming

science for society. **Water Resources Research**, v. 53, n. 5, p. 3550–3556, 2017.

SCHAEFFER, R.; SZKLO, A. S.; PEREIRA DE LUCENA, A. F.; MOREIRA CESAR BORBA, B. S.; PUPO NOGUEIRA, L. P.; FLEMING, F. P.; TROCCOLI, A.; HARRISON, M.; BOULAHYA, M. S. Energy sector vulnerability to climate change: a review. **Energy**, v.38, n.1, p.1-12, 2012.

SCOTT, C. A.; KURIAN, M.; WESCOAT, J. L. The water-energy-food nexus: enhancing adaptive capacity to complex global challenges. In: KURIAN, M.; ARDAKANIAN, R. (Ed.). **Governing the nexus**. Cham: Springer, 2015. p. 15–38.

SCOTT, C. A.; ZILIO, M. I.; HARMON, T.; TERAN, A. Z.; CARAVANTES, R. D.; HOYOS, N.; PERILLO, G. M. E.; MEZA, F.; VARADY, R. G.; RIBEIRO NETO, A.; VELEZ, M. I.; MARTÍN, F.; ESCOBAR, J.; PICCOLO, M. C.; MUSSETTA, P.; MONTENEGRO, S.; RUSAK, J. A.; PINEDA, N. Do ecosystem insecurity and social vulnerability lead to failure of water security? **Environmental Development**, v.38, e100606, 2020.

SENGUPTA, M.; HABTE, A.; WILBERT, S.; GUEYMARD, C.; REMUND, J. **Best practices handbook for the collection and use of solar resource data for solar energy applications**. 3.ed. 2021. Available from: <www.nrel.gov/publications>. Access on: 27 Apr. 2021.

SILVA, D.F.; GALVÍNCIO, J.D.; NOBREGA, R.S. Influência da variabilidade climática e da associação de fenômenos climáticos sobre sub-bacias do rio São Francisco. **Revista Brasileira de Ciências Ambientais**, n. 19, p. 46-56, 2011.

SISTEMA DE GESTÃO DA GEOINFORMAÇÃO - SIGEO. **Shapes disponibilizados pelo Comitê da BH do Rio São Francisco**. Available from: <<https://sosgisbr.com/2011/07/11/shapes-disponibilizados-pelo-comite-da-bh-do-rio-sao-francisco/>>. Access on: 5 July 2018.

SILVÉRIO, N. M.; BARROS, R. M.; TIAGO FILHO, G. L.; REDÓN-SANTAFÉ, M.; SANTOS, I. F. S.; VALÉRIO, V. E. M. Use of floating PV plants for coordinated operation with hydropower plants: case study of the hydroelectric

plants of the São Francisco River basin. **Energy Conversion and Management**, v. 171, p. 339–349, 2018.

SOLAR IRRADIANCE DATA - SOLARGIS. **Solar irradiance data**. Available from: <<https://solargis.com/>>. Access on: 24 Nov. 2020.

SRINIVASAN, V.; SETO, K. C.; EMERSON, R.; GORELICK, S. M. The impact of urbanization on water vulnerability: a coupled human–environment system approach for Chennai, India. **Global Environmental Change**, v. 23, n. 1, p. 229–239, 2013.

STIUBIENER, U.; CARNEIRO DA SILVA, T.; TRIGOSO, F. B. M.; BENEDITO, R. DA S.; TEIXEIRA, J. C. PV power generation on hydro dam's reservoirs in Brazil: a way to improve operational flexibility. **Renewable Energy**, v. 150, p. 765–776, 2020.

SUPERINTENDÊNCIA DO DESENVOLVIMENTO DO NORDESTE - SUDENE. **Resolução n ° 107/2017**: - delimitação do semiárido brasileiro. 2017. Available from: <www.sudene.gov.br>. Access on: 6 Nov. 2018

TANIGUCHIA, M.; ENDO, A.; GURDAK, J. J.; SWARZENSKI, P. Water-energy-food nexus in the Asia-Pacific region. **Journal of Hydrology: Regional Studies**, v. 11, p. 1–8, 2017.

UNITED NATIONS - UN. **Water security and the global water agenda**: a UN-Water analytical brief. 2013. Available from: <www.unwater.org/publications/water-security-global-water-agenda>.

UNITED NATIONS - UN. **The 17 goals**: sustainable development. Available from: <<https://sdgs.un.org/goals>>. Access on: 12 Nov. 2020.

U. S. DEPARTMENT OF ENERGY - USDE. **Valuation of energy security for the United States**. Washington, DC, 2017. Available from: <[www.energy.gov/sites/prod/files/2017/01/f34/Valuation of Energy Security for the United States %28Full Report%29_1.pdf](http://www.energy.gov/sites/prod/files/2017/01/f34/Valuation_of_Energy_Security_for_the_United_States_Full_Report_1.pdf)>. Access on: 27 Apr. 2018.

VAN LOON, A. F.; GLEESON, T.; CLARK, J.; VAN DIJK, A. I. J. M.; STAHL, K.; HANNAFORD, J.; DI BALDASSARRE, G.; TEULING, A. J.; TALLAKSEN, L. M.; UIJLENHOET, R.; HANNAH, D. M.; SHEFFIELD, J.; SVOBODA, M.;

VERBEIREN, B.; WAGENER, T.; RANGECROFT, S.; WANDERS, N.; VAN LANEN, H. A. J. **Drought in the anthropocene**. [S.l]: Nature Publishing, 2016.

VAN OEL, P. R.; MARTINS, E. S. P. R.; COSTA, A. C.; WANDERS, N.; VAN LANEN, H. A. J. Diagnosing drought using the downstreamness concept: the effect of reservoir networks on drought evolution. **Hydrological Sciences Journal**, v. 63, n. 7, p. 979–990, 2018.

VAN OEL, P. R.; ODONGO, V. O.; MULATU, D. W.; MUTHONI, F. K.; NDUNGU, J. N.; OGADA, J. O.; VAN DER VEEN, A. Supporting IWRM through spatial integrated assessment in the Lake Naivasha basin, Kenya. **International Journal of Water Resources Development**, v. 30, n. 3, p. 605–618, 2014.

VARIS, O.; KESKINEN, M.; KUMMU, M. Four dimensions of water security with a case of the indirect role of water in global food security. **Water Security**, v. 1, p. 36–45, 2017.

VASCO, A. N.; AGUIAR NETTO, A. O.; SILVA, M. G. The influence of dams on ecohydrological conditions in the São Francisco River Basin, Brazil. **Ecohydrology and Hydrobiology**, v.19, n.4, p.556-565, 2019.

VELLOSO, M. F. A.; MARTINS, F. R.; PEREIRA, E. B. Case study for hybrid power generation combining hydro- and photovoltaic energy resources in the Brazilian semiarid region. **Clean Technologies and Environmental Policy**, v.21, 2019.

VIEIRA, N. P. A.; BUENO, E. O.; PEREIRA, S. B.; DE MELLO, C. R. Water footprint of the sobradinho hydropower plant, Northeastern Brazil. **Revista Ambiente e Agua**, v. 13, n. 3, 2018.

VIEIRA, N. P. A.; PEREIRA, S. B.; MARTINEZ, M. A.; SILVA, D. D.; SILVA, F. B. Estimativa da evaporação nos reservatórios de Sobradinho e Três Marias usando diferentes modelos. **Engenharia Agrícola**, v. 36, n. 3, p. 433–448, 2016.

VIVIESCAS, C.; LIMA, L.; DIUANA, F. A.; VASQUEZ, E.; LUDOVIQUE, C.; SILVA, G. N.; HUBACK, V.; MAGALAR, L.; SZKLO, A.; LUCENA, A. F. P.;

SCHAEFFER, R.; PAREDES, J. R. Contribution of variable renewable energy to increase energy security in Latin America: complementarity and climate change impacts on wind and solar resources. **Renewable and Sustainable Energy Reviews**, v. 113, p. 109232, 2019.

WATER EVALUATION AND PLANNING SYSTEM - WEAP. **WEAP**: user guide. 2015. Available from: <<https://www.weap21.org/index.asp?action=208>>. Access on: 2 Nov. 2018.

WORLD BANK. . **Where Sun meets water**: floating solar market report. Washington, DC, 2019. Available from: <<http://documents1.worldbank.org/curated/en/670101560451219695/pdf/Floating-Solar-Market-Report.pdf>>. Access on: 3 Dec. 2020.

WORLD ECONOMIC FORUM - WEF. **Global risks report 2020**. 2020. Available from: <<http://reports.weforum.org/global-risks-report-2020/>>. Access on: 4 Nov. 2020.

YATES, D.; SIEBER, J.; PURKEY, D.; HUBER-LEE, A. WEAP21: a demand-, priority-, and preference-driven water planning model. Part 1: model characteristics. **Water International**, v. 30, n. 4, p. 487–500, 2005.

APPENDIX A - WATER EVALUATION AND PLANNING (WEAP) MODELING

The main model programming, input dataset and results extracted from the WEAP are presented in this section.

Figure A.1 – WEAP general rules for water allocation.

Inflows And Outflows Of Water

This step computes water inflows to and outflows from every node and link in the system for a given month. This includes calculating withdrawals from supply sources to meet demand. A linear program (LP) is used to maximize satisfaction of requirements for demand sites, user-specified instream flows, and hydropower generation, subject to demand priorities, supply preferences, mass balance and other constraints. The LP solves the set of simultaneous equations explained below. For details of how demand priorities and supply preferences affect calculations, see [Priorities for Water Allocation](#).

Mass balance equations are the foundation of WEAP's monthly water accounting: total inflows equal total outflows, net of any change in storage (in reservoirs, aquifers and catchment soil moisture). Every node and link in WEAP has a mass balance equation, and some have additional equations which constrain their flows (e.g., inflow to a demand site cannot exceed its supply requirement, outflows from an aquifer cannot exceed its maximum withdrawal, link losses are a fraction of flow, etc.).

Priorities For Water Allocation

WEAP uses three user-defined priority systems to determine allocations from supplies to demand sites and catchments (for irrigation), for instream flow requirements, and for filling reservoirs and generating hydropower: Demand Priority, Supply Preference, and Distribution Order.

Demand Priority

Competing demand sites and catchments, reservoir filling and hydropower generation, and flow requirements are allocated water according to their **demand priorities**. The demand priority is attached to the demand site, catchment, reservoir (priority for filling Conservation Zone, filling Buffer Zone, or generating hydropower), or flow requirement, and can be changed by right clicking on it and selecting General Info. By default, priorities can range from 1 to 99, with 1 being the highest priority and 99 the lowest, although you can change the lowest priority in [Basic Parameters](#). Reservoir filling priorities default to 99, meaning that they will fill only if water remains after satisfying all other higher priority demands. (Hydropower priorities for individual reservoirs are set in the Data View under [Reservoir Hydropower](#). To set a system hydropower priority, go to the Supply and Resources branch in the Data View.) Many demand sites can share the same priority. These priorities are useful in representing a system of water rights, and are also important during a water shortage, in which case higher priorities are satisfied as fully as possible before lower priorities are considered. If priorities are the same, shortages will be equally shared. Typically, you would assign the highest priorities (lowest priority number) to critical demands that must be satisfied during a shortfall, such as a municipal water supply. You may change the priorities over time or from one scenario to another.

Distribution Order

Additionally, if you want to be able to distribute differing amounts to branches within a demand site or catchment in case of shortage, you can set a **distribution order** for each branch. The distribution order does not affect how much water gets allocated to each demand site and catchment, only how the demand site or catchment distributes its allocation internally to its sub-branches. By default, this option is turned off; to turn it on, go to [Basic Parameters](#). Then, [set the distribution order](#) for each demand branch. Enter data at any level of the Data Tree. A value entered at one level will be used by all branches at lower levels, unless a value has also been entered at the lower level. Leave all blank to allocate to all branches equally. If coverage < 100%, WEAP will allocate water first to branches with distribution order 1, then second to order = 2, third to order 3, etc. If multiple branches have the same order, they will get the same percentage of their demand met. For catchments, these allocations will be used to calculate the soil moisture balance. If the demand site as a whole has 100% coverage, then each branch will also have 100% coverage. If the "Distribution Order" option has been turned on in Basic Parameters, three new reports will be available in the Results View, detailing how the water has been distributed within the demand sites: Supply Delivered by Branch, Unmet Demand by Branch, and Coverage by Branch.

Water demand

Figure A.2 – Method for data input and allocation on water demand.

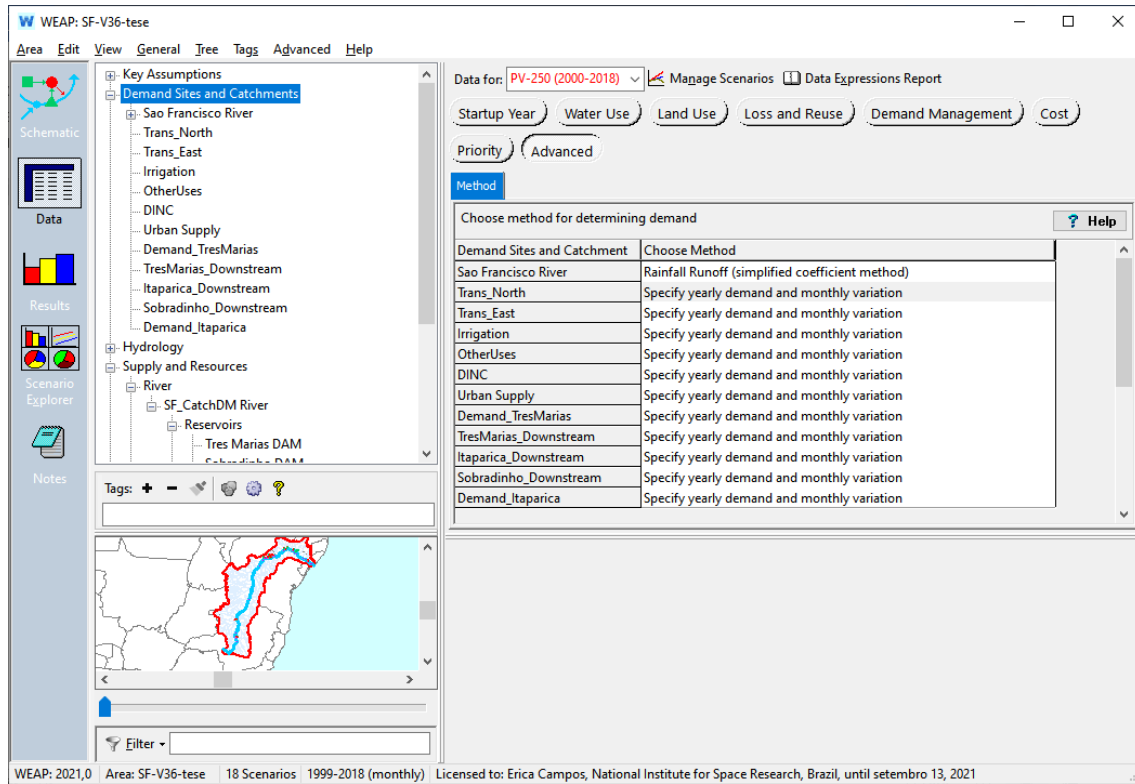
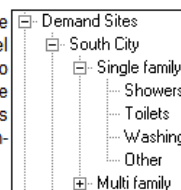


Figure A.3 – Method for quantifying the water demand.

Annual Demand

A demand site's (DS) demand for water is calculated as the sum of the demands for all the demand site's bottom-level branches (Br). A bottom-level branch is one that has no branches below it. For example, in the structure shown at the right, Showers, Toilets, Washing and Other (and four others underneath Multifamily that are not shown) are the bottom-level branches for South City.



$$AnnualDemand_{DS} = \sum_{Br} (TotalActivityLevel_{Br} \times WaterUseRate_{Br})$$

Figure A.4 – Data for annual activity level of water demand.

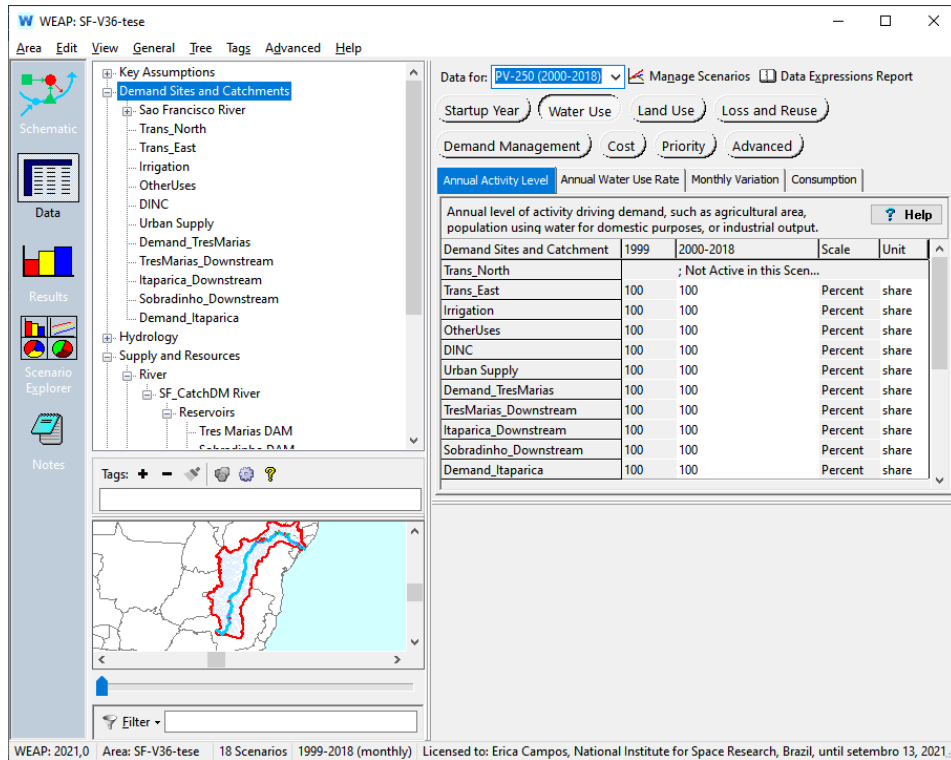
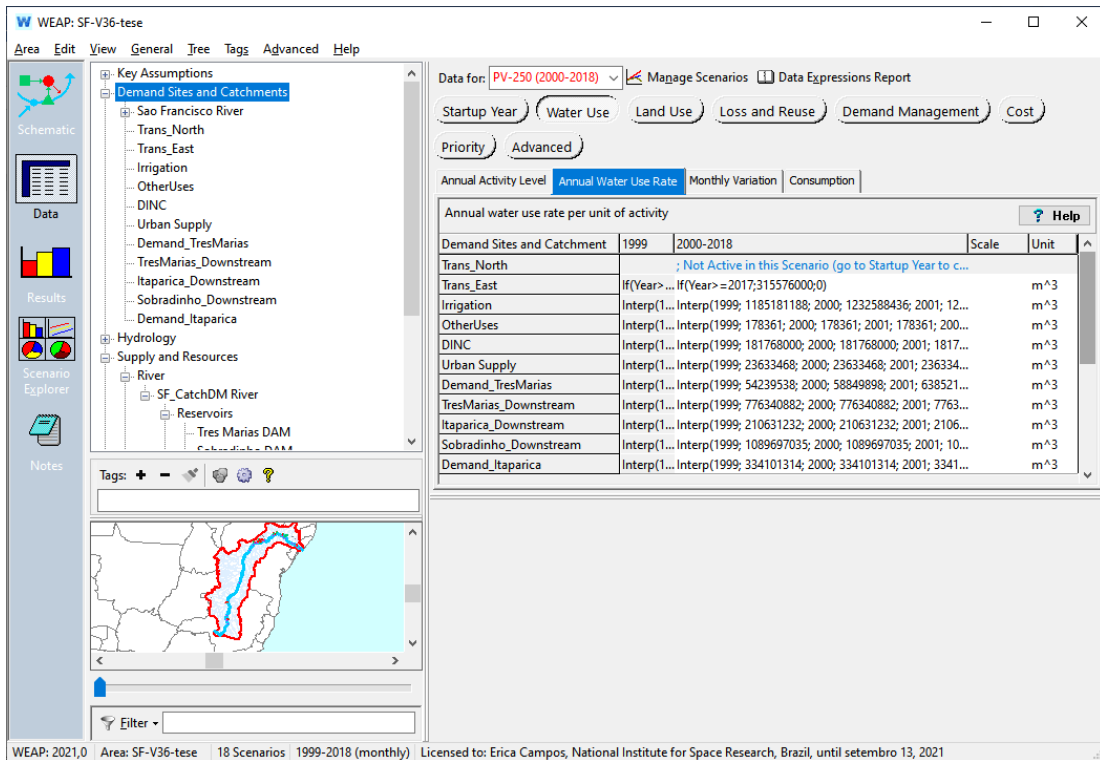


Figure A.5 – Data for annual water use rate.



Input dataset:

Trans_East: If (Year>=2017;315576000;0)

Irrigation (Sobradinho): Interp(1999; 1185181188; 2000; 1232588436; 2001; 1281891973; 2002; 1333167652; 2003; 1386494358; 2004; 1441954132; 2005; 1499632298; 2006; 1559617589; 2007; 1614034298; 2008; 1609848223; 2009; 2238051199; 2010; 2251584449; 2011; 1192445793; 2012; 1185181188; 2013; 2457588359; 2014; 2481506161; 2015; 2780917246; 2016; 2008978304; 2017; 2278733821; 2018; 2325450544)

Other Uses (Sobradinho): Interp(1999; 178361; 2000; 178361; 2001; 178361; 2002; 178361; 2003; 178361; 2004; 178361; 2005; 178361; 2006; 178361; 2007; 178361; 2008; 207893; 2009; 207893; 2010; 57893; 2011; 271053; 2012; 346613; 2013; 39821693; 2014; 39836093; 2015; 40024157; 2016; 40207144; 2017; 40277111; 2018; 40301518)

DINC (Sobradinho): Interp(1999; 181768000; 2000; 181768000; 2001; 181768000; 2002; 181768000; 2003; 181768000; 2004; 181768000; 2005; 181768000; 2006; 183414000; 2007; 216483000; 2008; 202661000; 2009; 168768000; 2010; 257780000; 2011; 221253000; 2012; 320646000; 2013; 326015962; 2014; 277580000; 2015; 310059000; 2016; 348295000; 2017; 393853000; 2018; 328188000)

Urban Supply (Sobradinho): Interp(1999; 23633468; 2000; 23633468; 2001; 23633468; 2002; 23633468; 2003; 23633468; 2004; 23633468; 2005; 23633468; 2006; 23633468; 2007; 23633468; 2008; 23633468; 2009; 23633468; 2010; 38416275; 2011; 37712524; 2012; 71040933; 2013; 64566101; 2014; 22911005; 2015; 18968775; 2016; 20521452; 2017; 18445298; 2018; 48106599)

Demand_TresMarias: Interp(1999; 54239538; 2000; 58849898; 2001; 63852140; 2002; 69279572; 2003; 75168335; 2004; 81557644; 2005; 88490043; 2006; 96011697; 2007; 104172691; 2008; 113027370; 2009; 122634697; 2010; 133058646; 2011; 144368631; 2012; 156639964; 2013; 169954361; 2014; 184400482; 2015; 200074523; 2016; 217080857; 2017; 235532730; 2018; 256625120)

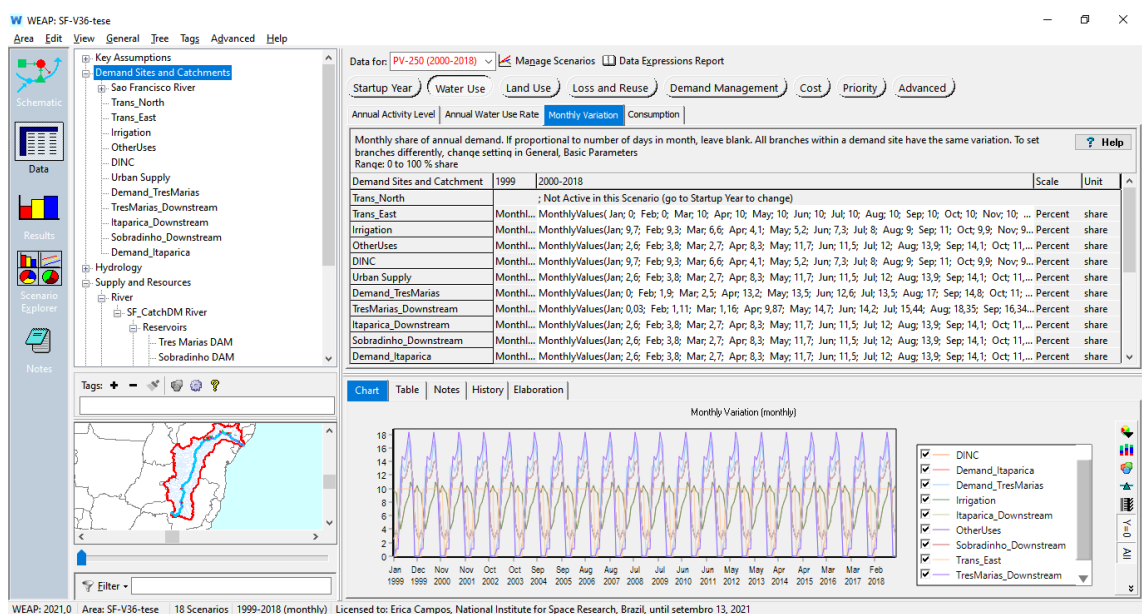
Tresmarias_Downstream: Interp(1999; 776340882; 2000; 776340882; 2001; 776340882; 2002; 776340882; 2003; 776340882; 2004; 776340882; 2005; 776340882; 2006; 776340882; 2007; 1199724240; 2008; 1222128360; 2009; 1236039069; 2010; 1238458518; 2011; 776340882; 2012; 849410899; 2013; 1728810450; 2014; 2228137702; 2015; 3183426709; 2016; 2283891493; 2017; 2925017046; 2018; 3027286922)

Itaparica_Downstream: Interp(1999; 210631232; 2000; 210631232; 2001; 210631232; 2002; 210631232; 2003; 210631232; 2004; 210631232; 2005; 227600865; 2006; 210631232; 2007; 211436208; 2008; 189649108; 2009; 229910699; 2010; 385246939; 2011; 730475698; 2012; 684013750; 2013; 1796427325; 2014; 1807552503; 2015; 1528046593; 2016; 1454054991; 2017; 639429334; 2018; 617202897)

Sobradinho_Downstream: Interp(1999; 1089697035; 2000; 1089697035; 2001; 1089697035; 2002; 1089697035; 2003; 1089697035; 2004; 1089697035; 2005; 1660408294; 2006; 1089697035; 2007; 1773602199; 2008; 1902947431; 2009; 2485031772; 2010; 2637345753; 2011; 2108575311; 2012; 2651364498; 2013; 3305408834; 2014; 3815178791; 2015; 2406949722; 2016; 2981350145; 2017; 1582165325; 2018; 2195131928)

Demand_Itaparica: Interp(1999; 334101314; 2000; 334101314; 2001; 334101314; 2002; 334101314; 2003; 334101314; 2004; 334101314; 2005; 334101314; 2006; 336889698; 2007; 349637452; 2008; 381227146; 2009; 373806098; 2010; 379067708; 2011; 384688502; 2012; 649676601; 2013; 692013280; 2014; 924347687; 2015; 690033096; 2016; 699048093; 2017; 489857766; 2018; 510582205)

Figure A.6 – Monthly variation of the water demand.



Input dataset:

Trans_East

MonthlyValues(Jan; 0; Feb; 0; Mar; 10; Apr; 10; May; 10; Jun; 10; Jul; 10; Aug; 10; Sep; 10; Oct; 10; Nov; 10; Dec; 10)

Irrigation (Sobradinho)

DINC (Sobradinho)

MonthlyValues(Jan; 9,7; Feb; 9,3; Mar; 6,6; Apr; 4,1; May; 5,2; Jun; 7,3; Jul; 8; Aug; 9; Sep; 11; Oct; 9,9; Nov; 9,5; Dec; 10,4)

Urban Supply (Sobradinho)

Other Uses (Sobradinho)

Itaparica_Downstream

Sobradinho_Downstream

Demand_Itaparica

MonthlyValues(Jan; 2,6; Feb; 3,8; Mar; 2,7; Apr; 8,3; May; 11,7; Jun; 11,5; Jul; 12; Aug; 13,9; Sep; 14,1; Oct; 11,2; Nov; 5; Dec; 3,2)

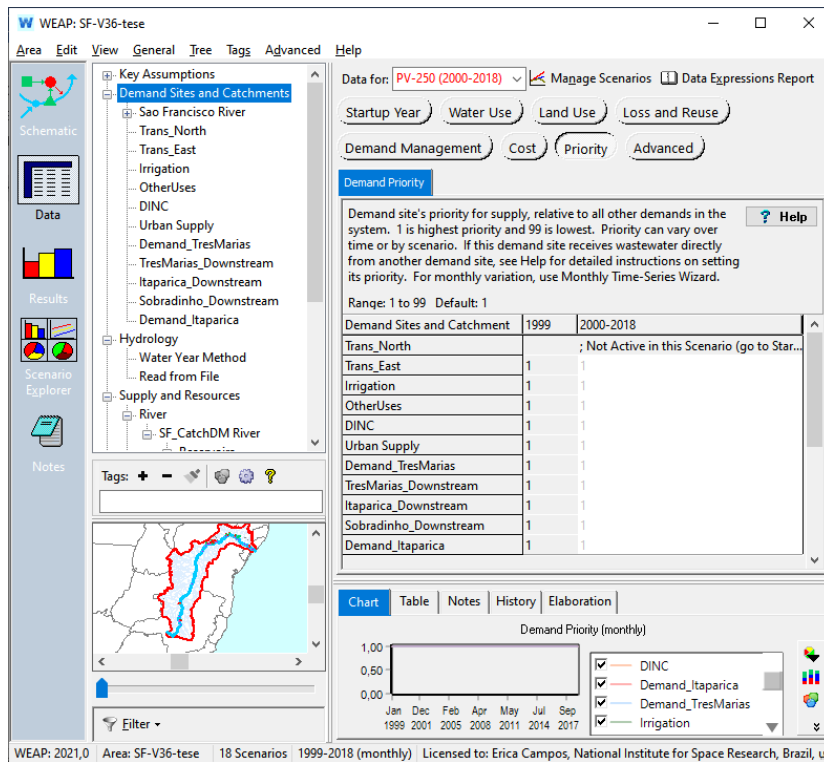
Tresmarias_Downstream

MonthlyValues (Jan; 0,03; Feb; 1,11; Mar; 1,16; Apr; 9,87; May; 14,7; Jun; 14,2; Jul; 15,44; Aug; 18,35; Sep; 16,34; Oct; 8,69; Nov; 0,12; Dec; 0)

Demand_TresMarias

MonthlyValues (Jan; 0; Feb; 1,9; Mar; 2,5; Apr; 13,2; May; 13,5; Jun; 12,6; Jul; 13,5; Aug; 17; Sep; 14,8; Oct; 11; Nov; 0; Dec; 0)

Figure A.7 – Priority rule for water allocation.



Reservoirs

Figure A.8 – WEAP programing for water storage and outflow of the reservoirs.

River Reservoir Flows

A reservoir's (Res) storage in the first month (m) of the simulation is specified as data (see [Supply and Resources\RiverReservoirStorage](#)).

$$BeginMonthStorage_{Res,m} = InitialStorage_{Res} \text{ for } m = 1$$

Thereafter, it begins each month with the storage from the end of the previous month.

$$BeginMonthStorage_{Res,m} = EndMonthStorage_{Res,m-1} \text{ for } m > 1$$

This beginning storage level is adjusted for evaporation. Since the evaporation rate is specified as a change in elevation (see [Supply and Resources\RiverReservoirPhysicalNetEvaporation](#)), the storage level must be converted from a volume to an elevation. This is done by a simple linear interpretation between adjacent points on the volume-elevation curve (specified as data--see [Supply and Resources\RiverReservoirPhysicalVolume Elevation Curve](#)).

$$BeginMonthElevation_{Res} = VolumeToElevation(BeginMonthStorage_{Res})$$

The elevation is reduced by the evaporation rate.

$$AdjustedBeginMonthElevation_{Res} = BeginMonthElevation_{Res} - EvaporationRate_{Res}$$

Then the adjusted elevation is converted back to a volume.

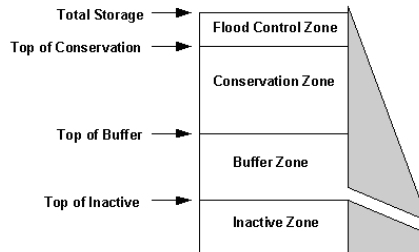
$$AdjustedBeginMonthStorage_{Res} = ElevationToVolume(AdjustedBeginMonthElevation_{Res})$$

A reservoir's operating rules determine how much water is available in a given month for release, to satisfy demand, instream flow and hydropower requirements, and for flood control. These rules operate on the available resource for the month. This "storage level for operation" is the adjusted amount at the beginning of the month, plus inflow from upstream, and demand site (DS) and treatment plant (TP) return flows that come in at that point.

$$StorageForOperation_{Res} = AdjustedBeginMonthStorage_{Res} + UpstreamInflow_{Res} + \sum_{DS} DSReturnFlow_{DS,Res} + \sum_{TP} TPReturnFlow_{TP,Res}$$

The amount available to be released from the reservoir is the full amount in the conservation and flood control zones and a fraction of the amount in the buffer zone (the buffer coefficient fraction is entered as data--see [Supply and Resources\RiverReservoirOperation](#)). Each of these zones is given in terms of volume (i.e. not elevation). The water in the **inactive** zone is not available for release.

$$StorageAvailableForRelease_{Res} = FloodControlAndConservationZoneStorage_{Res} + BufferCoefficient_{Res} \times BufferZoneStorage_{Res}$$



All of the water in the flood control and conservation zones is available for release, and equals the amount above Top Of Buffer (TOB) and other reservoir zones levels are entered as data--see [Supply and Resources\RiverReservoirOperation](#).

$$FloodControlAndConservationZoneStorage_{Res} = StorageForOperation_{Res} - TopOfBuffer_{Res}$$

or zero if the level is below Top Of Buffer.

$$FloodControlAndConservationZoneStorage_{Res} = 0$$

Buffer zone storage equals the total volume of the buffer zone if the level is above Top Of Buffer,

$$BufferZoneStorage_{Res} = TopOfBufferZone_{Res} - TopOfInactiveZone_{Res}$$

(continues)

Figure A.8 – Conclusion.

or the amount above Top Of **inactive** if the level is below Top of Buffer.

$$BufferZoneStorage_{Res} = StorageForOperation_{Res} - TopOfInactiveZone_{Res}$$

or zero if the level is below Top Of **inactive**:

$$BufferZoneStorage_{Res} = 0$$

WEAP will release only as much of the storage available for release as is needed to satisfy demand, instream flow and hydropower requirements, in the context of releases from other reservoirs and withdrawals from rivers and other sources. (As much as possible, the releases from multiple reservoirs with the same **reservoir filling priority** are adjusted so that each will have the same fraction of their conservation zone filled. For example, the conservation zone in a downstream reservoir will not be drained while an upstream reservoir remains full. Instead, each reservoir's conservation zone would be drained halfway. If, however, you would like to drain reservoir A before reservoir B, set reservoir A's priority lower than B's priority.)

$$Outflow_{Res} = DownstreamOutflow_{Res} + \sum_{DS} TransLinkInflow_{Res,DS}$$

where

$$Outflow_{Res} \leq StorageAvailableForRelease_{Res}$$

In addition, WEAP will not release more from the reservoir than its **maximum hydraulic outflow** (if this data value is set).

$$Outflow_{Res} \leq MaximumHydraulicOutflow_{Res}$$

However, this constraint is not binding if the reservoir is completely full. In this case, it can overtop the reservoir with no maximum flow constraint.

The storage at the end of the month is the storage for operation minus the outflow.

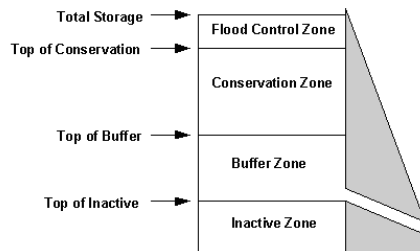
$$EndMonthStorage_{Res} = StorageForOperation_{Res} - Outflow_{Res}$$

The change in storage is the difference between the storage at the beginning and the end of the month. This is an increase if the ending storage is larger than the beginning, a decrease if the reverse is true.

$$IncreaseInStorageRes = EndMonthStorageRes - BeginMonthStorageRes$$

Reservoir Zones And Operation

Reservoir storage is divided into four zones, or pools. These include, from top to bottom, the flood-control zone, conservation zone, buffer zone and **inactive** zone. The conservation and buffer pools, together, constitute the reservoir's active storage. WEAP will ensure that the flood-control zone is always kept vacant, i.e., the volume of water in the reservoir cannot exceed the top of the conservation pool.



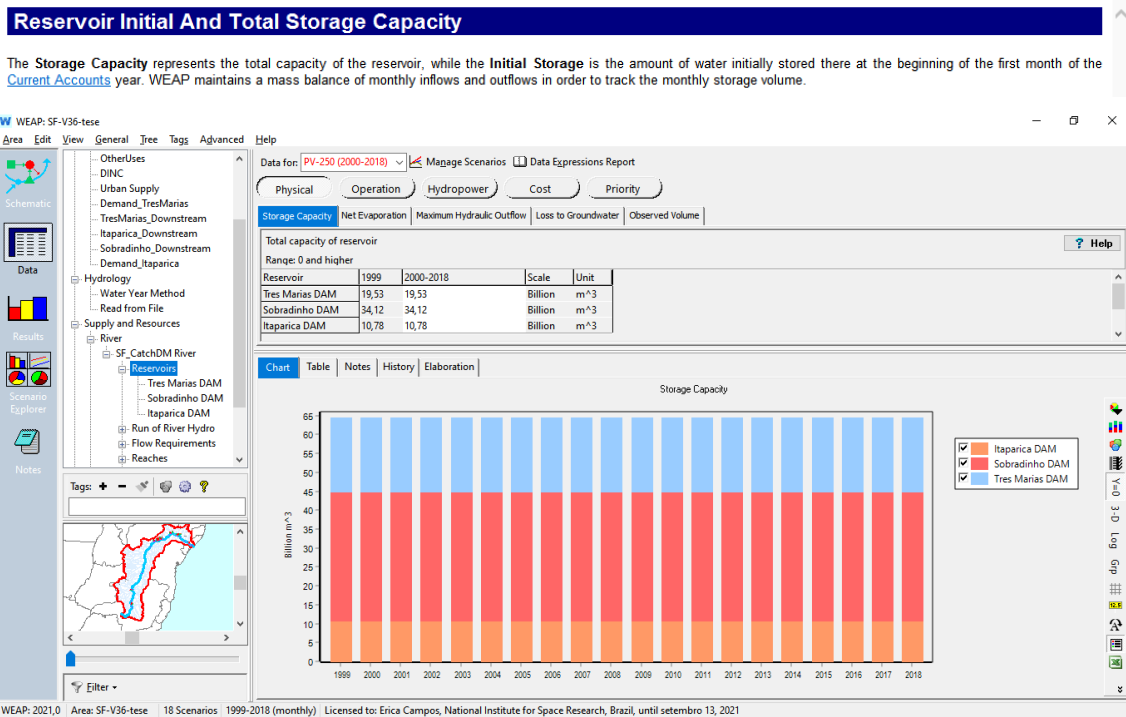
WEAP allows the reservoir to freely release water from the conservation pool to fully meet withdrawal and other downstream requirements, and demand for energy from hydropower. Once the storage level drops into the buffer pool, the release will be restricted according to the buffer coefficient, to conserve the reservoir's dwindling supplies. Water in the **inactive** pool is not available for allocation, although under extreme conditions evaporation may draw the reservoir into the **inactive** pool.

To define the zones, you enter the volumes corresponding to the top of each zone (**Top of Conservation**, **Top of Buffer** and **Top of inactive**). WEAP uses the **Buffer Coefficient** to slow releases when the storage level falls into the buffer zone. When this occurs, the monthly release cannot exceed the volume of water in the buffer zone multiplied by this coefficient. In other words, the buffer coefficient is the fraction of the water in the buffer zone available each month for release. Thus, a coefficient close to 1.0 will cause demands to be met more fully while rapidly emptying the buffer zone, while a coefficient close to 0 will leave demands unmet while preserving the storage in the buffer zone. Essentially, the top of buffer should represent the volume at which releases are to be cut back, and the buffer coefficient determines the amount of the cut back. **Note:** The buffer coefficient determines how much of the water that is in the buffer zone at the *beginning* of a timestep is available for release during that timestep. However, this doesn't restrict WEAP from releasing some or all of water that flows into the reservoir *during* the timestep. Even if the buffer coefficient is 0, WEAP can still release any water that flows into the reservoir that timestep if needed to meet downstream or hydropower demands—in this case, the storage level will not decrease, but it may not increase either.

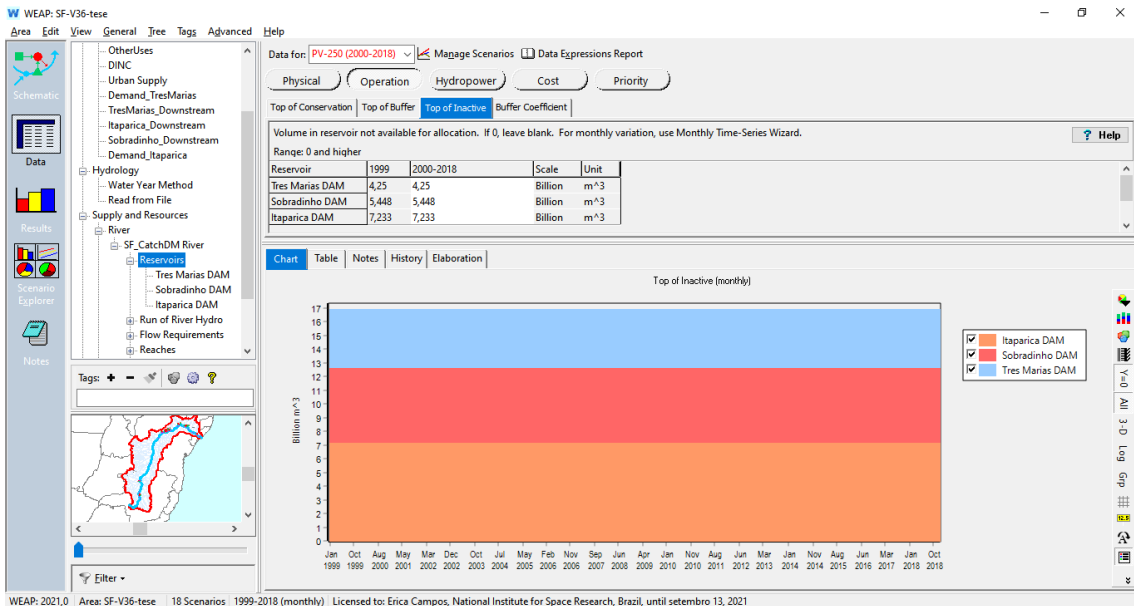
Reservoir Volume-Elevation Curve

In order to calculate the amount of evaporation and/or the amount of energy production from hydropower, WEAP must have a function to convert between volume and elevation. This function is defined by the points on the **Volume-Elevation Curve**. Values between the points are interpolated. You must enter at least one point, corresponding to the total storage capacity of the reservoir. If you choose to model the reservoir as a box with straight sides, you do not need to enter any other points.

Figure A.9 – Modeling of the reservoirs installed at SFR.
(A) Storage Capacity



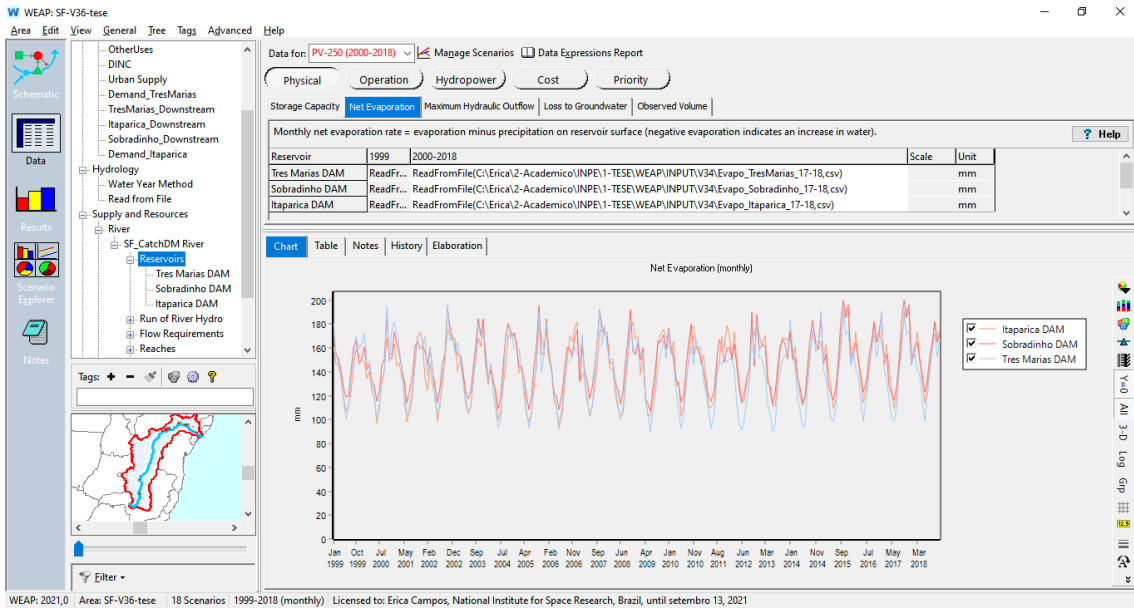
(B) Top of Inactive Volume



(continues)

Figure A.9 – Conclusion.

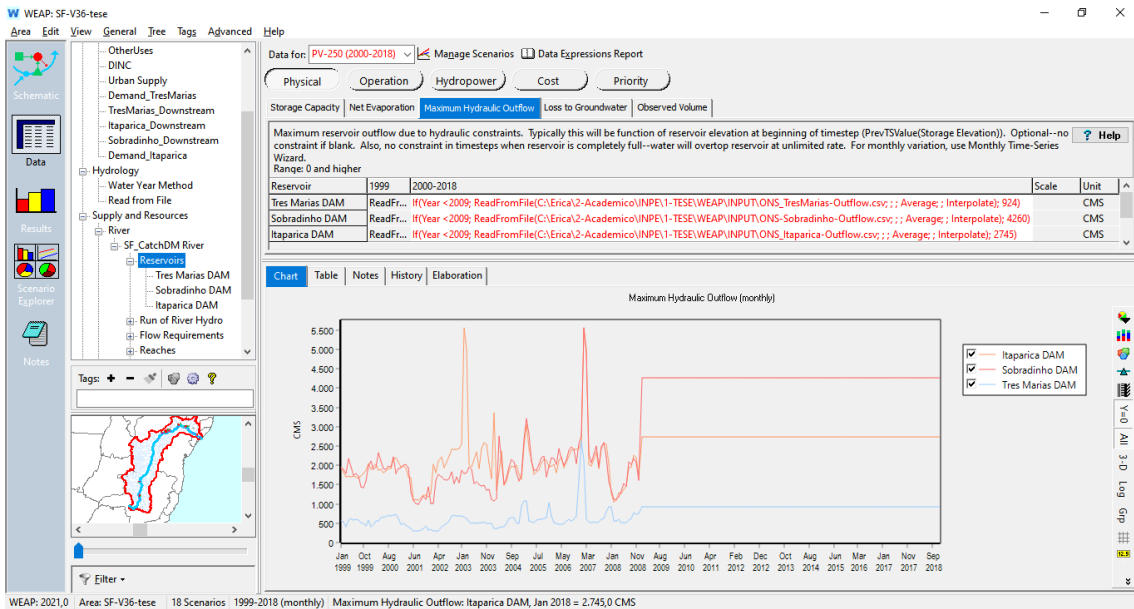
(C) Net Evaporation



(D) Maximum Hydraulic Outflow

Reservoir Maximum Hydraulic Outflow

Maximum reservoir outflow during the timestep due to hydraulic constraints. Typically this will be a function of reservoir elevation at beginning of timestep (PrevTSValue(Storage Elevation)). Optional--no constraint if blank (i.e., no limit on outflow). Also, no constraint in timesteps when reservoir is completely full--water will overflow the reservoir at an unlimited rate. Normally, when there is no maximum hydraulic outflow constraint, WEAP will never allow reservoir storage to exceed the top of conservation. However, if there is a maximum hydraulic outflow constraint, it is possible for the reservoir storage to exceed the top of conservation in timesteps where releases from the reservoir equal the maximum hydraulic outflow.



Input dataset:

Tres Marias DAM: `If (Year <2009; ReadFromFile (C:\Erica\2-Academico\INPE\1-TESE\WEAP\INPUT\ONS_TresMarias-Outflow.csv; ; ; Average; ; Interpolate); 924)`

Sobradinho DAM: `If (Year <2009; ReadFromFile (C:\Erica\2-Academico\INPE\1-TESE\WEAP\INPUT\ONS-Sobradinho-Outflow.csv; ; ; Average; ; Interpolate); 4260)`

Itaparica DAM: `If (Year <2009; ReadFromFile (C:\Erica\2-Academico\INPE\1-TESE\WEAP\INPUT\ONS_Itaparica-Outflow.csv; ; ; Average; ; Interpolate); 2745)`

Source for ONS_Reservoir_Outflow: ONS (2019a)

Hydropower

Figure A.10 – Modeling for quantifying the electricity generation at the hydropower plants.

Hydropower Calculations

Hydropower generation is computed from the flow passing through the turbine, based on the reservoir release or run-of-river streamflow, and constrained by the turbine's maximum flow capacity. Note that the amount of water that flows through the turbine is calculated differently for local reservoirs, river reservoirs and run-of-river hydropower. For river reservoirs, all water released downstream is sent through the turbines, but water pumped from the reservoir to satisfy direct reservoir withdrawals is not sent through the turbines.

$$Release_H = DownstreamOutflow_H$$

For local reservoirs, all linked demand sites are assumed to be downstream of the reservoir, so all reservoir releases are sent through the turbines.

$$Release_H = \sum_{DS} TransLinkInflow_{H,DS} + ExtraOutflowForHydropowerRequirement$$

For run-of-river hydropower nodes, the "release" is equal to the downstream outflow from the node.

$$Release_H = DownstreamOutflow_H$$

The volume of water that passes through the turbines is bounded by the maximum turbine flow (entered as data—see [Supply and Resources/ReservoirHydropower](#)). Note that if there is too much water, extra water is assumed to be released through spillways that do not generate electricity.

$$VolumeThroughTurbine_H = \min(Release_H, MaxTurbineFlow_H)$$

The gigajoules (GJ) of energy produced in a month,

$$EnergyFullMonthGJ_H = VolumeThroughTurbine_H \times HydroGenerationFactor_H$$

is a function of the mass of water ($1000 \text{ kg} / \text{m}^3$) through the turbines multiplied by the drop in elevation, the plant factor (fraction of time on-line), the generating efficiency, and a conversion factor (9.806 kN/m^3 is the specific weight of water, and from joules to gigajoules). The plant factor and efficiency are entered as data (see [Supply and Resources/ReservoirHydropower](#)).

$$HydroGenerationFactor_H = 1000 (\text{kg} / \text{m}^3) \times DropElevation_H \times PlantFactor_H \times PlantEfficiency_H \times 9.806 / (1,000,000,000 \text{ J} / \text{GJ})$$

For reservoirs, the height that the water falls in the turbines is equal to the elevation at the beginning of the month minus the tailwater elevation (entered as data—see [Supply and Resources/ReservoirHydropower](#)).

$$DropElevation_H = BeginMonthElevation_H - TailwaterElevation_H$$

For run-of-river hydropower nodes, the drop in elevation is entered as data (see [Supply and Resources/River/Run of River Hydropower](#)).

$$DropElevation_H = FixedHead_H$$

If a demand priority for hydropower energy has been set for an individual reservoir, WEAP will calculate the supply requirement (volume of water through the turbines) necessary to generate the energy demand.

$$SupplyRequirement_H = EnergyDemandFullMonthGJ_H / HydroGenerationFactor_H$$

(continues)

Figure A.10 – Continuation.

Hydropower Generation

If the reservoir does not generate hydropower, simply leave this entire section blank.

Hydropower will only be generated for flows up to the **Maximum Turbine Flow**. Note: you must enter a non-zero value for maximum turbine flow in order to generate hydropower. **Tailwater Elevation** is used to calculate the working water head on the turbine. The power generated in a given month depends on the head available, which is computed as the drop from the reservoir elevation (as computed by WEAP, using the [Volume Elevation Curve](#) and the storage volume at the beginning of the month) to the tailwater elevation. The **Plant Factor** specifies the percentage of each month that the plant is running. The plant **Generating Efficiency** defines the generator's overall operation effectiveness in converting the energy of the falling water into electricity.

Optionally, to accommodate situations in which you want to prioritize reservoir releases to generate hydropower, there are two methods for specifying hydropower energy demands in WEAP: as individual energy demands for each reservoir or run of river hydropower, or as an aggregate energy demand at the system level. You can choose either method, or even use both at the same time. See [Supply and Resources\System Hydropower Demand](#) for more information about system-level aggregate energy demands.

If you specify a non-zero **Hydropower Priority and Energy Demand**, WEAP will convert the energy demand into an equivalent volume of water that must be released from the reservoir that month to satisfy that demand. (Because hydropower generation is a function of the distance the water falls, this required volume will vary as the reservoir elevation varies each month.) Depending on the hydropower priority, this release requirement will be satisfied either before, after or at the same time as other demands for water on the river. If the hydropower priority is zero, WEAP will not release water solely to generate hydropower. You may change the priority over time or from one scenario to another.

Note: Water drawn from river reservoirs directly via transmission links does not pass through the turbines nor generate electricity. If you want to generate hydropower, attach the transmission link to the river immediately below the reservoir. It is the opposite for "local" reservoirs (not on a river)—flows through transmission links from a local reservoir do pass through hydropower turbines and do generate hydropower.

Hydropower Constraints

For individual reservoirs with a demand and priority for hydropower energy has been set for an , WEAP will calculate the supply requirement (volume of water through the turbines) necessary to generate the energy demand.

In order to limit the flow through the hydropower turbines to the maximum turbine flow, two new LP variables are created for each reservoir and run of river hydropower that either have individual hydropower priorities and demands, or that contribute to a system hydropower energy demand, representing the flow through the turbine and the flow that bypasses the turbine. A constraint is added, which equates these two variables with the total release from the reservoir or run of river hydropower.

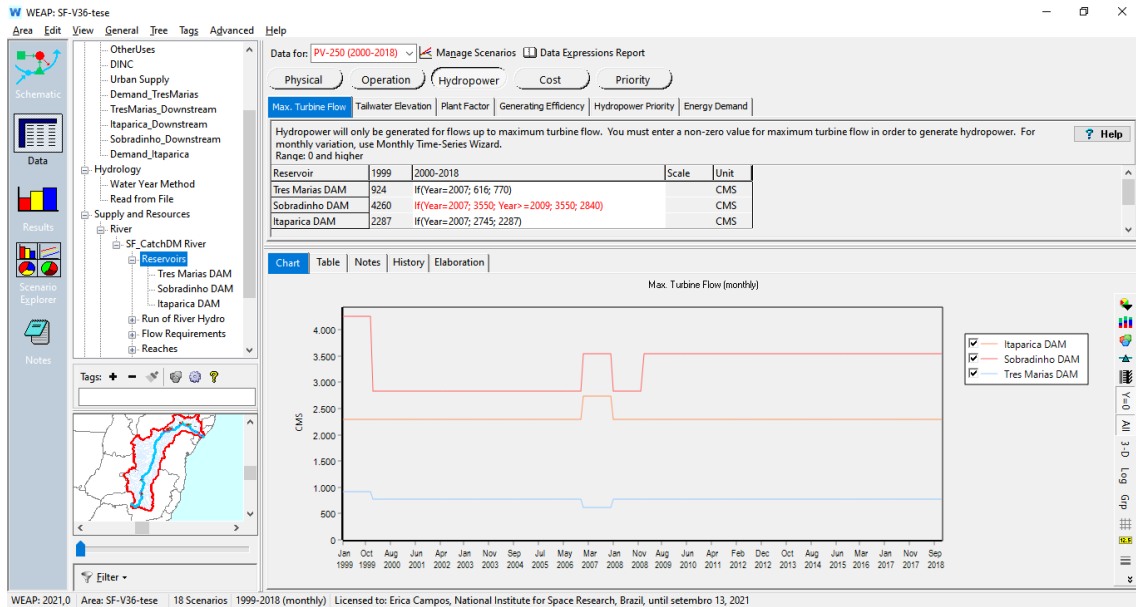
$$Release_H = VolumeThroughTurbine_H + VolumeNotThroughTurbine_H$$

And a constraint is set for the maximum turbine flow.

$$VolumeThroughTurbine_H \leq MaxTurbineFlow_H$$

Figure A.11 – Modeling of the hydropower plants installed at the SFR.

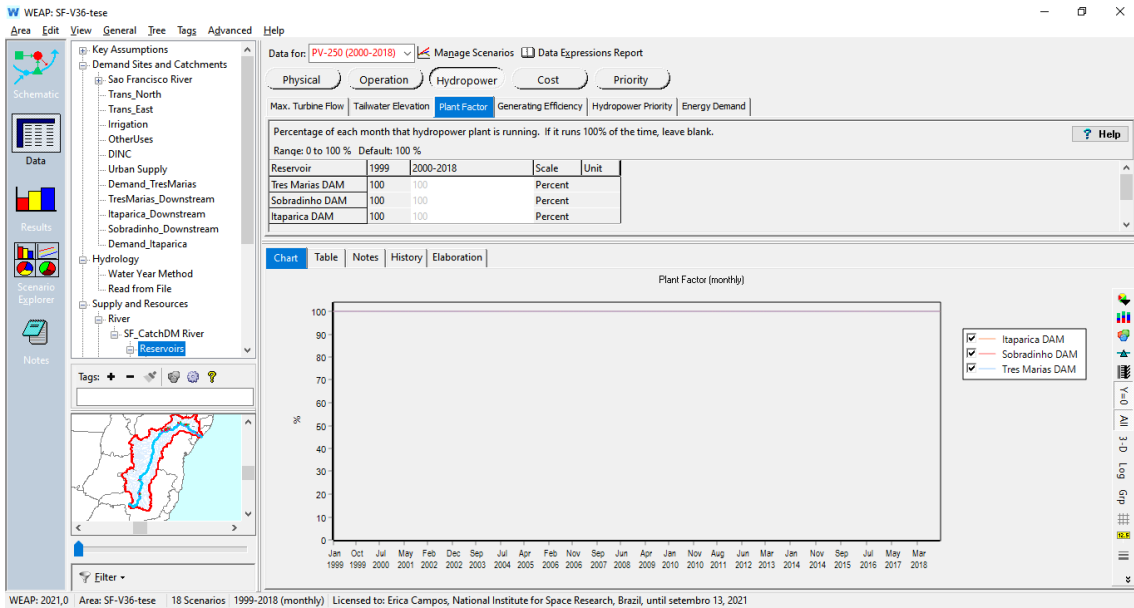
(A) Maximum Turbine Flow



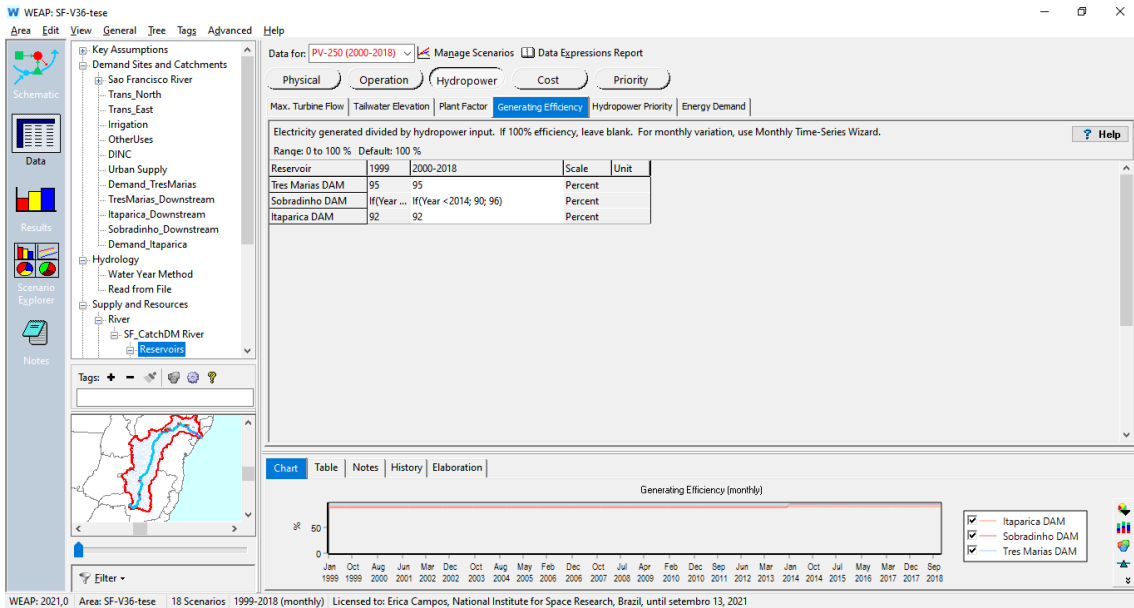
(continues)

Figure A.11 – Continuation.

(B) Plant factor



(C) Generating efficiency



(continues)

Figure A.11 – Continuation.

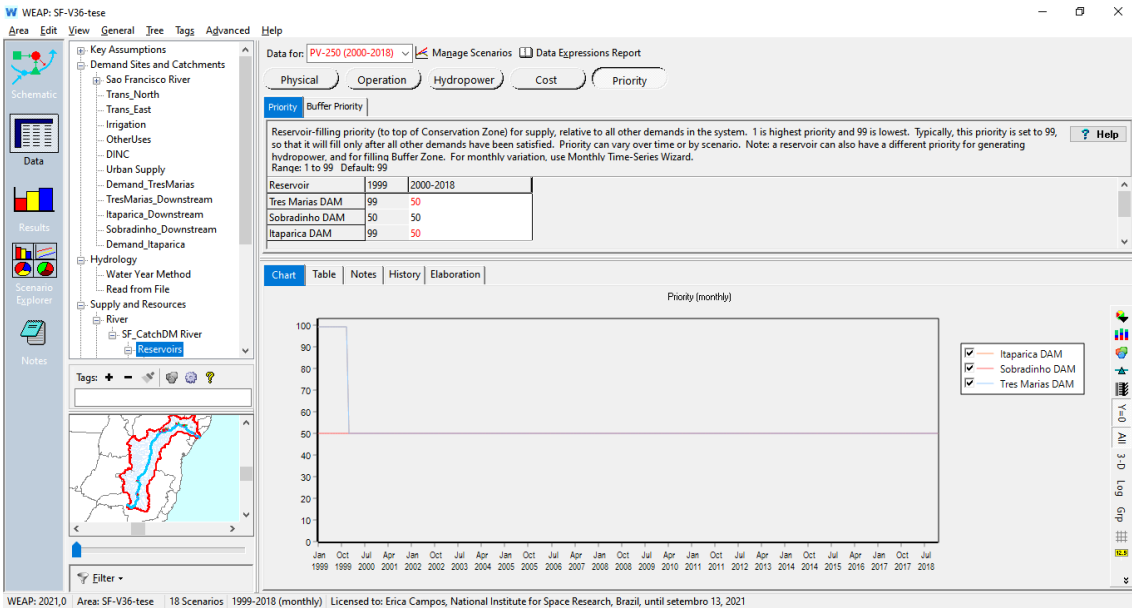
(D) Priority on filling the reservoir

Reservoir Filling Priorities

Each reservoir has one or two priorities for filling, relative to all other demands in the system. 1 is highest priority and 99 is lowest. Priorities can vary over time or by scenario. Note: a reservoir can also have a different priority for generating hydropower – see [Reservoir Hydropower](#) for details.

All reservoirs have a main reservoir-filling **Priority**, for filling the reservoir to the top of the Conservation Zone. By default, priorities can range from 1 to 99, with 1 being the highest priority and 99 the lowest, although you can change this in [Basic Parameters](#). Typically, this reservoir-filling priority is set to 99, so that it will fill only after all other demands have been satisfied. If you had two reservoirs, you could fill one before the other by setting the main reservoir-filling priorities of the two reservoirs to 98 and 99.

A reservoir may also have an optional **Buffer Priority**, for filling just to the top of the Buffer Zone. This allows for more control in how you allocate water in the system for filling various reservoirs. If specified, the buffer priority must be a higher priority than the main reservoir-filling priority (to top of Conservation Zone). Set buffer priority to zero if not used (this is the default).



(continues)

Figure A.11 – Conclusion.
(E) Run of river power plants

Run Of River Hydropower

Hydropower will only be generated for flows up to the **Maximum Turbine Flow**. *Note: you must enter a non-zero value for maximum turbine flow in order to generate hydropower.* The **Fixed Head** defines the working water head on the turbine—the distance the water falls. The **Plant Factor** specifies the percentage of each month that the plant is running. The **Plant Generating Efficiency** defines the generator's overall operation effectiveness in converting the energy of the falling water into electricity.

Optionally, to accommodate situations in which you want to prioritize reservoir releases to generate hydropower, there are two methods for specifying hydropower energy demands in WEAP: as individual energy demands for each reservoir or run of river hydropower, or as an aggregate energy demand at the system level. You can choose either method, or even use both at the same time. See [Supply and Resources\System Hydropower Demand](#) for more information about system-level aggregate energy demands.

Individual energy demands: If you specify a non-zero **Hydropower Priority** and **Energy Demand**, WEAP will convert the energy demand into an equivalent volume of water that must flow through the hydropower plant that month to satisfy that demand. Depending on the hydropower priority, this flow requirement will be satisfied either before, after or at the same time as other demands for water on the river. If the hydropower priority is zero, WEAP will not release water from upstream reservoirs solely to generate hydropower at this run of river plant. You may change the priority over time or from one scenario to another. See [Demand Priority, Supply Preferences and Allocation Order](#) for more information.

See [Hydropower Calculations](#) for calculation algorithms.

Entered on: **Data View**, Branch: Supply and Resources \ River \ <River Name> \ Run of River Hydro, Tabs: Max. Turbine Flow, Plant Factor, Generating Efficiency, Fixed Head, Hydropower Priority, Energy Demand

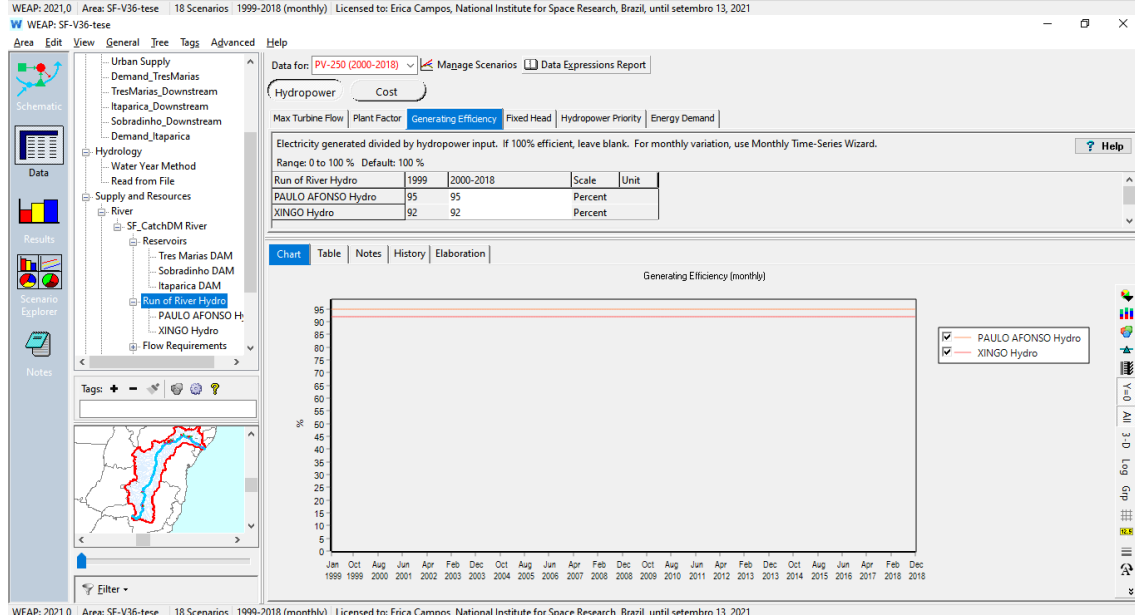
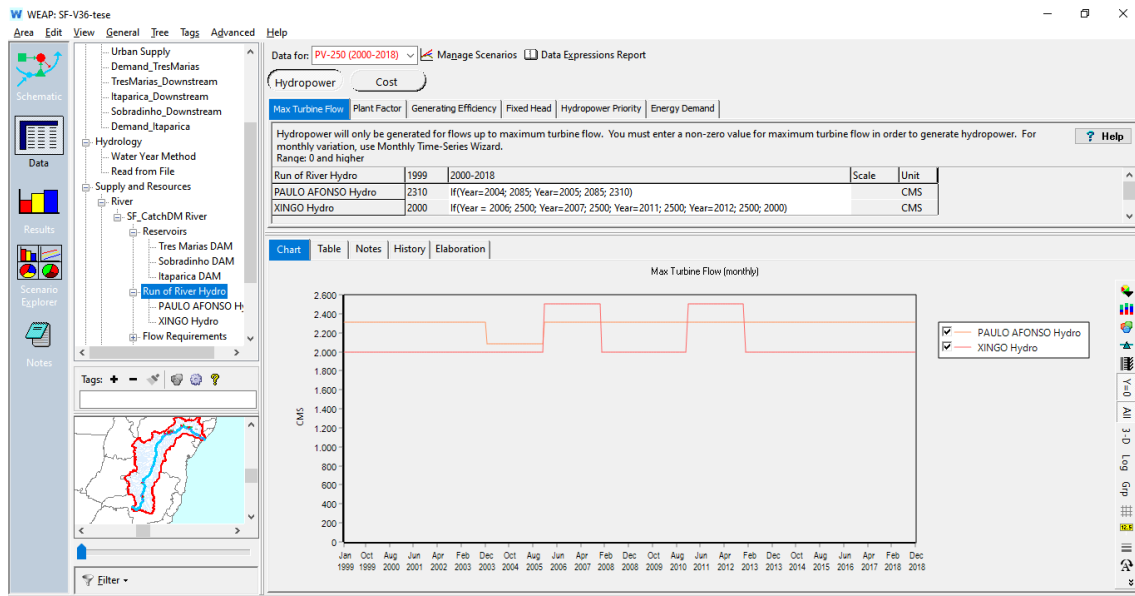
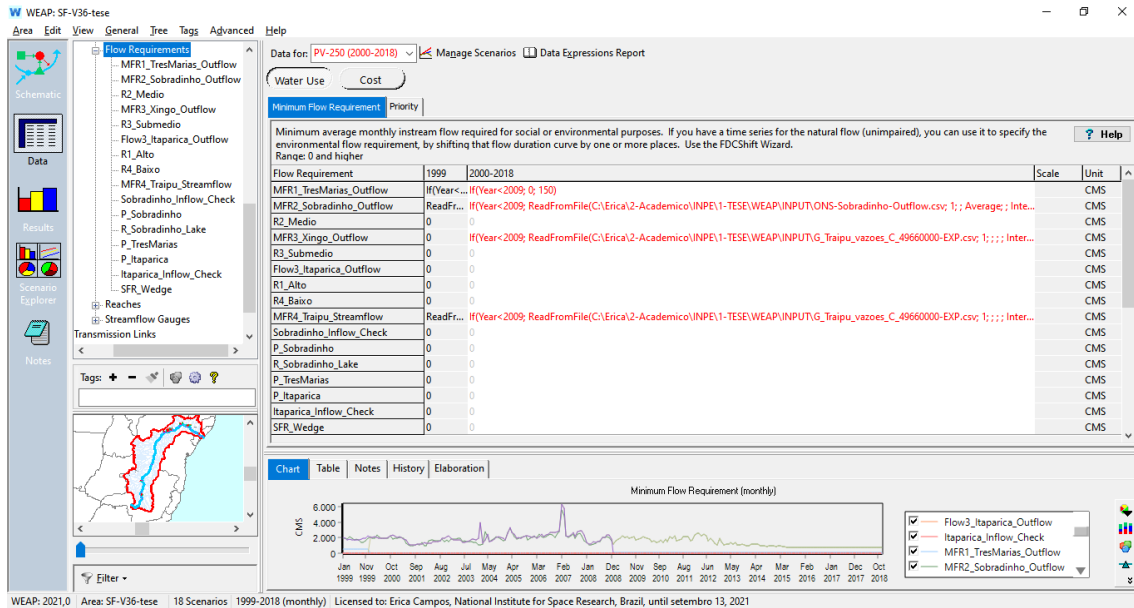


Figure A.12 – Model rules for Minimum Flow Requirement.



Input dataset:

MFR1_TresMarias_Outflow: If (Year<2009; 0; 150)

MFR2_Sobradinho_Outflow: If (Year<2009; ReadFromFile (C:\Erica\2-Academico\INPE\1-TESE\WEAP\INPUT\ONS-Sobradinho-Outflow.csv; 1; ; Average; ; Interpolate); (ReadFromFile (C:\Erica\2-Academico\INPE\1-TESE\WEAP\INPUT\ONS-Sobradinho-Outflow.csv; 1; ; Average; ; Interpolate) - Saved Flow)<800; 800; PrevTSValue (Supply and Resources\River\SF_CatchDM River\Reservoirs\Sobradinho DAM:Storage Volume[m^3])>22649400000; ReadFromFile (C:\Erica\2-Academico\INPE\1-TESE\WEAP\INPUT\ONS-Sobradinho-Outflow.csv; 1; ; Average; ; Interpolate); (ReadFromFile (C:\Erica\2-Academico\INPE\1-TESE\WEAP\INPUT\ONS-Sobradinho-Outflow.csv; 1; ; Average; ; Interpolate) - Saved Flow))

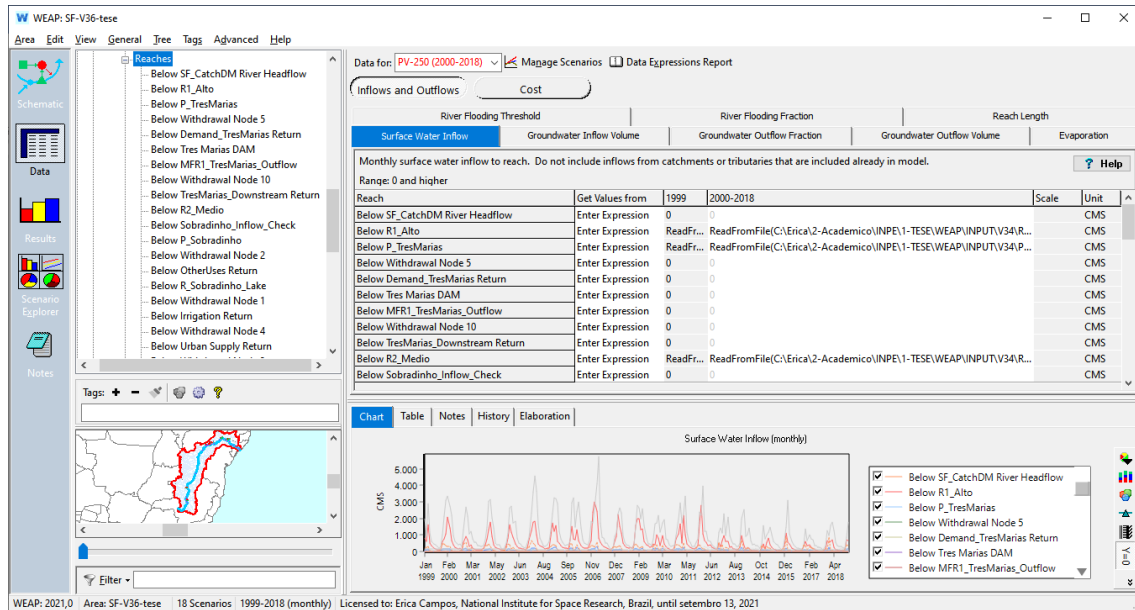
MFR3_Xingo_Outflow: If (Year<2009; ReadFromFile (C:\Erica\2-Academico\INPE\1-TESE\WEAP\INPUT\G_Traipu_vazoes_C_49660000-EXP.csv; 1; ; ; ; Interpolate); (ReadFromFile (C:\Erica\2-Academico\INPE\1-TESE\WEAP\INPUT\ONS-Sobradinho-Outflow.csv; 1; ; Average; ; Interpolate) - Saved Flow)<800; 800; PrevTSValue (Supply and Resources\River\SF_CatchDM River\Reservoirs\Sobradinho DAM:Storage Volume[m^3])>22649400000; ReadFromFile (C:\Erica\2-Academico\INPE\1-TESE\WEAP\INPUT\ONS-Sobradinho-Outflow.csv; 1; ; Average; ; Interpolate); (ReadFromFile (C:\Erica\2-Academico\INPE\1-TESE\WEAP\INPUT\ONS-Sobradinho-Outflow.csv; 1; ; Average; ; Interpolate) - Saved Flow))

MFR4_Traipu_Streamflow: If (Year<2009; ReadFromFile (C:\Erica\2-Academico\INPE\1-TESE\WEAP\INPUT\G_Traipu_vazoes_C_49660000-EXP.csv; 1; ; ; ; Interpolate); 0)

Source for ONS_Reservoir_Outflow: ONS (2019)

Saved Flow applied for the PV scenarios: Table 3.1

Figure A.13 – Rules for Reaches.



Input dataset

R1-Alto: ReadFromFile (C:\Erica\2-Academico\INPE\1-TESE\WEAP\INPUT\V34\R1-Alto.csv)

R2-Medio: ReadFromFile (C:\Erica\2-Academico\INPE\1-TESE\WEAP\INPUT\V34\R2-Medio.csv)

R3-Submedio: ReadFromFile (C:\Erica\2-Academico\INPE\1-TESE\WEAP\INPUT\V34\R3-SubMedio.csv)

R4-Baixo: ReadFromFile (C:\Erica\2-Academico\INPE\1-TESE\WEAP\INPUT\V34\R4-Baixo.csv)

P_TresMarias: ReadFromFile (C:\Erica\2-Academico\INPE\1-TESE\WEAP\INPUT\V34\P_TresMarias.csv)

P_Sobradinho: ReadFromFile (C:\Erica\2-Academico\INPE\1-TESE\WEAP\INPUT\V34\P_Sobradinho.csv)

P_Itaparica: ReadFromFile (C:\Erica\2-Academico\INPE\1-TESE\WEAP\INPUT\V34\P_Itaparica.csv)

R_Sobradinho Lake: ReadFromFile (C:\Erica\2-Academico\INPE\1-TESE\WEAP\INPUT\V34\R_Sobradinho_Lake.csv)

Table A.1 – Water input for incremental streamflow R1, R2, R3 and R4.

	R1- Upper	R2- Middle	R3- Lower-Middle	R4- Lower	Total
01/1999	830	2001	170	106	3107
02/1999	587	967	170	97	1821
03/1999	1623	2894	170	53	4740
04/1999	523	1145	170	82	1920
05/1999	371	611	170	68	1220
06/1999	209	474	170	65	918
07/1999	174	392	170	60	796
08/1999	89	299	170	85	643
09/1999	97	211	170	88	566
10/1999	116	318	170	112	716
11/1999	600	996	170	84	1850
12/1999	751	2130	170	167	3217
01/2000	1072	3121	170	102	4465
02/2000	2075	3364	170	122	5731
03/2000	1437	2744	170	123	4474
04/2000	664	2171	170	144	3149
05/2000	391	948	170	55	1564
06/2000	280	593	170	93	1136
07/2000	202	520	170	76	968
08/2000	143	409	170	70	792
09/2000	223	454	170	91	938
10/2000	98	306	170	119	693
11/2000	569	1306	170	194	2239
12/2000	906	2722	170	196	3993
01/2001	736	2131	170	22	3059
02/2001	313	1059	170	22	1564
03/2001	431	1221	170	22	1844
04/2001	193	751	170	22	1136
05/2001	135	555	170	22	882
06/2001	117	553	170	22	862
07/2001	100	354	170	22	646
08/2001	85	333	170	22	610
09/2001	106	316	170	22	614
10/2001	196	339	170	22	727
11/2001	428	697	170	22	1317
12/2001	788	1497	170	22	2477
01/2002	1304	3053	170	22	4549
02/2002	1794	3138	170	22	5124
03/2002	942	2020	170	22	3154
04/2002	402	1441	170	22	2035
05/2002	276	504	170	22	972
06/2002	206	415	170	22	813
07/2002	161	419	170	22	772
08/2002	86	217	170	22	495
09/2002	138	83	170	22	413
10/2002	75	258	170	22	525
11/2002	333	505	170	22	1030
12/2002	837	1112	170	22	2141
01/2003	1642	2673	96	22	4433
02/2003	1172	2746	96	22	4036
03/2003	871	1715	96	22	2704
04/2003	464	1831	96	22	2413

05/2003	300	825	96	22	1243
06/2003	224	525	96	22	867
07/2003	193	460	96	22	771
08/2003	149	316	96	22	583
09/2003	131	249	96	22	498
10/2003	88	182	96	22	388
11/2003	202	512	96	22	832
12/2003	716	863	96	22	1697
01/2004	1287	2326	96	22	3731
02/2004	1784	3624	96	22	5526
03/2004	1822	4575	96	22	6515
04/2004	1014	3666	96	22	4798
05/2004	448	1657	96	22	2223
06/2004	363	786	96	22	1267
07/2004	299	620	96	22	1037
08/2004	236	351	96	22	705
09/2004	167	285	96	22	570
10/2004	179	383	96	22	680
11/2004	203	603	96	22	924
12/2004	992	1310	96	22	2420
01/2005	1716	2311	96	22	4145
02/2005	1234	3239	96	22	4591
03/2005	1599	3196	96	22	4913
04/2005	603	2871	96	22	3592
05/2005	512	1198	96	22	1828
06/2005	362	727	96	22	1207
07/2005	273	522	96	22	913
08/2005	229	360	96	22	707
09/2005	220	374	96	22	712
10/2005	160	395	96	22	673
11/2005	720	680	96	22	1518
12/2005	1545	2956	96	22	4619
01/2006	759	3261	96	22	4138
02/2006	702	1496	96	22	2316
03/2006	1322	2460	96	22	3900
04/2006	646	2976	96	22	3740
05/2006	346	1419	96	22	1883
06/2006	257	715	96	22	1090
07/2006	222	474	96	22	814
08/2006	185	452	96	22	755
09/2006	203	411	96	22	732
10/2006	390	656	96	22	1164
11/2006	639	1830	96	22	2587
12/2006	2383	1707	96	22	4208
01/2007	3017	2575	96	22	5710
02/2007	2449	4138	96	22	6705
03/2007	795	5755	96	22	6668
04/2007	562	1690	96	22	2370
05/2007	383	782	96	22	1283
06/2007	300	732	96	22	1150
07/2007	247	453	96	22	818
08/2007	194	454	96	22	766
09/2007	151	231	96	22	500
10/2007	127	117	96	22	362
11/2007	247	150	96	22	515

12/2007	634	907	96	22	1659
01/2008	922	1107	96	22	2147
02/2008	2242	2294	96	22	4654
03/2008	1508	2613	96	22	4239
04/2008	1108	2257	96	22	3483
05/2008	500	901	96	22	1519
06/2008	353	516	96	22	987
07/2008	265	352	96	22	735
08/2008	212	272	96	22	602
09/2008	232	114	96	22	464
10/2008	195	170	96	22	483
11/2008	436	392	96	22	946
12/2008	1584	1509	96	22	3211
01/2009	2011	2780	96	22	4909
02/2009	1974	2641	96	22	4733
03/2009	1331	1957	96	22	3406
04/2009	1372	2523	96	22	4013
05/2009	599	1499	96	22	2216
06/2009	420	761	96	22	1299
07/2009	353	391	96	22	862
08/2009	280	369	96	22	767
09/2009	301	291	96	22	710
10/2009	447	724	96	22	1289
11/2009	424	1667	96	22	2209
12/2009	1008	1745	96	22	2871
01/2010	820	2189	96	116	3221
02/2010	359	1176	96	139	1770
03/2010	977	1742	96	148	2963
04/2010	472	1862	96	248	2679
05/2010	294	677	96	151	1218
06/2010	223	630	96	299	1248
07/2010	162	331	96	191	780
08/2010	101	222	96	121	540
09/2010	94	296	96	109	595
10/2010	250	304	96	203	853
11/2010	765	991	96	121	1974
12/2010	1056	1992	96	181	3325
01/2011	1680	2936	96	167	4879
02/2011	500	1723	96	187	2507
03/2011	2194	2307	96	219	4817
04/2011	1031	3345	96	68	4540
05/2011	465	1148	96	155	1864
06/2011	348	602	96	123	1170
07/2011	278	527	96	177	1078
08/2011	207	271	96	164	738
09/2011	140	267	96	230	733
10/2011	236	545	96	321	1198
11/2011	362	745	96	275	1478
12/2011	1742	2382	96	239	4459
01/2012	2792	2194	96	246	5328
02/2012	1055	3949	96	258	5359
03/2012	658	1229	96	289	2272
04/2012	553	1204	96	274	2127
05/2012	382	606	96	188	1272
06/2012	385	554	96	255	1291

07/2012	250	364	96	180	890
08/2012	185	261	96	221	764
09/2012	161	91	96	251	599
10/2012	137	169	96	189	591
11/2012	501	1154	96	125	1876
12/2012	321	1438	96	228	2083
01/2013	686	1144	96	200	2127
02/2013	961	2272	96	152	3481
03/2013	610	970	96	164	1840
04/2013	632	1982	96	169	2879
05/2013	260	856	96	185	1398
06/2013	289	586	96	158	1129
07/2013	178	386	96	212	873
08/2013	130	330	96	177	733
09/2013	110	219	96	219	644
10/2013	175	256	96	189	716
11/2013	258	507	96	156	1017
12/2013	947	1962	96	113	3119
01/2014	354	2564	96	117	3131
02/2014	125	919	96	184	1325
03/2014	181	1015	96	130	1422
04/2014	205	1318	96	184	1803
05/2014	99	559	96	193	947
06/2014	72	302	96	184	654
07/2014	69	346	96	163	674
08/2014	60	215	96	199	570
09/2014	32	205	96	203	537
10/2014	22	89	96	190	397
11/2014	204	476	96	184	960
12/2014	457	1562	96	135	2250
01/2015	148	766	96	120	1130
02/2015	547	1000	96	136	1780
03/2015	831	1156	96	90	2173
04/2015	431	1303	96	142	1972
05/2015	267	853	96	176	1392
06/2015	174	441	96	150	861
07/2015	120	313	96	155	684
08/2015	65	204	96	160	525
09/2015	95	67	96	155	413
10/2015	33	0	96	145	274
11/2015	166	68	96	85	415
12/2015	346	643	96	100	1185
01/2016	1105	1498	96	172	2871
02/2016	571	3077	96	90	3835
03/2016	463	1030	96	56	1645
04/2016	202	514	96	105	917
05/2016	143	279	96	122	640
06/2016	127	189	96	139	551
07/2016	76	100	96	132	404
08/2016	58	72	96	143	369
09/2016	38	32	96	161	328
10/2016	84	82	96	150	412
11/2016	296	365	96	89	846
12/2016	636	1380	96	73	2185
01/2017	355	660	96	78	1189

02/2017	389	1014	96	68	1568
03/2017	238	745	96	63	1142
04/2017	138	584	96	145	963
05/2017	167	190	96	183	636
06/2017	71	212	96	148	527
07/2017	29	132	96	314	571
08/2017	24	92	96	138	350
09/2017	7	23	96	137	264
10/2017	9	7	96	92	204
11/2017	166	343	96	52	657
12/2017	648	1259	96	41	2044
01/2018	553	953	96	49	1651
02/2018	635	1538	96	65	2335
03/2018	694	1754	96	70	2614
04/2018	247	1107	96	109	1559
05/2018	121	394	96	143	754
06/2018	95	230	96	145	566
07/2018	53	139	96	173	461
08/2018	49	98	96	203	446
09/2018	46	52	96	237	432
10/2018	143	75	96	204	518
11/2018	734	886	96	224	1940
12/2018	645	1795	96	186	2722

Table A.2 - Water input related to precipitation in the area of the reservoirs and runoff in Sobradinho.

	P_TresMarias	P_Sobradinho	P_Itaparica	R_Sobradinho_Lake
01/1999	86.0	90.9	30.9	209.0
02/1999	69.0	118.7	36.2	271.5
03/1999	101.6	142.4	47.9	319.3
04/1999	9.1	15.1	5.1	32.1
05/1999	2.1	9.7	5.3	21.5
06/1999	4.8	0.6	1.7	1.4
07/1999	1.3	2.2	2.5	5.3
08/1999	0.0	1.4	1.3	3.5
09/1999	15.8	15.4	6.7	44.4
10/1999	30.8	57.5	23.3	179.3
11/1999	102.8	136.1	60.1	457.0
12/1999	92.9	146.9	63.1	475.2
01/2000	131.2	146.7	54.2	382.7
02/2000	82.7	131.1	45.9	320.7
03/2000	89.5	148.3	45.0	318.6
04/2000	15.2	33.7	14.3	68.0
05/2000	1.7	2.9	2.4	6.0
06/2000	0.4	0.4	3.3	0.8
07/2000	3.2	2.5	2.8	5.5
08/2000	7.6	6.2	3.6	14.5
09/2000	29.1	26.1	10.2	63.8
10/2000	16.0	25.6	8.5	67.1
11/2000	106.7	162.8	62.2	478.5
12/2000	95.4	214.9	72.2	557.3
01/2001	60.0	56.7	19.2	132.9

02/2001	26.1	51.3	17.4	121.2
03/2001	56.1	105.6	39.5	256.4
04/2001	5.4	16.9	6.4	42.7
05/2001	17.9	18.3	7.4	48.0
06/2001	0.1	4.0	5.3	11.2
07/2001	2.8	1.5	3.2	4.4
08/2001	14.8	5.3	4.5	16.6
09/2001	18.0	8.0	4.5	26.4
10/2001	45.8	48.2	23.7	174.5
11/2001	80.1	94.3	43.7	356.7
12/2001	142.4	101.7	53.0	362.0
01/2002	84.9	158.9	69.2	451.6
02/2002	130.2	132.6	45.3	294.5
03/2002	38.4	63.8	21.0	132.8
04/2002	6.7	26.2	8.6	54.3
05/2002	12.1	14.9	7.2	31.8
06/2002	0.0	0.6	2.8	1.3
07/2002	5.3	2.3	2.7	5.2
08/2002	2.5	0.6	1.4	1.5
09/2002	29.1	34.1	11.8	89.3
10/2002	24.3	11.7	5.5	35.1
11/2002	75.9	73.9	31.2	241.1
12/2002	118.9	147.0	64.3	491.1
01/2003	156.5	144.0	59.8	413.0
02/2003	32.7	59.5	21.4	140.8
03/2003	74.8	124.5	41.6	285.8
04/2003	13.5	36.6	12.3	81.2
05/2003	13.5	25.4	10.0	57.4
06/2003	0.1	0.6	1.1	1.3
07/2003	3.1	0.5	1.6	1.2
08/2003	8.5	10.7	4.0	27.0
09/2003	11.5	5.5	2.8	14.6
10/2003	15.2	17.7	7.3	53.6
11/2003	62.9	72.1	31.7	239.3
12/2003	89.2	70.2	31.9	238.5
01/2004	117.7	209.7	100.7	656.3
02/2004	152.9	219.2	74.2	536.3
03/2004	67.5	207.4	51.5	404.9
04/2004	39.7	107.6	19.7	147.5
05/2004	8.8	5.9	4.3	7.6
06/2004	6.3	5.3	4.0	7.2
07/2004	15.5	7.6	3.7	10.9
08/2004	0.1	1.0	1.5	1.6
09/2004	2.2	0.5	1.0	1.0
10/2004	32.7	57.9	14.8	116.4
11/2004	50.9	119.8	32.3	255.2
12/2004	138.5	149.1	44.4	321.4
01/2005	128.7	195.3	55.3	398.4
02/2005	55.4	236.8	57.8	443.5
03/2005	97.9	242.4	55.4	383.3
04/2005	21.4	77.6	15.5	101.8
05/2005	23.2	52.4	15.3	68.5
06/2005	5.9	3.8	5.3	5.4
07/2005	2.2	0.9	2.2	1.5
08/2005	2.2	2.3	2.3	4.3

09/2005	25.5	25.5	7.4	50.4
10/2005	25.3	17.3	5.6	37.0
11/2005	111.1	206.9	59.1	467.4
12/2005	111.6	211.0	59.3	450.9
01/2006	55.9	42.1	12.3	79.3
02/2006	69.4	124.4	34.8	221.3
03/2006	98.3	249.7	63.2	452.0
04/2006	20.3	175.9	33.2	234.5
05/2006	9.0	25.4	7.2	33.3
06/2006	2.6	1.7	4.0	2.5
07/2006	0.5	0.9	3.2	1.6
08/2006	7.0	3.6	1.9	6.9
09/2006	27.9	29.1	9.6	60.5
10/2006	58.2	116.2	33.3	262.9
11/2006	94.8	165.8	49.6	382.4
12/2006	159.4	162.9	50.0	364.0
01/2007	155.4	136.5	40.4	273.5
02/2007	67.6	305.7	78.9	565.8
03/2007	20.1	30.7	10.9	47.3
04/2007	31.7	61.9	13.4	81.6
05/2007	7.6	4.6	4.9	6.6
06/2007	0.8	0.7	1.9	1.2
07/2007	6.6	0.9	2.5	1.8
08/2007	0.1	0.3	2.0	0.6
09/2007	0.8	0.7	1.1	1.6
10/2007	25.8	11.7	4.9	28.9
11/2007	59.5	80.3	31.1	241.3
12/2007	90.3	88.9	38.0	289.6
01/2008	153.3	90.5	40.6	267.8
02/2008	90.0	117.8	45.3	310.0
03/2008	95.7	155.8	57.4	354.2
04/2008	43.0	113.3	34.0	227.8
05/2008	1.7	6.2	6.0	11.9
06/2008	2.8	1.0	2.1	2.0
07/2008	0.1	0.2	2.4	0.5
08/2008	7.2	1.1	1.9	2.4
09/2008	30.3	19.3	7.1	44.2
10/2008	16.6	5.1	2.5	12.6
11/2008	82.5	132.6	45.8	377.0
12/2008	183.5	167.9	65.5	472.8
01/2009	118.1	152.9	50.3	365.4
02/2009	92.1	109.8	36.5	226.3
03/2009	76.2	151.4	40.2	284.8
04/2009	33.8	202.6	45.4	306.6
05/2009	7.6	51.6	16.9	66.9
06/2009	9.6	26.2	7.4	36.6
07/2009	1.0	1.1	1.9	1.8
08/2009	14.9	11.1	5.9	20.9
09/2009	28.2	24.9	7.4	48.8
10/2009	73.4	196.5	51.1	403.0
11/2009	52.6	71.8	19.6	147.6
12/2009	128.0	214.7	58.1	437.2
01/2010	58.9	94.8	27.9	184.5
02/2010	28.3	71.4	20.5	132.6
03/2010	85.1	199.9	51.4	388.8

04/2010	17.5	92.6	27.1	175.6
05/2010	16.7	19.9	6.5	38.2
06/2010	2.6	2.0	5.3	3.8
07/2010	0.8	1.4	3.0	2.8
08/2010	0.0	0.2	1.1	0.5
09/2010	21.6	7.9	4.6	17.6
10/2010	58.0	79.8	28.0	191.3
11/2010	109.1	163.3	50.9	408.0
12/2010	104.8	165.7	55.9	406.8
01/2011	87.1	134.6	43.5	310.5
02/2011	36.1	102.1	33.0	220.4
03/2011	138.6	243.2	70.3	513.8
04/2011	30.9	54.7	17.7	103.0
05/2011	2.1	8.1	7.6	13.9
06/2011	6.0	1.2	1.9	2.2
07/2011	0.1	0.6	2.1	1.2
08/2011	0.3	0.5	1.2	1.0
09/2011	1.5	0.6	1.3	1.2
10/2011	59.6	102.1	30.8	231.3
11/2011	71.7	160.5	47.7	385.2
12/2011	161.8	190.2	59.3	447.0
01/2012	127.3	130.7	39.4	277.3
02/2012	34.4	72.4	21.0	139.2
03/2012	53.5	91.7	22.8	165.1
04/2012	25.1	21.3	6.3	39.8
05/2012	11.9	20.5	6.3	40.5
06/2012	23.7	3.2	3.1	6.7
07/2012	0.8	0.4	1.7	0.9
08/2012	0.1	0.6	1.5	1.3
09/2012	10.4	3.9	2.0	9.7
10/2012	14.3	8.3	3.5	21.6
11/2012	100.5	214.1	70.8	591.0
12/2012	45.1	43.2	15.6	111.1
01/2013	117.7	158.7	56.8	419.8
02/2013	38.7	29.0	10.8	72.4
03/2013	76.8	109.6	34.5	263.5
04/2013	36.2	79.6	25.7	185.1
05/2013	21.9	7.3	5.1	16.4
06/2013	9.8	6.4	3.6	14.6
07/2013	2.5	0.9	3.5	2.1
08/2013	1.2	0.7	1.2	1.8
09/2013	20.3	10.6	4.4	26.2
10/2013	41.0	47.0	17.3	122.1
11/2013	68.2	106.0	38.1	300.9
12/2013	106.0	248.1	86.2	682.3
01/2014	33.7	37.7	12.2	86.6
02/2014	13.6	64.6	18.8	136.5
03/2014	41.2	114.7	33.2	248.9
04/2014	35.8	68.3	23.8	146.0
05/2014	4.9	8.7	5.4	18.6
06/2014	1.1	2.1	1.9	4.7
07/2014	19.7	3.9	4.5	8.9
08/2014	0.6	0.6	1.2	1.4
09/2014	3.1	2.3	1.6	5.8
10/2014	27.7	25.2	10.5	66.3

11/2014	85.0	116.0	47.6	352.9
12/2014	57.9	105.6	40.9	324.7
01/2015	44.7	27.1	12.2	79.2
02/2015	93.6	93.3	40.4	287.7
03/2015	89.2	75.3	34.1	229.1
04/2015	21.6	72.4	27.0	209.6
05/2015	18.8	21.1	9.6	60.6
06/2015	5.4	1.2	3.1	3.5
07/2015	0.8	0.9	3.0	2.8
08/2015	1.2	1.3	1.0	4.3
09/2015	30.9	3.6	3.6	12.5
10/2015	19.7	13.8	7.1	51.9
11/2015	59.5	54.6	27.7	221.6
12/2015	73.1	28.5	18.6	117.8
01/2016	139.8	224.0	117.0	887.5
02/2016	38.3	25.8	13.0	72.4
03/2016	46.1	46.0	17.2	115.2
04/2016	10.4	9.0	3.9	22.4
05/2016	3.7	1.8	2.9	4.5
06/2016	16.8	3.2	3.4	8.6
07/2016	0.2	0.6	1.0	1.6
08/2016	2.4	1.9	1.2	5.8
09/2016	13.9	12.1	5.6	40.5
10/2016	17.7	29.8	14.1	106.1
11/2016	99.6	115.4	46.0	434.0
12/2016	111.4	99.4	40.0	353.0
01/2017	44.7	23.7	12.2	79.2
02/2017	93.6	84.9	40.4	287.7
03/2017	89.2	71.6	34.1	229.1
04/2017	21.6	66.6	27.0	209.6
05/2017	18.8	18.7	9.6	60.6
06/2017	5.4	1.1	3.1	3.5
07/2017	0.8	0.8	3.0	2.8
08/2017	1.2	1.2	1.0	4.3
09/2017	30.9	3.3	3.6	12.5
10/2017	19.7	13.1	7.1	51.9
11/2017	59.5	54.3	27.7	221.6
12/2017	73.1	30.4	18.6	117.8
01/2018	139.8	263.0	117.0	887.5
02/2018	39.7	24.0	13.4	75.0
03/2018	46.1	44.4	17.2	115.2
04/2018	10.4	9.2	3.9	22.4
05/2018	3.7	1.9	2.9	4.5
06/2018	16.8	3.5	3.4	8.6
07/2018	0.2	0.7	1.0	1.6
08/2018	2.4	2.3	1.2	5.8
09/2018	13.9	15.6	5.6	40.5
10/2018	17.7	38.1	14.1	106.1
11/2018	99.6	152.3	46.0	434.0
12/2018	111.4	138.8	40.0	353.0